
Université de Liège – Faculty of Applied Sciences

# Development and implementation of a methodology for hybrid fire testing applied to concrete structures with elastic boundary conditions

Thesis submitted in partial fulfillment of the requirements for the degree of Doctor of Philosophy in Applied Sciences by

**Ana SAUCA**

December 2016


Université de Liège – Faculty of Applied Sciences

# Development and implementation of a methodology for hybrid fire testing applied to concrete structures with elastic boundary conditions

Thesis submitted in partial fulfillment of the requirements for the degree of Doctor of Philosophy in Applied Sciences by

**Ana SAUCA**

December 2016

*Supervisor*

Prof. Dr. Ir. Jean-Marc Franssen

*Co-Supervisor*

Prof. Dr. Ir. Boyan Mihaylov

*Research institute*

Structural Engineering unit
Department ArGEnCo
Faculty of Applied Sciences
University of Liege, Belgium

*Examination committee*

| | | |
|---|---|---|
| Prof. Dr. Ir.<br>Jean-Pierre Jaspart<br>(chairman) | University of Liege, Belgium<br>Faculty of Applied Sciences | Department ArGEnCo<br>Structural Engineering |
| Prof. Dr. Ir.<br>Jean-Marc Franssen<br>(supervisor) | University of Liege, Belgium<br>Faculty of Applied Sciences | Department ArGEnCo<br>Structural Engineering |
| Prof. Dr. Ir.<br>Boyan Mihaylov<br>(co-supervisor) | University of Liege, Belgium<br>Faculty of Applied Sciences | Department ArGEnCo<br>Structural Engineering |
| Dr. Ir.<br>Thomas Gernay | University of Liege, Belgium<br>Faculty of Applied Sciences | Department ArGEnCo<br>Structural Engineering |
| Prof. Dr. Ir.<br>Nicola Tondini | University of Trento, Italy | Department of Civil, Environmental and Mechanical Engineering |
| Dr. Ir.<br>Fabienne Robert | CERIB, France | Fire Testing Center |
| Prof. Dr. Ir.<br>Hervé Degée | Hasselt University, Belgium<br>Faculty of Engineering Technology | |

*Research funding*

The author would like to acknowledge CERIB for financial support of this thesis.

# ABSTRACT

Fire tests remain a precious tool to comprehend the behavior of structures under accidental fire conditions. The common practice in fire testing is to isolate the tested element in a furnace in which the mechanical support conditions are maintained constant throughout the test. However, such tests fail to capture the effect of the structure surrounding the element of interest when this effect cannot be realistically modeled by a free or fixed support condition. It has been observed in large-scale tests that the behavior of entire structures under fire is different compared with the behavior observed in traditional tests on isolated elements. This indicates the importance of capturing accurately the boundary conditions between the element and the remainder of the structure when characterizing the behavior of this element in fire.

The literature describes a few attempts at performing fire tests under realistic boundary conditions. In the latter, the tests were still performed on isolated elements but the boundary conditions were updated during the test taking into account the characteristics of the remainder structure. This technique, called hybrid testing, represents an appealing solution to test structural elements under realistic boundary conditions.

Hybrid testing is a methodology which offers the advantage of testing singular structural elements (or a group of structural elements) named physical substructure PS while at the same time considering the characteristics of the remainder substructure named numerical NS, thus allowing to model realistic boundary conditions. Pioneering work has been done in the seismic field where this technique is now well described, but the implementation of this methodology for structural fire testing raises important challenges due to the specificities of the field. A few hybrid fire tests have been performed in the past on columns and slabs. Their analysis shows that they all use a similar methodology, which is referred to as the first generation method in this work.

The objective of the thesis was to develop and implement a hybrid fire testing methodology on a reinforced concrete beam extracted from a moment resisting frame. Initially, it was intended to build on the first generation method, but after its detailed analysis in the development stage it has been observed that the process can be unstable. The value of the stiffness ratio between the numerical substructure and the physical substructures has been identified as critical in governing the stability of the test, dictating whether the hybrid test needs to be applied in displacement control or force control. This is a severe drawback of the first generation method, as the stiffness ratio is unknown and changing during the test; besides that, different degrees-of-freedom can require different procedures during the test. Therefore, it has been shown that the first generation method should not be applied as it can lead to instability prematurely during the tests.

To overcome the drawbacks of the first generation method, the objective was to develop a new technique that leads to interface equilibrium and compatibility while at the same time is unconditionally stable (i.e. independently of the stiffness ratio). Thus a new methodology was developed and applied to the case of a concrete beam (PS) being part of a concrete moment

resisting frame (NS). The new method makes use of the PS's stiffness in addition to the NS's stiffness as it was the case in the first generation method. The stiffness matrix of the PS is unknown during the test therefore the initial tangent stiffness matrix is considered during the calculations. The latter choice influences the value of the time step to be adopted during the test. Every time step the boundary conditions are updated and it will be discussed how the chosen value can influence the results.
A predetermined matrix is used to describe the behavior of the NS during the hybrid fire tests. This approach does not capture the nonlinearity of the remainder but at the same time the implementation is relative simple and the negative effect of the time calculation is eliminated. The procedure to compute the predetermined matrix of the NS is presented in this thesis. One possible direction in the future development of hybrid fire testing is to model the NS in a finite element model.
The algorithm of the proposed method is developed and implemented in the nonlinear finite element software SAFIR in order to perform virtual hybrid fire tests. The same algorithm is translated in order to be implemented by the company in charge of the control system at the CERIB furnace facility.
The thesis also presents a traditional fire test that has been performed on the beam, in order to highlight the differences when testing structural element without and with the real boundary conditions. For the hybrid test, three degrees-of-freedom are controlled at the interface. The furnace facility has an important role to perform successful test where the equilibrium and compatibility are ensured and no instability occurs during the test. The impediments encountered during the tests will be discussed along with the recommendation for a successful hybrid fire test.

**Keywords**: fire, substructures, physical substructure, numerical substructure, boundary conditions, hybrid fire test, SAFIR, virtual environment

# ACKNOWLEDGMENT

I am grateful to my advisor, Dr. Jean Marc Franssen, for his guidance and support throughout my doctoral studies. He is tremendous mentor and someone who I will always admire. He is the ONE who always had an answer for my questions accompanied by the best advice I could receive. I enjoyed every moment being part of the Fire Safety Engineering group and I am thankful that "you made something out of me".

I am thankful to my dissertation committee members, Dr. Jean-Pierre Jaspart, Dr. Boyan Mihailov, Dr. Thomas Gernay, Dr. Nicola Tondini, Dr. Fabienne Robert, Dr. Hervé Degée for their helpful advice in preparing this thesis. Dr. Boyan Mihailov was the co-supervisor of the thesis and I am grateful for all the help. Dr. Vincent Denoël and Dr. Jean François Demonceau offered valuable advices during the preparation and I express my appreciation.

I am particularly thankful to Dr. Robert Fabienne and Dr. Tessier Christophe. You were the first persons to believe in me and you offered me unbelievable support. I am fortunate to have had the possibility to learn from mentors like you and to be part of the CERIB family.

Dr. Thomas Gernay was the most perfect office colleague, one of the best researchers I know and moreover an incredible friend. I enjoyed working with you, I enjoyed our discussions and jokes and I have no words to express my gratitude for you. I am thankful for every advice and by the way, you know that you deserve all the chocolate from the world.

Cedric Collignon, Eric Leroy, Rija Niry, and Fabien Dumont helped immensely with the design and conduct of my project. They were always available for questions and devoted long hours of effort to help set up the specimens and taught me many technical skills.

The Fire Safety Engineering group, i.e. Anthony Scifo, Joao Ferreira, Elke Mergny, Eric Wellens, and Adil Ouardani, was a joy to work with. Their generosity and expertise created unique work environment.

I spent valuable time at CERIB with great people around from whom I learn all I know about the experimental work. I thank them for always making my stay there amazing and for sharing with me the French culture and not only.

I am particularly grateful to Dr. Oreste Bursi, Dr. Nicola Tondini and Dr. Giuseppe Abbiati who shared with me their experience on hybrid simulations.

My friends and ULg colleagues Anas, Andreea, Christophe, Daniela, Emil, Emna, Hélène, Hicham, Jian, Laura, Lina, Marina, Quang, Ruben, Teo, Timothée created a pleasant environment. I enjoyed our lunch discussions, holidays, gym or dancing nights, and I will always carry with me the memory of this amazing years.

Daniela, Dan, Oana, Getush, Lena, Maria, Melinda, Tudor si Morar have been always supportive and dear friends. I am thankful to Dr. Hortensiu Liviu Cucu and Dr. Mihai Nedelcu who believed in me more than anyone.

I am the most grateful to my beloved family who has been continuously supportive. My dear mom and dad “Mamuska tai Neneka”, my brother Ivan and my sister in law Maria, I am extremely fortunate to have you and my love goes to you.

Support for this project was provided by CERIB. Any opinions, findings, and conclusions expressed herein are those of the author.

# TABLE OF CONTENTS

# LIST OF FIGURES

# LIST OF TABLES

# 1. INTRODUCTION

## 1.1. Motivation of performing hybrid fire tests

The construction field is growing in terms of structural solutions and new material. In order to prevent catastrophic events, which can occur under accidental actions, the behavior of different types of structures in extreme conditions should be assessed by civil engineers. The ability to analyze the behavior of a structure under accidental loads requires first the knowledge of the material behavior. New materials or new structural elements made of well-known materials need to be tested in order to validate and calibrate the new models and methodologies.

Fire tests are required to understand the behavior of structures exposed to fire. Generally the fire tests are performed on single elements, with no restraint, neglecting the action of the remainder structure [1], [2]. Entire structures have been tested [3]-[5] but the high cost makes the practice uncommon. Keeping the advantage of testing only parts of the structure, but at the same time to consider the global behavior of the structure, hybrid fire testing methodology is a promising technique.

Hybrid testing is a methodology inspired from substructuring procedure, and can have applicability under different loading conditions caused by wind, blast, impact, waves, fire, traffic and seismic events. Even if the methodology can be used for many cases of loading conditions, only in seismic field important research has been done in this direction since early 1970s. The implementation of a method developed from the seismic field to the fire field remains a challenge and only a few hybrid fire tests have been performed. Laboratories such as BAM (Germany), CERIB (France) and NRC (Canada) have the experimental facilities that would allow, provided a proper methodology is available, to carry out Hybrid Fire Testing (HFT).

Here are just few of the reasons supporting the necessity of fire tests in general and hybrid fire tests in particular. Globally, the thermal expansion of the structural elements exposed to fire induces important changes in the structural behavior during the fire test. The changes are dependent on the boundary conditions adopted in the test. Locally, specific phenomenon occurs for some materials when exposed to fire such as the spalling of the concrete. This phenomenon is yet impossible to be numerically modeled therefore the fire tests in the appropriate conditions are required to comprehend the action along with the structural behavior. Hybrid fire testing is the key to get more realistic results of the tests and to understand the real behavior of structures exposed to fire, under real boundary conditions.

Despite the large amount of existing information related to hybrid testing in other fields, the application in the fire tests is not straightforward. This is due to the main characteristic of hybrid fire testing which requires hybrid tests performed in real time. The effect of the fire on the materials is immediate and continuous and the thermal expansion implies modification of the interface boundary conditions in real time. Thus the main challenge of hybrid fire testing

is to be able to develop a methodology specifically suited for the fire field which can be used in practice.

Therefore the objective of the thesis is to investigate the theoretical aspect of the methodology which can provide accurate results and ensure compatibility and equilibrium at the interface of the tested substructure and the remainder structure in real time. Next, the proper methodology will be implemented in a fire facility furnace followed by the experimental testing.

It is desired to develop the methodology to fully take advantage of the variety of the instrumentation devices, versatile equipment existing in the worldwide laboratories.

## 1.2. The influence of the boundary conditions on the fire test results

This section illustrates the capability of hybrid fire testing to capture the global behavior of the analyzed structure when testing individual structural elements.

For exemplification, the behavior of a concrete beam exposed to fire is next analyzed in different test configurations. The exposed beam is a structural component of a moment resisting frame, a common structure in practice.

The most common practice when testing structural elements is to ensure free or fixed boundary conditions. Different support conditions are possible, depending on the furnace facility. Table 1-1 present the configurations available when testing a beam exposed to fire.

**Table 1-1. Possible test configuration for beam structural elements**

**Configuration 1**

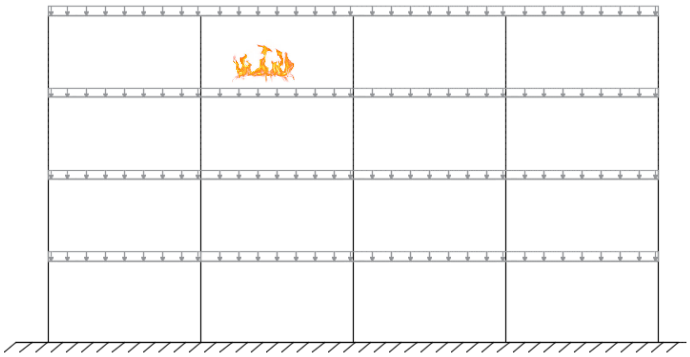

**Configuration 2**

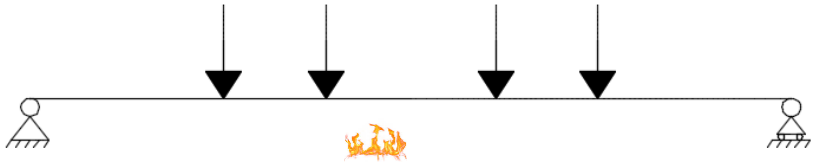

**Configuration 3**

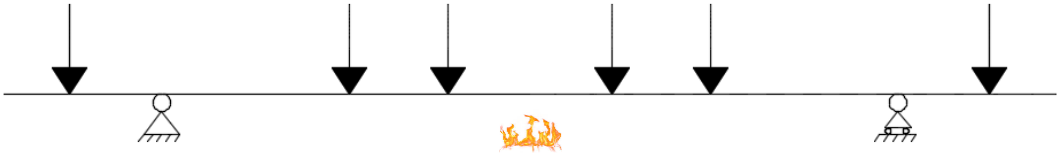

**Configuration 4**

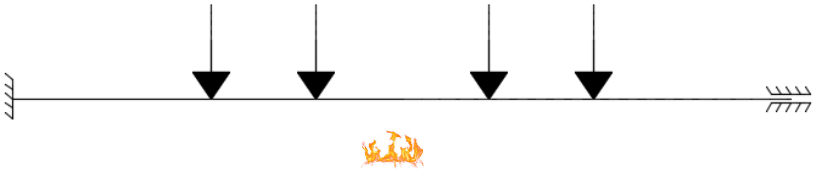

**Configuration 5**

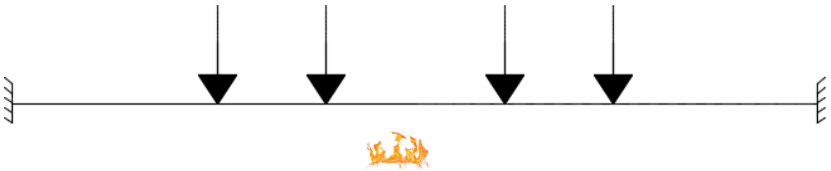

**Configuration 6**

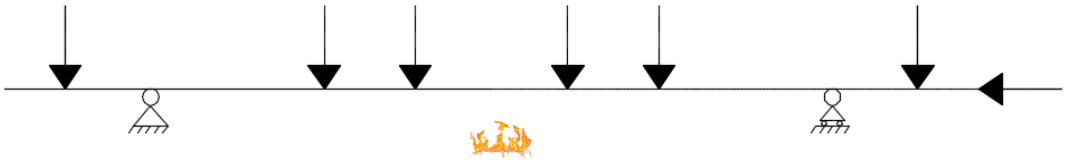

*Configuration 1* refers to full scale testing when only the roof beam of the span number two is exposed to fire.

*Configuration 2* represents the most common practice in the worldwide testing facilities. The beam is simply supported and loaded with equivalent forces such that the mid-span bending moment from the *Configuration 1* is reproduced.

*Configuration 3* is similar to *Configuration 2*. The beam is simply supported and in addition to the previous configuration, the supports bending moments are reproduced during the tests. The support bending moments are induced by the vertical jacks acting on the cold cantilever beam. The fire acts in between the supports and all the forces are constant during the entire test duration.

*Configuration 4* presents the beam test when the support rotations are fixed and the thermal expansion is free.

In the test *Configuration 5*, the support rotations as the thermal expansion are fixed. The difference between the *Configuration 4* and *Configuration* 5 is the fixation or not of the thermal expansion.

In the tests performed in the *Configuration 1* to *Configuration 5*, all the forces are constant during the test.

The *Configuration 6* is characteristic to hybrid fire testing. The support bending moments are applied by the vertical forces acting on the cantilever cold beam while the horizontal restrain of the surrounding structure is modeled via the horizontal force. Therefore, the action of the surrounding on the beam during the test is simulated by the vertical and horizontal forces. These forces vary during the tests depending on the characteristics of the tested elements and the characteristics of the rest of the structure. The vertical forces acting in the span of the beam are constant during the tests.

The beam is numerically modelled in the nonlinear software SAFIR in the specified configuration, in order to observe the behavior during the fire exposure. The standard fire exposure is considered, i.e. ISO 834, and the interest is to observe the time failure and failure mode.

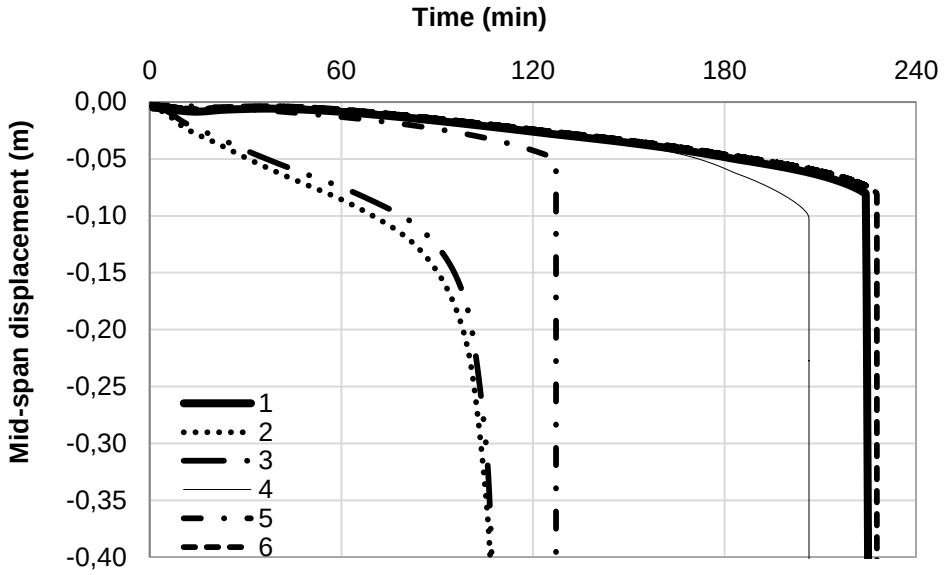


**Figure 1-1. The evolution of mid-span displacement in different testing configurations of the beam structural element**

Figure 1-1 presents the evolution in time of the mid-span displacement, in different configurations.

Similar results can be observed when testing the beam in *Configuration 2* and *Configuration 3*. The distribution of the bending moment is different in the mentioned configurations and this is the reason of the small differences. The beam experiences ductile failure around 100 min since the start of the fire.

The beam tested in the *Configuration 4* reproduces the behavior of the beam when full scale tested, until approximately 150 min since the beginning of fire. The failure occurs soon after 200min of fire exposure, with 100 min later than in the case of the simply supported beam.

When the boundary conditions of the beam are fixed, with no possibility of thermal expansion i.e. *Configuration 5*, the failure occurs around 130 min.

When performing hybrid fire testing, i.e. *Configuration 6*, the behavior of the full scale testing is reproduces with small differences. The difference is due to the hypothesis accepted to perform the hybrid fire test. More details about how the hybrid fire test was numerically modelled will be presented in the next chapters.

For this specific case studied, the provided results by means of hybrid fire testing reproduce the real behavior better than the other possible mentioned configurations.

The time failure along with the mode failure depends on the configuration of the fire tests.

During full scale testing the measured mid-span displacement is smaller compared with the mid-span displacement measured in the *Configuration 2 and 3*.

When performing hybrid fire testing, the mid-span displacement reaches the same range of values than in the case of the full scale testing.

Not only a variation of failure time depending on the test configuration is observed, but the failure mode can be different. A ductile failure is characteristic for tests performed in the *Configuration 2* or *Configuration 3*, while in all the other configurations the failure is brittle.

From all the possible tests configurations presented in this section, the global behavior is reproduced only by means of hybrid fire testing. The advantage of the hybrid fire testing compared with the full scale testing derives from the possibility to perform test on individual structural elements but at the same time to reproduce the global behavior. During the hybrid fire test, the effect of the surrounding is considered.

This section shows the importance and the capability of hybrid fire testing in order to capture the global behavior during the fire tests. All the other configurations reveal different behavior and different failure time compared with the real situations. A better understanding of structures exposed to fire can be provided only by means of hybrid fire testing.

## 1.3. Problem definition

Hybrid fire testing methodology must be validated for different structural elements, must be stable during the entire test, to ensure equilibrium and compatibility at the interface of the substructures and to reproduce the global behavior of the building.
Only few hybrid fire tests have been performed in the past when physically testing columns and slabs. The behavior of the surrounding structure is modeled by using a predetermined matrix (assuming elastic behavior) or nonlinear numerical software (which allows capturing the nonlinear behavior).
The authors of the former hybrid fire tests used methods tailored to suit their particular needs, without verifying the applicability for generic application.
Therefore there is a need of developing and implementing a method which is unconditionally stable, to ensure interface equilibrium and compatibility and to generate accurate results and to be valid for all types of configurations and members.

## 1.4. Research objectives and scope

The aim of the research was to investigate, develop and validate hybrid fire testing and to permit hybrid testing to address to more complex problems to be investigated, independently on the characteristics of the substructures, being stable during the test. To achieve the purpose, the research has been conducted following the objectives presented here bellow.

1. Review and evaluation of the existing concepts and frameworks in hybrid fire testing.
2. Review and evaluation of the existing concepts and frameworks in hybrid methodology developed in seismic field. A comparison between the seismic and fire fields is done, as well as the identification of the sources which suit the fire field.
3. Development of an unconditionally stable method to be suitable for various configurations and which provides correct results.
4. The implementation of the new method in CERIB fire testing facility.
5. The experimental validation of the method on a case study.

## 1.5. Organization of the thesis

This thesis is organized as follows:

Chapter 1 underlines the motivation to perform hybrid fire testing, defines the problems to be solved and the objectives of the current thesis.

Chapter 2 provides general information about hybrid fire testing. It starts describing the procedure and the components of the hybrid fire testing, underlining the advantages and challenges of the procedure. The particularities of hybrid fire testing are visible when making the comparison of the hybrid simulation in fire field versus seismic field. Intensive research has been performed in seismic field and the history of the hybrid simulation method is presented followed by the state of the art in the fire field.

In Chapter 3, the characteristics of the hybrid fire testing are discussed, such as, the global versus local system of coordinates, the representation of the numerical substructure, the importance of the time step during the simulation, and the possible errors during the test.

Chapter 4 describes in details the methodology considered in the previous hybrid fire tests. The discussion is done using one degree-of-freedom case study. The particularities of the first generation method are presented for displacement and force control procedure.

Chapter 5 presents the new developments and implementations of hybrid fire testing. A numerical example (performed on one degree-of-freedom case study) is presented in order to underline the particularities of the new method.

Chapter 6 presents the analyzed case study when using the new methodology. The analysis is first performed in the virtual environment (FE software) followed by the real hybrid fire tests. The proposed method is implemented in CERIB fire facility where the hybrid fire tests are performed.

Finally, Chapter 7 summarizes and draws conclusions about the new developments proposed in this thesis, from the numerical and experimental point of view.

# 2. HYBRID SIMULATION FUNDAMENTALS

## 2.1. Introduction

The fire behavior of the structural systems can be assessed by several methods.

The most common method is the individual testing method, meaning that individual elements are tested without considering the global behavior of the structural system. Such tests are relatively easy and economical to execute compared with the other fire testing methods, but the boundary condition and the loading rate do not reproduce the reality. When individual elements are tested, the thermal expansion is free and no additional forces develop in the specimen. Therefore, the question is if the fire resistance of the tested specimens is under- or overestimated for a specific project situation.

Full scale testing is a second form of testing the structural elements. These tests provide important data on the fire response of the structural system, considering real boundary conditions and loading rate. So far only few tests have been performed in full scale; the high cost needed in performing such tests makes the practice uncommon. Important amount of work needs to be done in building the structural system and installing the needed equipment to measure the required information.

A third method is hybrid simulation, which has been widely used in seismic field, inspired from substructuring methodology. The idea of hybrid simulation is to combine the advantages of individual testing method and full scale testing, meaning that individual element(s) will be tested while accounting for the surrounding's contribution. The surrounding can be modelled via nonlinear numerical software or a predetermined matrix (if elastic behavior of the surrounding is expected). The part of the structure tested in the furnace will be referred to as the physical substructure (PS), while the surrounding as the numerical substructure (NS). The method then consists in ensuring equilibrium and compatibility between these two substructures over the duration of the test. At each time step, data (displacements or forces) are measured at the substructure interfaces. Due to the fire exposure of the PS, equilibrium and compatibility at the interface are not generally satisfied any more at the end of the time step. To restore the equilibrium and compatibility at the interface, new data are computed (forces or displacements) and are imposed to the substructures, based on the measured data from the previous time step. At frequent intervals (time step $\Delta t$), the displacements or the forces at the interface are measured from the PS and this information is sent to the NS. The reactions (forces or displacements) of the NS at the interface are calculated and then sent back to the PS. There may be an additional delay of time $\Delta t_P$ requested for the calculation of the NS reaction and for application of the reaction to the PS. The procedure is either called force control procedure (FCP) or displacement control procedure (DCP), when reaction forces or displacements are sent back to the PS.

The key components in hybrid simulation will be next presented more in detail and the procedure will be described. Using the hybrid simulation, a variety of advantages is gained compared with the individual testing method and the full scale method. In addition, several types of challenges need to be addressed. The advantages and challenges when using hybrid simulations will be discussed. While in seismic field the method is widely studied, in fire field only few tests have been performed using hybrid methodology. The direct implementation of the method used in the seismic field to the fire field is not possible due to the fact that there are some obvious differences between the fields. The difference between the hybrid testing in seismic field and hybrid fire testing will be discussed together with the numerical and experimental errors which can affect the accuracy of the method. In the last chapters, the history of hybrid simulation and the state of the art in fire field is presented.

## 2.2. Components and procedure

To perform a hybrid simulation, there are several components which need to be controlled and interact during the test. The objective of the hybrid simulation is to analyze the behavior of a structural system by combining the experimental testing and the numerical analysis of the remainder. The interaction between the two parts should be ensured during the test in order to achieve equilibrium and compatibility at the interface. To do so, the key components needed in this process are next described and presented in Figure 2-1.

1. The **physical substructure** (PS) to be tested in a furnace is the key component of hybrid fire testing. The PS is the part of the structure which will be experimentally tested in the furnace. The choice of the PS will be done based on the following criteria: (i) unknown behavior of a new material or (ii) a new structural system difficult to be represented numerically.
2. The second key component is represented by the **numerical substructure** (NS) to be analyzed aside during the hybrid simulation. The NS can be modelled in a finite element (FE) model or it can be predetermined in a matrix. There are some differences in the hybrid simulation process depending on how it will be chosen to represent the NS.

   The FE model is recommended when parts of the NS are exposed to fire. The drawback of representing the NS by FE software is the time needed for every time-step calculation during the interaction. In hybrid fire testing the time of the calculation needs to be short in order to be able to reach equilibrium and compatibility at every interaction time step. The advantage of the method is the possibility of considering parts of the NS exposed to fire too.

   When the NS remains cold during the hybrid simulation, then the behavior of the NS can be accounted for by using the predetermined matrix. This means that a matrix will be defined before the hybrid simulation; therefore the calculation time of the NS is virtually zero. Predetermined matrix accounts for the stiffness of the NS, the load pattern and the condensation of DoFs at the interface.

   To reduce the time needed for one-step interaction in hybrid simulation the predetermined matrix is recommended to be used when possible.

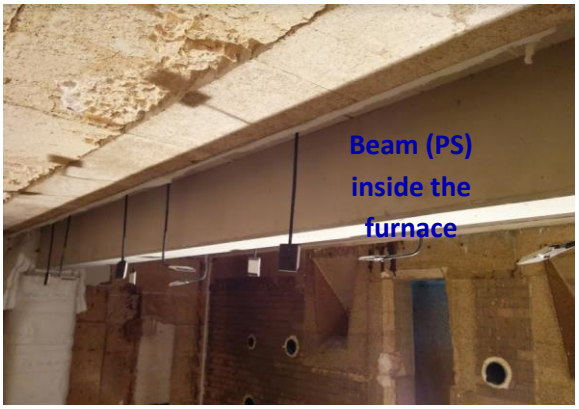


*Physical Substructure PS*

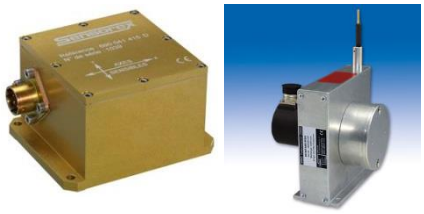

*Data-Acquisition System*

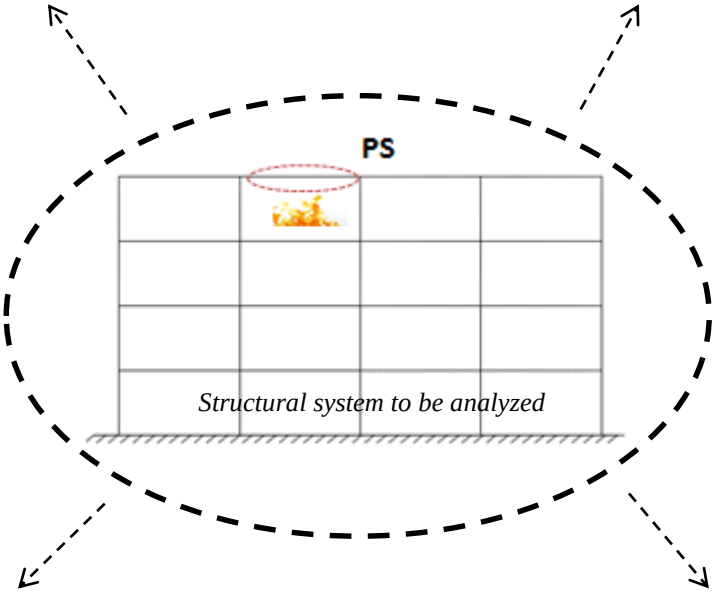


*Transfer System*

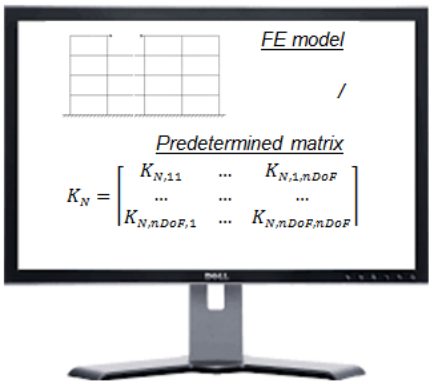


*Numerical Substructure NS*

**Figure 2-1. Components of hybrid fire testing**

3. The **transfer system** between the NS and PS;
   The transfer system means the actuators needed to apply the time step response (displacements in displacement control procedure and forces in force control procedure)
4. The **data acquisition system** in the furnace;
   The data-acquisition system refers to the instruments employed during the hybrid process in order to read the data from experimental process. Examples of such instruments are (i) the displacements transducers and inclinometers and (ii) load cells. The displacements transducers and the inclinometers are used to measure the evolution of displacements and rotations in time, while the loads cells have the properties to read the reaction forces (or restoring forces) in the actuators.

The procedure of hybrid fire testing is next described.
Hybrid fire testing can be performed in force control procedure (FCP) or displacement control procedure (DCP). The steps to be followed during the hybrid fire testing HFT as presented in the literature are described right below.

*Step 1*: Before starting the hybrid fire testing, the interface forces and displacements need to be determined for ambient conditions. To do so, analyze the entire structure (with the physical substructure included in the analysis) at ambient temperature under the loading relevant to the fire situation (called here "external loads") and obtain the corresponding effects of actions called here the reaction forces (bending moments, axial forces, shear forces, torsion moments) and displacements/rotations at the interface between the physical substructure and the numerical one.

*Step 2*: Run another analysis for the numerical substructure, but this time without the physical substructure, when the numerical substructure is subjected to the external loads and, at the interface, to the reaction forces (DCP)/displacements (FCP) resulted in Step1.

*Step 3*: For the physical substructure in the furnace, apply the initial forces or displacements at the interface obtained from step 1 and the external loads which are applied to the physical substructure. The fire test is now ready to start.

Note that when the physical specimen is loaded before starting the fire, it may be possible to get a different value of interface displacements (FCP)/reaction forces (DCP) than the ones calculated in the Step 1. In this situation some additional calculations are needed to restore the interface equilibrium and compatibility at ambient temperature, before the start of the fire. Section 5.2.3 presents more details about this activity.

*Step 4*: Turn the furnace on.

*Step 5*: Read the variation of reaction forces (DCP)/displacements (FCP) of the heated physical substructure at the interface after one time increment.

*Step 6*: From the situation obtained after step 3, impose this variation of reaction forces (DCP)/displacements (FCP) to the numerical substructure and calculate the effects of actions at the interface, displacements (DCP)/reaction forces (FCP). Note that using the finite element analysis, part of the NS can be exposed to fire too.

*Step 7*: Adjust the displacements (DCP)/reaction forces (FCP) forces applied to the interface of the physical substructure in the furnace. The time needed to perform the calculation of the NS and to apply the new corrections in the furnace will be referred to as the delay time $\Delta t_P$.

*Step 8*: Repeat Steps 5 to 7 for each time increment $\Delta t$, for the entire period of the test including the cooling phase if relevant.

After *Step 7* the equilibrium and compatibility at the interface need to be ensured. Due to the fire exposure, while performing the calculation of the NS, the interface conditions are changing. Therefore, at the end of the *Step 7* there is a risk not to satisfy the compatibility and equilibrium conditions if the calculation time is too big.

When the structure to be analyzed is divided in the PS and NS, the number of degrees-of-freedom (DoFs) at the interface is $ntDoF$. When PS is placed in the furnace the rigid body modes need to be suppressed, resulting $nDoF$ at the interface. This means that the total number of DoFs $ntDoF$ at the interface is reduced [6] in the number of DoFs which can be controlled in the furnace $nDoF$. By using a predetermined matrix to represent the NS, the condensation of DoFs is already implemented in the matrix and no additional calculations are needed. When the finite element analysis is used in the hybrid simulation, then the condensation of DoFs needs to be done during the test. More details about the condensation of DoFs will be presented in the chapter 3.3.

## 2.3. Advantages and challenges

Hybrid simulation technique combines the analytical and the experimental approaches to investigate the behavior of the structural system.

The most important advantages are summarized here bellow:

- Hybrid simulation consist in subdividing a structure in two substructures (i) the NS characterized by a well understood behavior reliably modelled in finite element models and (ii) the PS characterized by the fact that is difficult to be modelled numerically and is thus obtained from a physical test in a laboratory. The uncertainties will be reduced if the numerical model of the unreliable parts is replaced with actual physical components.
- Experimental and numerical models can take advantage of the different capabilities available in different laboratories using geographically distributed hybrid simulation.
- The global behavior of structures can be reproduced only by means of hybrid fire testing. This method presents the advantage of providing the real failure time during the fire exposure and the real failure mode.

The hybrid simulation method presents advantages compared with the other existing methods, but several challenges still need to be addressed by conducting further research in this field. The challenges of using hybrid simulation are presented next:

- During the hybrid simulation, data are measured and imposed on the PS every time step. The acquisition and transfer system (actuators and transducers) used to control the interface data (displacements/reaction forces) should be suitable for different types of configurations.
- Each implementation of hybrid fire testing done so far is dependent on the testing site and control, and on the data –acquisition system. The software framework is difficult to be adapted to different structural problems and even to different laboratories.
- The need of a common software framework for developing and performing hybrid simulation. The object-oriented software framework should be robust, transparent, easily extensible and environment independent.
- Using hybrid fire testing, there are different sources of errors which can affect the accuracy of the results: (a) modelling errors (e.g. discretization process); (b) experimental errors generated by the control and transfer system; (c) experimental errors introduced by the instrumentation devices; and (d) unappropriated method of performing hybrid simulations. All these errors can lead to instability during the test.
- Depending on the stiffness of the structures, tests with stiff physical substructure can be difficult to execute under displacement control. One solution to stiff structure would be to use a force control procedure. This means that the method should be suitable for this specific problem and other specific problems which can be identified.
- If the future geographically distributed hybrid simulation can be used, then the networks delays and breakdowns should be avoided and the communication speed needs to be improved as much as possible. A delay in communication can have a crucial effect on the results, due to the fact that during this time the fire exposure continues in the furnace.

## 2.4. Seismic vs. Hybrid Fire Testing

Some differences between the two fields when performing hybrid simulations will be presented in the Table 2-1 to highlight the impossibility of implementing the methods from seismic field directly to the fire field.

The first difference between the two fields is the equation that needs to be solved during the hybrid simulation. For the seismic field a dynamic equation governs the procedure while in the fire field the static equation needs to be solved. When the PS is exposed to fire the expansion develops slowly in time. Therefore, there is no need of a dynamic approach.

The static approach is characterized by the fact that the stiffness of the PS is used in the calculations and this represents a challenge considering that it is not easy to determine the stiffness of the PS. Due to the fire exposure, this value changes during the duration of the test and the change can be significant close to the failure. For floating subdomains (which experience rigid body movements) additional calculations need to be done to find the invert of the singular stiffness matrix. In seismic field, depending on the type of the considered solver, the evolution of the stiffness matrix during the test is not always requested.

One of the main challenges of hybrid fire testing is related to the necessity to conduct the HFT in real time; except for metallic elements in which a uniform temperature distribution can develop, the temperature distribution in most elements is highly non-uniform and time dependent and cannot be scaled down in time (this is particularly significant for concrete or timber elements). In seismic field, reduced scale tests are possible (similitude theory is needed in this case).

Real time testing is needed in fire field compared to seismic field, where slow tests, rapid tests, real time tests and smart shaking table tests are possible. In fire field, except for some specific elements, i.e. pure metallic unprotected structures, the evolution of the thermal gradient in the section of the PS continues even if the fire stops. This requests a real time testing and a fast interaction between the substructures during the hybrid simulation. In seismic field, the slow tests can be executed on extended time-scales of up to two orders of magnitude slower than the actual time-scale. To avoid force relaxation and actuator stick-slip difficulties, rapid tests have been implemented, where the inertial and viscous damping forces are generated in the physical substructures. Another alternative is to perform the hybrid simulation in real time or to execute smart shaking table tests. For every case, the algorithms to solve the dynamic equation are specific.

In fire fields, the structural elements are tested in furnaces, exposed to different fire load. This means that the structural elements need to be assembled (positioned) in such a way to build a closed space where the load fire can be reproduced properly. The structural elements can be totally or partially exposed to fire. The transfer system and data-acquisition system must be protected from the fire exposure (placed outsides the furnace) whereas in seismic field no protection is needed since the test is performed at ambient temperature.

Table 2-1 summarizes the differences between the seismic and fire hybrid testing.

**Table 2-1. Hybrid simulation in seismic versus fire field**

| Criteria for comparison | Seismic field | Fire field |
|---|---|---|
| *Equation to be solved* | Dynamic equations | Static equations |
| *Size of the PS* | Real<br>Scaled (Similitude Theory) | Real |
| *Time of performing tests* | Slow tests<br>Rapid tests<br>Real time tests<br>Smart shaking table test | Real time test |
| *The transfer system and data-acquisition system* | No matter the position | Limited position |

## 2.5. Numerical and experimental errors

In hybrid simulation process errors can be introduced into solution at different stages. A first classification of the errors is the numerical errors versus experimental errors.

A brief list of numerical and experimental errors is described herein.

- Since the fire exposure is continuous, the time needed to perform the calculation of the NS when using the finite element model and to apply the new values on the PS is a factor of error. While the calculation of the NS is undergoing the PS is still exposed to fire. This means that the interface data (reaction forces (DCP)/displacements (FCP)) from the calculations time step are different compared with the interface data (reaction forces (DCP)/displacements (FCP)) from the time when the data are imposed on the PS. Therefore the interface equilibrium and compatibility are not satisfied. The influence of the time calculation and the time needed to induce the target values on the PS needs to be carefully studied.
- The methodology used to perform the hybrid fire testing is another factor of errors. The applied method needs to be stable, to ensure equilibrium and compatibility and to be able to reproduce the global behavior. More information about the instability induced by the wrong methodology will be presented more in detail in the chapter 4.
- Other source of errors can be generated by the transfer system which imposes the calculated response quantities on the PS. The transfer system needs to be tuned correctly in order to avoid the poor results.
- Experimental errors are the most common errors when experimental tests are performed. For example the resolution of the instrumentation, the noise generated in the instrumentation and the calibration errors can produce inaccurate or incorrect measurements leading to poor test results.

More research needs to be done in this area to observe the influence of different errors on the results.

## 2.6. History of hybrid testing in the seismic field

In this section, a brief history of hybrid methodology within the years will be presented.
Searching for new methods to evaluate the dynamic behavior of structures, especially the seismic performance of large-scale structures, the hybrid simulation testing technique started to be developed in the early 1970s, but it was first published in 1975.
There are several methods for evaluating the seismic behavior of a structural system: quasi-static testing method, shaking table tests and hybrid simulation method.
The quasi-static tests are relatively easy and economical. The methodology consists in applying a predefined history of loads or displacements on the tested specimen. The advantage of the method is that the changes in the materials, the boundary conditions and other factors can be identified imposing the same loading on different series of specimens. But the load pattern does not model the change of the load distribution that a structure experiences during a real seismic event.
Shaking table tests are able to simulate the close conditions that would exist during a particular earthquake. The advantage of this method is that the dynamic response of a structure can be analyzed considering specific ground motion, the inertial and energy-dissipation characteristics of the tested structure. Most of the shaking tables are limited in size and capacity, so there is a need to implement dynamic similitude.

The hybrid simulation method represents a new way of testing method which is formerly called the pseudo-dynamic test method or the online computer-controlled test method.
The reader is referred to Schellenberg et al. in [7] for a comprehensive review of hybrid simulation as well as the history in the development. Herein only a short description will be presented.
Takanashi in [8]-[9] published the first official publication about hybrid simulation method. The method was referred to as "online test" and represents an alternative to the shaking table test. In time the method has been improved in terms of efficiency, accuracy and performance.
The experimental tests are sensitive to different types of errors, therefore it was needed to study the propagation of random and systematic errors after the initial developments were conducted by Mahin and William [10] and Shing and Mahin [11]. A summary of error propagation i.e. implementation techniques, experimental setup as the errors based on modeling is presented by Thewalt and Mahin in [12] and by Mosqueda et al. in [13].
The first studies about numerical algorithms for the integration of the equation of motion in hybrid simulation have been conducted by Shing and Mahin [14]. They investigated the implementation of stable explicit schemes, included Newmark method (based on the Newmark family of methods [15]). During the experiments it has been observed that the damage occurred in limited and specific regions of the entire structure. Consequently, Dermitzakis and Mahin [16] suggested using substructuring technique, meaning that a structure needs to be divided into experimental and numerical substructures to perform partitioned hybrid simulations. The explicit integration schemes are conditionally stable, and to overcome the instability of the process a mixed implicit-explicit algorithm was presented by Dermitzakis and Mahin [16], based on the previous developments made by Hughes and Liu [17], [18]. A summary of the all the activities in hybrid simulations, performed in U.S., have been published by Mahin and Shing [19]. The paper described the basic approach to the pseudo-dynamic testing method, and this includes the numerical integration algorithms, details about the implementation and also the capabilities and the limitation of the technique.
In the Nakashima [20]-[23] papers, the stability and the accuracy of the pseudo-dynamic testing method has been studied. A comprehensive summary of all the field activities developed in Japan have been presented by Takanashi and Nakashima [24]. Meanwhile, in U.S., Thewalt and Mahin [25] presented the research about the first multi-directional hybrid simulation, developed as force, mixed force and displacement control strategies, and proposed the "effective force" dynamic testing method. The first implicit unconditionally stable integration method has been presented in the framework of the same research based on the alpha method by Hilber et al. [26]. The need of unconditionally implicit integration methods results from the fact that the explicit integration methods are conditionally stable and impractical for multi-degrees of freedom and for multi-directional hybrid simulation.
Nakashima [27] proposed a specialized operator-splitting (OS) method for hybrid simulation, and later on, the same author [28] published the investigation of stability and accuracy of the later method. Unconditionally stable numerical algorithms to integrate the equation of motion were required to deal with large multi-degree-of-freedom hybrid models. The inspiration of the OS method was based on the implicit-explicit predictor-corrector scheme developed by Hughes [29]. It was found that the OS method possessed improved stability and error propagations compared to the explicit methods moreover any equilibrium iterations were

required. The updated summary of the developments about hybrid simulation were presented by Mahin [30].

The complexity of the structural systems increased as well as the growing number of partitioned hybrid simulations. The consequence was the development of the implicit unconditionally stable integration schemes for hybrid simulation. A new integration scheme based on the implicit Newmark method has been presented by Dorka and Heiland [31], Dorka [32] and Bayer [33].The method used a substepping approach in an inner loop of the algorithm (digital implementation of the force feedback). Shing et al. [34] and Shing and Vannan [35] proposed an integration method based on alpha method by Hilbert and employed an equilibrium solution algorithm with initial stiffness iteration. The algorithm was subsequently used in partitioned pseudo-dynamic tests on concentrically braced frames presented by Shing et al. [36]. Bursi et al. [37] extended the method in the way that the time-step size could be adapted during the hybrid simulation.

Nakashima et al. [38] present the first implementation of hybrid simulation for real-time testing. The dynamics actuators and a digital servo-mechanism were used in the implementation. To improve the computational efficiency, an interlace solution strategy (staggered integration) was employed.

Schneider and Roeder [39] modified the first time a finite element software package (DRAIN-2D) for hybrid simulations instead of using a problem-specific implementation. The next step was to develop the concept of replacing the numerical elements with experimental elements tested in the laboratory. As it was a challenge to estimate the stiffness matrix of the tested substructure during the test, Thewalt and Roman [40] developed a technique based on the measured forces and displacements during the test. Broyden-Fletcher-Goldfarb-Shanno (BFGS) algorithm represented the base in these developments.

Campbell and Stojadinovic [41] proposed geographically distributed structural subassemblies where the individual sited are connected through Internet. The new developments and activities in hybrid simulation made at the European Laboratory for Structural Assessment (ELSA) have been presented by Magonette and Negro [42].

Houriuchi et al. [43], [44] developed the actuator-delay compensation technique to improve the real-time execution of hybrid simulation. Magonnette [45] developed a system to execute continuous hybrid simulations without the real-time requirement in order to avoid the force relaxation.

Pan et al. [46], [47] developed an architecture where the physical test was conducted in one place while the numerical analysis was performed in a different location, where the communication between the substructure has been done via Internet. The reason was to take advantage of different existing testing sites.

The hybrid simulations can be performed using a force control procedure, displacement control procedure or a mixed force-displacement control procedure, depending on the particularities of the problem. Usually in seismic field, a displacement control procedure has been used. The procedure is not always suitable for all the problems types, especially for stiff physical substructures. Therefore the force control and mixed force-displacement control strategies have been developed by Elkhoraibi and Mosalam [48] and Wu et al. [49]. The switching between the force control and displacement control during the simulation is possible.

The real-time testing started to be the main studied area in hybrid simulation and details can be found in Bonnet et al [50] and Bursi et al. [51].
Saouma and Sivaselvan [52] provide information about the hybrid simulation theory, the implementations and applications.
As presented in this chapter, the hybrid simulation in seismic field was widely studied and important improvements were done. Some main differences between the seismic field and fire field when performing hybrid simulations have been presented. It has been underlined that the direct implementation of the existed methods is not straightforward but nevertheless the development done in seismic field are a good source of inspiration for the specific problems of hybrid simulation in fire field.

## 2.7. State of the art in the fire field

Schwarz in [53] (1890) applied the strategy "divide and conquer" to a mathematical problem where a complex domain was divided in two simple parts (a circle and a rectangle) in order to find a solution for the associated differential equations of the combined domains. The analytical solutions of both subdomains were known. To find the solutions on the interfaces an iterative way was used to converge to the solution on the complex domain. Therefore, the idea of *domain decomposition* can be seen as the ancestor of substructuring, where the subdomains are in fact the components of the total structural system.

In civil engineering, the idea of substructuring as a hybrid method has been successfully applied in earthquake engineering as presented in the previous chapter. The combination of numerical and experimental techniques is done in real-time. Pioneering work in that field has been done in Japan[54], USA [55] and Italy [56].

In fire engineering, only few hybrid tests can be found in the literature.

The first reported hybrid fire test was performed by Korzen at BAM [57]-[60] in 1999, where a column specimen was experimentally tested as part of a simulated building environment. The mode of action between both parts is exemplified on a one degree-of-freedom (DoF) basis, i.e. the axial column force is measured and adjusted continuously to the model force, which is represented through a – not necessarily constant – stiffness, in displacement control.

Figure 2-2 presents the idea of substucturing method implemented by Korzen.
Figure 2-2 b) presents the BAM column's furnace with six electro-hydraulic control channels equipped with displacement and force sensors. Depending on the type of the problem the following mechanical boundary conditions can be controlled during the hybrid testing: i.e. two bending rotations for the top and the bottom of the specimen, one axial displacement at the bottom and one horizontal displacement at the top. Therefore, during the hybrid test, thermal and mechanical actions are applied through this device to the PS. The thermal loads are known (the mean gas temperature in the furnace is defined as a function of time) before starting the test whereas the mechanical loads need to be calculated online during the hybrid fire test. The mechanical loads applied during the process take into consideration the contribution of the NS, therefore the real boundary conditions are modeled in the furnace.

During the hybrid fire test, forces at the boundaries of the specimen are measured and used for the computation of the corresponding displacements. The computed data are sent to the PS in order to keep the entire building in mechanical equilibrium with its prescribed overall boundary conditions.

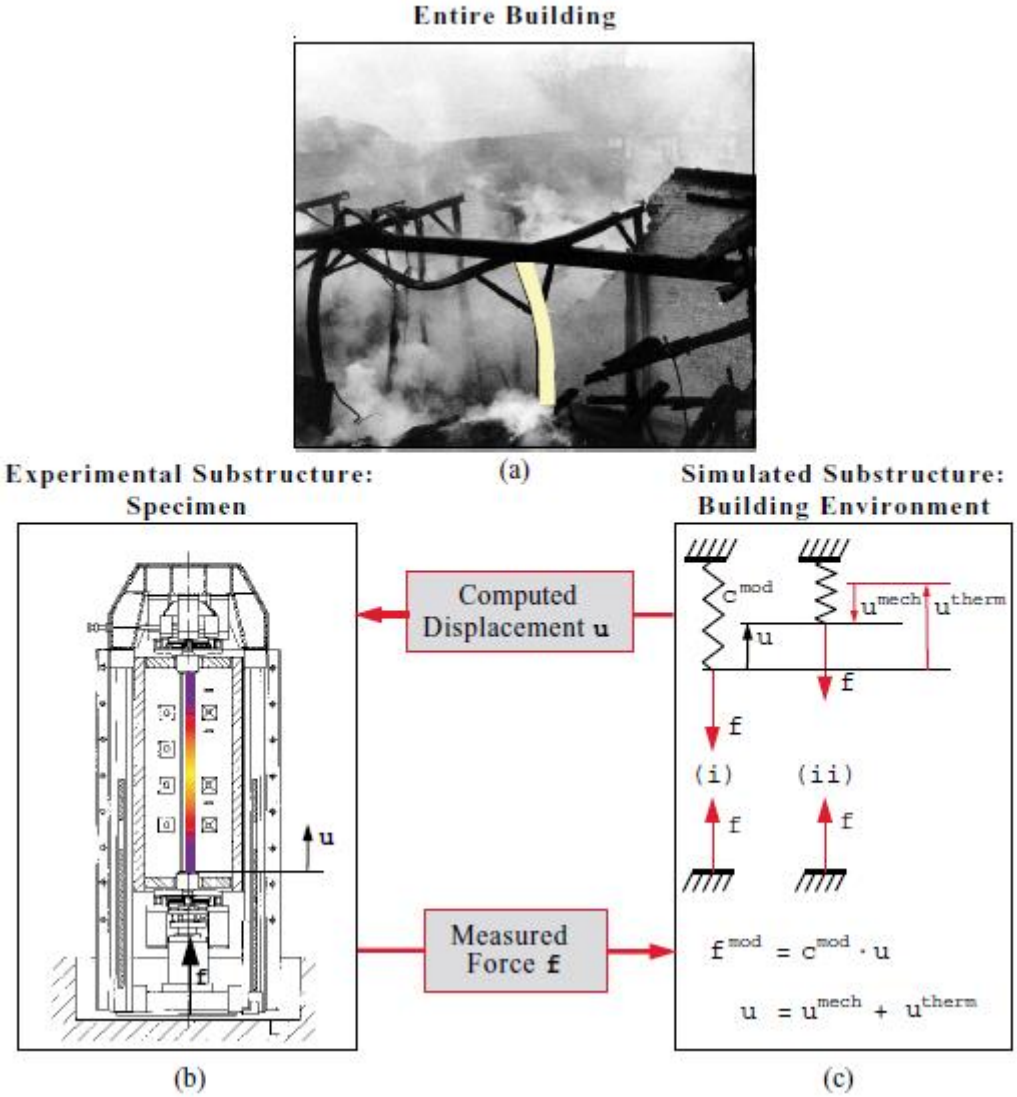


**Figure 2-2. Substructuring method applied at BAM, Germany (excerpt from Korzen [58])**
**a) Entire building; b) Experimental Substructure: Specimen; c) Simulated Substructure: Building Environment;**

Only the channel of the axial cylinder is controlled in the performed hybrid fire test while the remaining five channels are kept constant in displacement or rotation control. The considered loop for only one channel mode is displayed in Figure 2-2 b) – c).

If the hybrid simulation is not considered, then the tested specimen is free to expand when exposed to fire. In Figure 2-2 c) it can be seen that the free thermal displacement $u^{therm}$ is diminished by the mechanical displacement $u^{mech}$ in hybrid simulation. The controlled axial displacement during the HFT is composed of the thermal and mechanical components $u = u^{mech} + u^{therm}$. A compressive force $f^{mod}$ results on the column under test due to the stiffness $c^{mod}$ of the NS (surrounding). The function of the control loop is to change the

(total) displacement $u$ by moving the position of the electro-hydraulic axial cylinder in such a way that the model force $f^{mod} = c^{mod}\, u$ is equal to the measured force in the furnace $f$.
Figure 2-3 presents the results of the hybrid fire tests presented by Korzen in [58]. The value of the $c^{mod}$ is first defined and used in the calculations. It can be observed the increase of the axial force determined by the increase of the axial displacement.

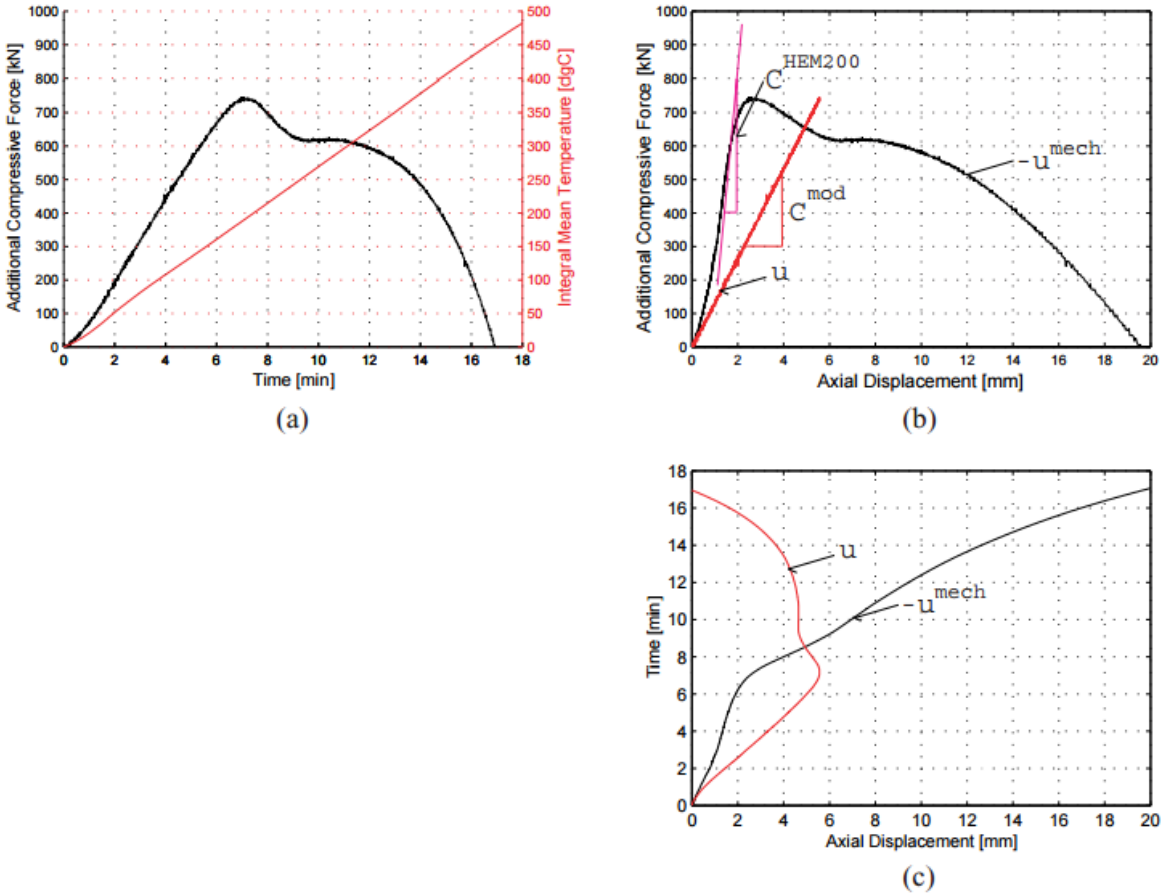


**Figure 2-3. Results of the hybrid fire test performed by Korzen (excerpt from Korzen [58])**

At Faculty of Sciences and Technology of the University of Coimbra (FCTUC) ([59], [60], [61]) performed tests on columns with restrained thermal elongation as presented in Figure 2-4. In other words, the NS is built outside the furnace with a direct effect on the thermal expansion. Several tests, with different characteristics are performed and compared with the tests performed at BAM.

The experimental results registered in the two furnaces are in good agreement. The differences stand from the small differences adopted in the configuration of the tests.
The conclusion of the tests indicates that the surrounding affects the time failure of the columns. Based on the BAM tests, the increase of the stiffness ratio between the NS and PS reduces the critical time. The FCTUC test results show that the increase of the stiffness ratio does not affect the critical time (the rotational restrained plays an important role during the tests cancelling the detrimental effect caused by the axial restrained).

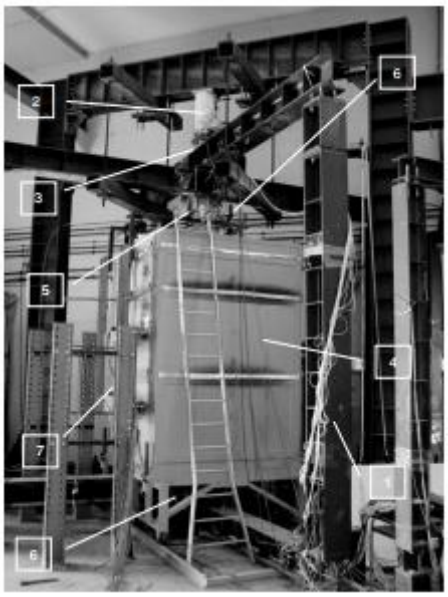

**Figure 2-4. Experimental set-up to tests columns at FCTUC (excerpt from Korzen [59])**

During the test performed by Korzen, the interface force is computed every time step. To apply the computed force on the physical substructure, the displacement control procedure is considered. Therefore, the interface displacement is controlled in such a way that the target force is reached.

Another hybrid fire test is performed and reported by Robert [62]-[64] in 2008. The PS consisted of a concrete slab whereas the NS was a surrounding one floor concrete building. Three DoFs were controlled, i.e. one axial DoF and two rotational DoFs. A force controlled procedure was employed. The behavior of the NS was modelled by a constant predetermined matrix, which had been calculated before the test.

The tested floor system (PS) was composed of 5 cm prestressed concrete floor in combination with a compression slab reaching 16 cm of total depth. The PS has been extracted from a building of 5 identical spans (5.6 m long) with the central span exposed to ISO fire (see Figure 2-5). The test has been stopped after three hours of testing without reaching the critical parameters for failure.
Promethee is the testing facility of fire testing center CERIB. In the fire test, the surrounding structure is replaced by 30 hydraulic jacks whose forces will be time dependent and calculated taking into account the deflected shape and the predetermined matrix of the NS. Compared to the previous tests (Korzen), the number of controlled DoFs increased.

The implemented approach in CERIB testing facility will be next presented.

*Step 1*: Definition of the predetermined matrix.
The predetermined matrix represents the elastic restraint of the cold surrounding (NS) imposed on the PS and it can be calculated by means of numerical simulations and/or by simplified approach considering the structural mechanics. After determining the bending moment / rotation dependency at support and axial forces / displacement dependency at

support, the stiffness coefficients are then calculated through the established relations. Figure 2-5 presents the configuration of the structure used to establish the predetermined matrix of the NS.

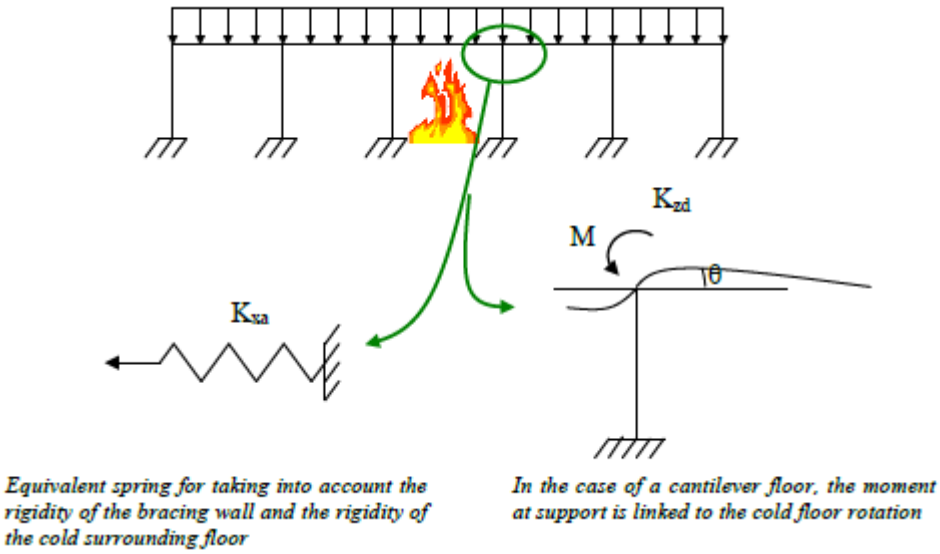


**Figure 2-5. The configuration of the considered structure (excerpt from Robert [64])**

*Step 2:* The configuration of the PS is establish

Figure 2-6 presents the configuration of the tested floor, i.e. the position of the data acquisition system and transfer system. Vertical and horizontal jacks are used to represent the action of the NS on the PS. The vertical jacks (constant during the test) acting in the span of the floor system represent the exterior load. The vertical jacks acting on the cold edge of the floor system simulate the support bending moment depending on the measured rotations and on the NS's stiffness. The horizontal restrain is provided by the horizontal jacks and depends on the horizontal measured displacement and NS's stiffness. In the same figure, the corresponding measured displacements during the test are presented.

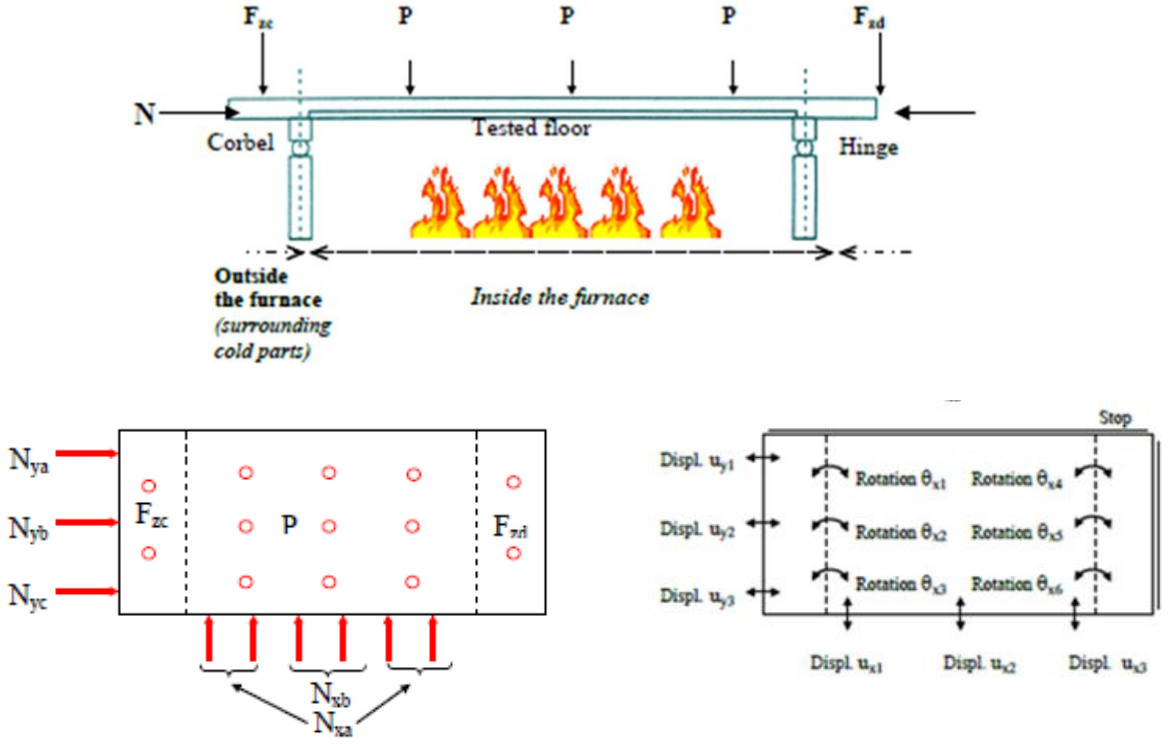


**Figure 2-6. The set-up of the PS (excerpt from Robert [64])**

*Step 3:* The start of the fire and the implementation of hybrid simulation

After the configuration of the PS is establish, the fire starts in the furnace. In the software of the furnace, the predetermined matrix is defined. At each time step the displacements and rotations are measured from the furnace and used in the computation of the target forces based on the static equation $F = K_N u + C$ where $F$ is the vector of target forces, $K_N$ is the predetermined matrix of the NS (elastic behavior), $u$ is the displacement vector and $C$ is the constant vector representing the initial conditions.

The calculated reaction forces of the NS are adjusted in the furnace inducing new displacements. During the entire process, the PS kept being exposed to fire, therefore to ensure equilibrium and compatibility the calculation should be restarted, meaning that the new displacements are measured and used for the computation of new target forces. The procedure is repeated until the end of the fire test and in this way the global behavior of the building is accounted for while testing only a part of the building.

Figure 2-7 presents the results of the hybrid fire test focusing on the evolution of the axial force developed during the hybrid test. The increase of the axial force in the first 90 minutes is due to the thermal expansion which is resisted by the surrounding. The stiffness of the exposed PS degrades in time, the mid-span displacement (noted as Z8) increases which leads to the decrease of the axial force.

No information is presented regarding the evolution of support bending moment i.e. the forces acting on the cold extremity of the slabs. The interface displacements/rotations are not presented either.

The tests is stopped after three hours in the conditions that no critical parameters for failure were reached.

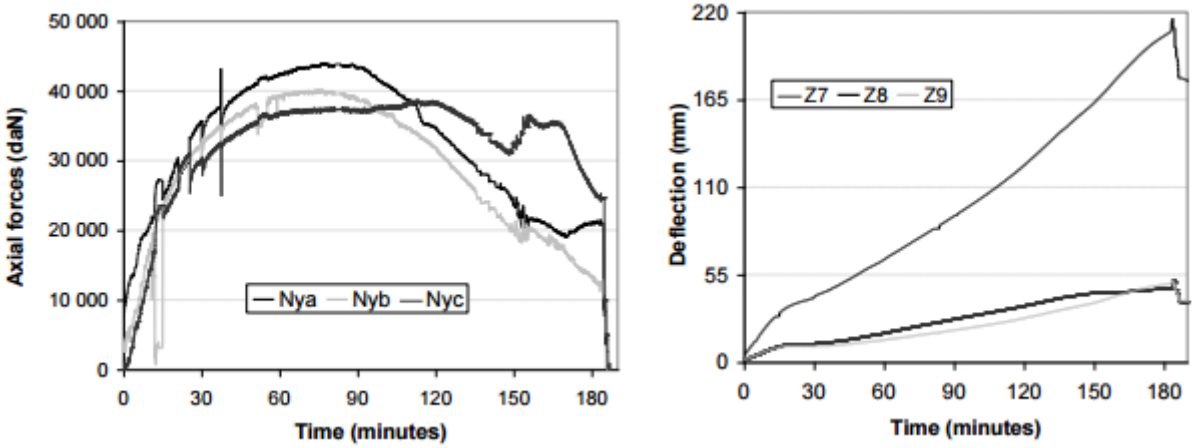


**Figure 2-7. The presented results of the hybrid fire test (excerpt from Robert [64])**

Finally, Mostafaei [65]-[66] reports in 2013 the hybrid fire test of the first floor central column part of a 3D concrete frame (see Figure 2-8). The column was tested in the furnace (PS) while the surrounding was numerically modelled in the non-linear finite element software SAFIR® [74]. Every time step, the interaction between the PS and NS was ensured manually by the user. In particular, the axial force in the column was controlled. Unlike the previous cases, a part of the NS was also exposed to fire.

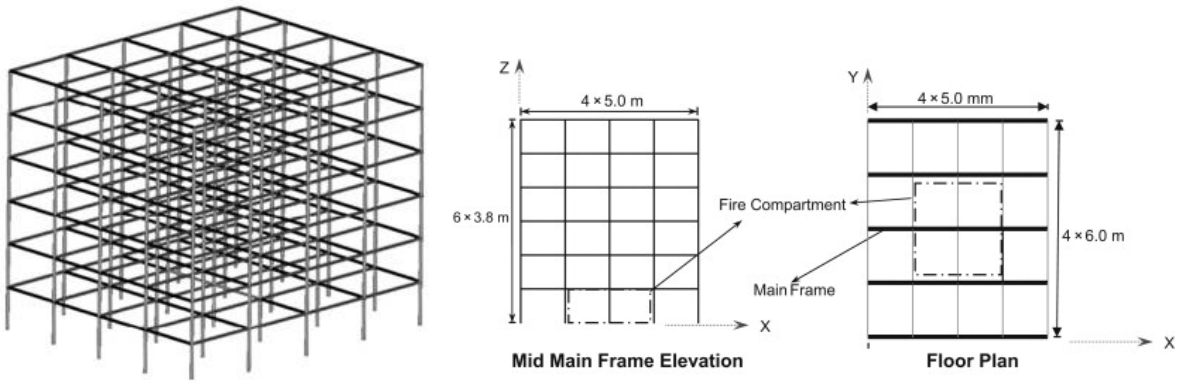


**Figure 2-8. The configuration of the structural system used by Mostafaei (excerpt from Mostafaei [66])**

The symmetry of the structural system and the symmetry of the fire compartment determine only the variation in time of the axial DoF for the central column. The HFT loop in Mostafaei's example is presented in Figure 2-9.

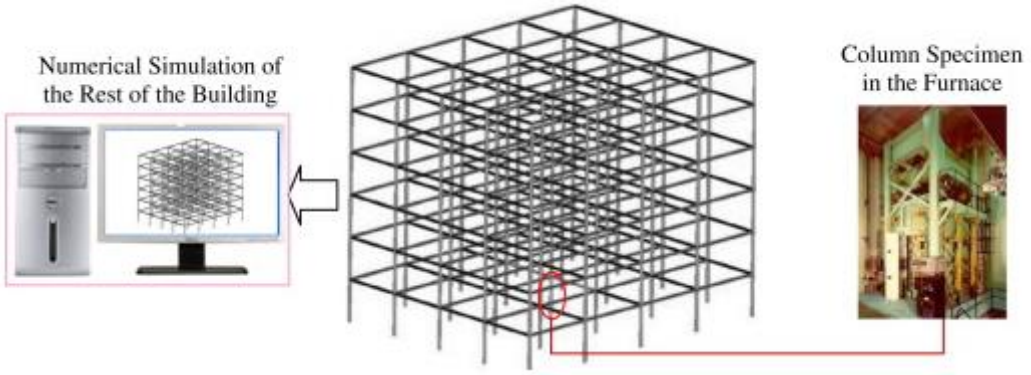


**Figure 2-9. HFT loop presented by Mostafaei (excerpt from Mostafaei [66])**

Compared with the previous test performed by Robert, no predetermined matrix has been computed. The steps applied in the hybrid fire test performed by Mostafaei are presented here bellow:

*Step 1*: Analyze the entire structure (with the physical substructure included in the analysis) at ambient temperature under the loading relevant to the fire situation (called here "external loads") and obtain the corresponding effects of actions (bending moments, axial forces, shear forces, torsion moments) and displacements at the interface between the physical substructure and the numerical one.

*Step 2*: Run another analysis for the numerical substructure, but this time without the physical substructure, when the numerical substructure is subjected to the external loads and, at the interface, to the displacements obtained in Step 1.

*Step 3*: For the physical substructure in the furnace, apply the initial forces equal to the effects of actions at the interface obtained from step 1 and the external loads which are applied to the physical substructure. The fire test is now ready to start.

When the physical specimen is loaded before starting the fire, it may be possible to get a different value of displacements than the ones calculated in the Step 1. In this situation the measured displacements before the start of the fire will become the reference displacements, and in Step 2 the analysis will be made with this new value. The adjustment will be done before starting the fire.

*Step 4*: Turn the furnace on.

*Step 5*: Read the variation of displacements of the heated physical substructure at the interface after one time increment.

*Step 6*: From the situation obtained after step 2, impose this variation of displacements to the numerical substructure; read the effects of actions at the interface.

*Step 7*: Adjust the forces applied to the physical substructure in the furnace with the effects of actions obtained from the analysis in Step 3.

*Step 8*: Repeat Steps 5 to 7 for each time increment, for the entire period of the test including the cooling phase if relevant.

The interaction between the PS and NS was done every 5 minutes by the user which provided reasonable accurate results. The PS and the NS are exposed to E119 standard curve for duration of 4 h. The evolution of the axial displacement along with the evolution of the axial force registered during the tests is presented in Figure 2-10. The thermal expansion of the PS leads to the increase of the axial force since the NS restrain the thermal expansion. The axial displacement and the axial force are plotted for the PS and for the NS. The two curves match each other therefore the equilibrium and compatibility are satisfied. The author does not present the solution resulted from the global analysis of the entire structure.

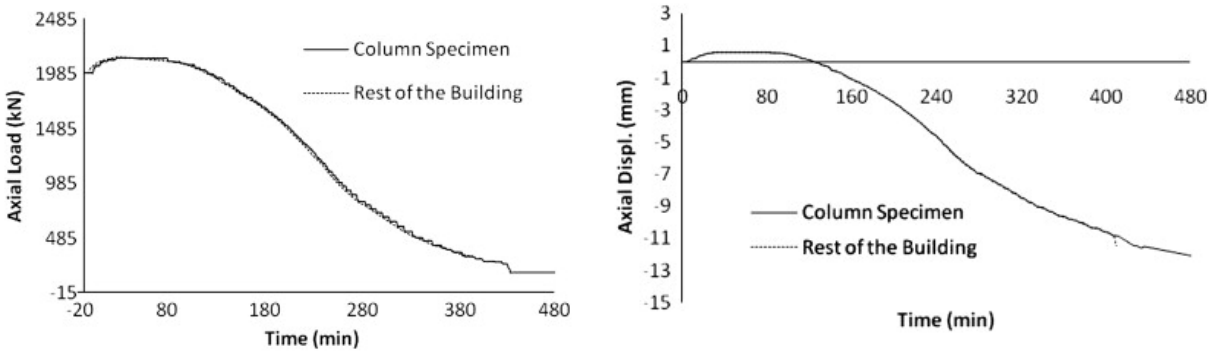


**Figure 2-10. Axial load versus the axial displacement during the hybrid fire tests presented by Mostafaei (excerpt from Mostafaei [66])**

Moreover, a comparison between the hybrid fire tests and a standard test is presented. The results show that the fire resistance determined by means of HFT is higher compared to the fire resistance of a standard test. In addition, the behavior of the exposed NS is presented in the same paper.

In the two examples presented by Robert and Mostafaei, the force control procedure (FCP) is considered. It means that the information received from the NS are reaction forces, and therefore these reaction forces are imposed on the PS.

Recently, i.e. 2016, the developments regarding the hybrid fire testing are addressed by other researchers as next presented.

New thermomechanical hybrid simulation method was presented by Whyte et al. in [68]. The objective of the project is to extend the mechanical hybrid simulation method of OpenFresco [69] and OpenSees [70] by introducing the temperature DoF and temperature loads. To do so, new developments of OpenFresco objects are done along with developing test execution strategy. The implementation is done at the ETH Zurich IBK Structural Testing Laboratory and the analyzed structure is a long-span girder fixed at both ends and supported at mid-span by a hanger exposed to fire (see Figure 2-11). The PS is a steel dog bone having the dimensions of the narrow portion of 75 mm long, 10 mm wide and 3.6 mm thick. A scaled version of ISO834 standard fire curve is applied and a force ramp. The presented results are

specific to explicit and implicit integration schemes. The both simulations show almost identic solutions and moreover the correct solution is reproduced as well. The simulation parameters are tuned prior the tests in order to avoid instability and to produce accurate results. More details about the optimal tuning of the parameters in this specific case are presented by White et al. in [71]. The paper presents some lessons learned while performing the test. During the calculation time the fire still affects the PS, therefore the measured force used for the calculation of new displacement will change by the time when this displacement is imposed on the PS. The continuous effect of fire induced instability during the process. Reflections are presented about how the chosen time step, the PS and the furnace can influence this effect. Nevertheless, the mentioned lessons show how important is the continuous effect of fire during the hybrid fire tests and underline the specificity compared with the other hybrid tests applied for different field.

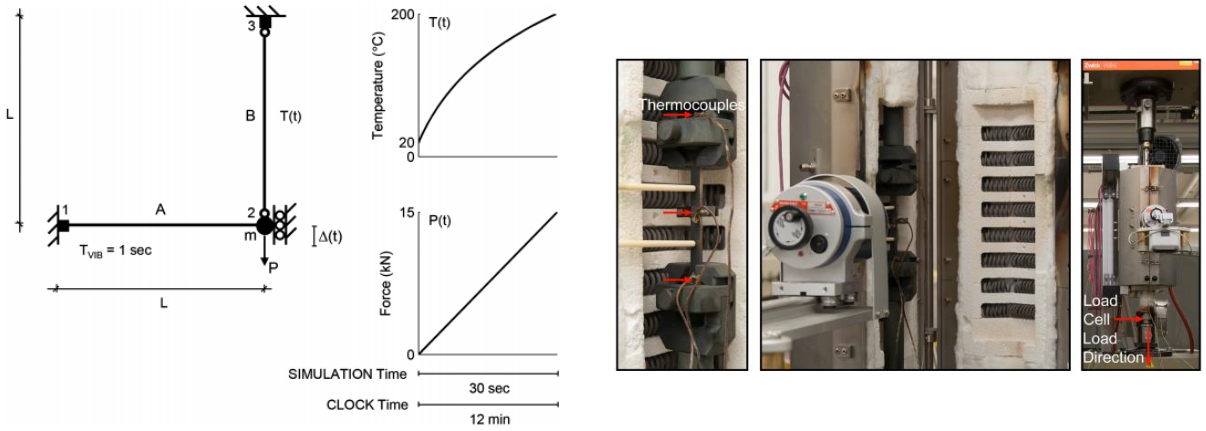


**Figure 2-11. Hybrid model with mechanical and thermal loading scheme. The ZWIck UTM and Konn Furnace (excerpt from Whyte et al. [68])**

Tondini et al. in [72] present a static partition solver for hybrid fire testing. The method is based on the FETI algorithm and is implemented for systems without floating subdomains, i.e. each subdomain is restrained with no singular matrices, and for floating domains, i.e. domains which experience rigid body motion. The validation of the method is done in a numerical environment considering a moment-resisting steel frame (see Figure 2-12). The robustness of the method is discussed, after the typical sources of errors i.e. noise and delay, are considered in the analysis. A displacement control procedure is implemented. The evolution of axial force in the PS along with the evolution of the axial displacements is presented. The results prove that the developed method ensures the compatibility and equilibrium at the interface, handles nonlinearities and is robust with respect to the possible sources of errors.

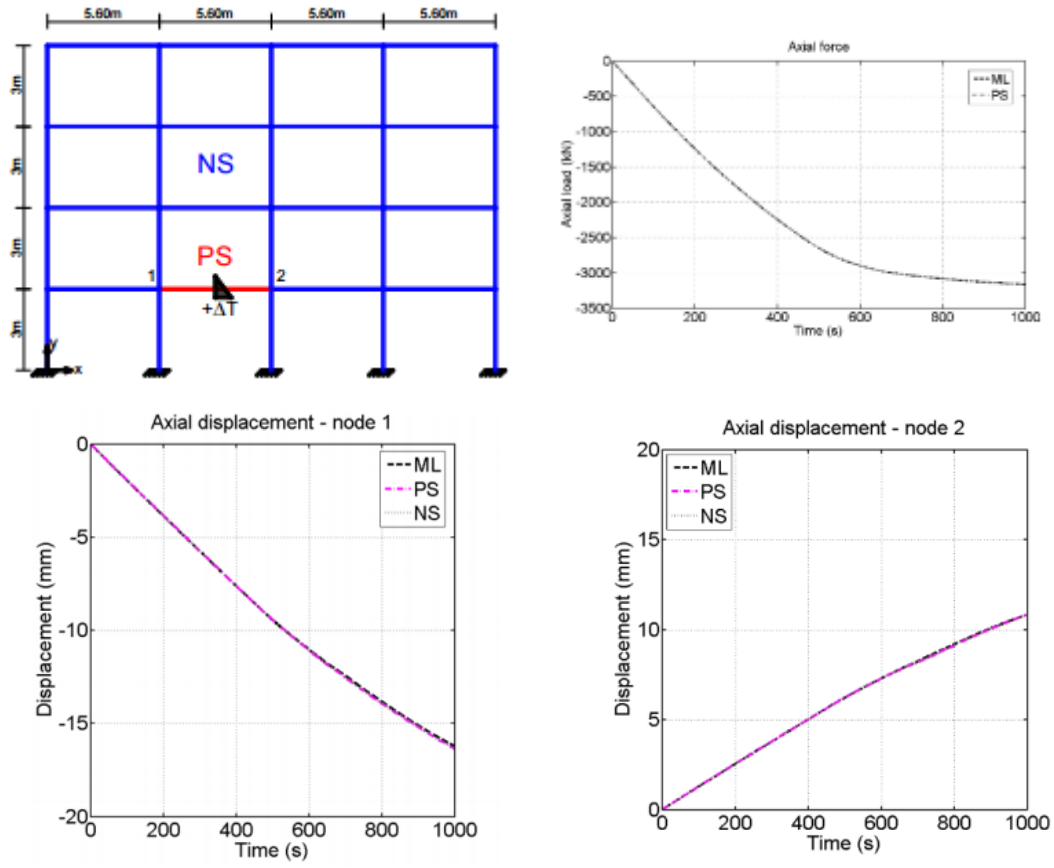


**Figure 2-12. Case study when FETI method is numerically applied (excerpt from Tondini et al. [72])**

Schulthess et al. in [73] present a case study of coupled thermomechanical hybrid simulation. The analyzed system consists of a static system of a simply supported beam that is connected to a truss element at mid-span (see Figure 2-13). The beam remains at ambient temperature throughout the full simulation while the truss element is additionally exposed to thermal loads. The truss element represents the steel coupon specimen that is mounted into the universal testing machine (UTM) inside the electric furnace. The objective is to compare the results of the pure physical test i.e. the PS and NS tested experimentally, with the one of the hybrid simulation. The first step was to conduct the hybrid test. Thus the NS is implemented in ABAQUS [74] and involves the entire structure of the benchmark problem (the beam and the truss element). The target displacements are sent to the PS while the restoring forces and measured displacements are registered and transferred to the FE model. Thus the stiffness of the PS i.e. the truss element, is updated every time step. The testing procedure is presented along with the analysis of the results in [73].

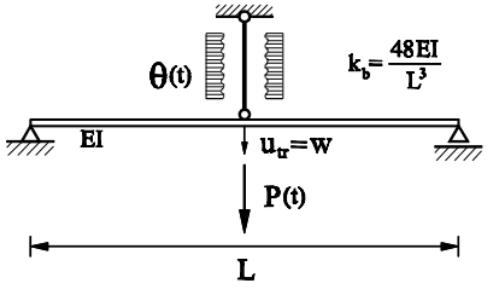


**Figure 2-13. Benchmark test for combined thermo-mechanical consolidated fire testing (excerpt from Schulthess et al. [73])**

The new developed research related to hybrid fire testing is validated either in numerical environment (Tondini et al. in [72]) or in an experimental approach (Whyte et al. in [68], Schulthess et al. in [73]). The mentioned experiments are performed on small scale structural elements. Nevertheless, the performed research helps understanding the hybrid fire testing and offers important information for the future developments.

The only hybrid fire tests performed on real size elements remain the tests reported by Korzen, Robert and Mostafaei.
The following differences are identified between the latter tests:

- The definition of the NS;
- The number of controlled DoFs;

The NS is defined as a constant matrix in the tests performed by Korzen and Robert, while the test reported by Mostafaei presents the NS modelled in the numerical software SAFIR. In the examples presented by Korzen and Mostafaei, the PS refers to a column therefore only one DoF is controlled at the interface, i.e. the axial DoF. The PS in the case of Robert is a concrete slab where three DoFs are controlled during the test.
The method to perform hybrid fire testing is similar in all the cases meaning that every time step of the calculations the reaction force of the NS is computed based on the measured displacements in the furnace. The computed reaction of the NS is next transferred to the PS with the objective to be generated in the PS.

## 2.8. Summary

Hybrid simulation is an attractive method to be applied in fire field, where the advantages of the individual testing method and full scale testing are combined. Only single structural elements are experimentally tested, but at the same time the global behavior of the building is considered by interacting during the tests with the modelled aside surrounding (NS).
It has been shown that there are key components in performing hybrid simulations; the physical specimen that is tested in the furnace; the surrounding modeled aside via finite element software or a predetermined matrix; a data-acquisition system needed to collect the needed information from the substructures to update the target response for every time step; and a transfer system including a controller and actuators to transfer the target response to the substructures. Depending on how the NS will be modelled, the hybrid simulation method will present some particularities. At the same time the hybrid fire testing can be performed in

displacement control procedure (DCP) or force control procedure (FCP) depending on the furnace facility and the particularities of the problem. It was possible to underline some advantages when using hybrid fire testing but at the time the challenges that needs to be addressed. Next a comparison between the hybrid simulation methods in seismic field versus fire field has been discussed just to highlight the fact that no straightforward application from seismic field is possible. Moreover, the numerical or experimental errors have been pointed out with the specification that more research needs to be performed in the field. A short presentation of the previous hybrid fire tests has been done along with the history of hybrid simulation in seismic field.

# 3. CHARACTERISTICS OF THE HYBRID FIRE TESTING

## 3.1. Introduction

The main advantage of hybrid fire testing is the capacity to reproduce the global behavior of the studied structure by testing individual structural elements.

To be able to do so, there are some particularities to be addressed and some of them are discussed in this chapter. The necessity to provide proper supports conditions during testing and how to deal with the transformation from global to local degrees of freedom (and vice versa) will be presented. The possibilities to model the NS during the hybrid fire tests will be analyzed along with the selection of the time step. In order to provide accurate results during the hybrid fire testing the errors must be minimized. The source of errors and the influence on the results are topics presented at the end of this chapter.

## 3.2. The supports of the PS and NS

The success of hybrid fire tests is influenced by the support conditions provided in the furnace during the test. The choice of the support conditions could lead to additional calculations in the hybrid process. Some conditions must be respected when selecting the supports conditions and more details will be presented in this chapter.
The boundary conditions of the PS during the hybrid test include the *supports* and the *interface conditions*. The NS's boundary conditions refer to the *supports* and the *interface conditions*. During the hybrid simulation only the *interface boundary conditions* will be updated depending on the properties of the PS and NS.
Figure 3-1 presents the supports and the interface conditions for a single span 2D frame. The left hand column represents the PS while the beam and the right hand column form the NS. Three degrees-of-freedom are controlled at the interface between the PS and NS i.e. the horizontal degree-of-freedom $D_x$, the vertical degree-of-freedom $D_y$ and the rotational degree-of-freedom $D_z$. The supports provided for the PS and NS are sufficient to avoid the rigid body motion during the hybrid fire test.

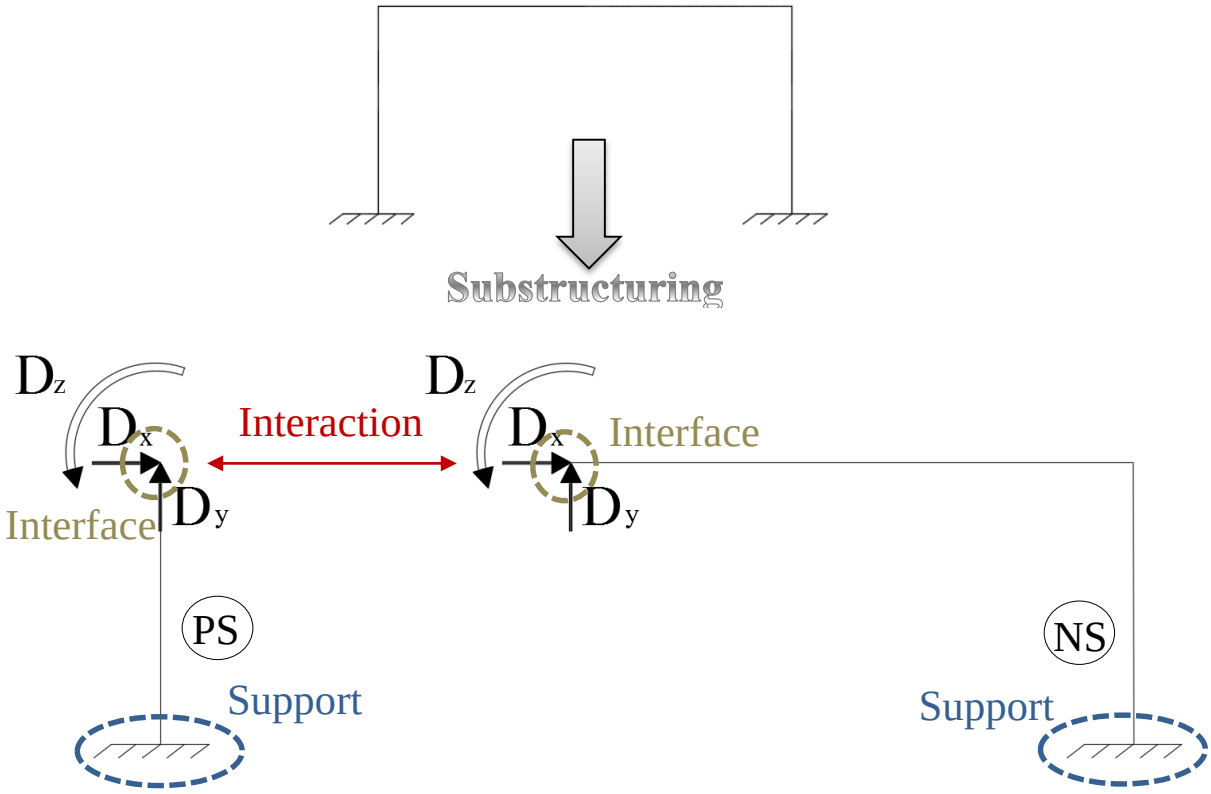


**Figure 3-1. Supports and boundary conditions in hybrid fire testing**

To avoid the rigid body motion during the hybrid fire test, proper number of support conditions during the tests must be ensured. Depending on the analyzed PS and NS, different solutions can be adopted during the hybrid fire test.

Some different situations which can be encountered will be next discussed.

Each rigid body situated in one plane has three degrees of freedom – three independent parameters determining its movement. By using support links, we limit this rigid body movement possibility. The structure with three links is called a determinate structure. If this body has less than three links then some movement will be possible. Such a body is called a mechanism. If we put more than three support links on the body then it is an indeterminate structure.

As a notation $N_{NS}$ represent the number of support links for the numerical substructure, and $N_{PS}$ the number of support links for the physical substructure. The number of degrees-of-freedom controlled at the interface is noted as $N_{Int}$.

In practice different cases can be encountered where the number of supports for the PS and NS will be sufficient to avoid the rigid body motion or not.

Here are some situations which can occur:

- The number of the link supports for the PS and NS is sufficient to avoid mechanism

$$N_{PS} \geq 3$$
$$N_{NS} \geq 3$$

- The number of the link supports for the PS and NS is insufficient

$$N_{PS} < 3$$
$$N_{NS} < 3$$

- The number of link supports is insufficient for the PS but sufficient for the NS

$$N_{PS} < 3$$
$$N_{NS} \geq 3$$

- The number of link supports is sufficient for the PS but insufficient for the NS

$$N_{PS} \geq 3$$
$$N_{NS} < 3$$

Next some examples will be presented for a better understanding of how the number of support will influence the hybrid simulation process.

*Example 1*

*Example 1* illustrate the case when the number of link supports for the PS and NS is sufficient to avoid the mechanism i.e. $N_{PS} \geq 3$ and $N_{NS} \geq 3$.

A moment resisting frame with fixed supports is presented. Following the substructuring procedure, the PS is represented by a one span frame while the rest of the structure will be modelled aside and considered the NS.

The supports of the PS and NS are presented and underlined in Figure 3-2. The number of supports for the PS and NS is equal to six ($N_{PS} = N_{NS} = 6$).

The number of degree-of-freedom to be controlled at the interface is equal to six ($N_{Int} = 6$). Thus the controlled degrees-of-freedom are as follows:

- The axial DoFs: $D_1$ and $D_4$
- The vertical DoFs: $D_2$ and $D_5$
- The rotational DoFs: $D_3$ and $D_6$

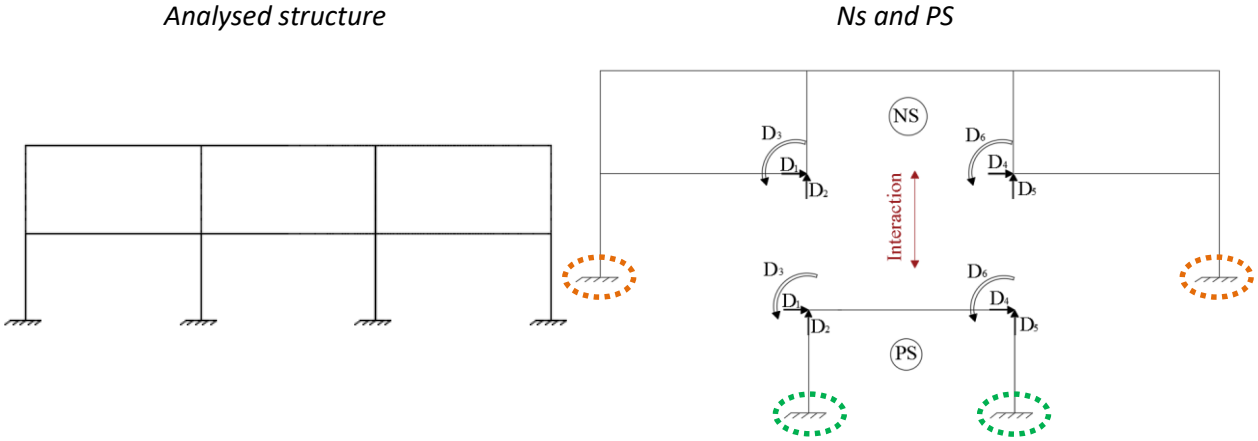


**Figure 3-2. Analyzed structure versus substructures. Sufficient number of link supports**

*Example 2*

*Example 2* illustrates the case when the number of link supports for the PS and NS is under the minimum numbered required, i.e. $N_{PS} < 3$ and $N_{NS} < 3$. The number of degrees-of-freedom controlled at the interface is equal to three i.e. $N_{Int} = 3$ (see Figure 3-3).

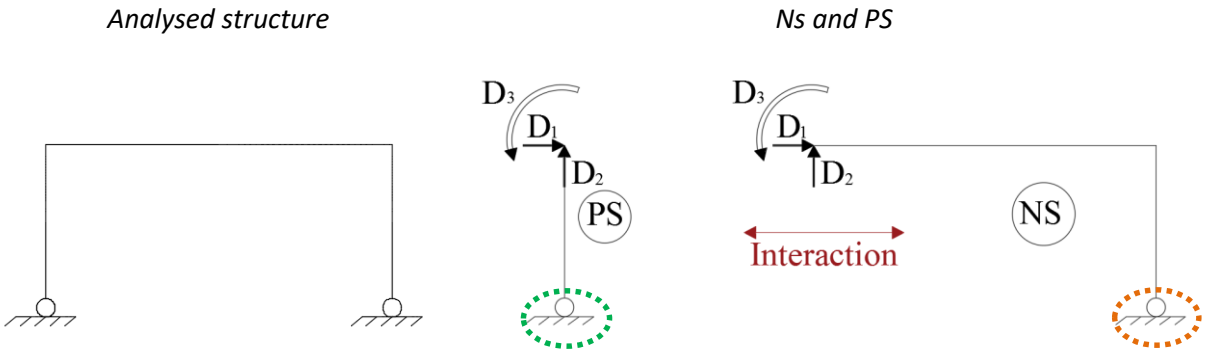


**Figure 3-3. Analyzed structure versus substructures. Insufficient link supports for the PS and NS**

*Example 3*

*Example 3* illustrates the case when the number of link supports for the PS is under the minimum numbered required $N_{PS} < 3$ whereas the NS provides the necessary number of link supports $N_{NS} \geq 3$.

The *Example 3* presents a moment resisting frame with hinged supports (see Figure 3-4).

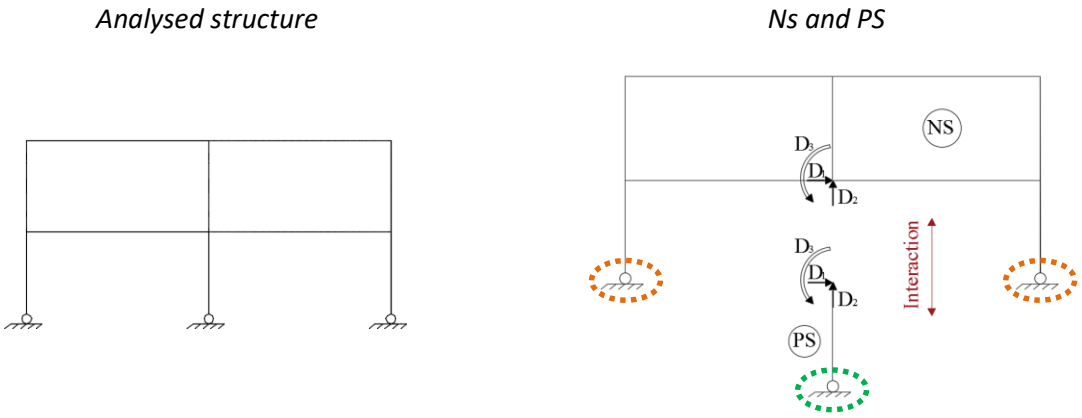


**Figure 3-4. Analyzed structure versus substructures. Insufficient number of link supports for the PS**

During the hybrid simulation process the PS is represented by the central column hinged at the bottom. Three DoFs need to be controlled during the hybrid test $N_{Int} = 3$, the horizontal DoF noted here as $F_1$, the vertical DoF noted $F_2$, and the rotational DoF referred to as $M_1$.

The number of link supports of the PS ($N_{PS} = 2$) does not satisfy the condition to avoid the mechanism. The number of link supports for the NS is enough to constitute a determined structure ($N_{NS} = 4$).

*Example 4*

*Example 4* illustrates the case when the number of link supports for the NS is under the minimum numbered required $N_{NS} < 3$ whereas the PS provides the necessary number of link supports $N_{PS} \geq 3$.

In Figure 3-5 a two storey frame with fixed supports is presented. The first floor frame is the PS meanwhile the upper storey represents the NS. The PS satisfies the requirement of having the minimum number of link supports, here $N_{PS} = 6$, while not the same comment can be done for the NS. No supports are present for the NS ($N_{NS} = 0$) only the interface boundary conditions which will be controlled during the hybrid simulation. The number of degrees-of-freedom controlled at the interface is equal to six i.e. $N_{Int} = 6$.

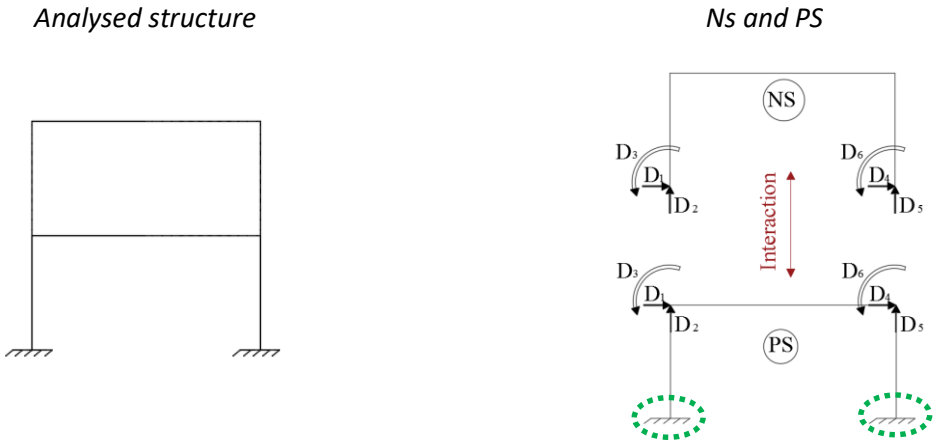


**Figure 3-5. Analyzed structure versus substructures. Insufficient link supports for the NS**

The above presented examples offer a better understanding of the different situations which may occur when performing hybrid fire testing. The PS and NS may have the sufficient number of link support or not. If the number of link supports is not sufficient then the substructures experience the rigid body motion.

To avoid the rigid body motion and to provide accurate results during the during the real hybrid fire test, the requested number of the link supports is recommended to be at least 3 for a 2D problem. Thus, it is recommended that the PS should be properly supported in the furnace to avoid the introduction of some measurements errors which may lead to instability or wrong results.

Depending on the stiffness of the PS, small variation of displacement can induce a big variation of force for one time step. Every small error in the measurement of displacements induces important variation of forces which can exceed the limit force early in the hybrid test. Therefore, a proper data-acquisition system is needed for hybrid fire tests to be able to measure appropriate displacements and rotations. Moreover, beside the capabilities of the data

acquisition system, it has been observed that in the case when controlling multiple DoFs, every actuator has an influence on the response of the other actuators. On top of what was just mentioned, imagine that some rigid body motion is registered. In this situation the measured displacement can induce forces which exceed the limit forces and the specimen can be destroyed.

If no link supports are provided, then every small error which appears during the test can lead to poor results or even to instability. The importance of providing proper link supports during the hybrid test has been observed when performing the hybrid fire test described later in this thesis.

Example 1 shows that the number of support links for the PS and for the NS is sufficient to build determined structures. So in this situation no mechanism is encountered. The PS can be tested in the furnace without additional transformations.

Example 2 presents the case when the number of the support links is insufficient for the PS and NS. In this case for the PS the needed number of sufficient links is provided in the furnace and controlling the local degrees-of-freedom at the interface.

Example 3 presents the case when the number of the support links for the PS is insufficient to build a determined structure. The solution to perform hybrid simulation in this examples is first to provide the necessary link supports in the furnace. Once the sufficient number of link supports is provided then the number of degrees-of-freedom controlled at the interface will be modified. Therefore, from a global number of DoFs at the interface (when substructuring is done) only the local number of DoFs will be controlled in the furnace (due to the fact that additional link supports have been introduced). This will imply some additional calculations during the hybrid simulation which are presented in the next chapter.

Example 4 presents the case when the number of link supports of the PS is sufficient, but not for the NS. This can also present a problem during the hybrid test, especially if the NS is modeled using a numerical nonlinear software and the needed calculations are made during the hybrid test. Some instability may occur during the calculations. A methodology which can treat the floating system should be adopted in hybrid simulation to avoid the instability. By floating system we understand a system with insufficient link supports.

## 3.3. The global versus local degrees-of-freedom

The necessary link supports should be provided for the experimental element in order to avoid rigid body motion. Thus, in some cases the number of degrees-of-freedom to be controlled in the furnace differs from the number of degrees-of-freedom in the numerical analysis (where the numerical substructure will be represented).
We refer to the degrees-of-freedom controlled in the furnace as the local degrees-of-freedom, while the degrees-of-freedom controlled in the numerical analysis as the global ones.

Figure 3-6 presents the global DoFs of the experimental element (beam) versus the local DoFss. In the global system of coordinates six degrees-of-freedom describe the interface conditions: $D_1$ and $D_4$ are the horizontal DoFs, $D_2$ and $D_5$ are the vertical DoFs while $D_3$ and

$D_6$ are rotational DoFs. By suppressing the minimum number of degrees-of-freedom to create the determinate structure in the furnace the local degrees-of-freedom are controlled during the hybrid test. $D_{1L}$ is the local axial DoF, $D_{2L}$ and $D_{3L}$ are the local rotational DoFs.

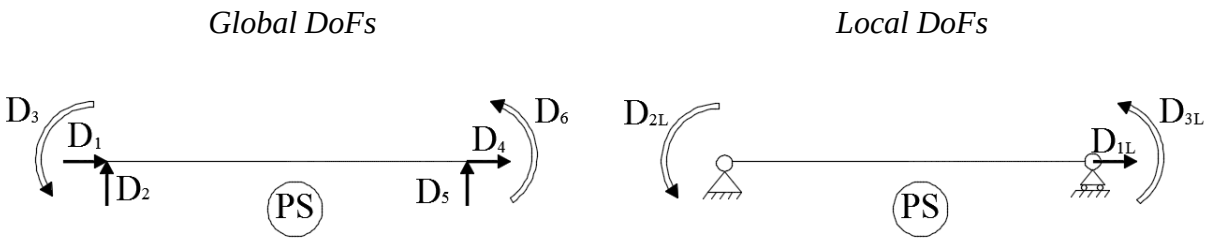


**Figure 3-6. Experimental element. Global versus local DoFs.**

During the hybrid test the global coordinate system of the NS needs to be transformed into the local system that is best suited for testing. Additionally, it needs to provide inverse transformation for the measured response quantities, from the local coordinate system back to the global coordinate system of the NS.

The transformation from the local DoFs to global DoFs (or other way around) takes into consideration the dimension of the problem 2D or 3D. In the examples presented in this chapter a 2D dimension has been considered.

Figure 3-7 presents the transformation of global DoFs to the local imposed DoFs in the furnace, for a bar. A displacement control procedure is assumed in this example meaning that the interface boundary conditions will be updated during the hybrid test by controlling the displacements in the furnace.

The update of the interface boundary conditions is done based on the properties of the PS and NS. Every time step the new displacements to be imposed in the furnace are computed in the global system of coordinated i.e. $D_1$, $D_2$, $D_3$, $D_4$, $D_5$ and $D_6$. The displacements to be imposed in the furnace (local system of coordinates) are $D_{1L}$, $D_{2L}$ and $D_{3L}$.

The transformation is done based on the Eq. **(1)**

$$D_{1L} = L_L - L$$
$$D_{2L} = \alpha - D_3 \quad (1)$$
$$D_{3L} = D_6 - \alpha$$

Where:

$L$ is the initial length of the PS (before the hybrid test starts);

$L_L$is the length of the PS in deformed configuration (this values will vary due to the thermal expansion and axial restrain) expressed by the Eq. **(2)**;

$$L_L = \sqrt{(D_5 - D_2)^2 + (L + D_4 - D_1)^2} \quad (2)$$

$\alpha$ is the rotation of the structural element from the undeformed to the deformed configuration is expressed by Eq. **(3)**;

$$\alpha = arctan\left(\frac{D_5 - D_2}{L + D_4 - D_1}\right) \quad (3)$$

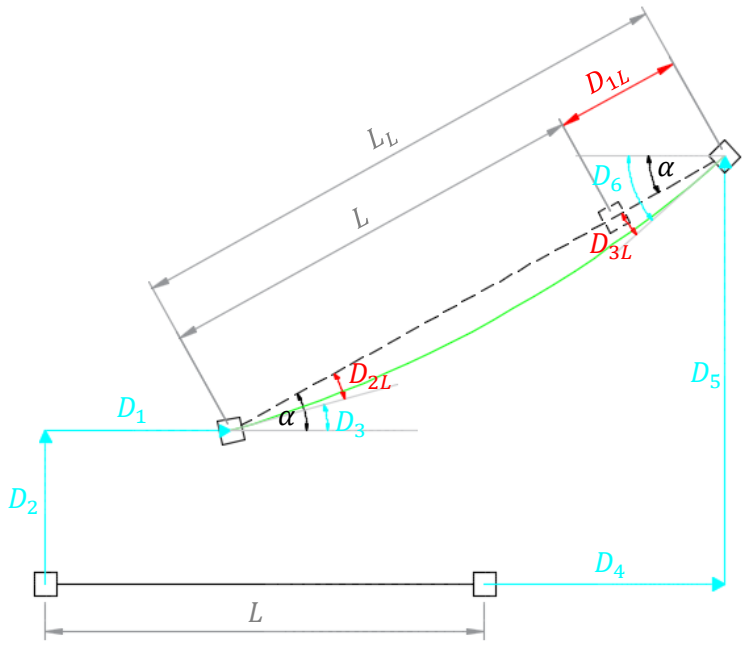


**Figure 3-7. Example of transformation of displacements from the global system of coordinates to the local system of coordinates**

After new displacements values are imposed in the furnace, reaction forces are registered and used for the update of the interface boundary conditions in the next time step.

The local reaction forces $F_{1L}$, $F_{2L}$ and $F_{3L}$ are registered and then transformed to the global reaction forces $F_1$, $F_2$, $F_3$, $F_4$, $F_5$ and $F_6$ as presented in Figure 3-8.

The transformation is described by the Eq. **(4)**.

$$\boldsymbol{F} = \boldsymbol{T}\,\boldsymbol{F_L} \quad (4)$$

The matrix $\boldsymbol{F}$ refers to the reaction forces in the global system of coordinate while the matrix $\boldsymbol{F_L}$ comprise the reaction forces registered in the furnace during the hybrid simulation thus in the local system of coordinates. The transformation is done based on the transformation matrix $\boldsymbol{T}$. The Eq (**4**) is explicitly written under the form presented by the Eq. (**5**).

$$\begin{bmatrix} F_1 \\ F_2 \\ F_3 \\ F_4 \\ F_5 \\ F_6 \end{bmatrix} = \begin{bmatrix} -\cos\alpha & -\frac{\sin\alpha}{L_L} & -\frac{\sin\alpha}{L_L} \\ -\sin\alpha & \frac{\cos\alpha}{L_L} & \frac{\cos\alpha}{L_L} \\ 0 & 1 & 0 \\ \cos\alpha & \frac{\sin\alpha}{L_L} & \frac{\sin\alpha}{L_L} \\ \sin\alpha & -\frac{\cos\alpha}{L_L} & -\frac{\cos\alpha}{L_L} \\ 0 & 0 & 1 \end{bmatrix} \begin{bmatrix} F_{1L} \\ F_{2L} \\ F_{3L} \end{bmatrix} \quad (5)$$

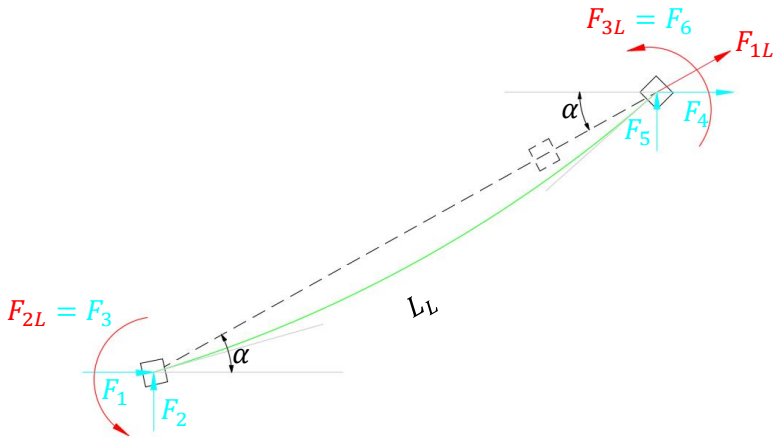


**Figure 3-8. Local reaction forces versus global reaction forces**

The local degrees-of-freedom are chosen to suit the furnace facility. In Figure 3-6 the local DoFs to be controlled are the axial displacement and the support rotations. If other configurations of the PS are more practical for the furnace facility then it will be adopted. Another theoretical solution is presented Figure 3-9 where the local DoFs to be controlled are the axial displacement $D_{1L}$ the vertical displacement $D_{2L}$ and the rotation $D_{3L}$ at one end of the beam. From the 3 local DoFs presented in Figure 3-7 some transformation can be done to get the local displacements presented in Figure 3-9 (see Schellenberg et al. in [7]).

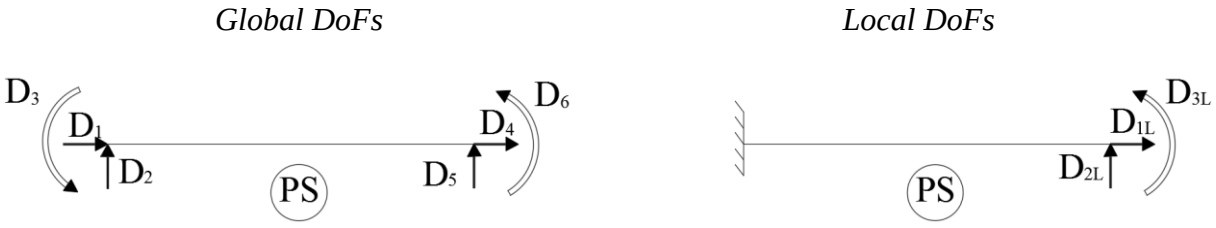


**Figure 3-9. Experimental element. Global versus local DoFs.**

One solution to make the transformation from global degrees-of-freedom to local degrees-of-freedom is presented by Mostafaei in [66], i.e. a column which is described by 6 global degrees-of-freedom at the interface controlling only 2 local degrees-of-freedom. The global degrees-of-freedom are the two axial DoFs, the two transverse DoFs, and the two rotational DoFs. The objective of Mostafaei is to control during the test only one axial DoF and one transverse DoF. The transformations that he used are suitable for a force control procedure.

In conclusion, proper supports needs to be implemented during hybrid fire testing in order to avoid the rigid body motion. Depending on the analyzed case study, the implementation of the proper support might lead to some traditional transformations between the local and global degrees-of-freedom. An example is presented when these transformations are performed in the case of a structural element characterized by 6 global DoFs and 3 local DoFs.

## 3.4. The Representation of the Numerical Substructure

While the PS is always exposed to fire, the NS can be heated or considered cold during the hybrid simulation depending on the considered fire scenario.

There are three possibilities to model the NS and these are:

- Finite element model;
- Predetermined matrix;
- Combination of the FE method and the predetermined matrix method;

*Finite element (FE) model*

When the NS is exposed to fire then only the FE model can be considered for the representation. The FE model should be capable of handling the heat transfer and to consider the large displacements which are characteristic to fire analysis.

The use of FE model in the hybrid simulation offers some advantages and drawbacks as well.

The main *advantage* of FE representation is the possibility of heating structural elements of the NS partially or heating all the structural components of the NS.

Hybrid fire testing is possible only in real time. The main reason of real time hybrid testing is the existence of the thermal gradient even if the burners are turned off in the furnace. The real time hybrid testing will request a fast calculation process of updating the interface boundary conditions. Therefore, the FE model should be able to perform every time step analysis in proper time.

The time needed to perform the analysis of the numerical substructure using the FE model is not neglected and it will be noted as $\Delta t_N$. More details about the time scale in hybrid fire testing will be presented in the section 3.5. Nevertheless the calculation time $\Delta t_N$ should not exceed some limit for proper results. If the time calculation is too big then the equilibrium at the interface will not be satisfied anymore. Moreover the errors from every time step will cumulate in time leading to incorrect results. The time calculation depends on the type of modelled structure.

During the hybrid fire test some specific phenomenon occurs such as, for example, spalling when concrete structures are exposed to fire. Spalling can occur in a short time and moreover during the calculation time $\Delta t_N$. The update of interface boundary conditions is done based on the previous existing boundary conditions. If the spalling occurs in the calculation time, then the solution applied on the PS does not correspond to the state of the boundary conditions used in the calculations. In this case the equilibrium/compatibility will not be satisfied and instability can be induced in the process.

When the NS is modelled in the FE software, the transformation from local to global system of coordinated and other way around (see section 3.3) is done in real time.

In conclusion, the main *advantage* of using a FE model to represent the NS is the possibility to consider the NS exposed to fire while the main *drawback* is the time needed to perform the calculations which have an effect on the results.

*Predetermined matrix*

Another solution to represent the NS is to use a predetermined matrix. By predetermined matrix we refer to the stiffness of the NS in some precise conditions.

The stiffness matrix of the interface DoFs is computed using displacement method. The displacement method implies to impose an increasing displacement in the direction of one interface DoF while the remaining interface DoFs are blocked. The nodes which do not constitute the interface are free to move. The NS is unloaded while performing the calculations of the stiffness matrix. The terms of the interface stiffness matrix result by dividing the reaction forces of every interface DoF by the imposed displacement. The stiffness calculated on the structure without load is an initial stiffness.

The predetermined matrix is determined using the same procedure as for the interface stiffness matrix. The only difference is that in this situation the NS is loaded with the exterior forces and the interface conditions. Before performing the hybrid fire test, the building already exists and is loaded, with some possible cracks. The loading is considered in the calculation of the predetermined matrix in order to model the real conditions of the structure. The stiffness calculated on the loaded structure is a tangent stiffness.

An example of how to establish the predetermined matrix will be presented in the section 6.2.2.

The *drawback* of using the predetermined matrix is that only the cold surroundings can be represented. If the NS is exposed to fire (no matter the fire scenario) then the matrix would be temperature dependent. The temperature dependency cannot be predetermined by using the matrix.

Even the nonlinear behavior of the cold NS can be captured by the predetermined matrix. Figure 3-10 presents the force displacement ($F-u$) curve which describes the nonlinear behavior of the NS. The curve can be approximated by linear segments for specific intervals of displacements. Every segment is characterized by a tangent stiffness matrix.

In the interval displacements of ($u_0$ , $u_1$] the behavior of the NS is described by the tangent stiffness $k_{0-1}$. Next, for the interval displacements of ($u_1$ , $u_2$] the tangent stiffness $k_{1-2}$ is considered while for the interval ($u_2$ , $u_3$] the tangent stiffness $k_{2-3}$ characterizes the behavior of the NS. Even the unloading of the NS can be accounted for by using the method of predetermined matrix as it can be seen in the Figure 3-10 where the tangent stiffness $k_{3-4}$ is specific for the interface displacements included in the interval ($u_3$ , $u_4$].

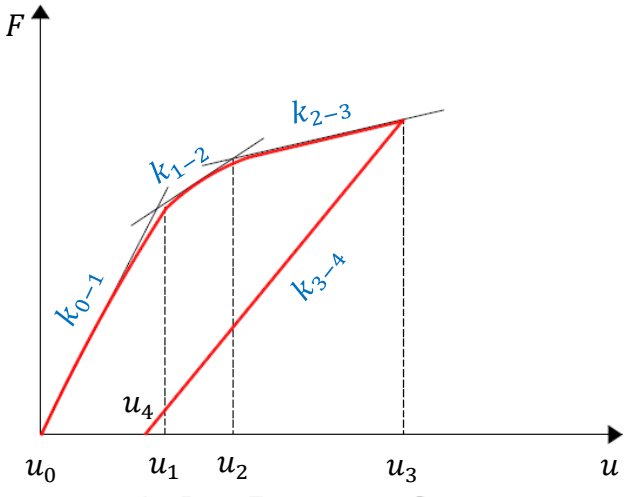


**Figure 3-10. The linearization of the nonlinear behavior**

The reaction forces $F_n$ of the NS when the predetermined matrix is used can be calculated using Eq. **(6)** where $K_N$ is the stiffness of the NS, $u_n$ is the displacement at the interface and $C$ is the constant at the interface.

$$F_n = K_N\, u_n + C \tag{6}$$

Depending on the values of the displacements, the stiffness $K_N$ of the NS and the constant values $C$ will adapt during the test as follows:

- If $u_0 < u_n < u_1$then the reaction force $F_n = k_{0-1}u_n + C_{0-1}$
- If $u_1 < u_n < u_2$then the reaction force $F_n = k_{1-2}u_n + C_{1-2}$
- If $u_2 < u_n < u_3$then the reaction force $F_n = k_{2-3}u_n + C_{2-3}$
- If $u_3 < u_n < u_4$then the reaction force $F_n = k_{3-4}u_n + C_{3-4}$

Two out of three former hybrid tests made use of a matrix to describe the behavior of the NS.

During the test performed by Korzen [57]-[60] the axial stiffness of the NS is considered in the calculations and remains constant during the entire test.
Robert in [62]-[64] present the hybrid fire test performed on a concrete slab where three DoFs have been controlled at the interface increasing the complexity of the problem. In this case the predetermined matrix describes the elastic behavior of the NS at the interface. Nevertheless the software which controls the hybrid simulation was developed to be able to account for the nonlinear behavior of the NS when required.
The hybrid fire test performed by Mostafaei [65]-[66] is the only case when the NS was represented in the nonlinear FE software SAFIR and parts of the NS are exposed to fire.

If a predetermined matrix is considered to model the NS instead of the FE method, then the time needed to perform the calculation is virtually equal to zero: $\Delta t_N = 0$.

Representing the NS by using the predetermined matrix can be advantageous (only if the NS is cold) in the situations when the size of the time step is crucial for a good quality of the results.

*Combination of the FE method and the predetermined matrix method*

The combination of both methods to represent the NS, i.e. predetermined matrix or FE model, can be considered during the hybrid fire test.

This would be justified in the cases where parts of the NS are exposed to fire but large calculation time of the NS is needed and the interface equilibrium and compatibility are not satisfied. Therefore, in order to reduce the size of the time step, the time calculation of the NS needs to be reduced. This can be fulfilled if only the exposed part of the numerical substructure is modeled via FE software, while the rest of the NS can be represented by a predetermined matrix.

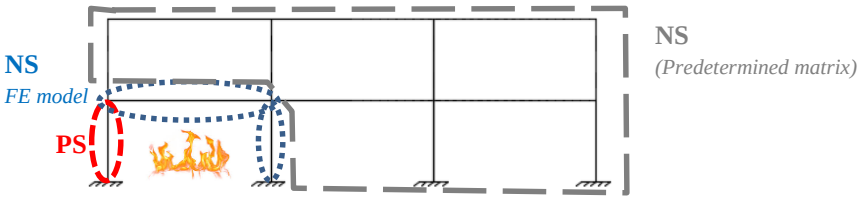


**Figure 3-11. FE model and the predetermined matrix used to represent the NS**

Figure 3-11 presents the main components of the substructuring when the fire compartment is located in the first span of the main floor. The exposed compartment is composed of the external column which will be tested in the furnace, thus the PS, while the rest of the fire compartment must be represented in FE software able to solve the heat transfer.

The subdividing of the NS will lead to a reduction of the time step when needed and implicitly to more accurate results where equilibrium and compatibility at the interface of the PS and NS are satisfied.

## 3.5. Time scale definition

The boundary conditions of the hybrid fire test need to be updated during the test accounting for the behavior of the PS (the tested element) and the NS (the surrounding building) in different moments of the process. In between the updates, i.e. during one time step, the boundary conditions are constant.

During one time step of hybrid simulation multiple action take place in order to induce new boundary conditions for the substructures. This actions comprise (i) the read of the current conditions (reaction forces and displacements at the interface) of the PS and NS; (ii) the registered data are transferred to the software where the new boundary conditions are computed (iii) the calculation of the new boundary conditions (iv) the transfer of the new boundary conditions to the substructures and (v) the new boundary conditions are induced in the substructure.

Let us note:

$\Delta t$ – The time step of the hybrid simulation characterized as a fixed value chosen before the test by the person in charge of the test.

$\Delta t_{PN}$ – The time to transfer the information to the numerical system. With modern electronic data logger, we will assume that $\Delta t_{PN} \cong 0$;

$\Delta t_N$ – The time needed for the numerical system to calculate the requested reactions. With a finite element model (nonlinear numerical software such as ANSYS, SAFIR), $\Delta t_N$ might not be negligible. If the NS is represented by a predetermined matrix (CERIB method) then $\Delta t_N \cong 0$;

$\Delta t_{NP}$ - The time to transfer the information from the numerical to the physical system and it is a negligible value $\Delta t_{NP} \cong 0$ ;

$\Delta t_P$ - The time needed by the transfer system to induce the new boundary conditions in the physical specimen (limited by the power of the hydraulic pump, necessity to avoid dynamic oscillations), $\Delta t_P$ is not negligible.

The time step $\Delta t$ should comprise the time needed for every action required to compute the new boundary conditions (see Eq. (7)).

$$\Delta t > \Delta t_{PN} + \Delta t_N + \Delta t_{NP} + \Delta t_P \tag{7}$$

As the time $\Delta t_{PN}$ and $\Delta t_{NP}$ are considered equal to zero the time step $\Delta t$ should be chosen based on Eq. **(8)**.

$$\Delta t > \Delta t_N + \Delta t_P \tag{8}$$

If the NS is represented by a predetermined matrix then the time step $\Delta t$ is made based on Eq. **(9)**.

$$\Delta t > \Delta t_P \tag{9}$$

Figure 3-12 presents the division of the time during the hybrid fire test

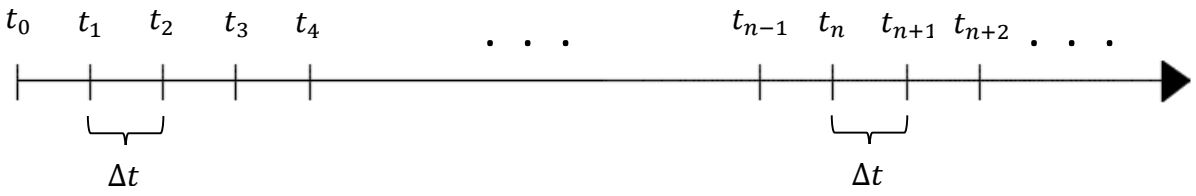


**Figure 3-12. Time scale for hybrid fire testing**

## 3.6. Influence of the errors in the results

A brief list of the errors has been mentioned in the Section 2.5.
The first objective of the hybrid fire testing is to establish a stable methodology to be used during the test.
Different factors can lead to incorrect results or they can even lead to instability of the process. The most important factors that influence the results and to be investigated next are presented here below:

- The methodology used to compute the new boundary conditions at the interface.
- The time step $\Delta t$ when the boundary conditions will be updated.
- Data acquisition system and transfer system.

*The methodology*

The static equation (see Eq. (10)) needs to be solved every time step to compute the new boundary conditions.

$$\boldsymbol{F} = \boldsymbol{K}\,\mathbf{u} \tag{10}$$

Where:

$\boldsymbol{F}$ is the force vector at the interface;

$\boldsymbol{K}$ is the stiffness of the assembly (the entire structure);

$\mathbf{u}$ is the displacement vector at the interface;

The stiffness of the analyzed structure is composed of the PS's stiffness $\boldsymbol{K_P}$ and NS's stiffness $\boldsymbol{K_N}$ as presented in the Eq. (11).

$$\boldsymbol{K} = \boldsymbol{K_P} + \boldsymbol{K_N} \tag{11}$$

The stiffness $\boldsymbol{K}$ used in the calculation process has an influence on the stability.

It will be shown that the stability when using the methodology of the previous hybrid fire test is not always ensured. The reason of instability comes from the value of the stiffness matrix used to solve the static equation. Only the stiffness of the NS is considered while the stiffness

of the PS is neglected (See Eq. (12)). Even if only the stiffness of the NS is considered in the calculation, the methodology can be successfully applied for specific cases, depending on the stiffness ratio between the substructures. In the situations when it can be applied, the error induced by neglecting the stiffness of the PS in the calculation is negligible. This subject will be discussed more in details in the chapter 4.

$$\boldsymbol{K} = \boldsymbol{K_N} \tag{12}$$

To overcome the drawback of the first generation method and to implement a stable methodology, a new method will be presented. The solution to avoid the instability caused by the first generation method is to include in the calculation the stiffness of the PS (see Eq. (13)).

$$\boldsymbol{K} = \boldsymbol{K_P^*} + \boldsymbol{K_N} \tag{13}$$

When exposed to fire the stiffness of the PS decreases in time. The decrease can be significant and will be amply if the fire specific phenomenon occurs, such as spalling for concrete structural elements. The measurement of the PS's stiffness during the test is not a common practice because it is very difficult to get accurate and reliable results based on the experimental measurements at the controlled degrees of freedom. Only few algorithms for estimating the tangent stiffness matrix based on the experimental measurements have been developed so far. One of these algorithms was presented by Bonelli and Bursi in [75]. The application and the benefits of updating the stiffness matrix during the test have not been demonstrated yet. A constant value of the stiffness matrix $\boldsymbol{K_P^*}$ will be used in the calculation, but this will imply some other decisions. The new method will be discussed in Chapter 5 where the principles and the recommendations will be presented.

*The time step* $\Delta t$

Section 3.5 presents the condition to select the minimum time step value.

The importance of the time step on the accuracy of the results will be next discussed. Improper value of the time step can lead to loss of equilibrium and compatibility at the interface. The solutions measured at the interface of the PS should coincide with the solution measured on the interface of the NS.

Since in hybrid fire testing the fire exposure is continuous, there will always be a difference between the solution registered at the interface of the PS and the one of the NS.

Figure 3-13 presents schematically the maximum value of error $\boldsymbol{\varepsilon_a}$which can be accepted in order to get accurate results. The difference between the measured solution of the PS and the calculated solution of the NS should not exceed the value of $\boldsymbol{\varepsilon_a}$.

It will be next explained why the equilibrium and compatibility cannot be ensured if an improper time step is chosen.
One of the most important factors which influence the choice of the time step is the constant stiffness matrix of the PS used in Eq. (13). The real stiffness of the PS will degrade during the

test while the estimated stiffness matrix used in the calculation process is constant. The difference between these values can be significant. The iterative process is implemented in order to converge to the correct solution, since a constant value of the PS's stiffness is considered in the calculations. During the iteration process, the boundary condition of the PS are changing, i.e. the reaction forces vary and are not constant.

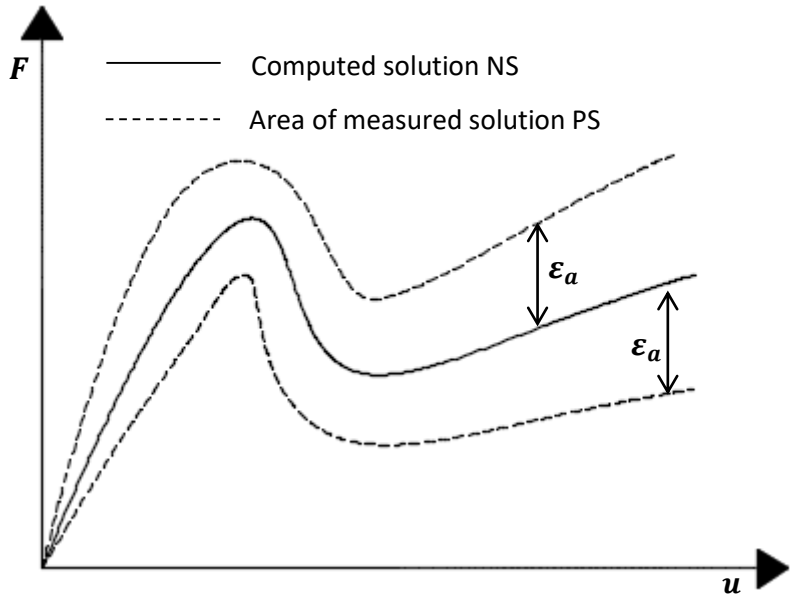


**Figure 3-13. The accuracy in hybrid simulation**

Hybrid fire test can be performed only in real time. Once the burners are on, the fire cannot be stopped. For example, if the PS is a concrete structural element, the thermal gradient still exists and advances in the section even if the burners are turned off. The continuous exposure makes the iteration process specific to hybrid fire testing and it will be next explained.

Figure 3-14 presents the reaction forces versus the imposed displacements of the PS for different time steps.

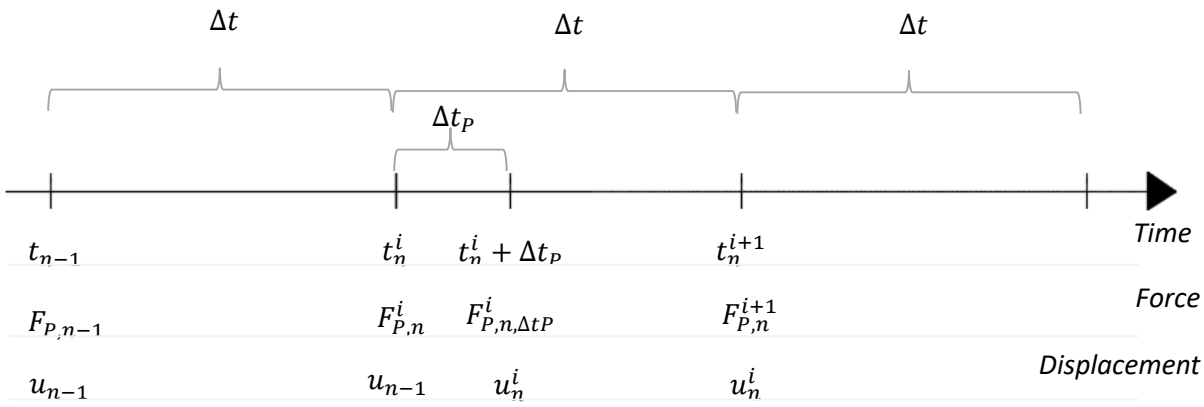


**Figure 3-14. Reaction forces versus displacements of the PS for different time steps**

For the time step $t_{n-1}$ the reaction force of the physical substructure $F_{P,n-1}$ is in equilibrium with the reaction force of the numerical substructure when the displacement $u_{n-1}$ is imposed on the substructure's interface. The next update of the boundary conditions will be done at the time $t_n^i = t_{n-1} + \Delta t$.

Between the time $t_{n-1}$ and $t_n^i$ the same displacements $u_{n-1}$ are imposed at the interface. The PS is heated inducing the increase of the PS's reaction force. In this moment, the reaction force of the PS is not in equilibrium with the reaction force of the NS. New displacements are computed to be imposed at the interface of the substructures in order to restore the equilibrium. The calculation of the new displacements to be imposed is done at the time $t_n^i$. The new displacements $u_n^i$ are updated in the furnace at the time $t_n^i + \Delta t_P$ and the value is computed based on the reaction force $F_{P,n}^i$ of the PS. By the time when the new displacements have been applied (considering the time delay $\Delta t_P$) the reaction force of the PS changed due to the fire exposure $F_{P,n,\Delta tP}^i \neq F_{P,n}^i$. If the delay time $\Delta t_P$ is negligible then it can be considered that $F_{P,n,\Delta tP}^i = F_{P,n}^i$, moreover the reaction force of the physical substructure is equal with the reaction force of the numerical substructure $F_{P,n,\Delta tP}^i = F_{N,n}^i$ and the equilibrium is satisfied.

The next update of the boundary conditions is done at the time $t_n^{i+1} = t_n^i + \Delta t$ following the same procedure.

Figure 3-15 presents the iteration process specific to hybrid fire tests when the initial tangent matrix of the PS is considered in the calculations.

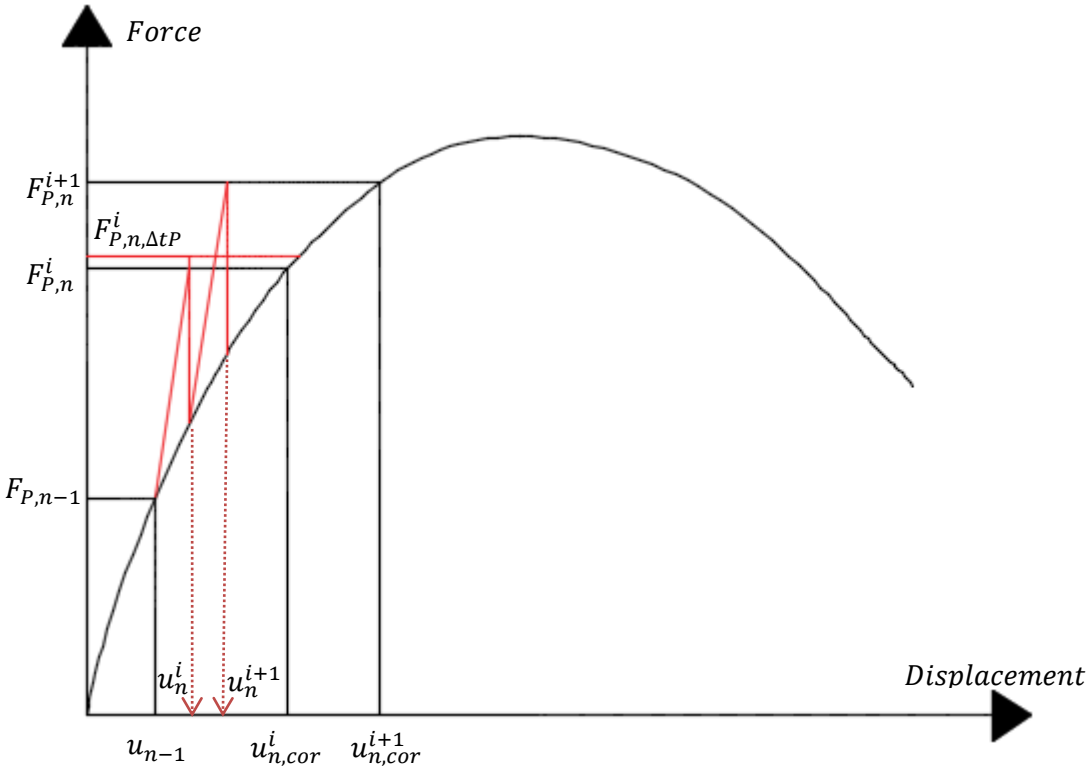


**Figure 3-15. Hybrid fire testing iteration process.**

For the time step $t_{n-1}$ the imposed displacements at the interface is $u_{n-1}$ inducing a reaction force $F_{P,n-1}$ in the furnace. The reaction force of the physical substructure is in equilibrium with the reaction force of the numerical substructure.

The new displacement to be imposed on the interface $u_n^i$ is computed based on the measured reaction forces ($F_{P,n}^i$ and $F_{N,n}^i$) and the stiffness of the PS and NS. The initial tangent stiffness of the PS will lead to a displacement value which is not equal to the correct value $u_n^i \neq u_{n,cor}^i$. Once the displacement is imposed in the furnace, the reaction forces of the PS, i.e $F_{P,n,\Delta tP}^i$, differs from the reaction force of the PS, i.e. $F_{P,n}^i$, used in the computation of the $u_n^i$.

The next computed displacement at the time step $t_n^{i+1}$ is $u_n^{i+1}$ and once again differs from the correct solution $u_{n,cor}^{i+1}$. The iterative process continues in order to converge to the correct solution. During the iterative process the correct solution modifies every iteration step due to the fire exposure.

The fire effect dictates a continuous iterative process in order to keep track of the correct solution.

The deviation from the correct solution is time dependent. If the chosen time step is too large, the boundary condition imposed every time step will diverge from the correct solution as it can be seen in the Figure 3-15.

The results of the hybrid fire tests when the time step is reduced compared with that of the Figure 3-15 is presented in Figure 3-16. By reducing the time step, the error between the computed solution and the correct one will significantly reduce. Therefore, in order to produce valuable results during the hybrid fire testing the time step used in the update of the boundary conditions needs to be reduced as much as possible. The contrivance is to perform continuous iterations in order to keep track of the correct solution.

Due to the fact that there is a time needed to adapt the new boundary conditions on the PS, during which the reaction force changes, the equilibrium will be approached but never reached. The difference between the NS's reaction force and PS's reaction force should be in the range of maximum value of error $(-\boldsymbol{\varepsilon_a}; \boldsymbol{\varepsilon_a})$ as presented in Figure 3-13**.**

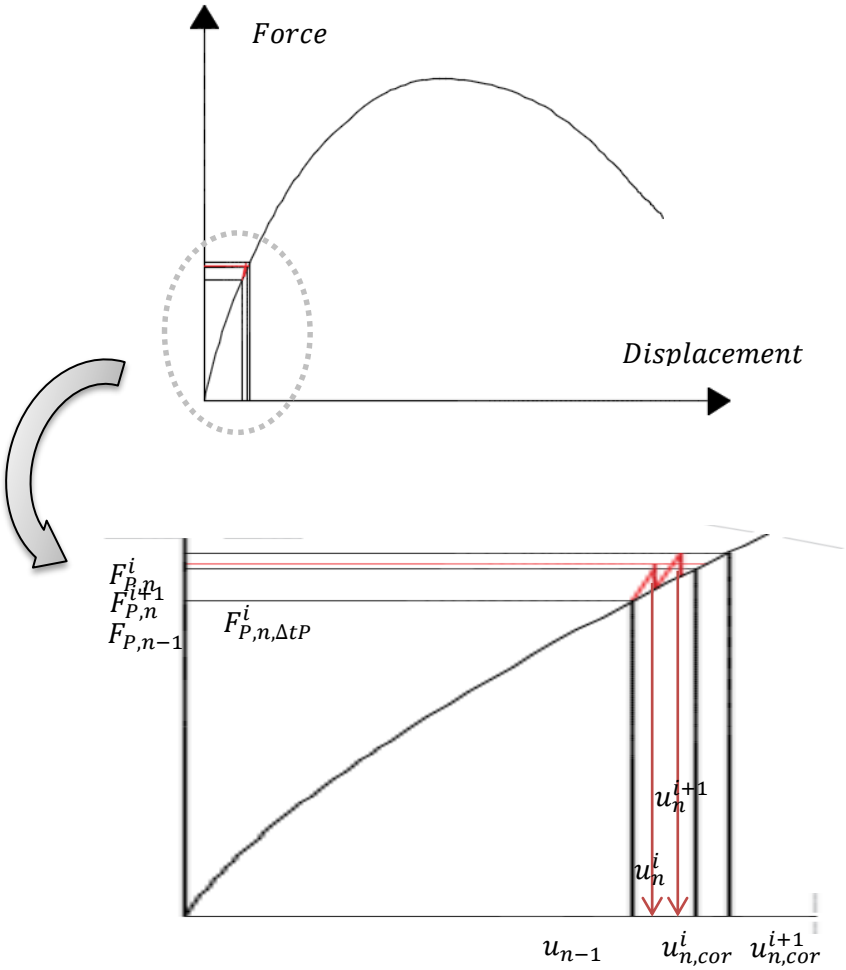


**Figure 3-16. Influence of the time step on the results in the iteration process.**

*Data acquisition system and transfer system*

Experimental errors generated by the transfer system are the most common errors affecting the results of hybrid simulation. The transfer system can be poorly tuned and not being able to impose the calculated response quantities leading to errors such as undershoots, overshoot or lag. The interaction of the transfer system with the supporting system of the PS can lead to additional systematic errors. In order to avoid the rigid body modes, the supporting system of the PS should be rigid and able to block certain specified degrees-of-freedom. The systematic errors modify the energy dissipation of the hybrid system and can lead to instability.

The data-acquisition systems along with the instrumentation devices represent a source of error. The resolution of the instrumentation, the noise generated in the instrumentation during the test and the calibration errors can produce very inaccurate or incorrect measurements leading to poor test results.

The effect of the mentioned sources of errors needs to be studied more in details in the case of hybrid fire testing.

## 3.7. Criterion for stability and accuracy

Prior the hybrid fire testing, the user is in the position to select some parameters to perform the hybrid tests in order to ensure the stability of the process and moreover to provide accurate results.

First, the proper method should be chosen if there are different methodologies available. In the section 4 and 5, two different methodologies for hybrid fire testing will be explained, i.e. first generation method and the second generation method. There is the possibility of inducing instability early in the test in some particular cases, which will be discussed in the next chapters.

Once the method is established, the next parameters are requested to be settled such as the value of the time step or the value of the PS's stiffness used in the calculation of the new boundary conditions.

Wrong selection of the values can lead to poor results such as loss of equilibrium and deviation from the correct solution.

In some specific cases, the inappropriate selection of the parameters can lead even to instability. All these situations will be analyzed in the next chapter.

The user can accept and define the value of acceptable errors in the process, depending on the objective of the project, the possibility of the experimental facility and the type of the analyzed structure.

First, there is the possibility to accept an error between the resulted solution of the PS and the one of the NS (no equilibrium and compatibility ensured). Thus the accuracy of the results is compromised but at the same time the user has the possibility to learn and understand the process especially in the implementation stage of the process.

Another possibility is to accept a defined error between the solutions resulted from the hybrid process compared with the solution resulted from the analysis of the structural system as an entity (the correct solution). The error can be defined as a percentage of the correct solutions depending on the main objectives.

## 3.8. Summary

The purpose of this chapter was to describe the characteristics of the hybrid fire testing.

A discussion based on the number of the link supports and the interface boundary conditions was done. If the number of the link supports is not sufficient in order to avoid the rigid body motion, the necessary number of the link supports will be provided during the hybrid test in the furnace. This decision implies the transformation of the global DoFs to the local DoFs (and vice versa) during the hybrid process. Some examples of transformation are presented with the mention that every furnace facility might request different transformations depending on the specificity of the facility.

Three cases were presented to be used in order to model the NS, i.e. FE model, the predetermined matrix, and the combination between the FEM and the predetermined matrix. The representation of the NS will have an impact on the selection of the time step.

The importance of selecting the appropriate value of the time step has been discussed. The continuous exposure of the PS implies a continuous iteration process, in order to follow the

correct solution. The iteration process of hybrid fire testing is discussed in details and the sources of errors are mentioned.
In the next chapter the methodology used in the former tests will be analyzed in details.

# 4. THE FIRST GENERATION METHOD

## 4.1. Introduction

Hybrid simulation method is a successfully applied technique and widely explored in different fields, for example seismic field.

In fire field mostly individual elements are tested in the furnace without considering the real boundary conditions.

In the specialized literature a number of state-of-the-art reviews on structural fire engineering testing, analysis and design can be found. For example Bisby at al. [76] present an overview of the fire resistance of concrete structures while Garlock et al. [77] present an overview of the fire behavior of steel structures.

Some laboratories, such as BAM (Germany), NRC (Canada) and CERIB (France) have the capability to carry out Hybrid Fire Testing (HFT) tailored for their purpose. The physical specimen (PS) tested at BAM and NRC was a column with one degree-of-freedom (DoF) at the interface. CERIB tested a slab by using hybrid testing technique, where the number of DoFs increased from one to three compared with the BAM and NRC tests. We will refer to the previous hybrid tests as the first generation test.

In this chapter the methodology of the first generation tests will be analyzed. We will show that, when computing the adjusted forces or displacements at the interface between the NS and the PS, only the characteristics of the NS are considered, disregarding the characteristics of the PS. A simple linear elastic system will be considered in the analysis just to simplify the understanding of the methodology. Description of the first generation method is followed by underlining the advantages and the drawbacks. Finally, recommendations are stated for users who want to implement the first generation method in their HFT.

## 4.2. Characteristics of the first generation method

### 4.2.1. Definition of the case study and nomenclature

The method considered in the former hybrid fire tests has been modelled analytically for a simple linear system with a single DoF located at the interface, which is the axial displacement at node 2 (see Figure 4-1). The temperature in the PS increases with time which induces thermal expansion but, for the sake of simplicity, the stiffness of the PS remains constant. The stiffness of the NS also remains constant during the entire duration of the test. The system is composed of two bars, the PS and the NS of length $L_P$ and $L_N$, respectively. The heated PS is defined by the axial stiffness $K_P$ and thermal coefficient of the material $\alpha$ whereas the cold NS is characterized by the axial stiffness $K_N$. In HFT the structure is

decomposed and the PS is placed in a furnace, while the NS is modelled via numerical software or characterized by a predetermined matrix.

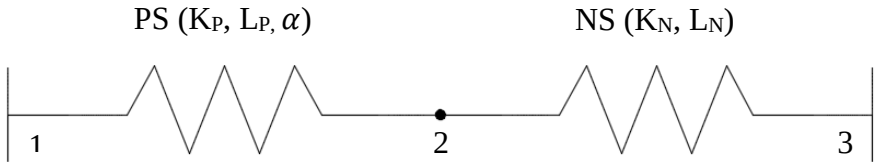


**Figure 4-1. Linear elastic system.**

The characteristics of the linear elastic system are summarized in Table 4-1.

**Table 4-1. The characteristics of the linear elastic system**

| Characteristics | PS | NS |
|---|---|---|
| **Stiffness** | $K_P$ | $K_N$ |
| **Length** | $L_P$ | $L_N$ |
| **Thermal coefficient of material** | $\alpha$ | - |

For a better understanding of the information presented in this chapter, the notations to be used in this paragraph are next described.

$\Delta t_P$ is the needed time for the calculations and for the transfer system to induce the new boundary conditions in the furnace. The time step $\Delta t$ should be selected as $\Delta t > \Delta t_P$, therefore the transfer system of the furnace facility and the calculation of the new boundary conditions influence the choice of the time step.

$n$ is the number of time steps from the beginning of the hybrid test.

$t_n$ is the time step $n$, i.e. $t_n = n\,\Delta t$.

$u_x(t_n)$ is the interface displacement of substructure $x$ (P for the PS and N for NS) at time $t_n$ (i.e. displacement of node 2 for the linear system), taken as positive when moving to the right.

$F_x(t_n)$ is the interface force of substructure $x$ (P for the PS and N for NS) at time $t_n$.

$T(t_n)$ is the temperature of the PS at time $t_n$.

For future discussion, the ratio between the stiffness of the NS and PS will be referred to as the stiffness ratio $R = \frac{K_N}{K_P}$.

### 4.2.2. The force control procedure

The first generation method using the force control procedure is applied step by step for the case study defined in the section 4.2.1:

a. First, the analysis of the entire system is performed in order to determine the forces and the displacements at the interface between the PS and NS before the fire starts.

b. The PS is placed in the furnace (in a real HFT) and loaded with the interface conditions (determined from step a.) and the external loads, while the NS is modeled aside. Herein the external loads, the interface forces and displacements are equal to zero.
c. The furnace is switched on so heating of the PS starts. In force control procedure, the PS is free to expand (i.e. it is the applied force at the interface which is controlled and it remains constant during a time step). The displacement is measured after a time step Δt. In this example, it yields to the value expressed by Eq. (14).

$$u_P(t_1) = \alpha L_P\, T(t_1) \tag{14}$$

d. The measured displacement (14) is imposed on the NS. This generates a reaction force that, in this case, can be computed analytically using Eq. (15).

$$F_N(t_1) = K_N\, \alpha\, L_P T(t_1) \tag{15}$$

e. The new reaction force is imposed on the PS (Eq. (16)). A time delay $\Delta t_P$ is used to capture the time needed to compute the reaction of the NS and to adjust the force in the jacks, as for a real HFT.

$$F_P(t_1 + \Delta t_P) = -K_N\, \alpha\, L_P T(t_1) \tag{16}$$

f. The new force induces a new displacement of the PS. Meanwhile, heating of the PS has continued and also induces variation in displacement. The updated displacement of the PS at the interface $u_P(t_2)$ is measured (given here by Eq. (17)) and imposed on the NS. This generates a new reaction force $F_N(t_2)$ given by Eq. (18).

$$u_P(t_2) = \alpha L_P\, T(t_2) + \frac{F_P(t_1 + \Delta t_P)}{K_P} = \alpha L_P \left( T(t_2) - \frac{K_N}{K_P} T(t_1) \right) \tag{17}$$

$$F_N(t_2) = K_N\, \alpha L_P \left( T(t_2) - \frac{K_N}{K_P} T(t_1) \right) \tag{18}$$

Steps *e* and *f* are repeated in order to maintain equilibrium and compatibility at the interface throughout the whole test.

Expanding Eq. (17) and (18), for $n$ time steps, the displacement can be expressed by Eq. (19), while the reaction force generated by the NS, by Eq. (20).

$$u_P(t_n) = \alpha L_P \sum_{i=0}^{n-1} \left[ (-R)^i\ T(t_{n-i}) \right] \tag{19}$$

$$F_N(t_n) = K_N\ \alpha\ L_P \sum_{i=0}^{n-1} \left[(-R)^i\ T(t_{n-i})\right] \tag{20}$$

Figure 4-2 presents one step of the hybrid fire testing when using the first generation method. To accomplish one step hybrid fire testing first the displacement $u_P$ is measured in the furnace and then imposed on the NS inducing a reaction $F_N$ which will be transferred to the PS ensuring the equilibrium and compatibility at the interface.

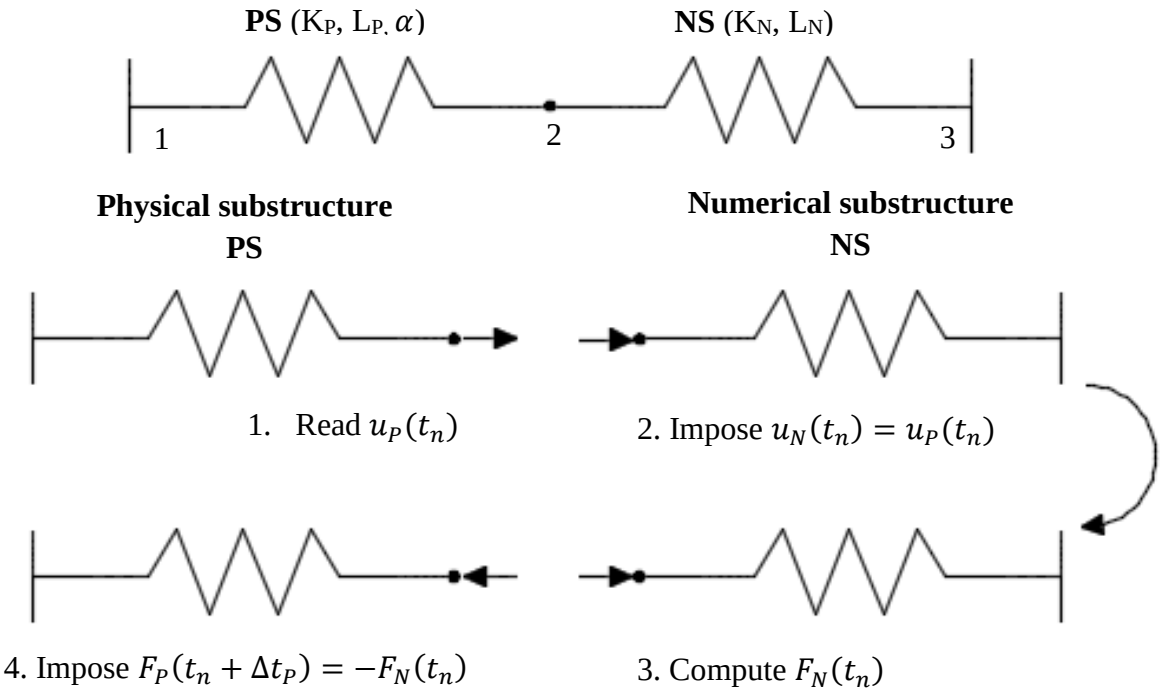


**Figure 4-2. One step of force control procedure. First generation method.**

### 4.2.3. The displacement control procedure

The same developments can be made for the displacement control procedure.

The steps *a* and *b* are the same as in the case of force control procedure. The next steps are modified as follows:

c. Heating of the PS starts. In displacement control procedure, no thermal expansion of the PS is allowed (i.e. it is the displacement at the interface which is controlled and it remains fixed during a time step). The reaction force is measured. In this example, it yields to the value expressed by Eq.(21).

$$F_P(t_1) = -K_P \alpha L_P\, T(t_1) \tag{21}$$

d. The measured reaction force (21) is imposed on the NS. This generates a displacement that is computed using Eq. (22).

$$u_N(t_1) = \frac{K_P}{K_N} \alpha L_P \, T(t_1) \tag{22}$$

e. The new displacement is imposed on the PS (Eq.(23)). A time delay $\Delta t_P$ is used to capture the time needed to compute the reaction of the NS and to adjust the displacements in the actuators, as for a real HFT.

$$u_P(t_1 + \Delta t_P) = \frac{K_P}{K_N} \alpha L_P \, T(t_1) \tag{23}$$

f. The new displacement induces a new reaction force of the PS. Meanwhile, heating of the PS has continued and also induces variation in force. The updated reaction force of the PS at the interface $F_P(t_2)$ is measured (given here by Eq.(24)) and imposed on the NS. This generates a new displacement $u_N(t_2)$ given by Eq. (25).

$$F_P(t_2) = -K_P \alpha L_P \left( T(t_2) - \frac{K_P}{K_N} T(t_1) \right) \tag{24}$$

$$u_N(t_2) = \frac{1}{R} \alpha L_P \left( T(t_2) - \frac{K_P}{K_N} T(t_1) \right) \tag{25}$$

Steps *e* and *f* are repeated in order to maintain equilibrium and compatibility at the interface.
In this case, the measured reaction force can be determined using Eq.(26), while the displacements can be calculated using Eq. (27).

$$F_P(t_n) = -K_P \, \alpha \, L_P \sum_{i=0}^{n-1} \left[ \left( -\frac{1}{R} \right)^i \, T(t_{n-i}) \right] \tag{26}$$

$$u_N(t_n) = \frac{1}{R} \alpha L_P \sum_{i=0}^{n-1} \left[ \left( -\frac{1}{R} \right)^i \, T(t_{n-i}) \right] \tag{27}$$

Next, Figure 4-3 presents one step of the displacement control procedure when using the first generation method. To accomplish one step hybrid fire testing first the reaction force $F_P$ is measured in the furnace and then imposed on the NS inducing a displacement $u_N$ which will be transferred to the PS ensuring the equilibrium and compatibility at the interface.

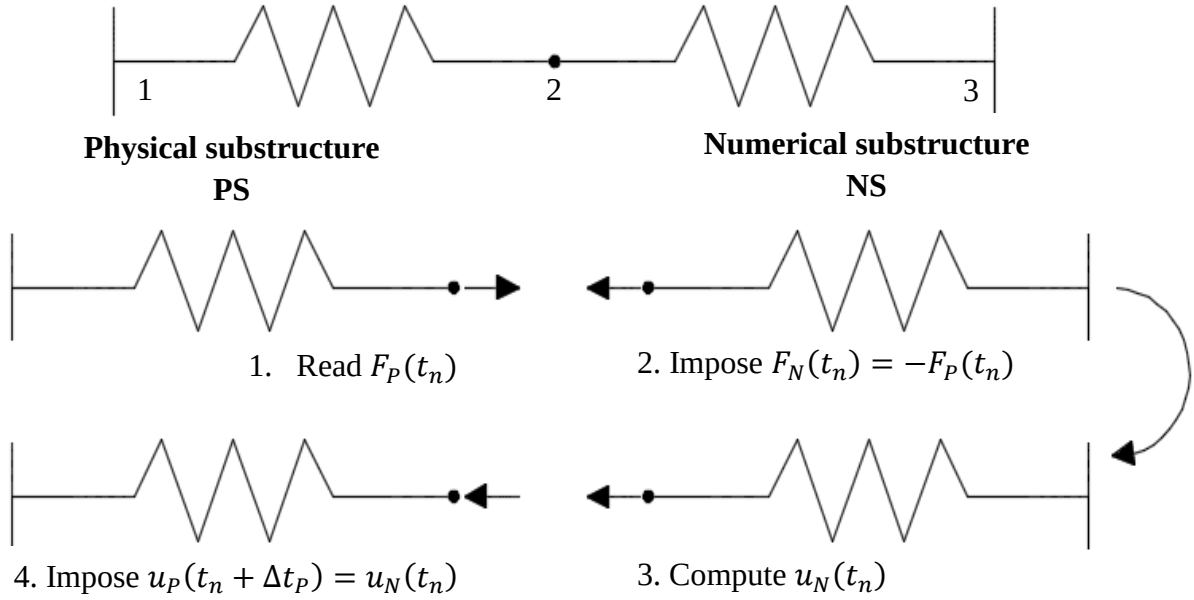


**Figure 4-3. One step of displacement control procedure. First generation method.**

To conclude the first generation method, Table 4-2 presents the measured data in the furnace and the calculated reaction of the NS when the first generation method is considered.

**Table 4-2. Measured and calculated data for one DoF case study**

| First generation method | Force control procedure (FCP) | | Displacement control procedure (DCP) | |
|---|---|---|---|---|
| *Measured data of the PS* | $\boldsymbol{u_P(t_n)}$ | Eq. (19) | $\boldsymbol{F_P(t_n)}$ | Eq. (26) |
| *Calculated reaction of the NS* | $\boldsymbol{F_N(t_n)}$ | Eq. (20) | $\boldsymbol{u_N(t_n)}$ | Eq. (27) |

## 4.3. Discussion

### 4.3.1. Analysis of the first generation method

In the previous section the first generation method has been illustrated by considering a simple linear system. For the force control procedure and for the displacements control procedure the steps applied during the hybrid tests have been described. The measured data in the furnace and the calculated reaction of the NS have been expressed for any time step $t_n$.

As shown by Equations ((19), (20), (26), (27)), the results are influenced by the properties of the substructures which compose the system such as the length of the bars, the stiffness of the bars, the thermal coefficient of the material, and the temperature of the heated substructure for different time steps. The stiffness ratio $R = \frac{K_N}{K_P}$ which appears in the equations play a particular role, as will be discussed hereafter.

The stability of the first generation method depends on the stiffness ratio $R$ between the two substructures that are subject to HFT. Indeed, for the process to be stable, the value of the parenthesis which involves the stiffness ratio in Equations ((19), (20), (26), (27)) should be smaller than 1, i.e. $R < 1$ for the force control procedure and $\frac{1}{R} < 1$ or $R > 1$ for the displacement control procedure. If not, the value tends toward infinity when the number of iteration $i$ increases, irrespectively of the size of the time steps, and the process becomes unstable.

It might seem straightforward to choose which of the two procedures (DCP versus FCP) has to be applied, based on the calculation of the stiffness ratio once the two substructures have been defined. However, in practice, this choice may be complex or even virtually impossible, for the following reasons:

*a) The stiffness ratio will vary during the test*

When exposed to fire, structural components are affected and their stiffness decreases.
The physical substructure, tested in a furnace, is by definition exposed to fire and therefore will have its stiffness reduced over the time of the HFT. On the other hand, the numerical substructure, modelled aside, may or may not be heated.
During the fire exposure the degradation of stiffness is significant and it may be amplified when some specific phenomenon occurs while heating the structural elements e.g. spalling of the concrete.
If the NS is kept cold, stiffness degradation is not as significant as in the case of fire exposure, but it may still happen due to large displacements and material nonlinearities.

Let us analyze the two procedures more in detail.

*Force control procedure*
The force control procedure is stable if the stiffness ratio is smaller than one during the entire test: $R < 1$. This involves the numerical substructure being more flexible than the physical substructure (i.e. the PS being stiffer than the NS).
If at ambient conditions the stiffness ratio satisfies the condition for stability, $R < 1$, when exposed to fire the stiffness ratio will generally start increasing as a result of the PS being exposed to fire (assuming the NS is kept cold). As a reminder, the denominator of the stiffness ratio is the stiffness of the PS. The stiffness ratio can increase until the critical value of 1 is reached and this corresponds to the moment when the instability occurs.
If the stiffness ratio does not exceed the value of 1 for the entire test duration, then the force control procedure can be safely used.
When the NS is exposed to fire then the evolution of the stiffness ratio becomes even harder to be predicted.

*Displacement control procedure*
The displacement control procedure is stable if the stiffness ratio is larger than one $R > 1$, meaning that the NS is stiffer than the PS.

As mentioned, when the NS is cold, then the stiffness ratio increases due to the degradation of the PS's stiffness. Therefore the displacement control procedure is stable once the stability condition is fulfilled at ambient conditions ($R > 1$).
When the NS is considered exposed to fire then the evolution of the stiffness ratio is difficult to be predicted.

The above discussion proves that the stability of the first generation method is governed by the evolution of the stiffness ratio during the hybrid test.

*b) The different degrees-of-freedom involved may require different procedures*

In applications when the PS is extracted from the analyzed structure, multiple DoFs will need to be controlled during the test. For some DoFs one procedure would be adequate while for the other DoFs the opposite procedure is. One solution to control multiple DoFs is to make use of both procedures (displacement and force control) during the same hybrid test. For now, the use of combined procedures during one test has not been tried in fire field. More research is needed to prove the feasibility of the combined procedures in terms of the quality of the results. From the experimental point of view, to control the displacements along with the forces might be complicated or even impossible for some facilities.

To avoid the instability which might occur prematurely in the hybrid fire tests, a new method needs to be developed independent on the stiffness ratio between the substructures.

### 4.3.2. Use of the first generation method in the previous hybrid fire tests

In the previous hybrid tests [57]-[66] the force control procedure has been applied. A posteriori analysis of the configuration of these tests shows that, in all cases, the NS was more flexible than the PS during the hybrid test. Therefore, the FCP was adequate and its application did not result in any stability issue during the tests.

The test by Korzen [57]-[61] has been performed on concrete column, whereas the NS was represented by a constant matrix.

Mostafaei in [65]-[66] presents the hybrid fire test performed on a column while the NS (3D concrete moment resisting frame) was modeled in SAFIR.

The axial stiffness of a column is very large with respect to the axial stiffness of the NS (moment resisting frames). Therefore, the stiffness ratio was much lower than 1. During Korzen's hybrid fire test, the stiffness ratio increased but never reached the critical value of stability. In the case of the hybrid test performed by Mostafaei, the NS was subjected to fire inducing a decrease of stiffness. In this case the increase of the stiffness ratio is slower compared with the situation when the NS is kept cold.

Robert in [62]-[64] presents a hybrid test where the physical substructure is represented by a reinforced concrete slab. The stiffness of the numerical substructure is predefined before the

test using a predetermined matrix. Three DoFs were controlled at the interface, one axial DoF and 2 rotational DoFs. It was considered during the test that the stiffness of the numerical substructure is elastic, and the axial DoF is uncoupled with the rotational DOFs.

The stiffness ratio was equal to 0.167 for the axial DoF while for the rotational DoFs, the ratio was equal to 0.756. During the test the stiffness of the NS was constant (elastic behavior) compared with the stiffness of the PS, which was decreasing due to the fire exposure. For the axial DoF the stiffness ratio is significantly smaller than 1, but it is not the case for the rotational DoFs where the stiffness ratio approaches the value of one. No instability occurred during the test, suggesting that the stiffness ratio did not exceed the value of 1. It has to be mentioned that in the hybrid fire test performed by Robert, some safety measurements have been adopted such as to avoid the possible instability.

## 4.4. Numerical example

### 4.4.1. The correct solution of the interface

The correct interface solution of the case study (one degree of freedom linear elastic system) can be expressed analytically using Eq. (28) for the time step $t_n$. The displacement of node 2 is calculated analyzing the entire structural system without substructuring.

$$u(t_n) = \frac{F^e(t_n) + F^i(t_n)}{K_N + K_P} \tag{28}$$

$$F^e(t_n) = 0 \tag{29}$$

$$F^i(t_n) = \mathrm{E}_P A_P \alpha T(t_n) \tag{30}$$

Where:

$u(t_n)$ is the interface displacement of the structural system analyzed without substructuring for the time step $t_n$;

$F^e$ is the external force eventually applied at the node that constitutes the interface. In this example no external force is considered.

$F^i$ is the internal force that would develop in a completely restrained substructure. This force depends on the time $t_n$;

$E_P$ is the Young modulus for the PS;

$A_P$ is the sectional area of the PS;

$T(t_n)$ is the temperature for the time step $t_n$;

During the hybrid test, the measured displacements (force control procedure) or the imposed displacements (displacement control procedure) should be equal to the correct displacement of the system.

In this exercise the degradation due to the fire exposure of the PS's characteristics such as stiffness (implicit Young modulus) is not considered.

### 4.4.2. Instability of the first generation method

In this section a numerical example will be presented to illustrate the dependency of the first generation method on the stiffness ratio $R$.
The linear truss system is considered with the following input data:

- Coefficient of thermal expansion of the material of the PS : $\alpha = 12\, e^{-6}\, \frac{1}{K}$
- Young modulus for the PS and NS: $E_P = E_N = 210000\, \frac{\mathrm{N}}{mm^2}$
- Sectional area of the PS and NS: $A_P = A_N = 20000\ \mathrm{mm}^2$
- The physical substructure is heated at a constant rate of 0.5 K/s;

The length variation of each substructure induces different relative stiffness of the substructures. For simplicity, the stiffness of the PS is kept constant during the exercise. In a real hybrid test the stiffness of the PS will decrease due to the fire exposure.
The objective of the exercise is to plot the reaction forces and displacements at the interface for the NS and PS versus the correct solution. The plots will be done for two different stiffness ratios $R < 1$ and $R > 1$ using the force control procedure and displacement control procedure. The length of the PS is equal to 1.50 m while the length of the NS is equal to 3.00 m when $R < 1$. For the stiffness ratio $R > 1$ the length of the PS is 3.00 m while the length of the NS is 1.50 m

*Force control procedure*

Figure 4-4 presents the evolution of interface forces and displacements in time for a stiffness ratio $R < 1$. The chosen time step is $\Delta t = 50\ sec$ with a delay time of the actuator equal to $\Delta t_P = 10\ sec$. For every graph three solutions are illustrated, the correct one and the solutions at the interface of the PS and NS.

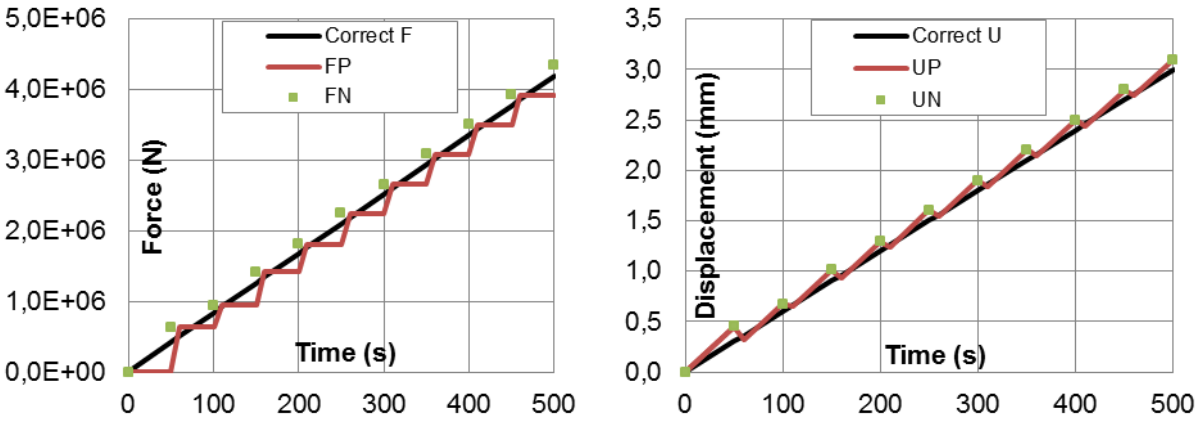


*The interface force* *The interface displacement*

**Figure 4-4. The boundary conditions when using a force control procedure ($R < 1$)**

The objective of hybrid fire testing is to maintain equilibrium and compatibility at the interface of the substructure while capturing the behavior of the structure as an assembly.

The interface equilibrium and compatibility translate from the graphical point of view by matching the solution of the PS with the solution of the NS. More than that, the interface solutions should match the correct solution. The correct solution results by analyzing the structural system as an assembly without considering the substructuring (which can be done analytically in this simple case).

During one time step $\Delta t$, in force control procedure, the force remains constant while the displacement varies due to the fire exposure. The force is constant once the actuator succeeded to apply with the delay time $\Delta t_P$ the new computed value of the interface force.

In this particular example before starting the hybrid simulation the interface displacements and forces are equal to zero (unloaded system). During the first time step $\Delta t$ the interface force is equal to zero while the displacement is increasing until 0.45 mm due to the thermal expansion. When the time $t_1 = \Delta t$ is reached the interface displacement $u_P(t_1) = 0.45$ (mm) of the PS is registered and used in the calculation of the interface force to be applied on the substructures. The interface force resulted from the NS analysis $F_N(t_1) = 0.63E^{+6}$ (N) is applied on the PS. Due to the delay time the force in the furnace is reached after 10 sec since the calculation has been performed $F_P(t_1 + \Delta t) = -F_N(t_1) = -0.63E^{+6}$. In all this time the PS continues to be heated, thus expanding. The new force acting on the PS leads to a decrease in displacements. Again the force is kept constant and the displacement is free until the next update of the interface forces.

Please note that in the graph the forces of the PS are represented in the absolute value to facilitate the understanding.

The interface solution of the PS and NS oscillates around the correct solution.

In the case of the stiffness ratio $R < 1$ the force control procedure is stable and showing results oscillating around the correct solution.

Figure 4-5 presents the evolution of the interface force and displacement for a case of stiffness ratio $R > 1$ when the force control procedure is considered. The same steps are followed as in the previous example, but it can be observed right from the start of the test how the solution diverges from the correct solution leading to the instability in the process.

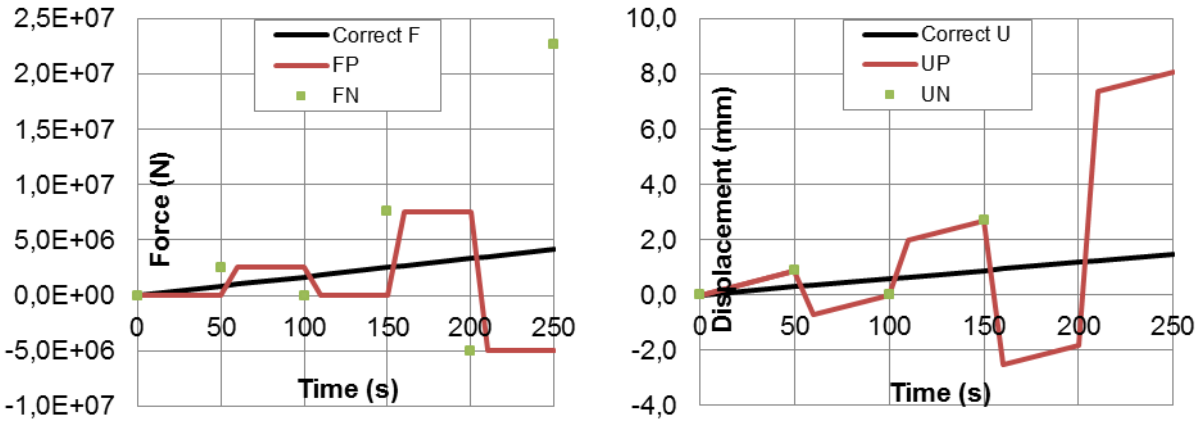


*The interface force* *The interface displacement*

**Figure 4-5. The boundary conditions when using a force control procedure ($R > 1$)**

To be able to understand the cause of instability the force control procedure presented in the chapter 4.2.2 will be interpreted making use of the graphs presented in Figure 4-4 and Figure 4-5.

The principle of hybrid simulation states that for a time step $t_{n-1}$ the same values of forces and displacements should be registered at the interface of the substructures, as presented in the Eq. (31).

$$u_P(t_{n-1}) = u_N(t_{n-1})$$
$$F_P(t_{n-1}) = F_N(t_{n-1}) \tag{31}$$

Until the next time step, the PS is continued to be heated inducing a change in the interface displacements. Thus the interface displacements of the PS at the time step $t_n$ is different compared with the displacement from the previous time step $t_{n-1}$. At the same time the NS is kept cold with the same interface conditions as in the previous time step.

$$u_P(t_n) \neq u_P(t_{n-1})$$
$$u_N(t_n) = u_N(t_{n-1}) \tag{32}$$

Equation (32) expresses the loss of compatibility at the interface of the substructure meaning that the interface displacement of the PS differs from the interface displacement of the NS as presented in the Eq. (33).

$$u_P(t_n) \neq u_N(t_n) \tag{33}$$

The objective is to restore the compatibility at the interface. To do so based on the measured interface displacements new values of forces are computed and applied at the interface just to restore the equilibrium. For the static case is equivalent by writing the Eq.(34), where $\Delta F(t_n)$ is the incremental force and $\Delta u(t_n)$ is the incremental displacement at the time step $t_n$. Note that the form of the Eq.(34) in the case of force control procedure will be explained in section 5.5.

$$\Delta F(t_n) = \left(\frac{1}{K_P} + \frac{1}{K_N}\right)^{-1} \Delta u(t_n)$$
$$\mathrm{F}(t_n) = \mathrm{F}(t_{n-1}) + \Delta F(t_n) \tag{34}$$

The new force $\mathrm{F}(t_n)$ is applied on the PS and NS which leads to equal displacements on the substructures (equilibrium and compatibility ensured). Note that the computed force $\mathrm{F}(t_n)$ will be applied with a delay time, therefore the compatibility is ensured at the time $t_n + \Delta t_P$.

$$u_P(t_n + \Delta t_P) = u_N(t_n + \Delta t_P) \tag{35}$$

To reach interface equilibrium and compatibility the key is to update the interface forces every time step using in the calculations the total stiffness of the assembly $K_P + K_N$.

In the case of the first generation method, application of the formulas expressed in section 4.2.2 leads to a different value of stiffness considered in the update of the boundary conditions at every time step, as shown hereafter.

The increment of the force is determined based on the Eq. (36) where the expression of $F(t_n)$ and $F(t_{n-1})$ are the one presented by the Eq. (20).

$$\begin{aligned}\Delta F(t_n) &= F_N(t_n) - F_N(t_{n-1}) \\ &= K_N\, \alpha\, L_P \sum_{i=0}^{n-1}\left[(-R)^i\ T(t_{n-i})\right] - K_N\, \alpha\, L_P \sum_{i=0}^{n-2}\left[(-R)^i\ T(t_{n-i})\right]\end{aligned} \tag{36}$$

The increment of the displacement is determined based on the Eq. (37) where the expression of $u_P(t_n)$ it the one presented by the Eq. (19) and $u_N(t_n) = \frac{F_N(t_{n-1})}{K_N}$, where $F_N(t_{n-1})$ is presented by the Eq. (20).

$$\begin{aligned}\Delta u(t_n) &= u_N(t_n) - u_N(t_{n-1}) \\ &= \alpha\, L_P \sum_{i=0}^{n-1}\left[(-R)^i\ T(t_{n-i})\right] - \alpha\, L_P \sum_{i=0}^{n-2}\left[(-R)^i\ T(t_{n-i})\right]\end{aligned} \tag{37}$$

Based on the equation (36) and (37) it can be written that the incremental force is equal the incremental displacement multiplied the stiffness of the NS (see Eq. (38)) which is not conform with the Eq. (34).

$$\Delta F(t_n) = K_N \, \Delta u(t_n) \tag{38}$$

In conclusion, the first generation method accounts only for the stiffness of the NS in the update of the boundary conditions at every time step. This is the reason why the first generation method is conditionally stable on the stiffness ratio between the substructures.

*Displacement control procedure*

Figure 4-6 presents the interface force and displacement for a case where the stiffness ratio is smaller than one while making use of displacement control method. The achieved solution by using the hybrid process diverges from the correct solution right after the beginning of the simulation.

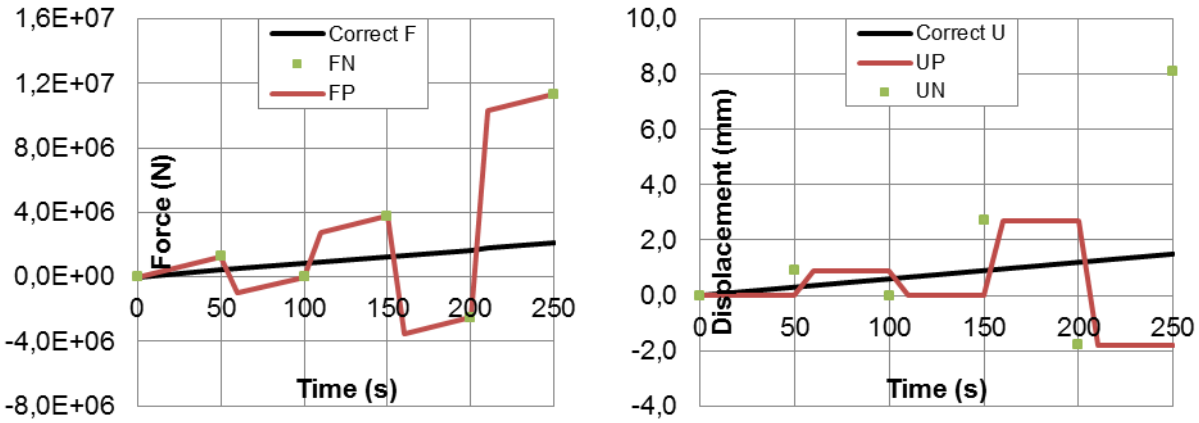


*The interface force* *The interface displacement*

**Figure 4-6. The boundary conditions when using a displacement control procedure ($R < 1$)**

Figure 4-7 presents the interface solution of the truss system when the stiffness ratio is bigger than one. The process is stable, and the solution oscillates around the correct solution.

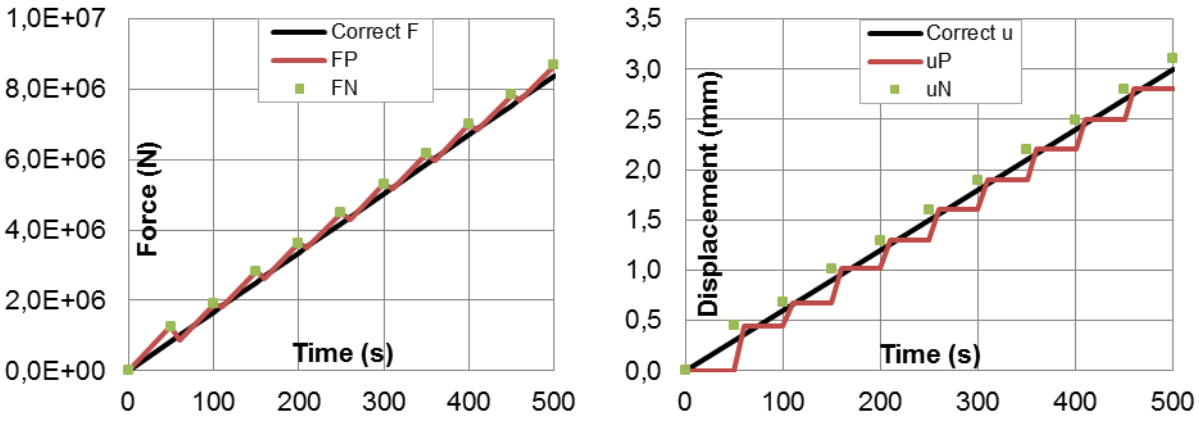


*The interface force* *The interface displacement*

**Figure 4-7. The boundary conditions when using a displacement control procedure ($R > 1$)**

The displacement control implies every time step an update of the interface displacements. Thus it can be observed in the same figure that the displacement is constant in between the updates. As a consequence, the interface force will vary between the two time steps. The time step and the delay time step are considered with the same values as in the force control procedure example, respectively $\Delta t = 50$ s and $\Delta t_P = 10$ s. In this particular example when a constant value of displacement is kept at the interface the reaction force increases due to the fire exposure. Once the interface displacement is updated the force reduces.

In displacement control procedure the displacements are fixed at the interface of the substructures during one time step. Meanwhile the PS is continued to be heated leading to a change in the reaction force.

Thus, based on the principle of the hybrid simulation the interface compatibility and equilibrium must be satisfied every time step (see Eq. (31) for the time step $t_{n-1}$).

Since the reaction force of the heated substructure is not anymore in equilibrium with the reaction force of the cold substructure (see Eq.(39)), the equilibrium needs to be restored.

$$F_P(t_n) \neq F_N(t_n) \tag{39}$$

Based on the measured interface reaction forces, new values of displacements are computed and applied at the interface just to restore the equilibrium. For the static case is equivalent by writing the Eq.(40).

$$\begin{aligned} \Delta u(t_n) &= (K_P + K_N)^{-1} \Delta F(t_n) \\ \mathrm{u}(t_n) &= \mathrm{u}(t_{n-1}) + \Delta u(t_n) \end{aligned} \tag{40}$$

Note that the computed displacement $u(t_n)$ will be applied at the time $t_n + \Delta t_P$ on the PS leading to equal reaction forces on the substructures as presented in Eq. (41) (equilibrium and compatibility ensured).

$$F_P(t_n + \Delta t_P) = F_N(t_n + \Delta t_P) \tag{41}$$

The stiffness of the assembly $K_P + K_N$ is required to be used in the hybrid process to ensure equilibrium and compatibility and moreover to ensure stability of the process.

For the force control procedure it has been mentioned that only the stiffness of the NS is considered in the hybrid process.

The value of stiffness considered in the update of the boundary conditions every time step for displacement control procedure is next identified.

The value of $\Delta F(t_n)$ and $\Delta u(t_n)$ are next expressed. The increment of the force is determined based on the Eq.(42), where the expression of $F(t_n)$ and $F(t_{n-1})$ are the one presented by the Eq.(26).

$$\begin{aligned}\Delta F(t_n) &= F_N(t_n) - F_N(t_{n-1}) \\ &= K_P\,\alpha\,L_P \sum_{i=0}^{n-1}\left[\left(-\frac{1}{R}\right)^i\ T(t_{n-i})\right] - K_P\,\alpha\,L_P \sum_{i=0}^{n-2}\left[\left(-\frac{1}{R}\right)^i\ T(t_{n-i})\right]\end{aligned} \tag{42}$$

The increment of the displacement is determined based on the Eq. (43) where the expression of $u_N(t_n)$ and $u_N(t_{n-1})$ is the one presented by the Eq. (27).

$$\begin{aligned}\Delta u(t_n) &= u_N(t_n) - u_N(t_{n-1}) \\ &= \frac{K_P}{K_N}\alpha\,L_P \sum_{i=0}^{n-1}\left[\left(-\frac{1}{R}\right)^i\ T(t_{n-i})\right] - \frac{K_P}{K_N}\alpha\,L_P \sum_{i=0}^{n-2}\left[\left(-\frac{1}{R}\right)^i\ T(t_{n-i})\right]\end{aligned} \tag{43}$$

Based on the equation (42) and (43) it can be written that the incremental displacement is equal the incremental force multiplied the inverse of the NS's stiffness (see Eq.(44)) which is not conform to the Eq. (40).

$$\Delta u(t_n) = {K_N}^{-1}\,\Delta F(t_n) \tag{44}$$

The first generation method could be unstable due to the fact that only the stiffness of the NS is considered in the hybrid process.

### 4.4.3. Graphic representation

In this section, a graphic representation of how the hybrid methodology works when applying the first generation method is provided to illustrate the instability that might occur. Therefore for every time step two cases will be illustrated ($R > 1$ versus $R < 1$).

The PS and NS are represented by segments with different slopes, thus different stiffnesses.

*Force control procedure*

At the ambient temperature there is no external load acting on the structure. The only load considered in example is the fire load. Thus, no initial force is applied to the physical substructure before heating at the time $t_0$ (see Figure 4-8).

The NS and the PS will intersect in the origin, where the interface displacement and forces are equal to zero as presented in the Eq. (45).

$$\begin{aligned}u_P(t_0) = u_N(t_0) = 0 \\ F_P(t_0) = F_N(t_0) = 0\end{aligned} \tag{45}$$

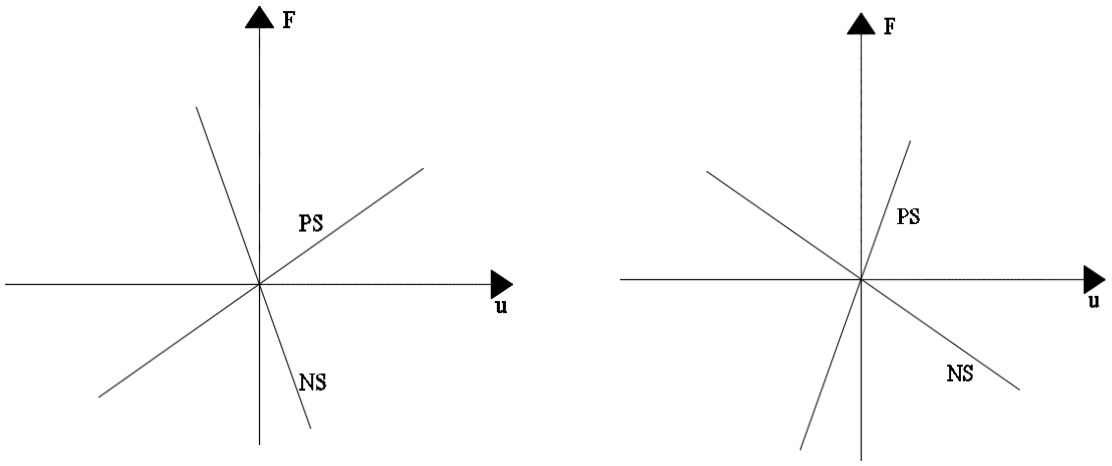


*a)* $R > 1$ *b)* $R < 1$

**Figure 4-8 Graphic representation of the PS and NS for the time $t_0$**

The physical substructure is starting to be heated. In force control procedure the heated substructures are free to expand. In this situation the displacement is registered in the furnace and sent to the NS in order to compute the force to be updated next at the interface. The measured displacement of the physical substructure is expressed by the Eq. (46) for the time $t_1$ .

$$u_P(t_1) = \alpha L_P T(t_1) \tag{46}$$

The heated PS is represented with the red color and is translated from the center of the system. The intersection of the segment with the horizontal axis represents the measured displacement of the PS during this step.

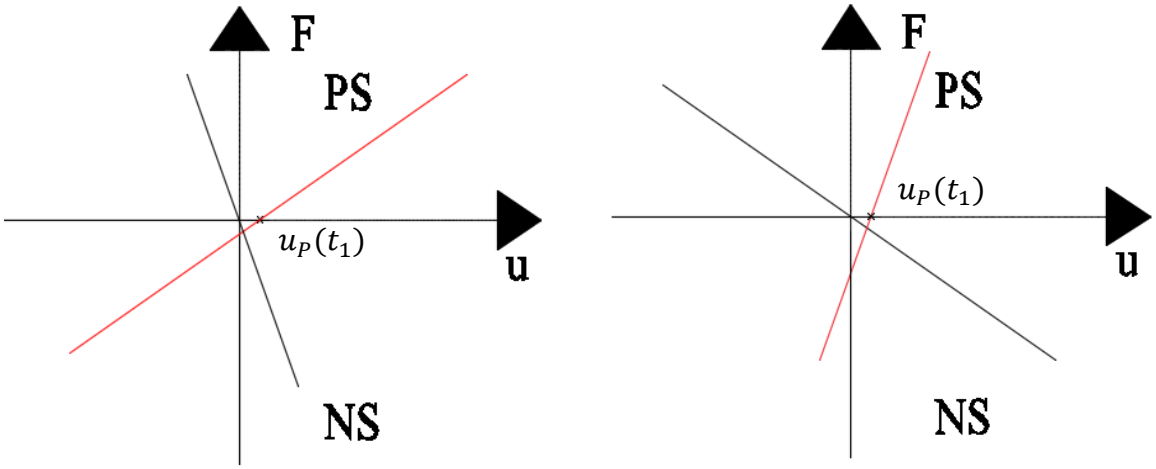


*a)* $R > 1$ *b)* $R < 1$

**Figure 4-9 Graphic representation of the first read of displacement (FCP)**

The next step is to run the analysis of the numerical substructure subjected to the displacement measured in the furnace and obtain the corresponding force presented by Eq. (47).

$$F_N(t_1) = K_N\ \alpha\ L_P T(t_1) \tag{47}$$

The measured displacement in the furnace is used to compute the reaction of the numerical substructure at the time $t_1$. The green color from the Figure 4-10 illustrates this step. Note that the correct displacement and the correct interface force is the one obtained at the intersection of the two segments, the NS segment with the PS segment. So it can be clearly seen that in the situation when the stiffness ratio is bigger than one the estimated reaction of the NS $F_N(t_1)$ is much too big compared with the correct value.

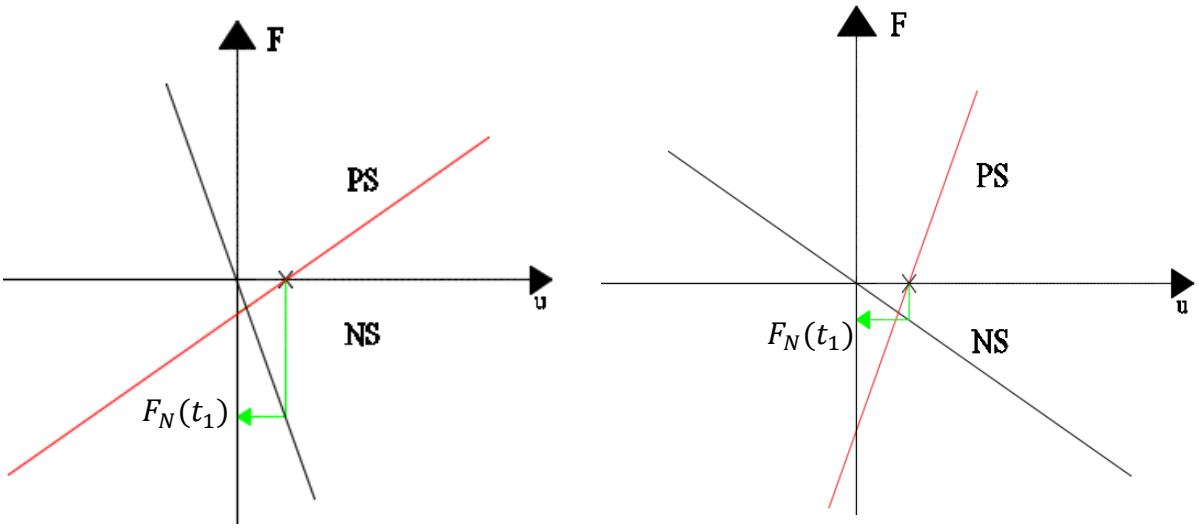


*a)* $R > 1$ *b)*$R < 1$

**Figure 4-10 Graphic representation when computing the reaction of the NS for the time $t_1$(FCP)**

The next step is to adjust the computed force in the furnace accordingly. Figure 4-11 presents the adaptation of the new force in the furnace at the time $t_1+\Delta t_P$. The force will be applied with a delay of $\Delta t_P$, which depends on the reaction time of the actuators in the furnace. So this is why, in the furnace we have a different displacement by the time when we applied the new load than the one which was used for the calculation of the force. This is represented in the graphs by the shift of the grey segment (which represented the PS at the time $t_1$) in the red segment (which represents the PS at the time $t_1+\Delta t_P$). So applying a new force on the PS (the one calculated in the previous step) leads to a new displacement of the PS.

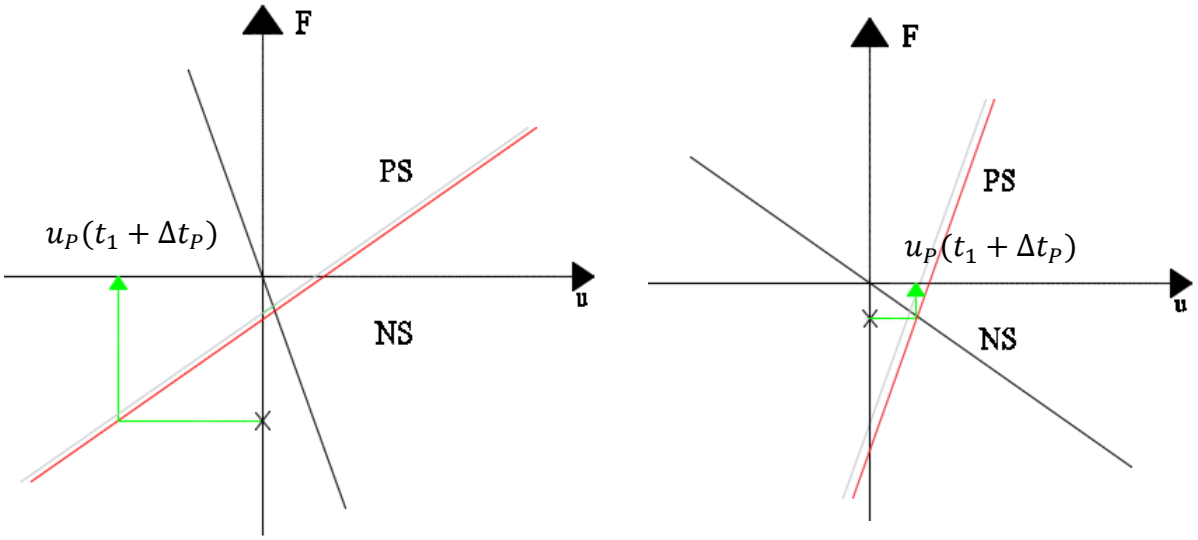


*a)* $R > 1$ *b)* $R < 1$

**Figure 4-11 Graphic representation of the new force and displacement induced in the PS for the time $t_1+\Delta t_P$**

It can be seen clearly from the first steps that in the case when the stiffness ratio is bigger than one, instability will occur. Due to the fact that stiffness of the numerical substructure is bigger compared with the physical one, the force to be applied every time step on the PS results with big values thus it cannot be supported by the PS, leading to instability. In the case when the PS is stiffer than the NS ($R < 1$) the force control procedure is stable and showing good results, i.e. results close to the correct solution.

*Displacement control procedure*

As in the case of force control procedure, the elastic truss system is unloaded before the start of the hybrid test. The forces and the displacements of the PS and NS are equal to zero and the two segments are intersecting each other in the origin of the coordinate system (see Figure 4-8).

The PS starts to be heated. If in force control procedure the PS is free to expand, in displacement control procedure no free expansion is allowed. Since the displacement of the heated PS is blocked, a reaction force $F_P(t_1)$ builds up as presented in Figure 4-12. From the graphical point of view the heated PS is represented by the translation of the segment representing the PS. The intersection of the segment with the vertical axis of the system is the reaction force which will be measured on the PS. The intersection of the segment with the horizontal axis of the system represents the thermal displacement of PS which corresponds to the measured reaction force.

No formulas will be presented for the measured and computed values at every time step. The values are according to the ones presented in the section 4.2.3. More details are specified for the case of force control procedure to facilitate the understanding.

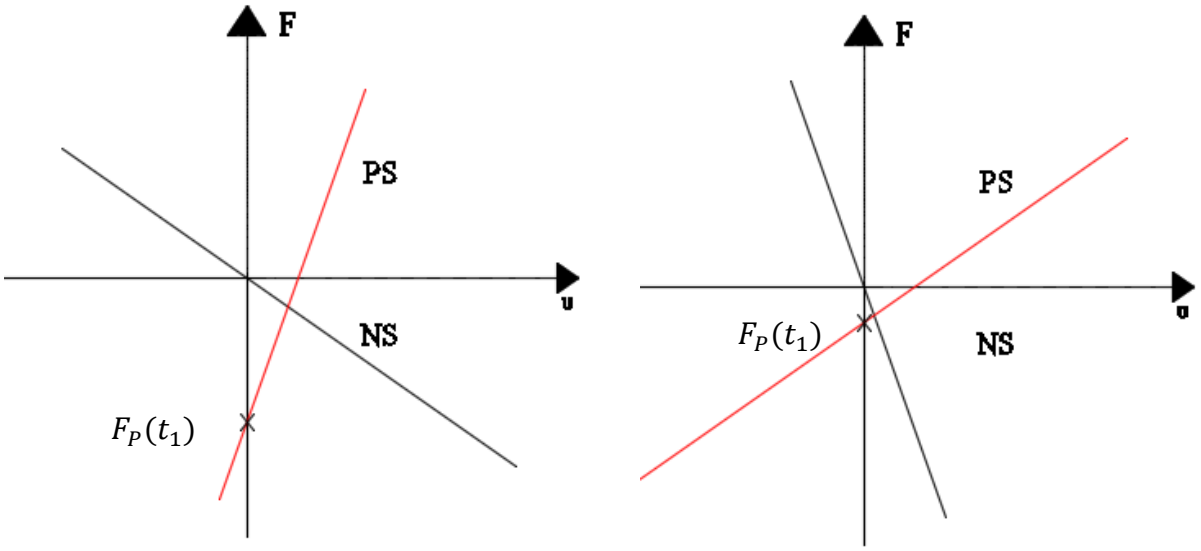


*a)* $R < 1$ *b)* $R > 1$

**Figure 4-12 Graphic representation of the first read $t_1$ (DCP)**

The measured reaction force of the PS will serve next to compute a new value of displacements to be imposed on the boundaries of the substructures. The measured reaction force is sent to the NS and in the calculation of the displacements only the stiffness of the NS is considered. The action of this step is presented in Figure 4-13.

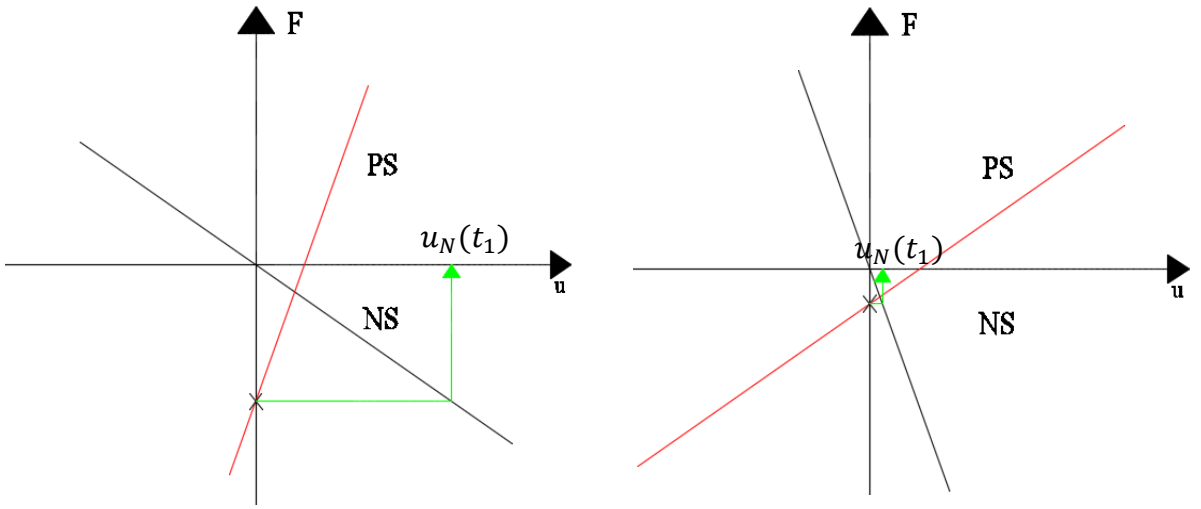


*a)* $R < 1$ *b)* $R > 1$

**Figure 4-13 Graphic representation when computing the displacement of the NS for the time $t_1$**

The calculated displacements from the previous step are imposed in the furnace on the PS with a delay time $t_1 + \Delta t_P$. During the delay time $\Delta t_P$ the PS continues to be heated. From the graphic point of view the position of the segment representing the PS is translated compared with the position during the time $t_1$. The new position is represented with the red color while

the position from the time step $t_1$ is represented by grey color. The Figure 4-14 presents the new reaction force resulted when the displacement $u_N(t_1)$ is imposed on the substructures.

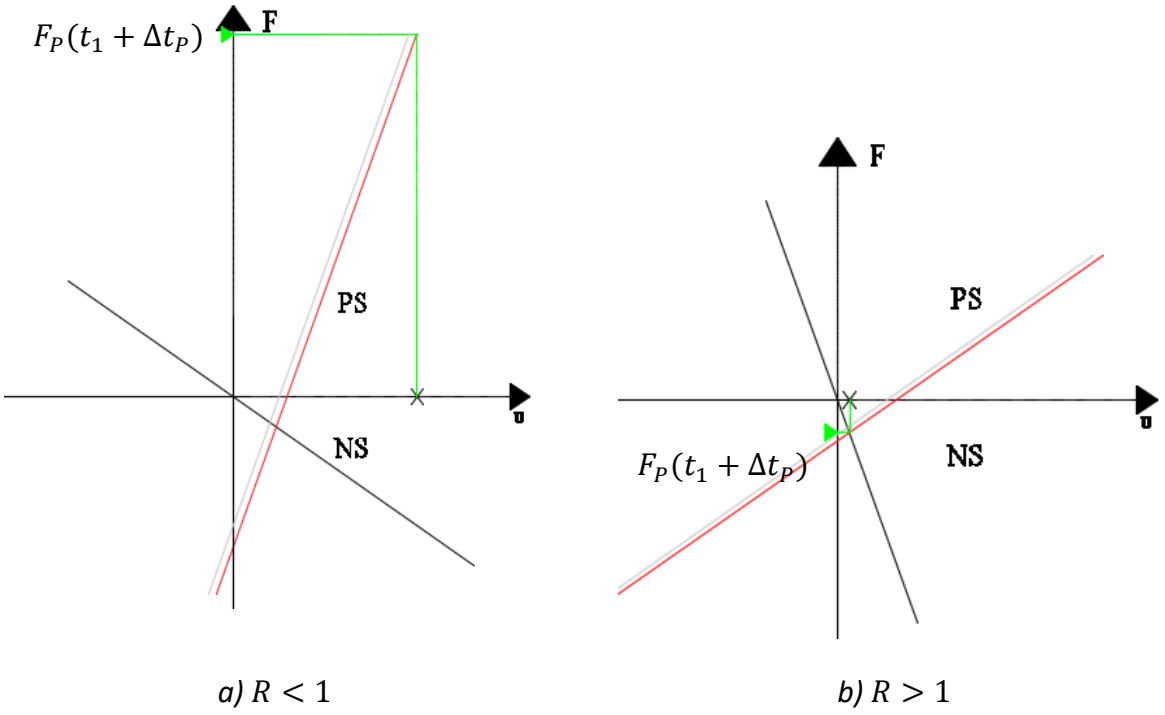


*a)* $R < 1$ *b)* $R > 1$

**Figure 4-14 Graphic representation of the new force and displacement induced in the PS for the time $t_1 + \Delta t_P$**

The instability occurs right at the beginning of the hybrid test when the PS is stiffer than the NS i.e. $R < 1$. For the stiff structural elements small variation of displacements induces big variation of forces. Therefore, the reaction force of the stiff PS is significant and will induce large displacements in the NS. The large displacement imposed on the stiff PS will induce too large reaction forces to be next imposed on the NS. Since the NS is more flexible than the PS will not support the load and the hybrid simulation ends right at the start of the test.

If the first generation method is used for the proper stiffness ratio, the solution provided by the hybrid fire testing will follow the correct solution (the intersection of the 2 segments, NS and PS).

### 4.4.4. Error estimation for the first generation method

Next, the objective is to analyze the accuracy of the results considering the following dependency:

- The time step $\Delta t$ and the delay time $\Delta t_P$;
- The stiffness ratio $R$;

Independently on the stiffness ratio, the value of the time step and the delay time has an influence on the results. One characteristics of the hybrid fire testing is the impossibility of turning off the fire during the test. Thus the fire exposure determines the change of the PS

boundary conditions during the *time of the calculations*, the *time of transfer* data from the PS to NS and vice versa, and the *delay time* of the actuators to induce the target values. As it has been mentioned already, the transfer time of the information is negligible. The calculation time is negligible if the NS is represented by a predetermined matrix. If the NS is represented via the FE model then the calculation time is important. The delay time of the actuators is important in the accuracy of the results.

Next, the linear elastic truss system is considered to observe the influence of the stiffness ratio on the results as well as the influence of the time step $\Delta t$ and the delay time $\Delta t_P$.

*Time step $\Delta t$ and the delay time $\Delta t_P$*

The influence of the time step and the delay time on the results will be discussed in this section for the displacement control procedure and for the force control procedure. The characteristics of the linear elastic truss system i.e. Young modulus, sectional area, the thermal coefficient of the material, the temperature evolution and the stiffness of the substrucutres, are the one presented in the section 4.4.2. As a recall, the physical substructure is heated at a constant rate of 0.5 K/s, the temperature evolution is considered as a function of the time step $T(t) = \frac{t}{2}$. In this example, the stiffness of the PS is kept constant during the exercise.

- *Force control procedure*

The example presented in Figure 4-1 will be next analyzed. The stiffness of the PS and NS is constants during the hybrid simulation in this particular example.

To be able to apply the force control procedure the stiffness ratio needs to be smaller than the critic value of one, thus in this example $R = 0.50$ while the delay time caused by the actuators is considered $\Delta t_P = 1s$.

The evolution of interface forces and displacements is presented for different values of the time step, i.e. 1 min (see Figure 4-15 a)), 5 min (see Figure 4-15 b)), 10 min (see Figure 4-15 c)) and 15 min (see Figure 4-15 d)). A deviation equal to 2%, 5% and 10% of the correct value is printed in the same graphs.

The principle of the force control procedure assumes a constant force during one time step meanwhile the interface displacements varies due to the fire exposure.

Every time step the variation of the displacement is registered and used in the computation of a new force to be imposed on the PS, thus the registered displacement is imposed at the interface DoFs of the NS. The next step is to compute the reaction force of the NS and to be imposed at the interface of the PS. The new force is imposed at the interface of the PS at time $\Delta t + \Delta t_P$. Thus the interface force of the PS equals the interface force of the NS (equilibrium). More than that, the new force acting on the PS induces a new displacement on the PS which is different compared with the displacements at the interface of the NS (compatibility not ensured).

In conclusion, the first generation method does not ensure the interface equilibrium and compatibility every time step. If the difference between the NS's interface solution and PS's is defined as acceptable by the user then the methodology can be applied. More than that, besides ensuring the interface equilibrium and compatibility, the two solutions should reproduce the real behavior of the structure when analyzed as an entire assembly (here specified the correct solution).

The admissible error is defined by the user depending on the type of structure analyzed and the furnace facility characteristics.

In this example the admissible error is randomly defined as a percentage (2%, 5% and 10%) of the correct value.

It is clear from the Figure 4-15 that a reduced time step provides results which oscillate around the correct solution and the deviation decreases once with the reduction of the time step. In these cases the interface solution is in the range of the admissible defined values for this example. Once the time step increases, the interface solution deviates from the correct solution and also from the admissible defined values.

A too much reduced time step chosen for the update of the interface conditions might cause problems on the experimental site. In a short time, the variation of the interface displacements and forces can exceed the minimum values which can be registered by the data acquisition system and transfer system. The values to be registered in the furnace should be bigger than the resolution of the transducers and inclinometers.

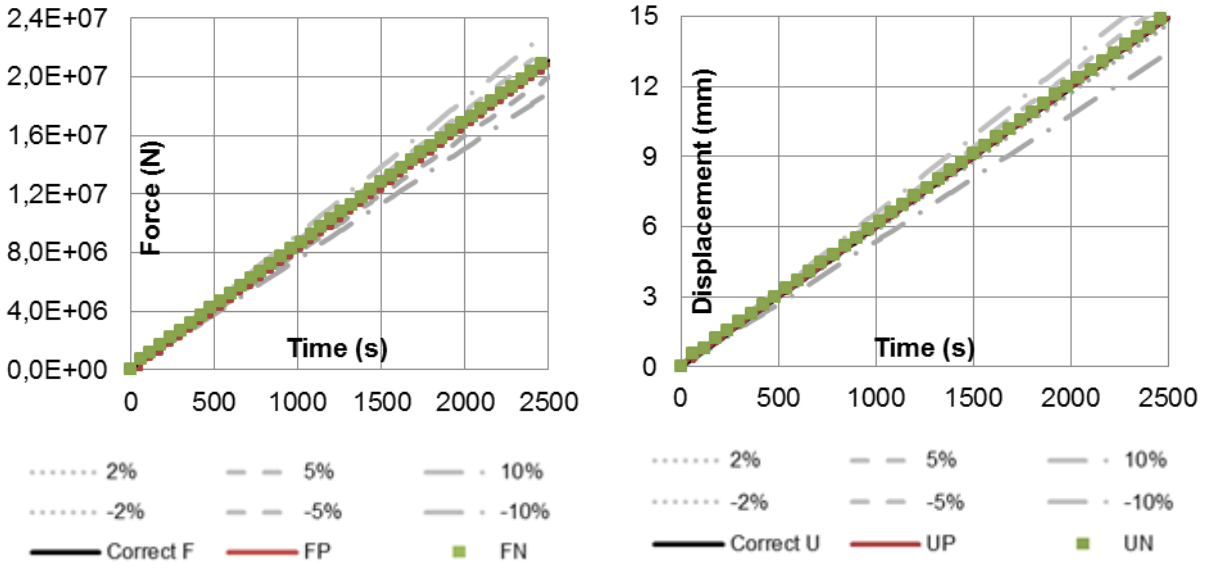


***a)*** $\Delta t = 60\ s; \Delta t_P = 1\ s$

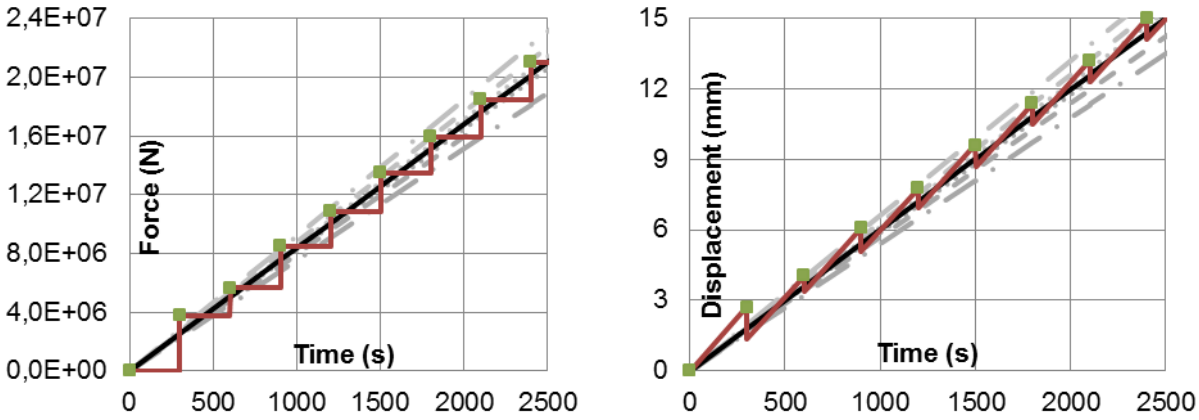


***b)*** $\Delta t = 300\ s;\ \Delta t_P = 1\ s$

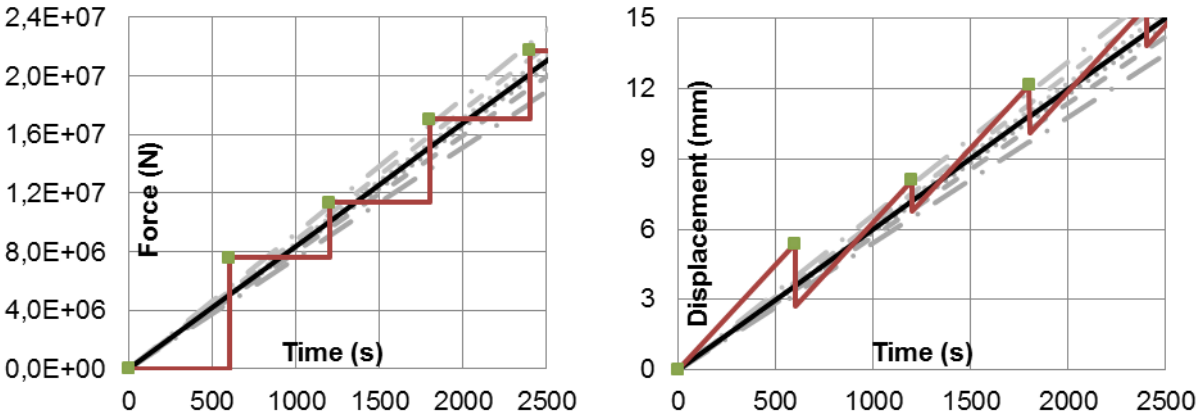


***c)*** $\Delta t = 600\ s;\ \Delta t_P = 1\ s$

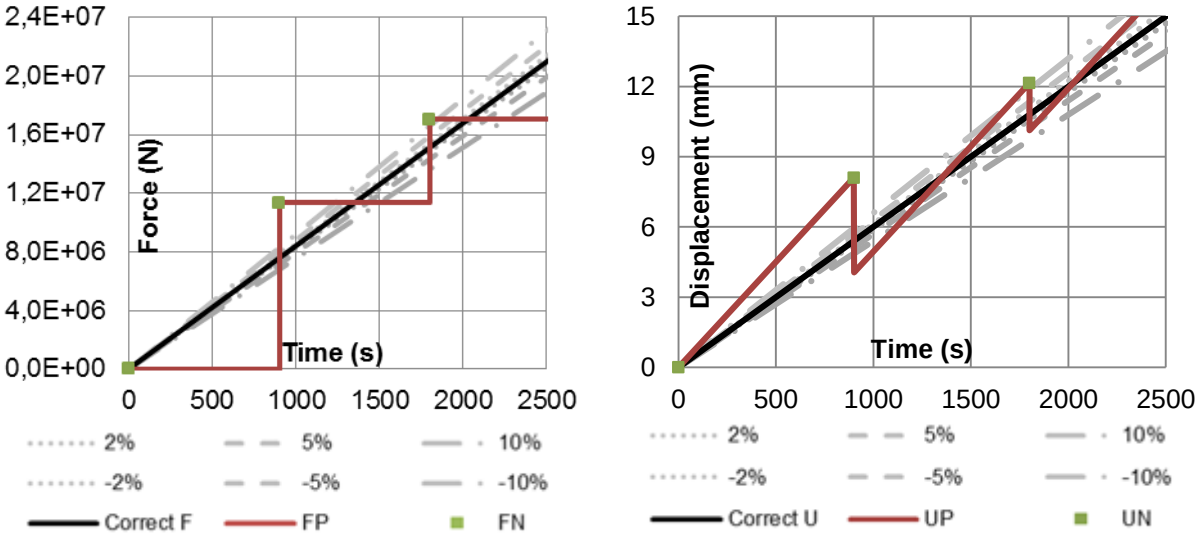


***d)*** $\Delta t = 900\ s;\ \Delta t_P = 1\ s$

**Figure 4-15. The evolution in time of interface force and displacement when the time step $\Delta t$ varies**

It has been shown in the previous case that the use of a reduced time step leads to results which oscillate around the correct solution. The value of $\Delta t = 60\ s$ proved to offer results with an accuracy of less than 5%. Thus the same value of the time step is next considered to study the influence of the delay time on the accuracy of the results.

Figure 4-16 presents the evolution of interface forces and displacements in time in the case of the delay time variation. The imposed values of force at the interface of the PS will induce a variation of displacement. The force is imposed at the time $\Delta t + \Delta t_P$ and once with the increase of this value, the resulted displacement will deviate from the correct solution.

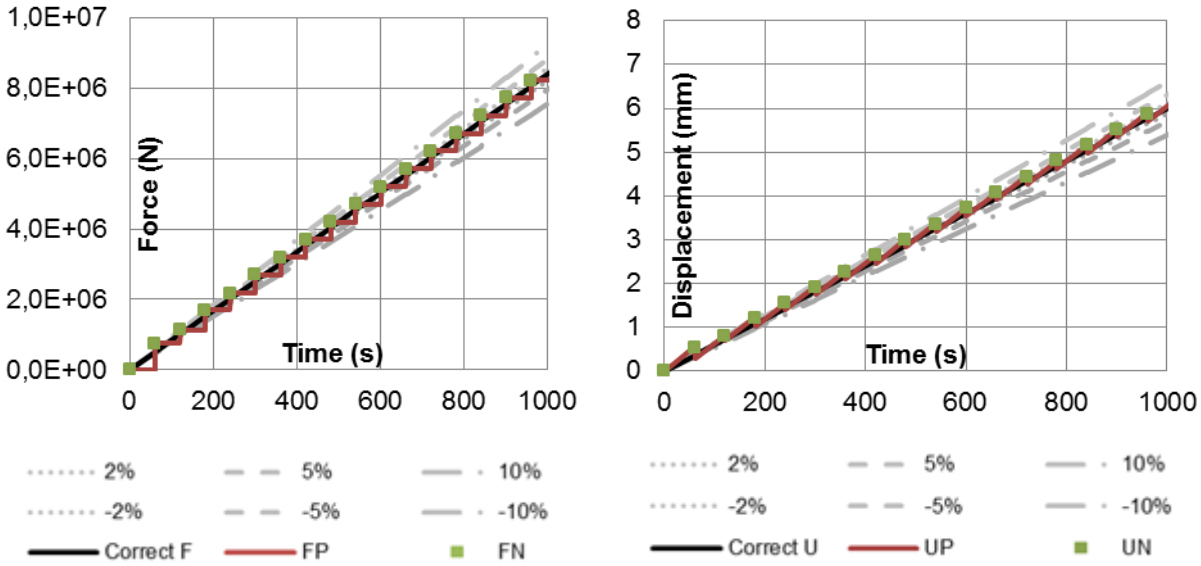


***a)*** $\boldsymbol{\Delta t = 60\ s;\ \Delta t_P = 1\ s}$

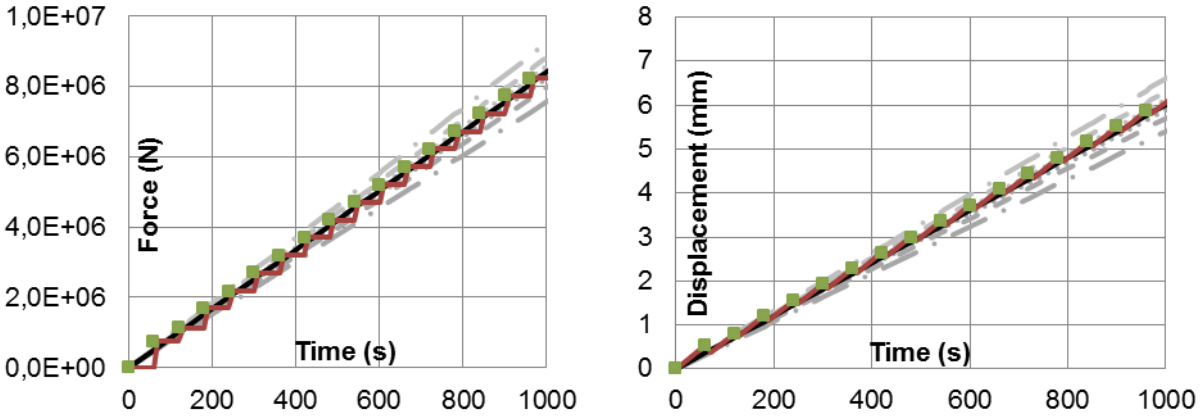


***b)*** $\boldsymbol{\Delta t = 60\ s;\ \Delta t_P = 10\ s}$

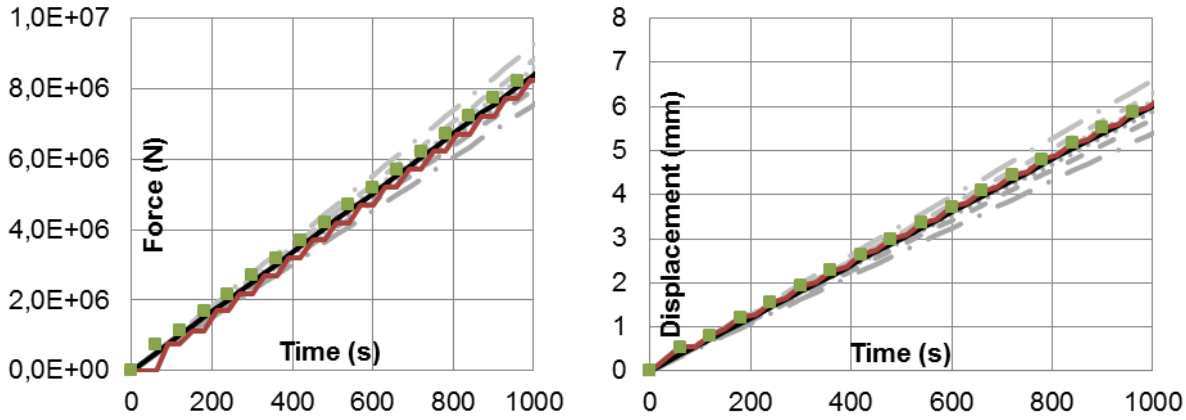


*c)* $\Delta t = 60\ s;\ \Delta t_P = 30\ s$

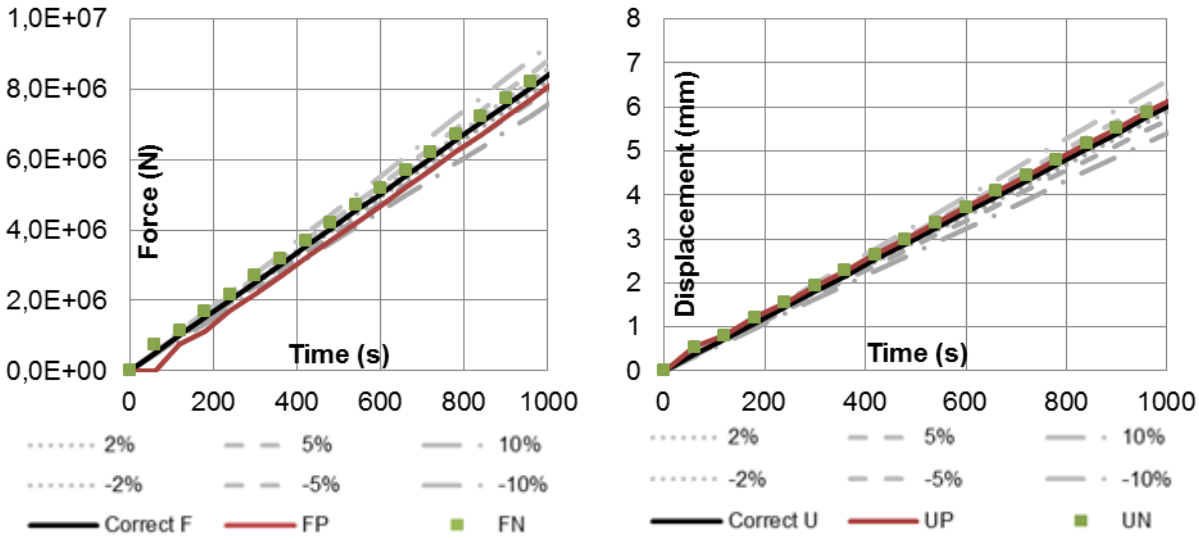


*d)* $\Delta t = 60\ s;\ \Delta t_P = 60\ s$

**Figure 4-16. The evolution in time of the interface forces and displacement when the delay time $\Delta t_P$ varies**

The conclusion of this exercise is that the value of the time step along with the delay time influences the accuracy of the results. The values of $\Delta t$ and $\Delta t_P$ depend on the type of the analyzed structure and the furnace facility.

For the structures where the variation of the interface forces and displacements is slow during the test it might be sufficient a bigger time step and delay time compared with the structures where the variation of the interface forces and displacements is fast during the test.

The furnace facility influences the value of the delay time. The delay time represents the time needed for the actuator to impose new values on the interface.

The furnace facility influences the value of the delay time. The delay time represents the time needed for the actuator to impose new values on the interface.

Note that the resolution and the precision of the data acquisition system and transfer system have an influence on how to choose the values for the time step and delay time. If the time step is small and the variation of the interface forces and displacements is also small then the values cannot be physically measured in the furnace.

Once the above presented conditions are full field the user should perform a study in order to be able to choose the correct value of the time step and delay time and thus to produce accurate results during the hybrid process.

- *Displacement control procedure*

The same exercise as for the force control procedure is done for the displacement control procedure.

The objective is to observe the results when the stiffness ratio is kept constant along with the delay time of the actuators. The time step instead will vary inducing different results at the interface of the PS and NS.

In this numerical exercise, the correct behavior is known and it will be used to make the comparison with the solution generated by the hybrid methodology.

The value of the stiffness ratio considered in this example is $R = 2$ while the delay time caused by the actuator is considered $\Delta t_P = 1s$.

The evolution of interface forces and displacements is presented for different values of the time step $\Delta t$, i.e. 1 min (see Figure 4-17 a)), 5 min (see Figure 4-17 b)), 10 min (see Figure 4-17 c)) and 15 min (see Figure 4-17 d)). The various values of the time step are chosen randomly for this example to observe the influence on the results. More than that, for every graph a deviation from the correct solution is printed. The deviation is also selected randomly as a percentage of the correct value such as 2%, 5% and 10%.

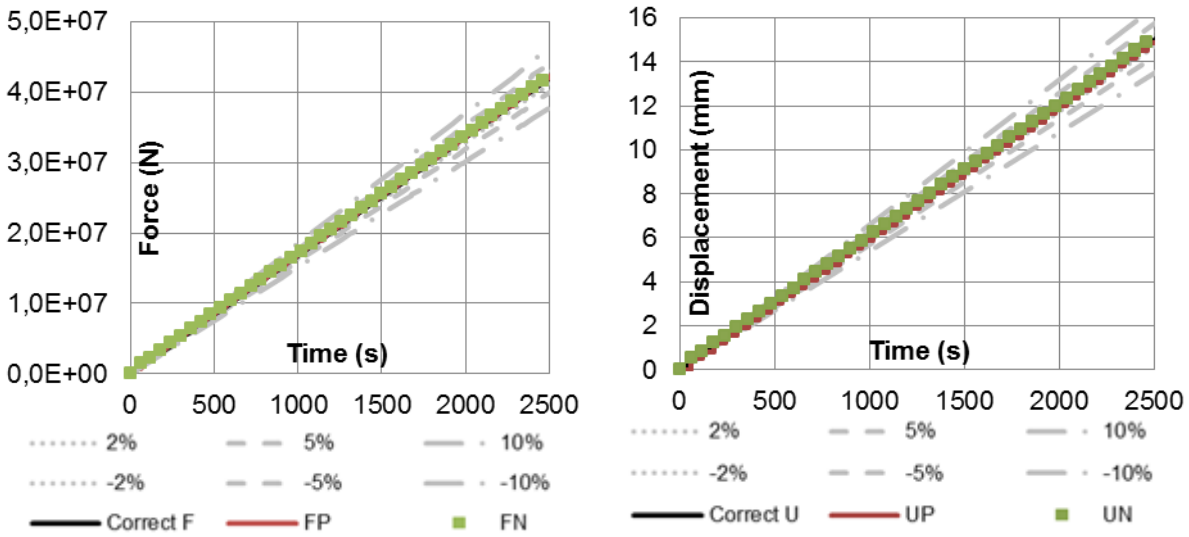


*a)* $\Delta t = 300\ s;\ \Delta t_P = 1\ s$

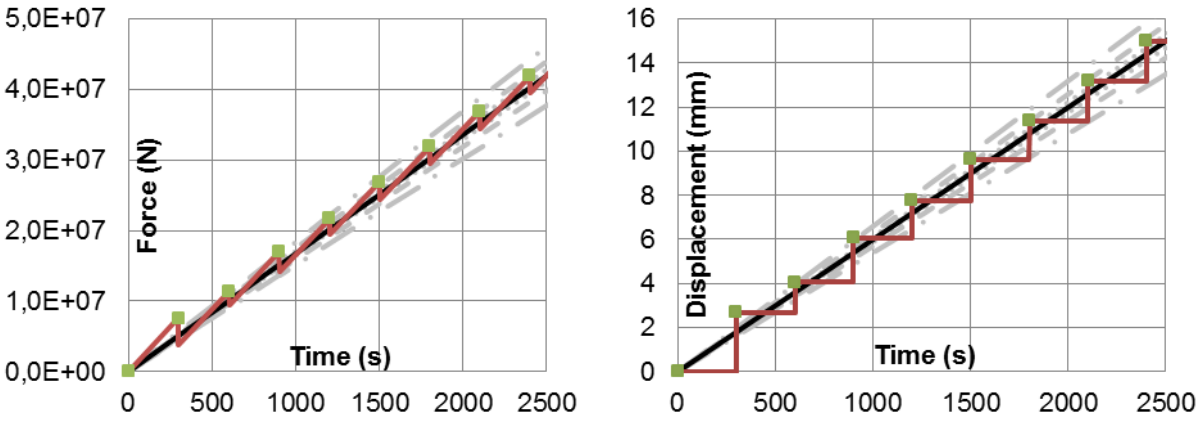


*b)* $\Delta t = 300\ s;\ \Delta t_P = 1\ s$

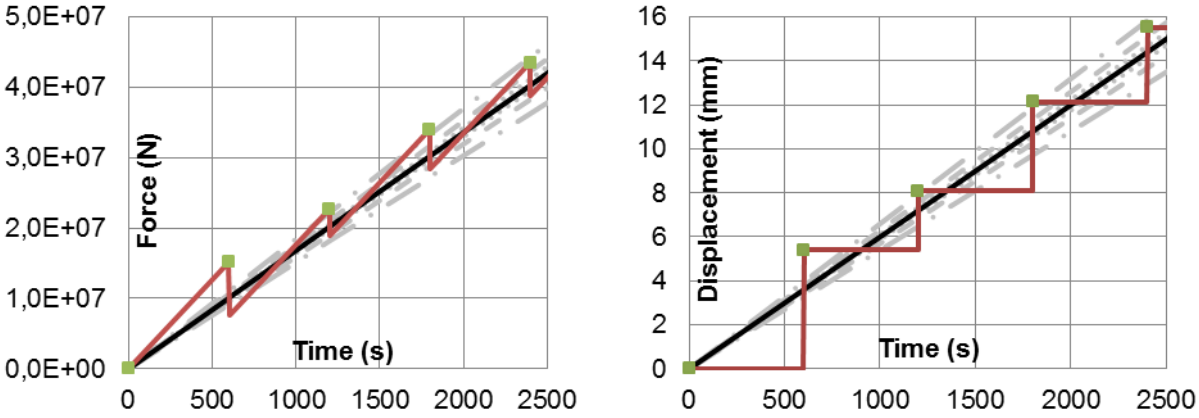


*c)* $\Delta t = 600\ s;\ \Delta t_P = 1\ s$

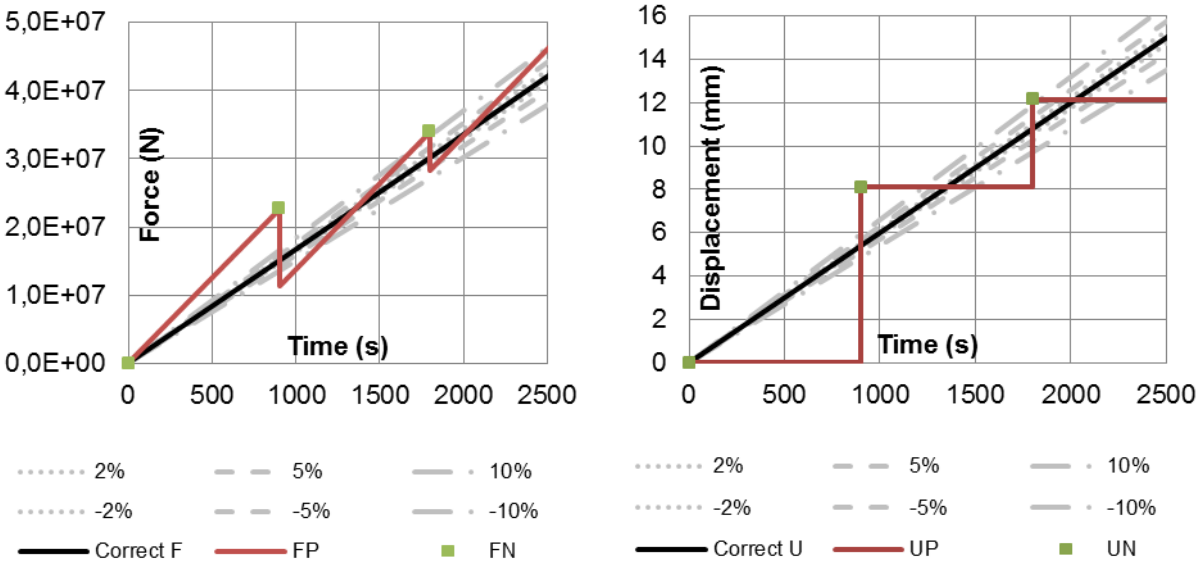


*d)* $\Delta t = 900\ s;\ \Delta t_P = 1\ s$

**Figure 4-17. Evolution of the boundary conditions when $R > 1$ and $\Delta t$ varies in DCP**

When the time step is equal to 1 min then the resulted solution at the interface of the PS and NS does not exceed the correct value more than 5% of the correct solution.

Once with the increase of the time step, the solution provided by the hybrid process deviates more and more from the correct solution. Nevertheless, the hybrid solution oscillates around the correct solution.

Generally, the value of the time step depends on the delay time of the actuators, on the time calculation of the new solution to be applied and the time transfer of the information between the substructures. More details about the components of the time step are discussed in the section 3.5.

Another component to influence the choice of the time step is the structural element to be tested. Some structural elements undergo large deformation early in the test. Thus the change of the interface condition is more pronounced in a short time. For example, the steel exposed structure experience larger displacements in a shorter time compared with the concrete structural elements exposed to fire. In this situation the needed time step might results with more reduced values than in the case of a concrete structure. The user defines the value of the time step based on the characteristics of the furnace facility as well as the type of the analyzed structural system but at the same time aiming accurate results.

The hybrid process is not only characterized by the stability criterion but also from the accuracy point of view. The results are considered accurate if the interface solution of the PS does not exceed a certain percentage of the interface solution of the NS as presented in the section 3.6. The solution provided by the hybrid fire testing needs to reproduce the correct solution too. Depending on the objective of the project, the deviation will be defined by the user.

In practice, in some cases the correct behavior of the analyzed structure is not predictable. These cases refer to the situation when the behavior of the PS is unknown and therefore impossible to be modeled in the FE model.

Next, stiffness ratio is kept constant $R = 2$ along with the time step $\Delta t = 60s$ and the influence of the actuators delay time $\Delta t_P$ will be analyzed. Figure 4-17 a) shows accurate results in the hybrid process if the time step is chosen equal to 60s.

Figure 4-18 presents the force-displacement evolution at the interface of the substructures along with the correct solution when the actuators delay time varies. It can be observed that the PS solution can diverge from the NS solution once the delay time of the actuator increases.

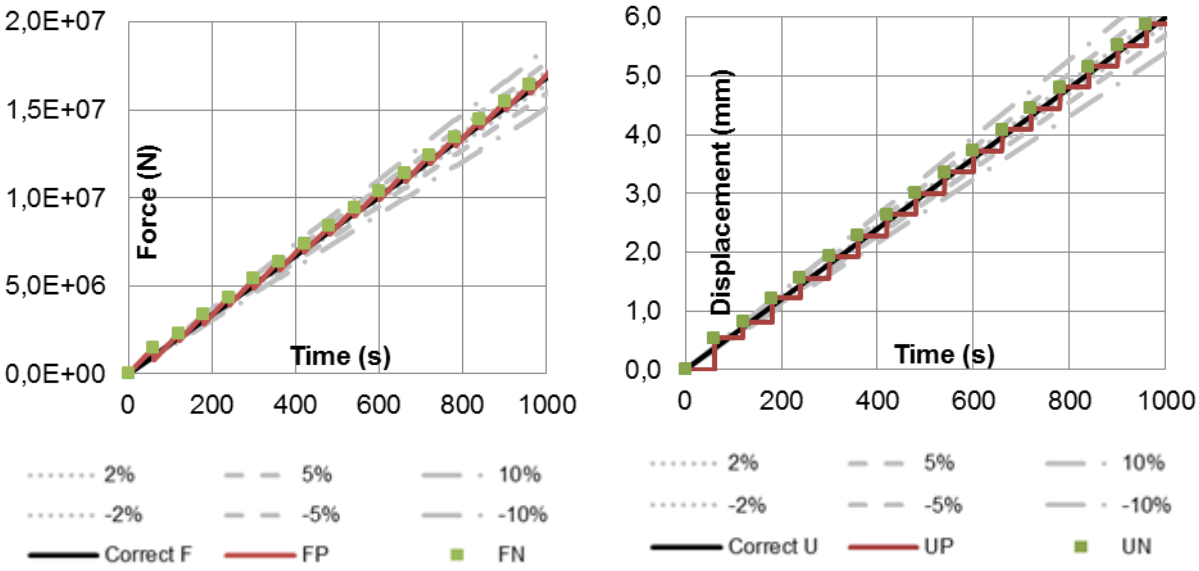


*a)* $\Delta t = 60\ s;\ \Delta t_P = 1\ s$

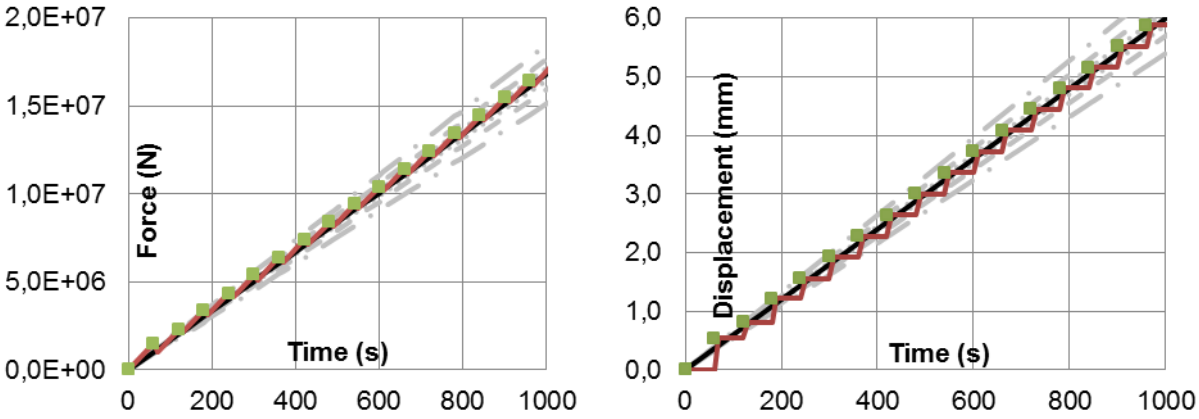


*b)* $\Delta t = 60\ s;\ \Delta t_P = 10\ s$

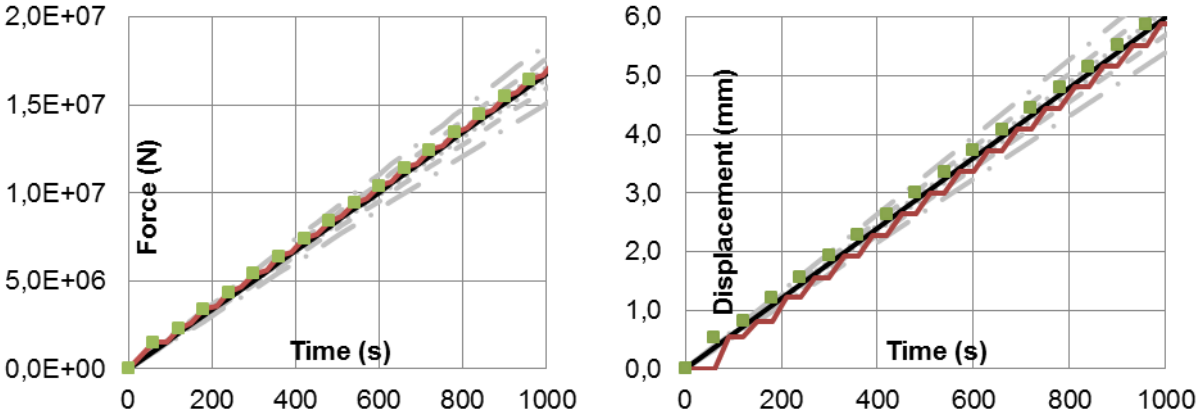


*c)* $\Delta t = 60\ s;\ \Delta t_P = 30\ s$

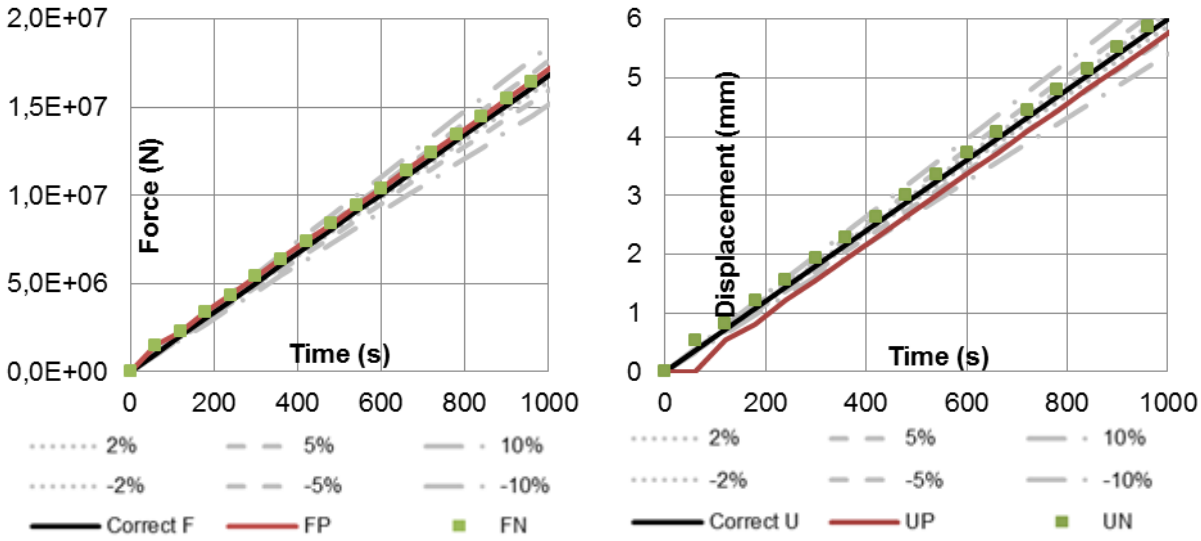


*d)* $\Delta t = 60\ s;\ \Delta t_P = 60\ s$

**Figure 4-18. The evolution in time of the interface forces/displacements when the time step $\Delta t_P$ varies**

Every time step $\Delta t$ the interface data (forces and displacements) of the substructures are used to compute the new solution to be updated at the interface. To reach the interface equilibrium and compatibility requires applying the new solution on the interface while the forces and displacements have the same value as the ones used for the calculation of the new solution. There is a delay time to impose the new solution on the interface due to the time response of the actuators. In all this time the PS continues to be heated and the interface forces and displacements change. The difference between the time when the calculation of the new solution is done until the same solution is applied on the substructures varies from case to case.

Importance is given to the total needed time to apply the new solution such as the equilibrium and compatibility are reached and the correct solution is reproduced. Just for reminder, the correct solution represents the solution at the interface when the studied structure is analyzed as a single entity (with no substructuring).

In Figure 4-17 it can be observed that with the increase of the time step, the equilibrium and compatibility are not satisfied. The user can choose to define a permissible error value to be reached during the hybrid tests with the condition that the quality of the results is not perturbed. Some specific situation might require an important time to update the solution in the furnace. In this cases if the defined error value is not exceeded then the hybrid process can be still applied.

*The variation of the stiffness ratio*

- Force control procedure

The objective of the exercise in this section is to see if the decrease of the stiffness ratio induces changes in the accuracy of the results. Thus the stiffness ratio varies from values of 1

until 0.02. The time step of $\Delta t = 60\ s$ and the delay time of the actuators of $\Delta t_P = 10\ s$ is considered sufficient for this exercise.

Figure 4-19 shows that the reduction of the stiffness ratio value still produce accurate results (in the defined range).

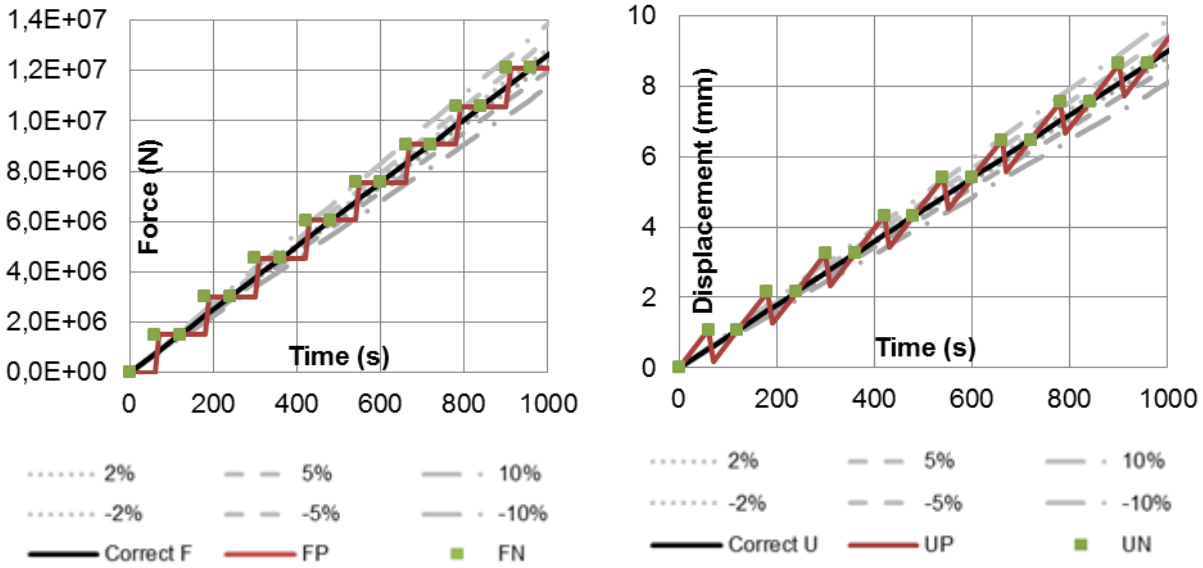


***a)*** $\boldsymbol{R = 1}$

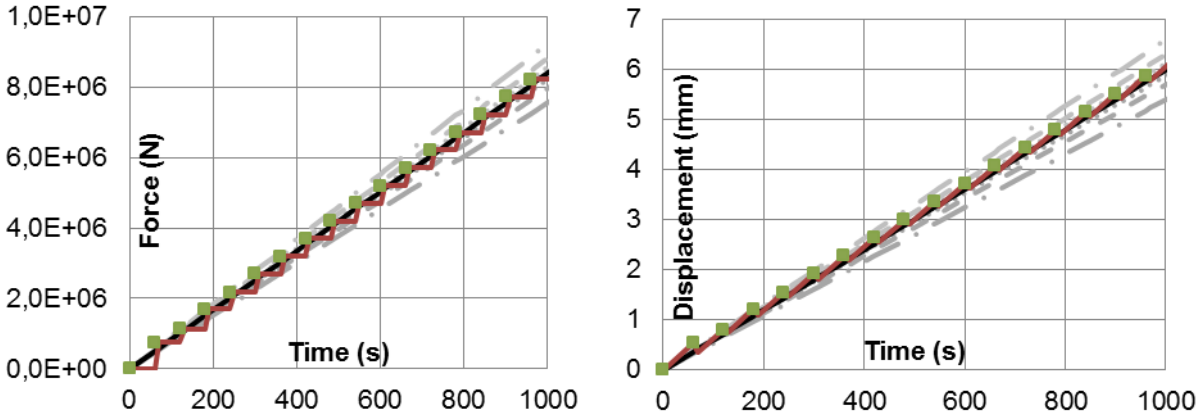


***b)*** $\boldsymbol{R = 0.50}$

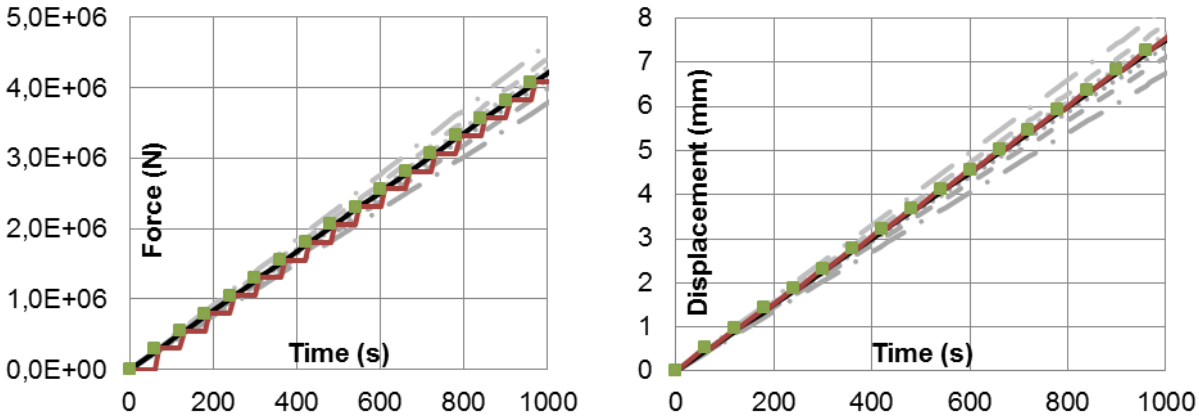


*c)* $R = 0.20$

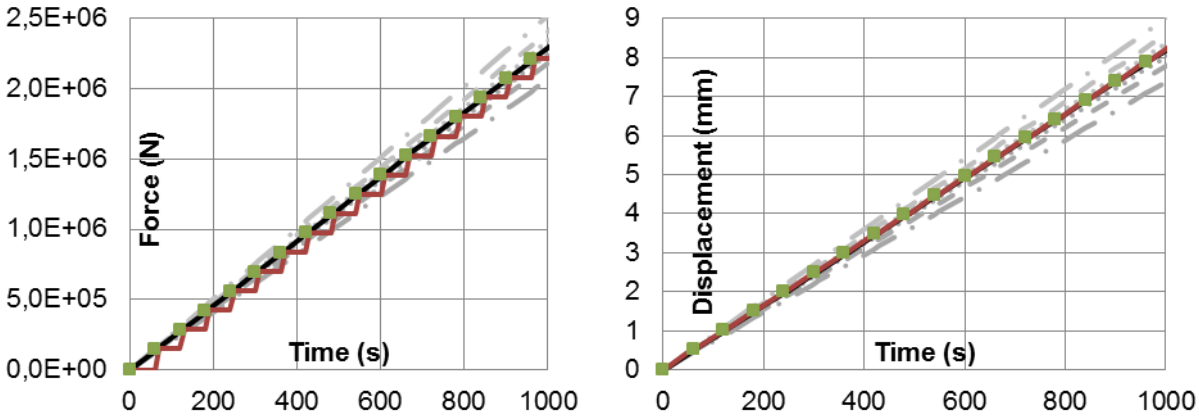


*d)* $R = 0.10$

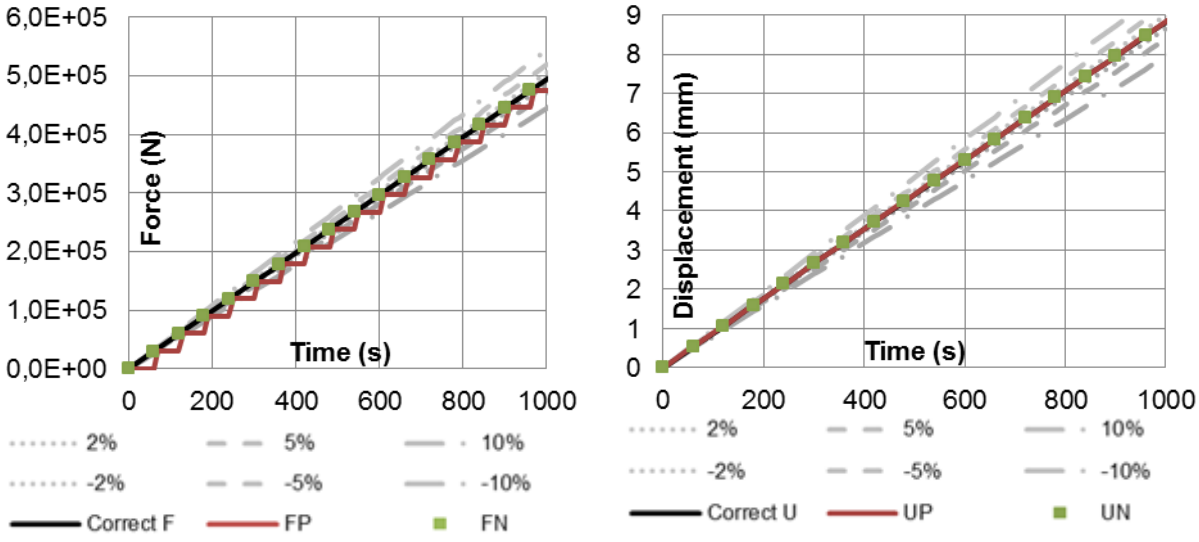


*e)* $R = 0.02$

**Figure 4-19. Evolution of interface forces and displacements for different stiffness ratios (FCP)**

- *Displacement control procedure*

The first generation method produces damage (instability) during the tests when the NS and PS have the same stiffness, i.e. stiffness ratio equal to one. The stiffness ration can be either smaller than one during the entire hybrid tests or on the contrary the stiffness ratio should always be bigger than one in order to apply the first generation method (and to avoid the instability of the process).
The influence of the stiffness ration on the accuracy of the results is next studied. Figure 4-20 presents the evolution of interface forces versus displacements when the time step and the delay time of the actuators are constant and the stiffness ratio varies. The time step is $\Delta t = 60\ s$ and the delay time of the actuators is $\Delta t_P = 10\ s$. The stiffness ratio varies from values of $R = 1$ until $R = 50$.
In the same figure it can be observed that the increase of the stiffness ratio does not affect considerably the error on the PS's interface. Moreover in this specific case the error decreases while the fire advances.

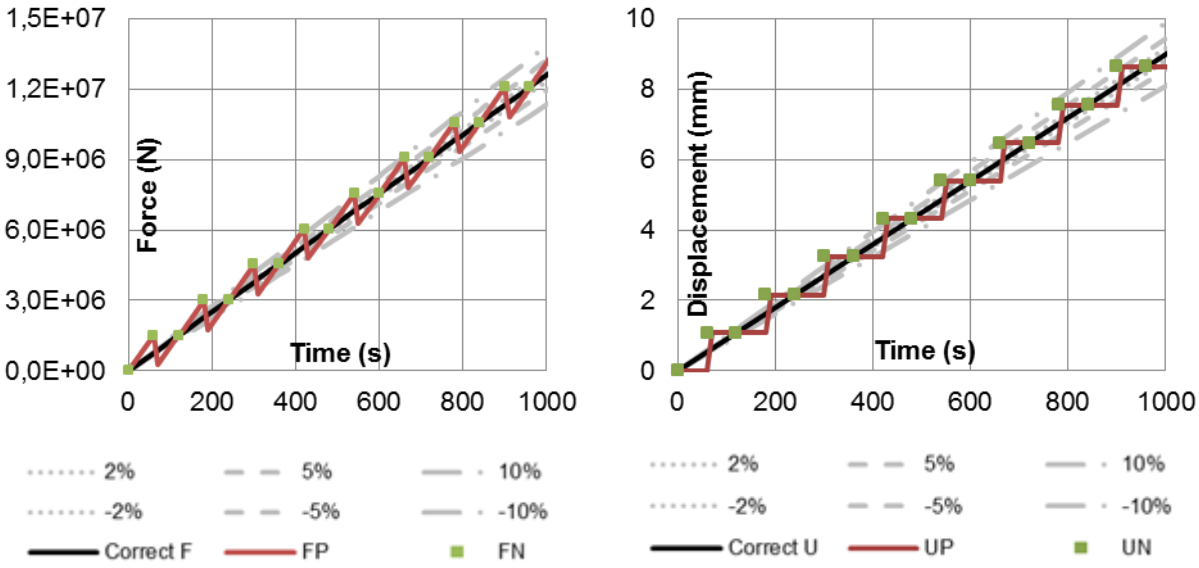


***a) $R = 1$***

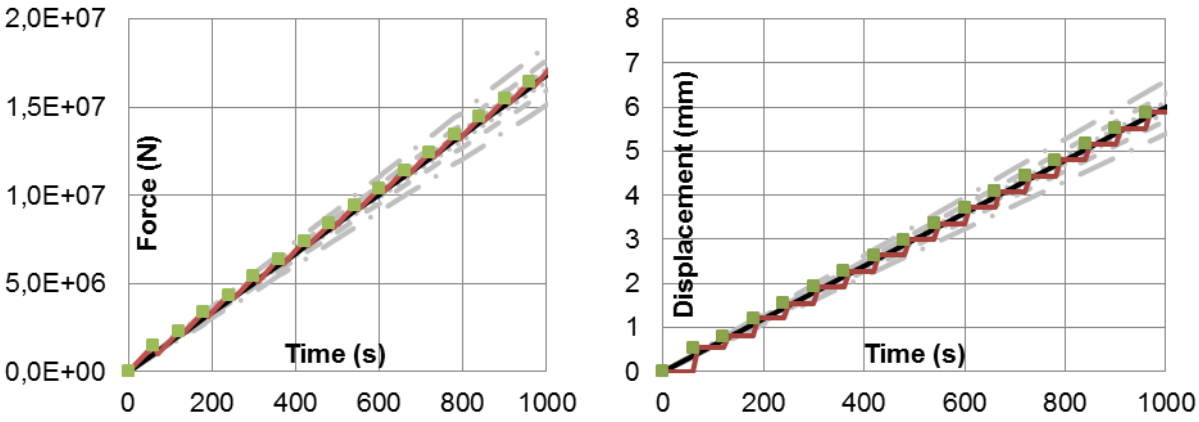
2,0E+07
1,5E+07
1,0E+07
5,0E+06
0,0E+00
Force (N)
Time (s)
0
200
400
600
800
1000
8
7
6
5
4
3
2
1
0
Displacement (mm)
Time (s)
0
200
400
600
800
1000

*b)* $R = 2$

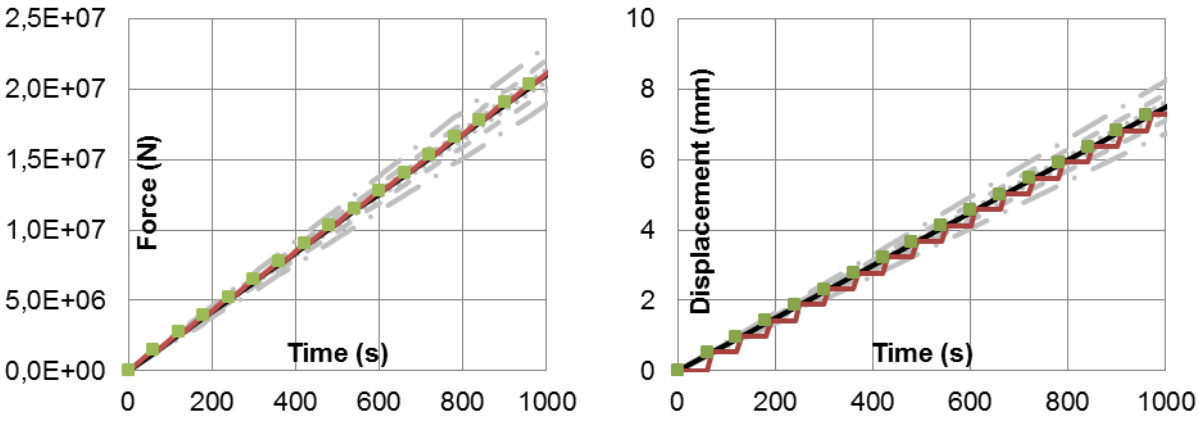
2,5E+07
2,0E+07
1,5E+07
1,0E+07
5,0E+06
0,0E+00
Force (N)
Time (s)
0
200
400
600
800
1000
10
8
6
4
2
0
Displacement (mm)
Time (s)
0
200
400
600
800
1000

*c)* $R = 5$

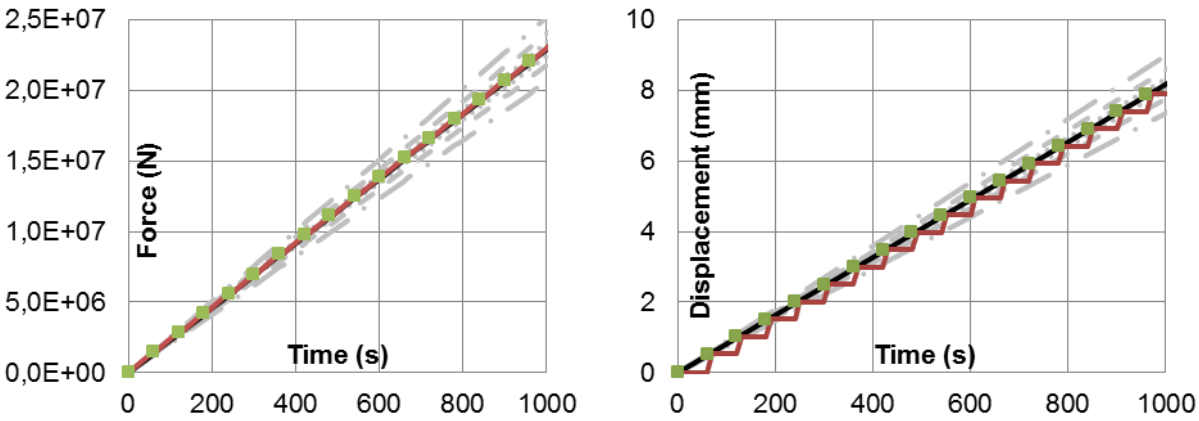
2,5E+07
2,0E+07
1,5E+07
1,0E+07
5,0E+06
0,0E+00
Force (N)
Time (s)
0
200
400
600
800
1000
10
8
6
4
2
0
Displacement (mm)
Time (s)
0
200
400
600
800
1000

*d)* $R = 10$

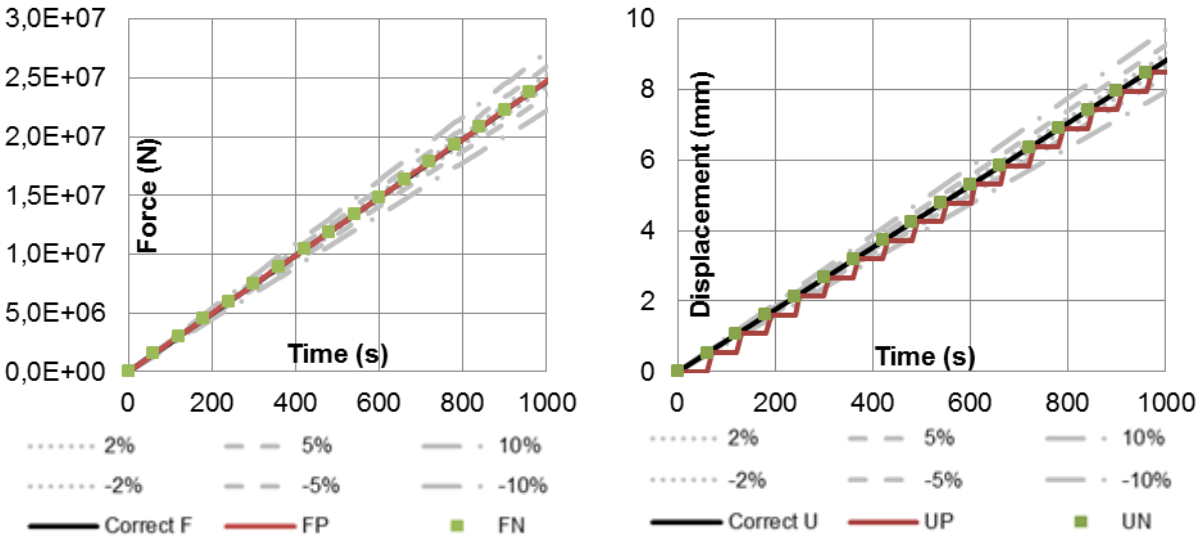


***e)*** $\boldsymbol{R = 50}$

**Figure 4-20. Evolution of interface forces versus displacements for different stiffness ratios R (DCP)**

# 5. PROPOSED METHOD FOR HFT: THE SECOND GENERATION METHOD

## 5.1. Introduction

In the previous chapter the stability conditions of the first generation method have been discussed. The latter method can be applied under specific conditions in order to be successful.

Depending on the stiffness ratio between the numerical substructure NS and the physical substructure PS, referred to as the stiffness ratio and noted as $R$, two procedures can be adopted when performing hybrid testing. One of the procedures is to control displacements at the interface while the other is to control forces. The choice of the procedure depends on the value of the stiffness ratio. When the stiffness of the NS is bigger than the stiffness of the PS during the test, i.e. $R > 1$, the displacements need to be controlled in order to ensure the stability while for the case when the stiffness of the PS is bigger than the one of the NS, i.e. $R < 1$, the force control procedure is required.

At ambient conditions the stiffness ratio can be estimated but is not the case when the structure is exposed to fire. The heat will lead to a decrease of stiffness of the exposed substructure thus the stiffness ratio will be changing during the hybrid test. The estimation of change in the stiffness ratio is not easy to be done therefore the chosen procedure at ambient conditions can become inappropriate once the fire exposure advances inducing instability in the process.

Inspired from seismic field one solution to avoid the instability can be the *switch* from one procedure to another during the hybrid test by the time when the stiffness ratio is approaching the critical value of one. In order to be able to change the procedure, the time when the value of stiffness ratio changes from a value smaller/bigger than one to a value bigger/smaller than one needs to be known. But as discussed previously the prediction in change of the stiffness ratio is almost impossible to be done. First because the stiffness ratio measured during the test can be incorrect due to the experimental errors encountered during the tests. Some attempts have been done to establish the stiffness of the PS during the test [79] but more research is needed to prove the advantage of doing so. Secondly some specific phenomenon can occur when the PS is exposed to fire. For example concrete elements can experience spalling, phenomenon which occurs suddenly inducing an important change in the stiffness. The prevision of this phenomenon cannot be done either the time of switching the procedure. Therefore, even the use of different procedures during one hybrid test is challenging due to the same reasons of being almost impossible to predict the change in the stiffness ratio due to the fire exposure and the entire specific phenomenon which are induced by the fire. The switch needs to be stable and fast beside the disadvantage of not knowing the time when it

should occur. Moreover, the testing laboratory should dispose on accurate force and displacements control at the same time. Research needs to be done in this field just to see if the change in the stiffness ratio can be estimated during the hybrid test and if the switch of procedure can be applied. In the case of multiple degrees-of-freedom, the stiffness ratio for each DoF can be bigger than one or smaller than one. Having different stiffness ratio for different DoFs would imply the use of different procedures during the same hybrid fire test. No hybrid fire tests have been performed when using different procedures in the same test. In seismic field, Elkhoraibi and Mosalam [80] implemented switch control hybrid simulation, switching between displacement and force control depending on the secant stiffness and the restoring force.

The displacement or force control procedures have their own advantages and challenges. Conventional hybrid simulation in seismic field is conducted in displacement control procedure. The main advantage of displacement control procedure is that the numerical models are developed to solve for displacements during the hybrid test. Some challenges can be underlined in this situation such as the difficulty of testing stiff specimens, or when performing fast tests and even when multiple DoFs are tested (depending on the loading direction). Dynamic effects in the physical model can be induced in case of fast tests. In the case of stiff specimens every small variation in displacements causes big variation in forces. Small errors during the experimental process when reading the imposed displacements can induce forces which are inappropriate leading to incorrect results or even to failure. One solution can be the use of accurate transducers with high resolution being able to estimate correctly the imposed displacement as presented by Whyte in [78]. The other solution is to use a force control procedure to avoid the errors coming from the small displacements to be imposed when stiff structures are tested. Challenges in the force control method are the fact that most numerical models are implemented in displacement control, along with some experimental errors.

Hence to overcome the instability of the first generation method it is necessary to utilize mixed force/displacement control, or switching during simulation between force and displacement control.

The mixed force/displacement control is recommended for multiple DoFs with different stiffness ratios (smaller or bigger than one) while the switch of the procedure could be done in the situation when the stiffness ratio for one DoF would exceed the frontier value of one. However, very little research has been conducted in these challenging areas so far. The disadvantage of doing so is the fact that these procedures induce complexity in the experimental process and if are not correspondently used the results can lead to incorrect values and instability.

To avoid these complex combinations between the force control procedure and displacement control procedure a new method should be developed independently on the stiffness ratio between the substructures. Thus the instability is avoided and this eliminates the necessity of knowing the time when the switch of the procedures should be done (depending on the stiffness ratio evolution during the test). In this way the methodology can be applied either in

displacement control procedure or force control procedure and there is no need for mixed force/displacement procedure.

Therefore, this chapter describes a new methodology which has been developed for hybrid fire testing, as an original contribution of this thesis. This methodology is called "second generation method" in this work as an acknowledgment of the fact that it follows the pioneering works of previous researchers using straightforward force/displacement control procedures for HFT, yet is built on a different formulation of the problem that leads to (virtually, i.e. under perfect testing conditions) unconditional stability as will be presented in the following parts. The chapter describes first the theoretical background of the methodology, with links to the finite element tearing and interconnecting (FETI) method. Then, the principle and equations of the methodology are given. Finally, some examples are presented.

## 5.2. Theoretical background of the second generation method

### 5.2.1. FETI method. Description. Characteristics

The new method needs to be stable independently on the stiffness ratio between the NS and PS, to ensure the equilibrium and compatibility at the interface and moreover to provide accurate results, i.e. results which correspond to what would be obtained if the structure was tested as a complete structure.

If the methodology is stable independently on the stiffness ratio then:

- The degradation of the stiffness ratio does not need to be accounted during the test;
- Only one procedure can be used during the entire test (displacement control procedure or force control procedure) avoiding the complex solution of applying the mixed force/displacement procedure or switching the procedures during the test when the case;
- Multiple DoFs can be controlled independently on the stiffness ratio;

Farhat and Roux in [79] have described the method called "Finite element tearing and interconnecting method (FETI)" which has been developed for spatial domain needed to be partitioned into a set of totally disconnected subdomains, each assigned to an individual processor. Lagrange multipliers are introduced in order to inforce compatibility at the interface nodes. Only the solution for the static problems is treated in the paper which is a departure from the classical method of substructures. The solution includes the case of floating subdomains (substructure which experiences rigid body movements). Valk in [82] presents an extension of the method presented by Farhat and Roux for dynamic cases.

Next, a general description of the method in static case will be made based on the information presented in [79].

The algebraic system presented in equation (48) is considered to ensure the equilibrium and compatibility between the substructures.

$$\begin{aligned} K_P u_P &= E_P + B_P^T \lambda \\ K_N u_N &= E_N - B_N^T \lambda \\ B_P u_P &= B_N u_N \end{aligned} \tag{48}$$

Where:

$K_j$ is the stiffness matrix of the substructure, $u_j$ is the displacement vector while $E_j$ is the prescribed force vector associated with the substructure. The subscript $j$ becomes $P$ when referring to the PS and $N$ for the NS. The vector of Lagrange multipliers $\lambda$ represents the interaction forces between the two substructures at the interface. $B_j$ represents the connectivity matrix. The connectivity matrix is a Boolean matrix (only terms of one and zero) with the role of connecting the DoFs of one substructure with the corresponding DoFs of the other substructure.

Each substructure $j$, is described by the interior nodal unknowns and the interface nodal unknowns. The number of the interior nodal unknowns will be referred to as $n_j^S$ and the number of interface nodal unknowns as $n_j^I$. The total number of interface nodal unknowns is noted by $n_I$. In the particular case of two substructures note that $n_I = n_1^I = n_2^I$. The form of the two connectivity matrices $B_P$, and $B_N$ depends on the how the numbering of the interior and interface DoFs is considered. If the interior degrees of freedom are numbered first and then the interface ones, the connectivity matrix is described by Eq. (49) where $O_j$ is an $n_j^I$ x $n_j^S$ null matrix and $I_j$ is the $n_j^I$ x $n_j^I$ identity matrix. The vector of Lagrange multipliers $\lambda$ is $n_I$ long.

$$B_j = (O_j \quad I_j) \qquad \text{j=1, 2} \tag{49}$$

The displacement of the substructures can be deduced by using the first two equation of the system described by (48) only if both $K_P$ and $K_N$ are non-singular. The two displacements will be replaced in the third equation (the compatibility equation) and grouped depending on the Lagrange vector. Eq. (50) presents the discussed steps.

$$\begin{aligned} u_P &= {K_P}^{-1}(E_P + B_P^T \lambda) \\ u_N &= {K_N}^{-1}(E_N - B_N^T \lambda) \\ (B_N {K_N}^{-1} B_N^T + B_P {K_P}^{-1} B_P^T)\lambda &= B_N {K_N}^{-1} E_N - B_P {K_P}^{-1} E_P \end{aligned} \tag{50}$$

Finally the solution is obtained by solving first the third equation of the system for the Lagrange multipliers $\lambda$, then substituting these in the first and second equation back solving for $u_P$ and $u_N$.

The described methodology was widely used in the numerical simulations just to gain some time in the calculation and to be able to model complex structure.

In the case of hybrid simulation process the approach of FETI method will be next presented.

The first and second equation can be expressed in the form presented by Eq. (51).

$$\begin{aligned} K_P u_P - (E_P + B_P^T \lambda) = 0 \\ K_N u_N - (E_N - B_N^T \lambda) = 0 \end{aligned} \tag{51}$$

The left term of the equations can be replaced by $r_j(u_j)$ and we will refer to it as the residual vector (see Eq. (52)). The residual vector needs to be always equal to zero to satisfy the equilibrium condition between the substructures.

$$\begin{aligned} r_P(u_P) = 0 \\ r_N(u_N) = 0 \end{aligned} \tag{52}$$

Let us express the residual equation in terms of $n+1$ time step displacement $u_{n+1}$ only, as it is presented in Eq. (53).

$$r(u_{n+1}) = 0 \tag{53}$$

Thus to find the interface solution a set of the non-linear equation are required to be solved. Most of the methods for solving a set of non-linear equations make use of linearization techniques.

If $u_{n+1}^k$ represents an approximate value of $u_{n+1}$ resulting from iteration *k* then the residual equation can be replaced with enough accuracy by the linear expression given by Eq. (54).The replacement is done in the neighborhood of the value $u_{n+1}^k$.

$$r(u_{n+1}^{k+1}) = r(u_{n+1}^k) + \left[\frac{\partial r}{\partial u}\right]_{u_{n+1}^k} (u_{n+1}^{k+1} - u_{n+1}^k) \tag{54}$$

For equilibrium the residual force for the iteration *k+1* should be equivalent with zero as presented in Eq. (55).

$$r(u_{n+1}^{k+1}) = 0 \tag{55}$$

Further on, Eq. (54) can be rewritten under the form presented in Eq. (56) accounting for the fact that the residual force for the iteration *k+1* is equal to zero as presented in Eq. (55).

$$-\left[\frac{\partial r}{\partial u}\right]_{u_{n+1}^k} (u_{n+1}^{k+1} - u_{n+1}^k) = r(u_{n+1}^k) \tag{56}$$

Where:

$$\left[\frac{\partial r}{\partial u}\right]_{u_{n+1}{}^k} = \left[\frac{\partial}{\partial u}(Ku - (E_P + B_P^T \lambda))\right]_{u_{n+1}{}^k} = K \tag{57}$$

The final form of the Eq. (56) is presented in the Eq. (58) where $\frac{\partial r}{\partial u}$ represent in this case the variation of the internal forces with respect to displacements and thus represents the tangent stiffness matrix $K$.

$$\left(u_{n+1}^{k+1} - u_{n+1}^{k}\right) = -K^{-1}\, r\left(u_{n+1}^{k}\right) \tag{58}$$

For the iteration *k+1* the solution results by solving the non-linear system in an iterative manner by means of the Newton-Raphson method.
An iterative process needs to be implemented due to the fact that the stiffness of the PS is unknown in the solving process.

The Eq. (59) presents the residual of the physical and numerical substructures for every iteration, depending on the Lagrange multipliers. The Eq. (59) has been written based on the equation (51) and (52). The terms $K_P u_{P,n+1}^{k}$ and $K_N u_{N,n+1}^{k}$ represent the interior forces of the PS and NS, $E_{n+1}^{P}$ and $E_{n+1}^{N}$ represent the exterior loads applied on the PS and NS, while the last term of the residual force is given by the interface forces $\lambda_{n+1}^{k+1}$ affected by the transpose of the connectivity matrix $B_P^T$ and $B_N^T$. In this stage of the problem the restoring forces of the substructure and the exterior loads are known. The only unknowns are the interface forces, this being the next step of solving one step hybrid simulation problem. In hybrid fire testing the $E_{n+1}^{P}$ and $E_{n+1}^{N}$include the effect of fire on the substructure. Therefore during the test in the furnace the registered reaction force is the couple $(K_P u_{P,n+1}^{k} - E_{P,n+1})$. For the numerical substructure the reaction force used in the calculation is $(K_N u_{N,n+1}^{k} - E_{N,n+1})$.

$$r\left(u_{P,n+1}^{k}\right) = K_P u_{P,n+1}^{k} - E_{P,n+1} - B_P^T \lambda_{n+1}^{k+1}$$

$$r\left(u_{N,n+1}^{k}\right) = K_N u_{N,n+1}^{k} - E_{N,n+1} + B_N^T \lambda_{n+1}^{k+1} \tag{59}$$

Based on the Eq. (58) the displacements for iteration *k+1* can be written in the form of the Eq. (60). This values are expressed in terms of displacements computed at *k* iteration $u_{P,n+1}^{k}$ and $u_{N,n+1}^{k}$, the stiffness's of the substructures $K_P^*$ and $K_N^*$ plus the value of residuals presented in Eq. (59). Please note that the stiffness values of the substructure is affected by the superscript "*" suggesting that the considered stiffness in the calculation it might be different than the real one. It has been discussed that the estimation of the PS's stiffness is difficult to be done during the test so the initial tangent stiffness will be considered in the calculations. The stiffness of the NS can be predetermined before the test if the NS is cold while for the exposed NS the stiffness can be computed every time step. Therefore the stiffness of the NS usually is known but in the presented formulation the superscript "*" will be still conserved.

$$u_{P,n+1}^{k+1} = u_{P,n+1}^{k} - K_P^{*-1} r\left(u_{P,n+1}^{k}\right)$$

$$u_{N,n+1}^{k+1} = u_{N,n+1}^{k} - K_N^{*-1} r\left(u_{N,n+1}^{k}\right) \tag{60}$$

To fulfil the compatibility condition the same displacement are imposed at the interface for each iteration as presented in Eq. (61) with the connectivity matrix to match the displacement of the PS with the displacements of the NS. The displacements in the Eq. (61) have the values presented by the Eq. (60).

$$B_P u_{P,n+1}^{k+1} = B_N u_{N,n+1}^{k+1} \tag{61}$$

The Eq. (61) is grouped in two parts (i) one part with the terms including the Lagrange multiplier and (ii) the rest of the terms. Then the Lagrange multiplier $\lambda_{n+1}^{k+1}$ results with the expression described by the Eq. **(62)**.

$$\lambda_{n+1}^{k+1} = \frac{B_P K_P^{*-1} K_P u_{P,n+1}^{k} - B_P K_P^{*-1} E_{P,n+1} - B_N K_N^{*-1} K_N u_{N,n+1}^{k} + B_N K_N^{*-1} E_{N,n+1}}{B_N K_P^{*-1} B_N{}^T + B_P K_N^{*-1} B_P{}^T} \tag{62}$$

Once the Lagrange multiplier is known, the residual forces presented by the Eq. (59) are computed. In the final stage of one iteration the displacements presented by Eq. (60) are solved.

The computed displacements are imposed on the PS and NS. The compatibility is ensured as the interface displacements of the PS are equal to the interface displacements of the NS. The imposed displacements will generate reaction forces (or restoring forces). The interface forces of the PS need to be in equilibrium with the restoring forces of the NS. Just because in the calculation process the initial tangent stiffness of the PS $K_P^*$ is considered (without considering the degradation due to the fire exposure) the resulting reaction force in the furnace will be different than the reaction force of the NS. Thus the equilibrium will not be satisfied.

To reach the equilibrium iterations are needed in order to converge to the correct solution with equilibrium and compatibility ensured at the interface of the substructures.

There is specificity though in the field of fire engineering. When the iteration process is undergoing, the interface forces are required to be constant. The difficulty in hybrid fire testing comes from the fact that the interface forces are always changing due to the fire exposure. This means that the equilibrium at the interface is never reached. By the time when new displacements are computed all the information of the previous step (including reaction forces) are considered. When the computed displacements are applied on the substructures, the reaction forces of heated substructures (the PS is always exposed to fire whereas the NS is exposed to fire or not) does not correspond anymore with the one used in the calculation. So the computed displacements are not correct anymore just because do not force equilibrium at the interface.

Therefore, it had been challenging to find a solution on how to ensure the compatibility and equilibrium at the interface by still using in the calculation the initial tangent stiffness of the PS.

Note that the FETI method is applied in displacement control.

Next the steps of the presented solution will be described along with the reasons which leaded to the new hybrid fire method.

### 5.2.2. Flowchart of the FETI method

To fully understand how the method is applied in hybrid fire testing the information presented in the previous subchapter will be organized in a flowchart.

Before the flowchart every step will be explained in details.

*Steps of hybrid fire testing with FETI method*

1. The first step is to divide the analyzed structure in the PS and NS. By dividing we mean to choose the part of the analyzed structure which presents interest to be tested in the furnace (PS) while the remainder of the structure (NS) will be modeled aside via FE model or a predetermined matrix.
2. The PS is placed in the furnace, loaded with the external loads (usually maintained constant during the fire test) and interface loads (variable depending on the fire exposure).
3. The NS is modelled aside. One solution is to use a FE model to represent the NS or by using the predetermined matrix. If the FE model is considered, then before starting the hybrid test the NS will be loaded with the corresponding exterior forces and the interface forces. If the predetermined stiffness matrix is chosen to be used instead, will account for the effect of the loading on the NS.
4. The fire starts in the furnace and will induce changes into the boundary conditions of the PS. The equilibrium and compatibility are not anymore satisfied at the interface, thus the boundary conditions are required an update. The time step when the update will be done during the hybrid test is noted with $t_n^k = t_{n-1}^k + \Delta t$ where *n* is the number of the step and *k* is the number of the iteration within one step.
5. From the previous time step $t_{n-1}^k$ to the current time step $t_n^k$ the same displacements have been conserved on the interface. During one time step the reaction forces of the heated substructures will change due to the fire exposure. The reaction forces of the PS are registered in the furnace ($F_{P,n} = K_P u_{P,n-1}^k - E_{P,n}$). The reactions of the NS ($F_{N,n} = K_P u_{P,n-1}^k - E_{P,n}$) are computed using the predetermined matrix if the case, or are solved in the FE model in the other case. The reaction forces of the PS and NS correspond to the time step $t_n^k$.
6. The stiffness of the numerical substructure is known (if the NS is cold), but the stiffness of the PS is unknown. Thus the initial tangent stiffness is considered in the hybrid process and noted $K_P^*$. The stiffness of the NS considered in the calculation is noted with $K_N^*$.

7. The Lagrange multiplier $\lambda_n^{k+1}$ is computed using the reaction (restoring) forces of the substructures and the stiffness of the substructures.
8. Once the Lagrange multiplier is known, the new displacements $u_{P,n}^k$ and $u_{N,n}^k$which will be applied on the substructures can be computed. The resulted displacement of the PS and the NS are always equal.
9. The time calculation of one step is neglected therefore the new displacements are applied on the substructure at the time $t_n^k$. The time when the displacement is induced in the furnace is $t_n^k + \Delta t_P$. Due to the fact that the initial tangent stiffness of the PS is considered in the calculations the reaction forces resulted in the substructure will not be in equilibrium. The equilibrium can be restored only if the iterative process is implemented. During the iterative process k is incremented $k = k + 1$. The time delay is the second factor after the initial tangent stiffness matrix of the PS which will lead to loos of equilibrium as discussed in the section 3.6.
10. Once the equilibrium is restored, the iteration step is set to zero $k = 0$ while the step number is incremented $n = n + 1$ and we repeat the steps 5-9.

*Flowchart of hybrid fire testing with FETI method*

The flowchart is presented in the **Figure 5-1** with the mention that $ENR$ refers to the energy norm rate while $\varepsilon$ is the acceptable error. Information about the energy norm rate and the acceptable error will be given later on in the thesis.

**Figure 5-1. FETI method**

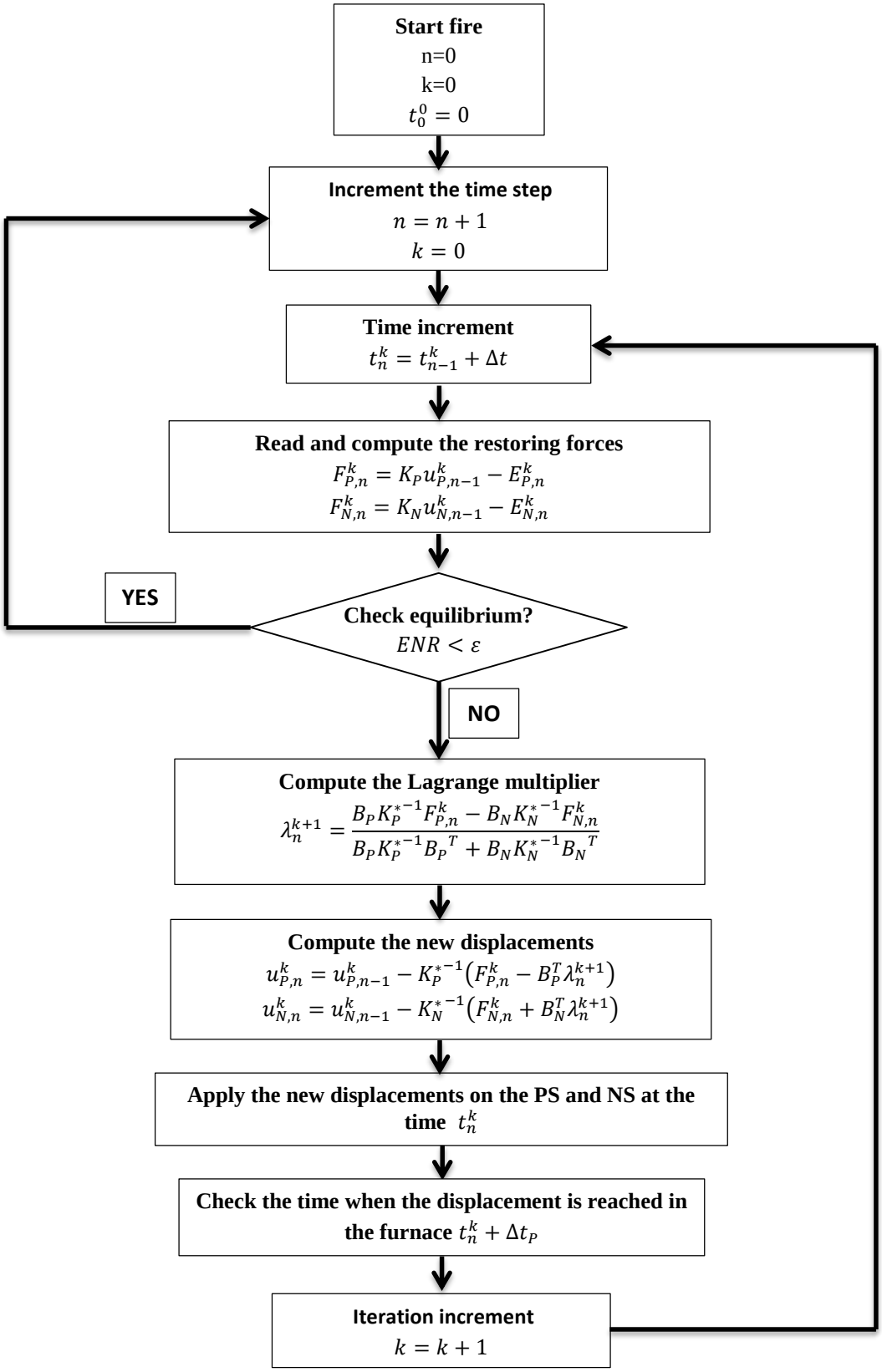

### 5.2.3. Equilibrium and compatibility at ambient temperature

The section 5.2.2 presents the steps of the hybrid fire testing when using FETI method.

The flowchart presents the method once the fire started.

Before starting the hybrid fire test, the equilibrium and compatibility at ambient temperature must be ensured.

Different reasons lead to the necessity of restoring the equilibrium at ambient temperature and the reasons will be next discussed.

Before starting the test, the PS is loaded in the furnace with the exterior loads and the interface conditions. When the loads are totally applied the interface reaction forces should be in equilibrium with the interface reaction forces of the NS. The compatibility is ensured by the fact that a displacement control procedure is considered (the same displacements are imposed at the interface).

Generally the equilibrium will not be ensured, the reaction forces of the PS will not equal the reaction forces of the NS.

Here are some possible reasons to explain why the equilibrium is not reached:

- The material behavior;
- Experimental site: supports, data acquisition system and transfer system;

The behavior of some materials is defined in the numerical model based on some hypothesis. This is why some difference occurs between the results measured during the experiments and the results from the numerical analysis. In this case, the equilibrium needs to be restored at ambient temperature before starting the hybrid fire test.

The experimental site can induce some differences in the PS's results compared with the results in the NS. For example, the provided support condition can be inappropriate and can induce some differences. Other sources of errors are the characteristic of data acquisition system and transfer system (e.g. inappropriate resolution of data acquisition system, poor tuning of the actuators etc.). The measurements in the furnace should be accurate in order to provide accurate results.

The conclusion of the above discussion is that the interface equilibrium will not be ensured right after the loads are applied on the substructure for different reasons. Before starting the hybrid fire test additional actions are required to endorse equilibrium.

A solution to restore the equilibrium at ambient conditions is to correct the interface displacements based on the out of balance forces. Thus the reaction forces of the substructures, the initial tangent stiffness of the PS along with the stiffness of the NS are used to compute new interface displacements.

The restoring of the interface equilibrium along with the new methodology will be presented in the section 5.3.

## 5.3. Development of the second generation method

The new hybrid methodology aims the following objectives:

- To be stable independently on the stiffness ratio between the substructures;
- To be simple and easy to apply;
- To ensure accurate results by forcing the interface equilibrium and compatibility every time step.

The method has been inspired from the finite element tearing and interconnecting method (FETI) and it controls the displacements during the HFT, based on the out of balance forces between the substructures. By analyzing the FETI method, it has been observed that the stiffness of the PS and NS is considered in the calculation of the boundary conditions. Therefore, in the second generation method besides the use of the NS's stiffness in the calculations, the stiffness of the PS will be also considered. In this way, the new method is unconditionally stable, independently on the stiffness ratio between the substructures.

### 5.3.1. Theoretical formulation

The key idea behind the second generation method is the fact that the stiffness of both the PS and the NS needs to be considered when relating the forces with the displacements at the interface. This contrasts with the first generation method, employed in all previous hybrid fire tests documented in the literature, in which only the NS's stiffness was considered.

This modification is far from trivial. In fact, it will allow the hybrid process to be stable independently of the ratio between the NS stiffness and the PS stiffness. In other words, it becomes possible for a fire laboratory which works in displacement control to perform a hybrid fire test for example on a concrete column axially restrained (R<1) as well as on a beam with rotational restraint (R>1), without the need to change their control system. More important, HFT in which several degrees of freedom are controlled can be conducted with a unique methodology.

In theory, the second generation method can be used in displacement control or in force control. The formulation to combine the PS's stiffness and the NS's stiffness differs for the two control strategies.

The displacement control configuration resembles a parallel circuit since the displacement at the interface is imposed to be the same for the PS and the NS. Therefore, the total stiffness of the two subsystems is equal to the sum of their individual stiffnesses, see Eq. (63).

$$K = K_P + K_N \tag{63}$$

Force control configuration, on the other hand, resembles a series circuit. The force at the interface is imposed to be the same for the PS and the NS. Therefore, the total stiffness of the

two subsystems is equal to the reciprocal of the sum of the reciprocals of their individual stiffnesses, see Eq. (64). Note that, in this case, the total stiffness is always smaller than the value of the smallest stiffness.

$$K = \left(\frac{1}{K_P} + \frac{1}{K_N}\right)^{-1} \quad \textbf{(64)}$$

### 5.3.2. The steps of the new methodology

A step by step description of the method is given here below.

a. The interface forces and displacements are determined before the start of the test by performing the analysis of the entire structure.
b. The PS is placed in the furnace and loaded with the exterior loads and interface displacements, while the NS is modeled aside. If a FE model is used to model the NS, the exterior forces and the interface displacements calculated at step *a* are applied on the NS. If a predetermined matrix is used to represent the behavior of the NS, then the matrix includes the effect of the loads on the NS.
c. The interface equilibrium for the ambient temperature will be restored if the case.
d. Heating of the PS starts. The interface displacements of the PS are blocked for the duration of a time step (displacement control procedure) and the reaction forces are measured.
e. Meanwhile, the displacements are blocked at the interface of the NS and the reaction forces of the NS are computed. If the NS is heated, the reaction forces vary during one time step. If the NS is kept cold, then the reaction forces is constant during one time step.
f. The measured reaction forces of the PS are compared with the computed reaction forces of the NS. Generally, the equilibrium is not ensured due to the fire effect.
g. To restore the equilibrium, the incremental displacement vector $\Delta\mathbf{u}$ will be calculated and applied at the interface. The calculation is based on the measured reaction forces of the PS and NS (the vector of out of balance forces $\Delta\mathbf{F}$ ). In the calculation process, the stiffness of the PS and the NS are accounted for, according to Eq. (65). This is the main difference with the first generation method (in which only the stiffness of the NS was considered) and the most important contribution that allows ensuring stability of the method.

$$\Delta\mathbf{u}(t_n) = (\boldsymbol{K}_P^* + \boldsymbol{K}_N^*)^{-1}\Delta\boldsymbol{F}(t_n) \quad \textbf{(65)}$$

h. The new calculated displacements are imposed on the PS and NS. There is some time needed to compute the reaction of the NS and to adjust the new displacements in the furnace.
i. The new imposed displacements will generate new reaction forces in the PS and NS. So the steps *e-g* are repeated until the end of the fire test.

To be able to make a comparison between the first generation method and the new method, the Eq. (66) illustrates the equation used to correct the interface displacements every time step for the first generation method (for displacement control procedure).

$$\Delta\mathbf{u}(t_n) = (\boldsymbol{K}_N^*)^{-1}\Delta\boldsymbol{F}(t_n) \quad \textbf{(66)}$$

By comparing the Eq. (65) with the Eq. (66) notice that the new method make use of the PS's stiffness for the correction of every time step displacements. As the stiffness of the PS is generally unknown during the HFT, several iterations would normally be needed at each time step to converge to the correct solution. As discussed previously, in a fire test, the evolution of temperature in the PS cannot be put to hold during the period requested to perform the iterations at every time step. During the time needed to perform the calculation in the computer and for the testing equipment to apply the corrections of displacements, the temperatures are still increasing, which modifies the stiffness of the PS, the restraint forces, etc. Hence, the convergence process tends to achieve an equilibrium that is constantly changing. As a result, it is not relevant to distinguish between iterations and time steps. Instead, the test can be performed by applying continuously Eq.(65), with a cycling frequency that is as high as possible, which requires computing techniques and testing equipment that has a short response time (hence the advantage of representing the NS by a predetermined matrix). Note that the compatibility is continuously respected, as the same displacements are imposed on the PS and NS at the interface. The purpose of the methodology is thus to constantly adapt these displacements to satisfy equilibrium between the substructures throughout the entire test duration.
The new methodology has been implemented in CERIB facility (Promethee furnace) and the developed algorithm will be presented in the next section.

### 5.3.3. Implemented algorithm in CERIB fire facility

The proposed method is implemented in Promethee furnace in displacement control. In the first step of development, the NS can be only represented by the predetermined matrix.
The implemented algorithm is next described.

*General description of the method*

The Promethee furnace was conceived to perform complex fire tests. Hybrid fire testing is possible since the first generation method was implemented, more specific the force control procedure. The idea is now to implement the new method in displacement control.

Note that the description to follow is suitable when the NS is represented by a predetermined matrix. When the NS is represented in a FE model then the reduction from the total number of DoFs at the interface to the number of DoFs to be controlled in the furnace (and other way around) is implemented in the algorithm.

*Input of the data to be introduced by the user for each test*

1. **nDOF, integer, ϵ [1, nDOFmax], unit [-]** – number of controlled degrees of freedom at the interface between the PS and NS used in the furnace;
   nDOFmax the maximum number of DoFs that can be controlled by Promethee.

Note: nDOF is not necessarily the total number of DoFs at the interface between the PS and NS when the whole building is considered. This total number of DoFs will be noted here

ntDOF. It is important for the user to know how to derive nDOF from ntDOF but, once the user has calculated nDOF, only nDOF is entered as a data in the algorithm. The algorithm does not use ntDOF.

2. $\boldsymbol{K_N}$**, reals, dimension [nDOF x nDOF],** $\epsilon$ **[-∞, ∞], unit [N, m]** – the predetermined matrix representing the behavior of the numerical substructure;

$$\boldsymbol{K}_N = \begin{bmatrix} K_{N,11} & \dots & K_{N,1,nDOF} \\ \dots & \dots & \dots \\ K_{N,nDOF,1} & \dots & K_{N,nDOF,nDOF} \end{bmatrix}$$

In the present stage of development of the algorithm, this matrix will remain constant during the whole test. It is foreseen to develop the capabilities of the algorithm in a way that the terms of the matrix $K_N$ change during the course of the test as a function of amplitude of the displacements at the interface.

3. $\boldsymbol{K_P}$**, reals, dimension [nDOF x nDOF],** $\epsilon$ **[-∞, ∞], unit [N, m]** – the stiffness of the physical structure PS;

$$\boldsymbol{K}_P = \begin{bmatrix} K_{P,11} & \dots & K_{P,1,nDOF} \\ \dots & \dots & \dots \\ K_{P,nDOF,1} & \dots & K_{P,nDOF,nDOF} \end{bmatrix}$$

It is known that, in fact, real values of $K_P$ in the PS will not be exactly equal to the ones that have been calculated by the user, because of uncertainties on material properties and on constitutive models. Furthermore, the stiffness matrix of the PS will change during the course of the test, because of material degradation due to heating, but these variations are not easily measured. At this stage, the algorithm is based on the constant, initially calculated value of $K_P$.

4. $\boldsymbol{F_{N,initial}}$**, reals, dimension {nDOF},** $\epsilon$ **[-∞, ∞], unit [N, m]** – Forces (or moments) at the interface at ambient temperature defined for the numerical substructure;

$$\boldsymbol{F}_{N,\boldsymbol{initial}} = \begin{bmatrix} F_{N,\boldsymbol{initial}}(1) \\ \dots \\ F_{N,\boldsymbol{initial}}(nDOF) \end{bmatrix}$$

These forces have been obtained from the analysis of the whole building (with the PS included in the analysis).

5. $\boldsymbol{u_{initial}}$**, reals, dimension {nDOF},** $\epsilon$ **[-∞, ∞], unit [m, rad]** – Displacements (or rotations) at the interface at ambient temperature.

$$\mathbf{u}_{\boldsymbol{initial}} = \begin{bmatrix} u_{\boldsymbol{initial}}(1) \\ \dots \\ u_{\boldsymbol{initial}}(nDOF) \end{bmatrix}$$

6. $\boldsymbol{T_P}$**, reals, dimension [nDOF x nDOF],** $\epsilon$ **[-∞, ∞], unit [m] –**Transformation matrix for forces.

$T_P$, is a diagonal matrix which contains the value of the arm of every restoring force measured in the furnace and it will be used to calculate the moments. For a restoring force that must generate a moment the value of the lever arm will be introduced in the matrix in the right position. If a restoring force will not generate a moment, then the value of the lever arm will be equal to 1.

$$\boldsymbol{T}_P = \begin{bmatrix} arm_1 & \dots & 0 \\ \dots & \dots & \dots \\ 0 & \dots & arm_{nDOF} \end{bmatrix}$$

7. $\boldsymbol{T_U}$**, integers, dimension [nDOF x nDOF],** $\epsilon$ **[-1 ; 1], unit [-] –**Transformation matrix for displacements.

$$\boldsymbol{T}_U = \begin{bmatrix} \pm 1 & \dots & 0 \\ \dots & \dots & \dots \\ 0 & \dots & \pm 1 \end{bmatrix}$$

$T_U$, is a diagonal matrix which will be used to transform the displacements from the global system of coordinates GSC in the local system of coordinates LSC.

8. **nP, integer,** $\epsilon$ **[0, nPmax], unit [-]** - Number of hydraulic jacks used to apply the constant loads on the PS.
   nPmax: maximum number of hydraulic jacks that can be used in a HFT with Promethee.

9. **P, reals, dimension {nP},** $\epsilon$ **[-∞, ∞], unit [N, m] -** limits to be defined by CERIB depending on the equipment of Promethee.

$$\mathbf{P} = \begin{bmatrix} P(1) \\ \dots \\ P(nP) \end{bmatrix}$$

These forces are the one that are applied on the PS when it is present in the whole building. They are normally applied in the span of the specimen and will remain constant during the test.

10. $\Delta \boldsymbol{t}$**, real,** $\epsilon$ **[0, maxval], unit [s]** – the duration during which the algorithm is on pause, before next reading of the forces at the interface. It can be bigger or equal to 0, and smaller than the maximum value defined. It depends on the facility of the furnace.

11. $\boldsymbol{eps}$ , **real,** $\epsilon$ **[minval, 1), unit [-]** – the tolerance for the convergence

    This value will drive the stop of the iteration process at a given step. It should be smaller than 1.0 e.g. $2x10^{-3}$. The appropriate value for **minval** will be found by users build up on their experience in HFT.

12. $\boldsymbol{eps_{jack}}$**, real,** $\epsilon$ **[minval, maxvalue), unit [m, rad]** – the tolerance for the jacks

The minimum value of displacement which can be applied by the system and it is different for every furnace facility and, maybe, from every DoF.

*Data to read from the testing equipment*

1. $\boldsymbol{R_P}$**, reals, dimension {nDOF},** $\epsilon$ **[-∞, ∞], unit [N]** – reaction forces at the interface.

$$\boldsymbol{R}_P = \begin{bmatrix} R_P(1) \\ \dots \\ R_P(nDOF) \end{bmatrix}$$

2. $\boldsymbol{u_P}$**, reals, dimension {nDOF},** $\epsilon$ **[-∞, ∞], unit [m, rad]** – displacements at the interface.

$$\mathbf{u}_P = \begin{bmatrix} u_P(1) \\ \dots \\ u_P(nDOF) \end{bmatrix}$$

*Information to send to the testing equipment*

1. $\boldsymbol{u_{initial}}$**, reals, dimension {nDOF},** $\epsilon$ **[-∞, ∞], unit [m, rad]** – Displacements (or rotations) at the interface at ambient temperature.

$$\mathbf{u}_{\boldsymbol{initial}} = \begin{bmatrix} u_{\boldsymbol{initial}}(1) \\ \dots \\ u_{\boldsymbol{initial}}(nDOF) \end{bmatrix}$$

2. **P, reals, dimension {nP},** $\epsilon$ **[-∞, ∞], unit [N, m] –** constant forces.

$$\mathbf{P} = \begin{bmatrix} P(1) \\ \dots \\ P(nP) \end{bmatrix}$$

3. $\boldsymbol{u}$**, reals, dimension {nDOF},** $\epsilon$ **[-∞, ∞], unit [m, rad]** – displacements at the interface calculated by the algorithm.

$$\mathbf{u} = \begin{bmatrix} u(1) \\ \dots \\ u(nDOF) \end{bmatrix}$$

*START of the test*

**Step 1**: apply initial values of the loads **P** and displacements at ambient temperature $\mathbf{u}_{J,initial}$

The user gives to the algorithm the instruction to start step 1.

$$\mathbf{u}_{J,initial} = \boldsymbol{T}_u * \mathbf{u}_{\boldsymbol{initial}}$$

The algorithm applies $\mathbf{u}_{J,initial}$ and **P** on the PS. Either these values are applied in a continuous manner taking a certain duration (to be introduced as a data) or they are applied in a series of successive steps, the amplitude of each step to be introduced as a data.

**Step 2**. Apply corrections at ambient temperature.

The user gives to the algorithm the instruction to start step 2.

Because of the uncertainties on the material properties and on the constitutive models of the PS, the restoring forces existing at the interface of the PS are not exactly equal to the ones that had been calculated in the analysis of the entire structure. Equilibrium has to be restored.
Energy norm rate ENR is used to check the convergence. Before iterations, this value must be bigger than the tolerance and, during the procedure, it will be recalculated every iteration and compared with the tolerance to check if convergence has been obtained.

$$ENR = 10\ eps$$
$$i = 0$$
$$\mathbf{u}_{20}^{i} = \mathbf{u}_{initial}$$

2.1.Read from the furnace the reaction forces of the PS, $\boldsymbol{R}_{P,20}^{i}$.

$$\boldsymbol{R}_{P,20}^{i} = \begin{bmatrix} R_{P,20}^{i}(1) \\ \dots \\ R_{P,20}^{i}(nDOF) \end{bmatrix}$$

2.2.Calculate the forces and moments of the PS, $\boldsymbol{F}_{P,20}^{i}$.

$$\boldsymbol{F}_{P,20}^{i} = \boldsymbol{T}_{P} * \boldsymbol{R}_{P,20}^{i} = \begin{bmatrix} F_{P,20}^{i}(1) \\ \dots \\ F_{P,20}^{i}(nDOF) \end{bmatrix}$$

2.3.Calculate the restoring forces (or moments) in the NS, $\boldsymbol{F}_{N,20}^{i}$corresponding to $\boldsymbol{u}_{20}^{i}$.

$$\boldsymbol{F}_{N,20}^{i} = \boldsymbol{K}_{N}\left(\mathbf{u}_{20}^{i} - \mathbf{u}_{initial}\right) + \boldsymbol{F}_{N,initial}$$

2.4.Check the convergence

If (i>1)

Calculate the energy norm rate ENR for the PS and NS (numerator and denominator are obtained by scalar products of two vectors:
Numerator = $\mathrm{SUM_i} \parallel a_i\ b_i \parallel$).

$$ENR_{P} = \left| \frac{\Delta\mathbf{u}_{20}^{i\ T}(\mathbf{F}_{P,20}^{i} + \mathbf{F}_{P,20}^{i-1})}{\Delta\mathbf{u}_{20}^{1\ T}(\boldsymbol{F}_{P,20}^{1} + \boldsymbol{F}_{P,20}^{0})} \right|$$
$$ENR_{N} = \left| \frac{\Delta\mathbf{u}_{20}^{i\ T}(\boldsymbol{F}_{N,20}^{i} + \boldsymbol{F}_{N,20}^{i-1})}{\Delta\mathbf{u}_{20}^{1\ T}(\boldsymbol{F}_{N,20}^{1} + \boldsymbol{F}_{N,20}^{0})} \right|$$

$$ENR = \max(ENR_{P}, ENR_{N})$$

If $ENR < eps$ then

Inform the user by writing on the screen **"Convergence fulfilled, ready to start the fire"**

Go to step 3.1

endif

endif

2.5. Increase the iteration step.

$$i = i + 1$$

2.6. Calculate the increment of displacements $\Delta\mathbf{u}_{20}^{i}$.

$$\Delta\mathbf{u}_{20}^{i} = -(\boldsymbol{K}_{P}{}^{*} + \boldsymbol{K}_{N})^{-1} * (\boldsymbol{F}_{P,20}^{i-1} + \boldsymbol{F}_{N,20}^{i-1})$$

2.7. Correct the interface displacement $\mathbf{u}_{20}^{i}$ (compatibility respected at the interface) for GSC.

$$\mathbf{u}_{20}^{i} = \mathbf{u}_{20}^{i-1} + \Delta\mathbf{u}_{20}^{i}$$

2.8. Calculate the displacements to be applied by the jacks.

$$\mathbf{u}_{J,20}^{i} = \mathbf{T}_{u} * \mathbf{u}_{20}^{i}$$

2.9. Promethee imposes the new value of the displacements $\mathbf{u}_{J,20}^{i}$ on the PS with a margin of errors of $\pm eps_{jack}$. The resolution of the data acquisition system permits reading only certain values of displacements.

$$\mathbf{u}_{J,20}^{i} \in [\mathbf{u}_{J,20}^{i} - eps_{jack}; \mathbf{u}_{J,20}^{i} + eps_{jack}]$$

2.10. Continue with step 2.1

Before the start of the fire, Figure 5-2 presents the flowchart of the procedure to restore the equilibrium at ambient temperature

**Figure 5-2. The procedure to restore equilibrium at ambient temperature**

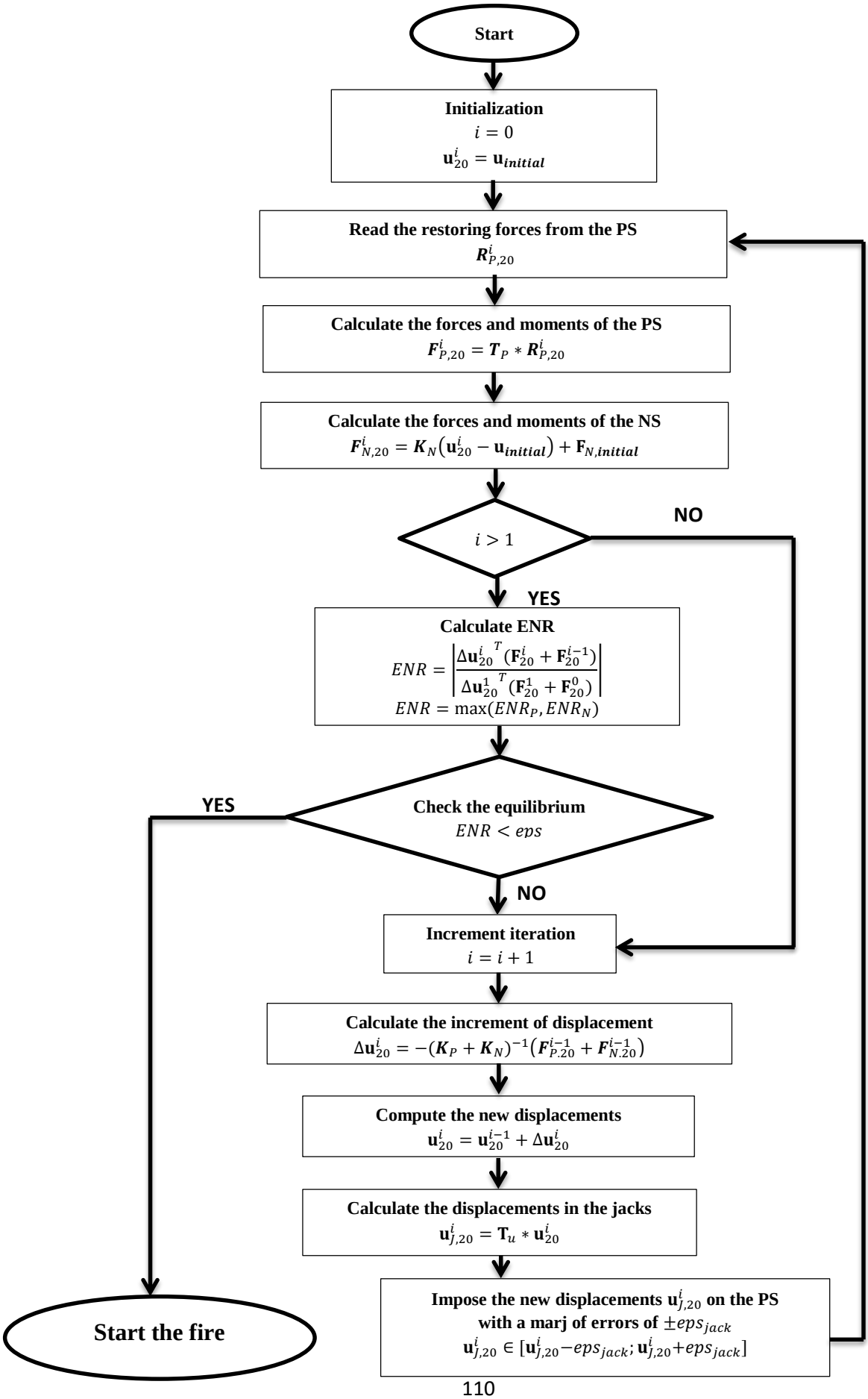

**Step 3**. Running the fire test.

The user gives to the algorithm the instruction to start step 3 right after the equilibrium at ambient temperature is restored.

Initialization of the parameters needed for the iteration process

$$n = 0$$
$$\mathbf{u}_0 = \mathbf{u}_{20}^{i}$$
$$t_0 = 0$$
$$T_{test} = 0$$

Where:
$n$ is the time step indices for a new read and calculation;
$t_0$ is the time when the fire starts.

Read time "$t$" from the internal clock of the system
$T_{initial} = t$

Promethee ignites the burners and, from now on, will take care that the prescribed time-temperature curve is followed in the furnace.

*Calculation procedure after the beginning of the fire*

3.1.The time step is incremented by 1 and time is incremented.

$$n = n + 1$$
$$t_n = t_{n-1} + \Delta t$$

Do while ($T_{test} < t_n$)
Read time $t$ from the internal clock of the system
$T_{test} = t - T_{initial}$
End do

3.2.Read from the furnace the restoring forces of the PS

$$\boldsymbol{R}_{P,n} = \begin{bmatrix} R_{P,n}(1) \\ \dots \\ R_{P,n}(nDOF) \end{bmatrix}$$

3.3.Calculate the forces and moments of the PS, $\boldsymbol{F}_{P,n}$.

$$\boldsymbol{F}_{P,n} = \boldsymbol{T}_P * \boldsymbol{R}_{P,n} = \begin{bmatrix} F_{P,n}(1) \\ \cdots \\ F_{P,n}(nDOF) \end{bmatrix}$$

3.4. Calculate the restoring forces and moments of the NS, $\boldsymbol{F}_{N,n}$ .

$$\boldsymbol{F}_{N,n} = \boldsymbol{K}_N(\mathbf{u}_{n-1} - \mathbf{u}_{initial}) + \boldsymbol{F}_{N,initial}$$

3.5. Calculate the increment of displacements $\Delta\mathbf{u}_n$.

$$\Delta\mathbf{u}_n = -(\boldsymbol{K}_P + \boldsymbol{K}_N)^{-1}\left(\boldsymbol{F}_{P,n} + \boldsymbol{F}_{N,n}\right)$$

3.6. Calculate the new value of the displacements in the global system of coordinates GSC

$$\mathbf{u}_n = \mathbf{u}_{n-1} + \Delta\mathbf{u}_n$$

3.7. Calculate the displacements to be applied by the jacks in the LSC.

$$\mathbf{u}_{J,n} = \mathbf{T}_u * \mathbf{u}_n$$

3.8. Promethee imposes the new value of the displacements $\mathbf{u}_{J,n}$ on the PS with a marj of errors of $\pm eps_{jack}$, depending on the characterics of the data acquisition system and transfer system.

$$\mathbf{u}_{J,n} \in [\mathbf{u}_{J,n} - eps_{jack}; \mathbf{u}_{J,n} + eps_{jack}]$$

3.9. Go to step 3.1

The flowchart for the hybrid fire testing making use of the proposed method is presented in **Figure 5-3**.

**Figure 5-3. New method of hybrid fire testing.**

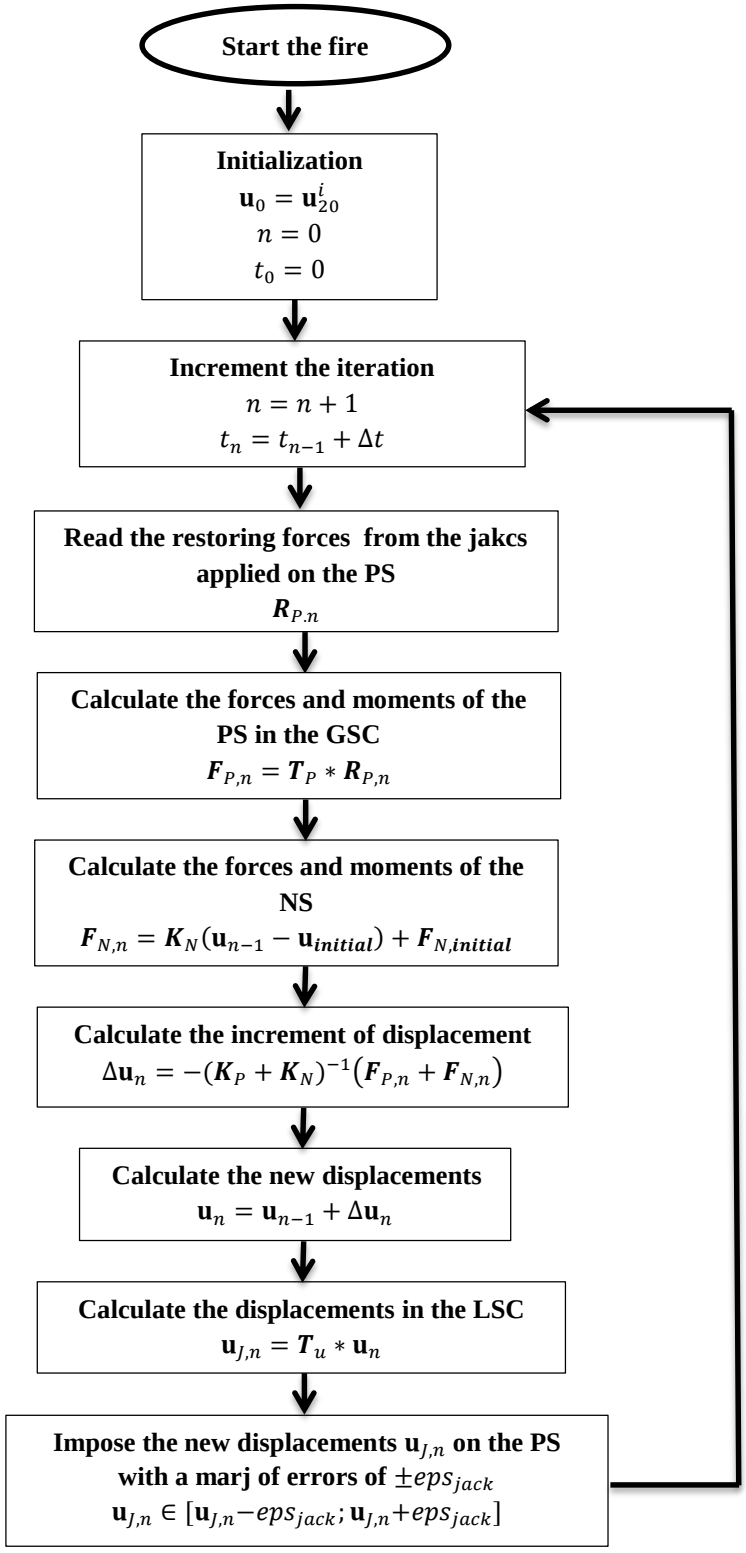

### 5.3.4. Local versus global system of coordinates in the new methodology

During the hybrid fire testing the measurement of the data (forces/displacements) in the furnace is done via the data acquisition system. The measured data is done in the local system of coordinates LSC. The LSC depends on the site where the hybrid test will be performed.

The new methodology will compute the new boundary conditions to be applied in the global system of coordinates (GSC).

Hence the transformation from the local system of coordinates to the global one is needed when the measured data in the furnace are sent to the software which computes the new boundary conditions. Once the calculations are done and sent back to the transfer system the values from the global system of coordinates will be transformed back to the local system of coordinates.

The local system of coordinates depends on how the data acquisition system is defined to measure the needed information in the furnace and on the other side on how the transfer system is defined to apply the new boundary conditions.

Every fire facility is unique in term of the furnace configuration. Therefore, the transformation from local-global and global- local system of coordinates will be adopted independently on the fire facility.

For a better understanding an example based on the available sign conventions in Promethee fire facility is presented in APPENDIX B.

## 5.4. Numerical example. Simple elastic truss

The behavior of the simple elastic truss analyzed in section 4 will be next observed in the conditions of using the new methodology.
The evolution of the interface displacements and forces is first presented assuming that there is no degradation of the PS's stiffness due to the fire exposure. The chosen time step is $\Delta t = 60s$ while the delay time is set to $\Delta t = 10s$. The new method is implemented in displacement control procedure.
Figure 5-4 present the interface displacements and forces obtained with the new method when the stiffness ratio is smaller than the critical value of one.

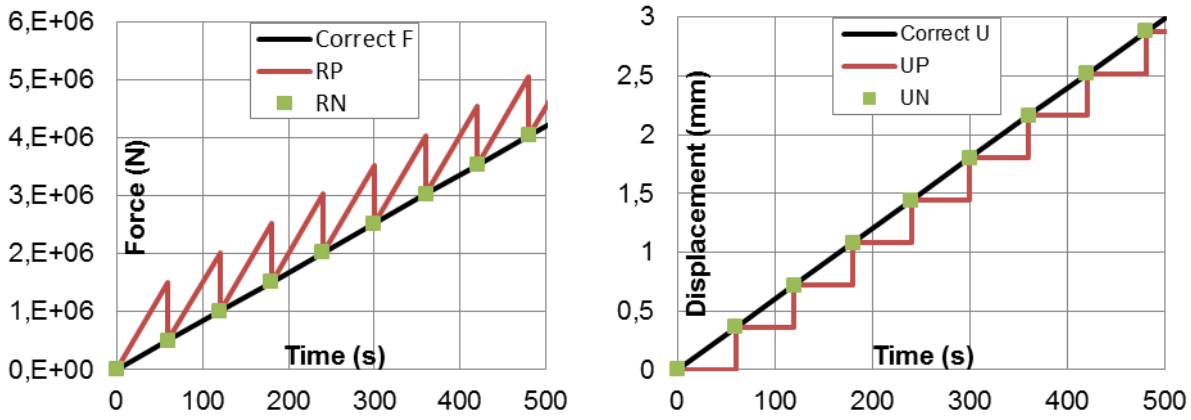


*The interface force* *The interface displacement*

**Figure 5-4. Interface conditions when the stiffness ratio $R < 1$**

When displacement control procedure is considered then the interface displacements are fixed in between the two readings. Since the PS is exposed to fire the blocked interface displacements between the readings induces changes of the reaction (restoring) forces. The reading of restoring forces of the PS are registered every 60 s and used to compute new displacements to be imposed at the interface of the PS and NS. The NS is cold (in this particular example) thus the reaction force (the interface force) is constant in between the two readings or during one time step. The interface equilibrium is lost, thus the out of balance forces serve to compute a new value of displacement to be imposed in order to restore the equilibrium. The new displacement is imposed on the PS with a delay time of 10 s. The new displacement induces new reaction forces in the PS as well as in the NS. The objective is to ensure compatibility (the same displacements at the interface of the PS and NS) and equilibrium (the same value of reaction forces at the interface of the PS and NS). To be mentioned that the behavior resulted when applying the hybrid process should replicate the "correct" behavior of the structure, i.e. the behavior resulted when the structure is analyzed as entity. The "correct" behavior (or we can call it the real behavior) is represented in the graph with black curve. The interface solution of the PS is represented in the graphs with red while the solution of the NS with green.

We can conclude that the interface solution of the substructure converges to the correct solution. The same displacements are imposed on the PS and NS, thus compatibility is ensured, and almost the same forces result at the interface of the substructures every time $\Delta t + \Delta t_P$.

It has just been underlined that ***almost*** the same forces result at the interface of the substructures. The difference between the interface forces is induces by the value of the delay time $\Delta t_P$. While the new displacement is imposed in the furnace, during the delay time $\Delta t_P$, the PS continues to be heated. The heat induces changes of the reaction force during this period. Thus the reaction force existing at the interface at the time $\Delta t + \Delta t_P$ (when the new displacement is induced at the interface of the PS) is different compared with the interface force at the time $\Delta t$ (when the displacements are computed to be updated at the interface). To reduce the difference between the substructures reaction forces is necessary to reduce the delay time step. The delay time step can be just reduced and not eliminated.

Figure 5-5 presents the interface displacement and forces when the stiffness ratio is bigger than one.

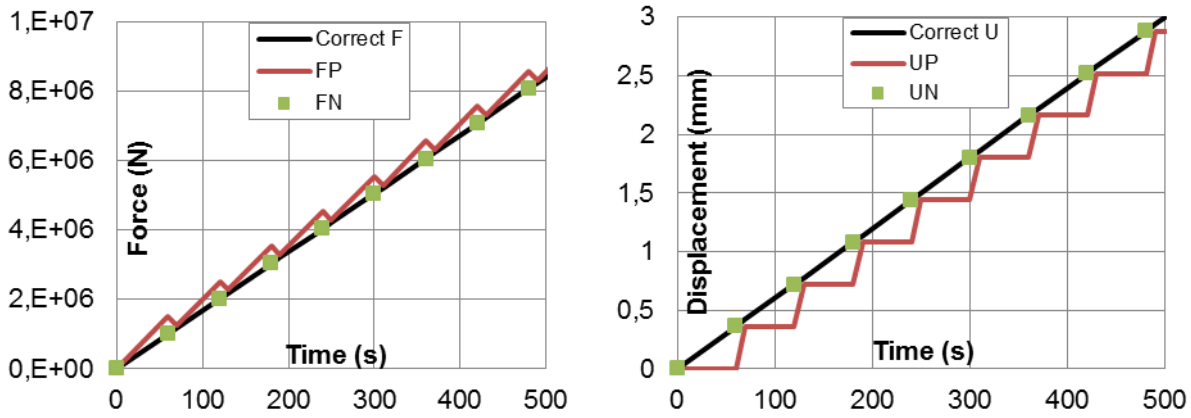


*The interface force* *The interface displacement*

**Figure 5-5. Interface conditions when the stiffness ratio $R > 1$**

The same principle explained for the case when R<1 is valid for the case when R>1.
The main conclusion after visualizing the figures just mentioned is that no instability occurs during the hybrid process when using the new method, no matter the value of the stiffness ratio.
The new method considers the stiffness value of the PS and NS in the calculation process, whereas the first generation method considers the sole stiffness of the NS. The stiffness of the heated substructure cannot be predicted during the hybrid process (or is not safe to be predicted), thus the initial tangent stiffness of the heated substructure is considered. By using a constant value of the PS's stiffness influences the interface compatibility and equilibrium.
In the previous example the stiffness of the PS (heated substructure) is considered no to degrade due to fire exposure, thus the effect of considering the initial tangent stiffness of the PS in the hybrid process cannot be observed.
The same example is next considered when the stiffness matrix of the PS will degrade in time, depending on the registered temperature. A linear degradation is chosen and a zero Young modulus occurs when the temperature of 1000°C is reached.
The time step and the delay time is chosen as in the previous case thus $\Delta t = 60\ s$ and $\Delta t = 10\ s$. The value of the PS's stiffness used in the calculations is considered as the initial tangent stiffness during the entire process.

Figure 5-6 presents the evolution of interface forces and displacements for the case when the stiffness ratio is smaller than one, more specific $\boldsymbol{R = 0.50}$.

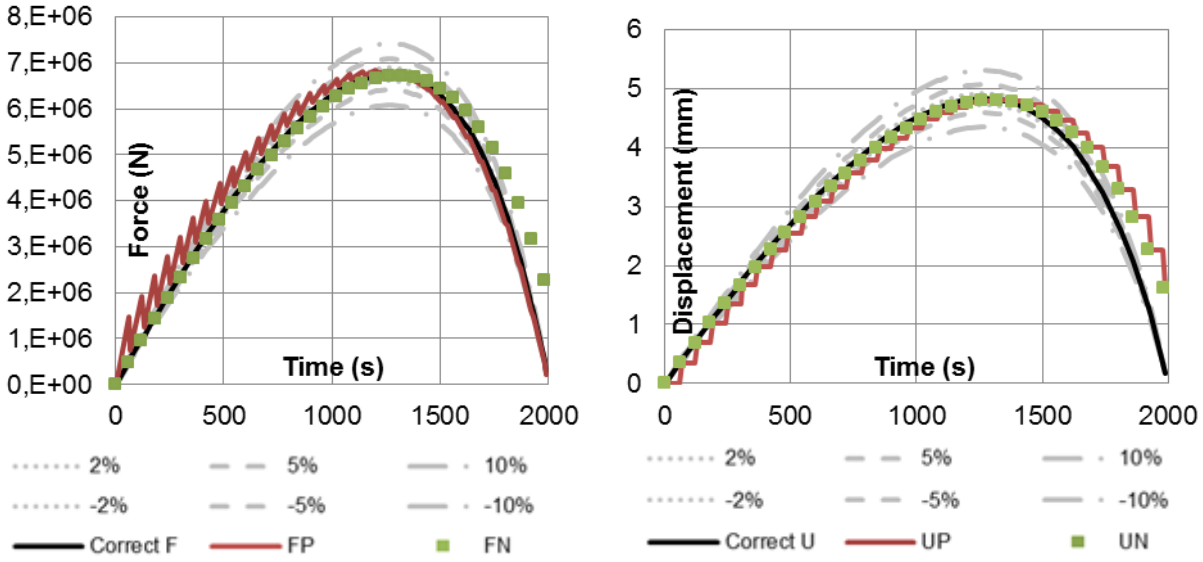


*The interface force* *The interface displacement*

**Figure 5-6. Interface conditions when the stiffness ratio $R < 1$ and the stiffness of the PS degrades**

Figure 5-7 presents the evolution of interface forces and displacements for the case when the stiffness ratio is bigger than one, more specific $\boldsymbol{R = 2}$.

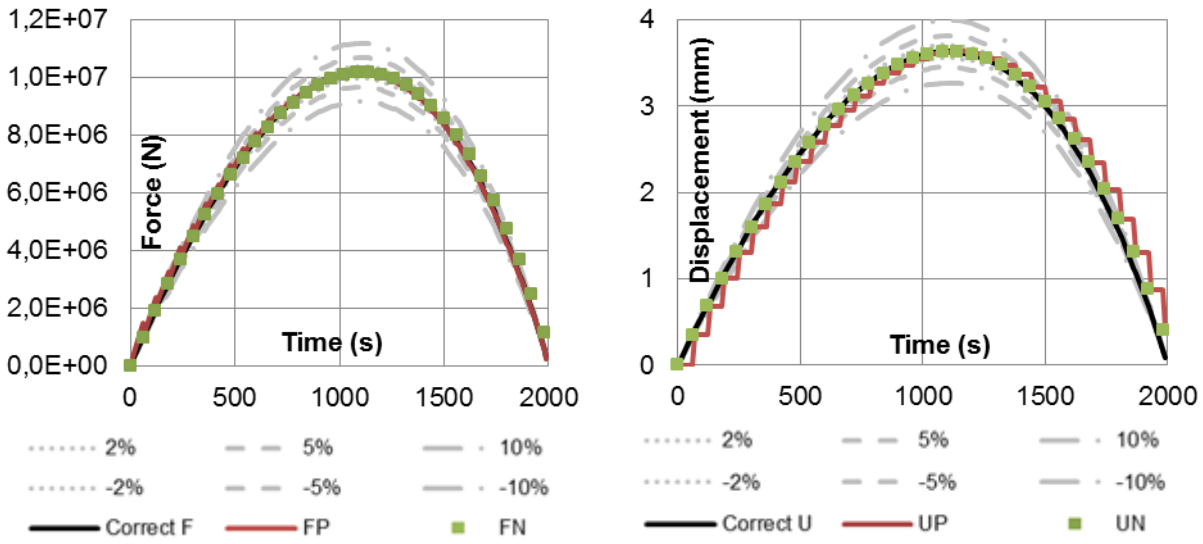


*The interface force* *The interface displacement*

**Figure 5-7. Interface conditions when the stiffness ratio $R > 1$ and the stiffness of the PS degrades**

An imposed error is printed in the graphs representing 2%, 5% and 10% error of the correct value. The admissible error is defined by the user depending on the objectives of the project.

It can be observed that close to the final stage of the process, the solution resulted by using hybrid methodology can slightly diverge from the correct solution. Moreover, the interface

forces are not in equilibrium. The just mentioned facts occur especially if the stiffness ratio is smaller than one. The reason will be next explained.

The chapter 3.6 presents the importance of choosing the correct value of the time step in order to be able to reach compatibility, equilibrium and moreover to converge to the correct solution.

In fire cases, the effect of fire induces a variation of the boundary conditions even in the process of the calculations of the new solution and even when the new displacements are imposed at the interface. Using a constant value of the stiffness matrix in the calculation, whereas in reality the stiffness varies due to the fire exposure, request an iterative process in order to converge to the correct solution. The condition of performing iterations is to keep the interface forces constant during this procedure. But as mentioned the interface forces are never constant since the fire is turned on during the test. Thus, it has been observed that is important to choose a time step as small as possible in order to produce results which are accurate. It is recommended to choose the value of the time step equal with the value of the delay time $\Delta t = \Delta t_P$. It means that depending on the testing facility, once the new displacement is imposed on the PS and NS, the restoring forces are registered and used for the calculation of new displacements. This process is repeated during the entire hybrid process as if continues iterations are performed.

The accuracy of the results as well as the possibility of instability will be next observed, while different parameters are studied to see the impact on the results. The mentioned parameters are:

- The time step;
- The stiffness of the PS used in the calculation process;
- The stiffness ratio between the substructures;

### 5.4.1. The influence of the time step on the results

Next the interface forces and displacements are presented when $\Delta t = \Delta t_P$ and the initial tangent stiffness is considered $K_P^* = K_P$. The $K_P^*$ is the stiffness of the PS used in the calculation process, when the new displacement is computed using the out of balance forces. The $K_P$ is the initial tangent stiffness of the PS. The objective is to observe the variation of the results when the time step varies.

Figure 5-8 presents the variation of the interface forces and displacements for a system characterized at the beginning of the test by a stiffness ratio smaller than one, i.e. $R < 1$. This is equivalent by writing that $K_N < K_P$, condition which is available just for a certain period of the hybrid fire tests. The stiffness of the PS is degrading during the test (due to the fire exposure) while the stiffness of the NS is constant in this particular case. Thus the value of the stiffness ratio can become bigger than one during the hybrid test.

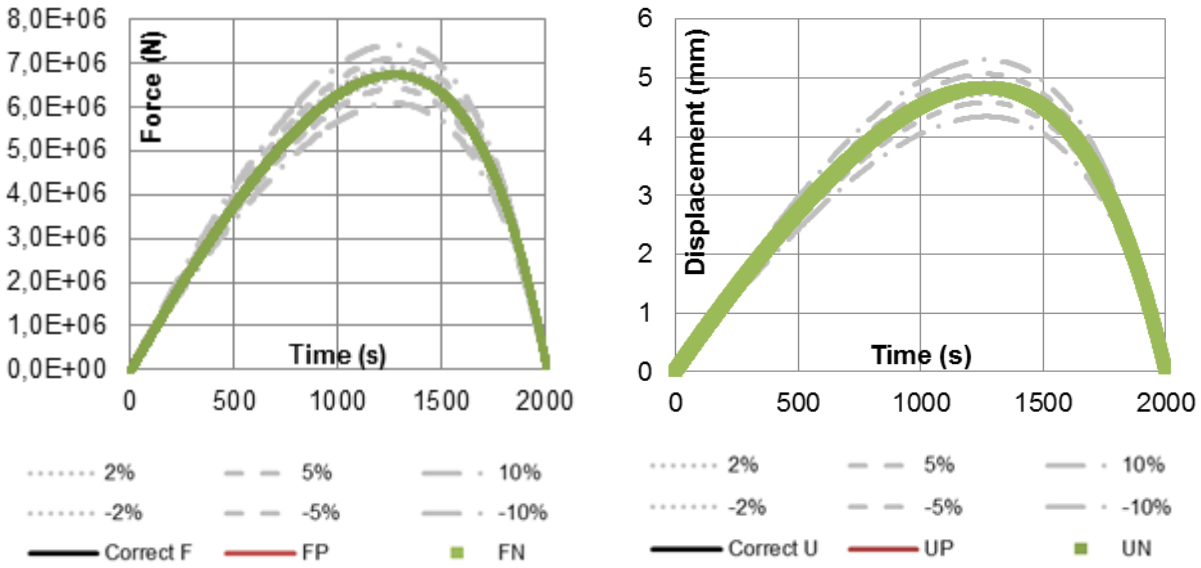


***a)*** $\Delta t = \Delta t_P = 1\ s$

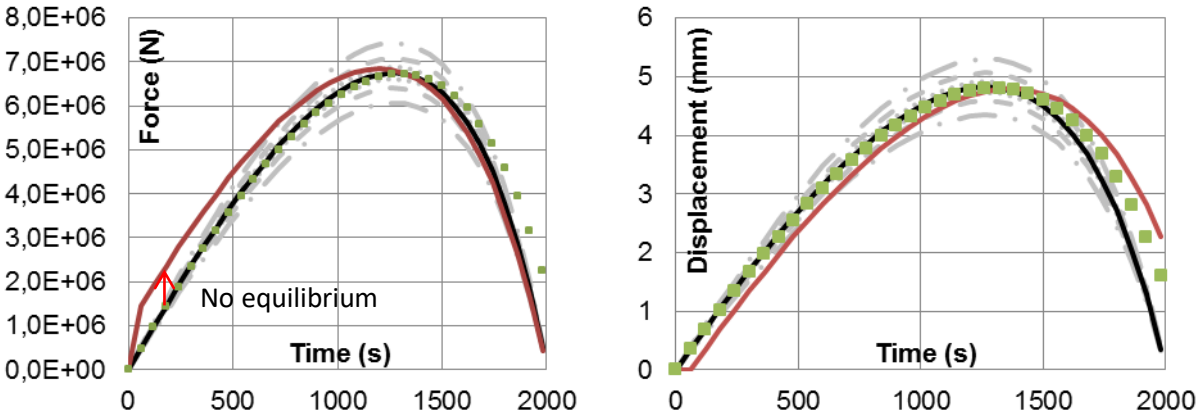


***b)*** $\Delta t = \Delta t_P = 60\ s$

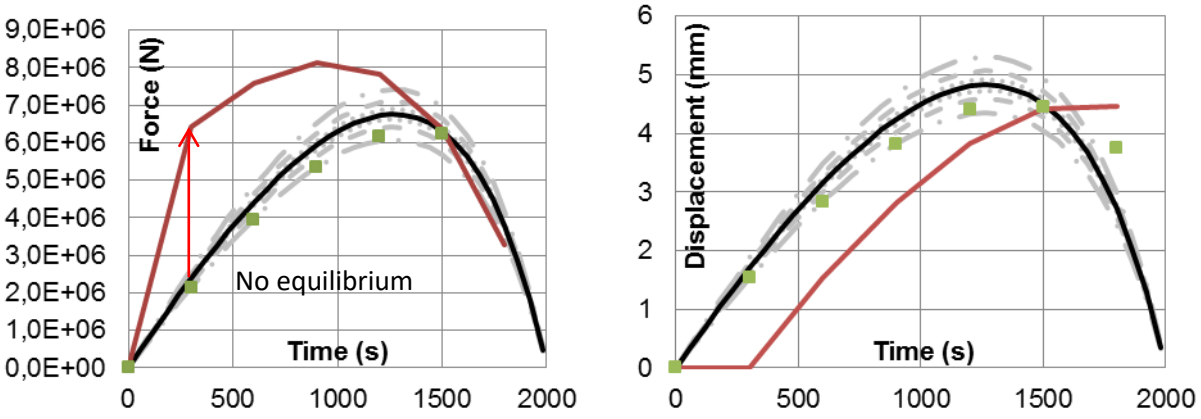


***c)*** $\Delta t = \Delta t_P = 300\ s$

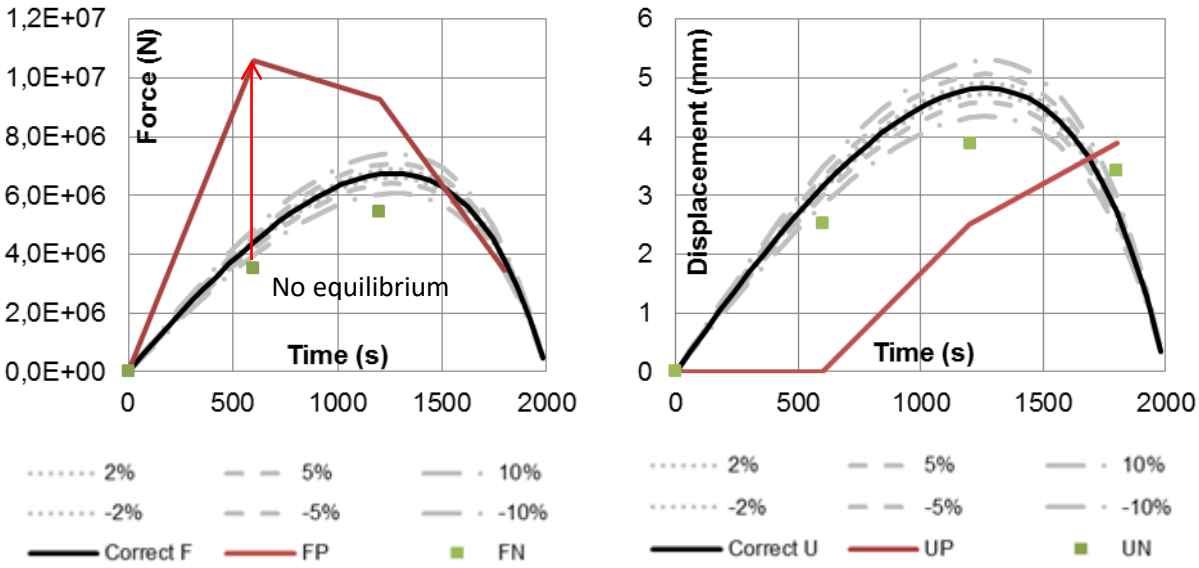


***d)*** $\Delta t = \Delta t_P = 600\ s$

*The interface force* *The interface displacement*

**Figure 5-8. Interface conditions when $R < 1$ and the time step varies**

Figure 5-9 presents the variation of the interface forces and displacements for a system characterized at the beginning of the test by a stiffness ratio bigger than one, i.e. $R > 1$. In this case the value of the stiffness ratio will be always bigger than one with the condition that the stiffness of the NS is constant while the stiffness of the PS is decreasing in time. Thus it can be written that $K_N > K_P$ during the entire test.

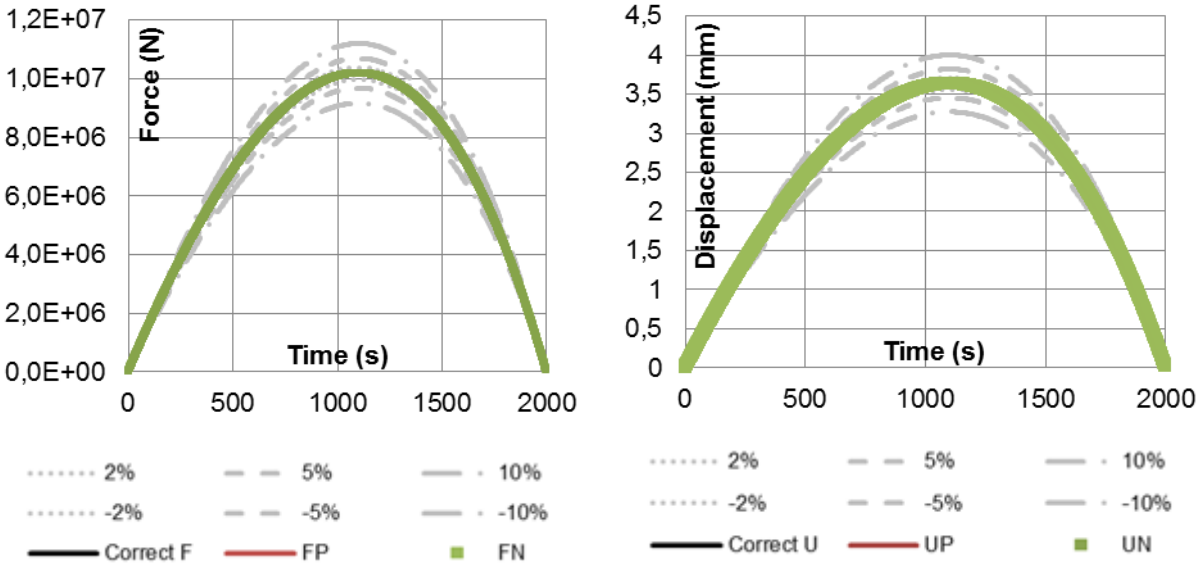


***a)*** $\Delta t = \Delta t_P = 1\ s$

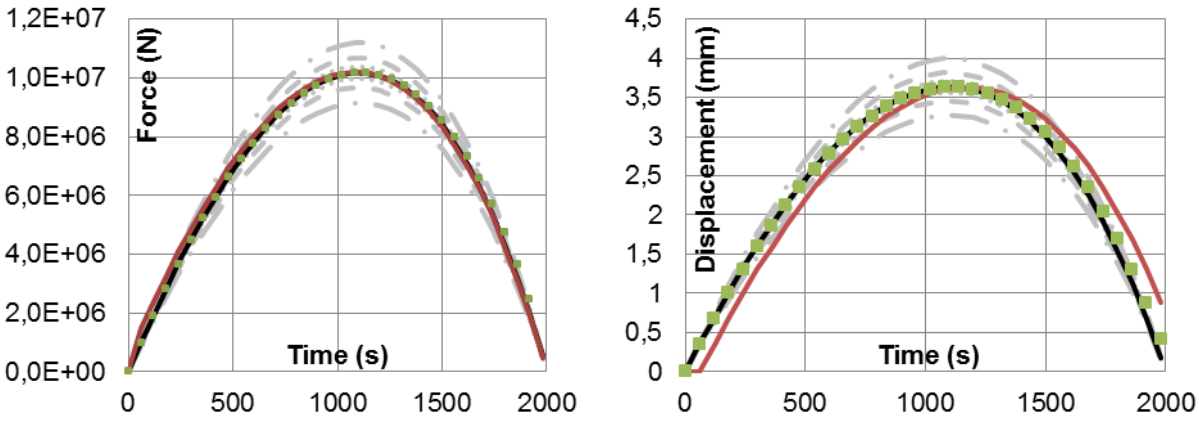


**b)** $\Delta t = \Delta t_P = 60\ s$

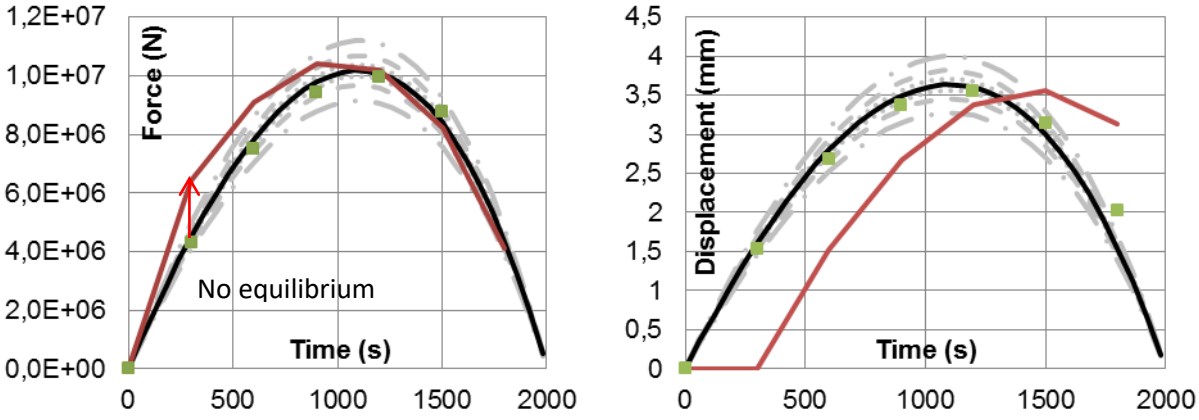


**c)** $\Delta t = \Delta t_P = 300\ s$

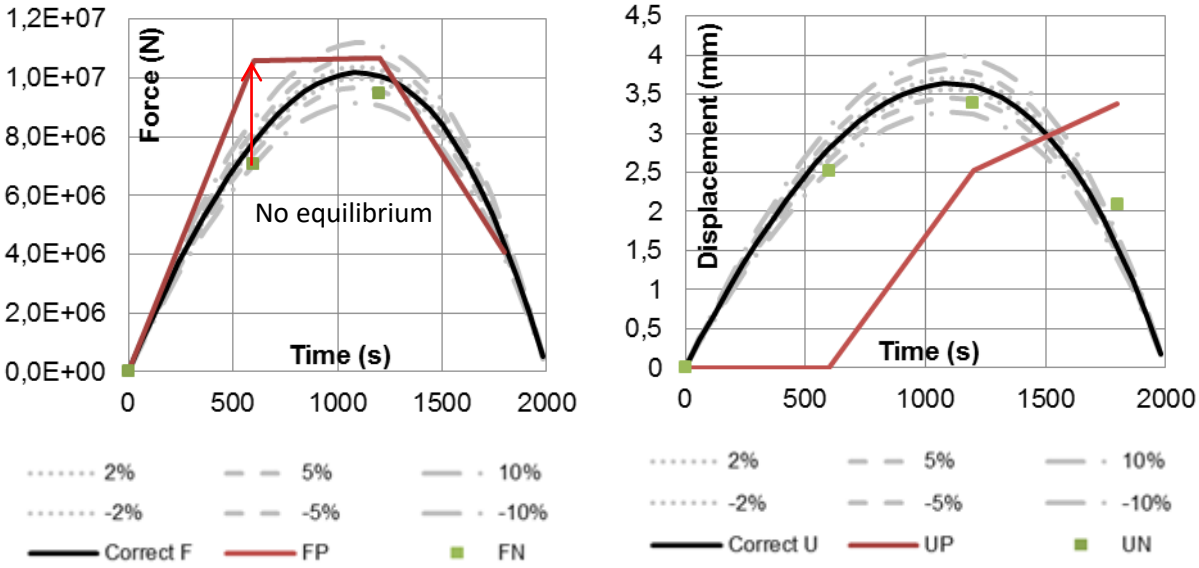


**d)** $\Delta t = \Delta t_P = 600\ s$

*The interface force* *The interface displacement*

**Figure 5-9. Interface conditions when $R > 1$ and the time step varies**

In this specific example the time step is chosen to vary with the following values: 1 s, 60 s, 300 s and 600 s. We assume that the time needed for the actuators to impose the new boundary conditions in the furnace is equal with the time step, i.e. $\Delta t = \Delta t_P$. The initial tangent stiffness matrix of the PS is considered in the calculations of every time step displacements. Every graph presents the interface solution of the PS and NS, along with the correct solution. Moreover, 2%, 5% and 10% percentage error of the correct solution is printed.

Several ideas can be underlined if observing the just mentioned figures.

First it is obvious that the increase of the time step does not ensure equilibrium and compatibility at the interface. Since the new displacement to be imposed is computed, until the update of displacement in the furnace, the heat induces some changes of the boundary conditions. Thus, when the new displacement is imposed in the furnace the resulted reaction force of the PS is not the one expected and therefore is not equal with the reaction force of the NS (no equilibrium satisfied). In addition to the effect of the time step, by considering the initial tangent stiffness matrix in the calculation process will increase the error in the results.

The main objective of the hybrid process is to ensure equilibrium and compatibility at the interface and to reproduce the behavior of the structure as an assembly (correct solution). Depending on the objectives of the project, the user can define an acceptable error in the results.

It can be accepted that the interface solution deviates from the correct solution with a percentage of the correct solution, as presented in these figures.

Another error which can be defined refers to the difference between the PS solution and the one of the NS. In the figures above an arrow shows the difference between the reaction force of the PS and NS for one time step. It can be accepted a difference which is defined by the user depending on the main objectives of the project.

The second observation which can be made towards the figures is that the same time step induces a bigger or a smaller error in the solution depending on the stiffness ratio of the substructures. Thus we can conclude that the time step to be chosen is dependent first on the fire facility (the reaction time of the facility every time step) but it also depends on the type of the structure to be analyzed.

If the time step is chosen to be equal to 1 s then we can observe that the results are accurate in the sense that the correct solution is reproduced while the equilibrium and the compatibility are satisfied. The remark is available for the situation when $R < 1$ as well as for $R > 1$.

If a time step of 10 s is selected instead, the error is more significant for the case when $R < 1$ than for the case when $R > 1$. For the time step equal to 300 s and 600 s the same conclusion is valid.

### 5.4.2. Influence of the tangent stiffness matrix of the PS on the results

The same exercise is next repeated but in this case the time step is kept constant while the initial tangent stiffness matrix will vary. Since the time step equal to 1 s showed good results for the case of a stiffness ratio smaller than one as well as for the stiffness ratio bigger than one, the same value will be kept while the initial tangent stiffness varies.

Figure 5-10 presents the evolution in time of the boundary conditions when the time step is set to be constant but the tangent stiffness of the PS used in the calculations varies. To be mentioned that the stiffness ratio between the substructures is smaller than one. The stiffness value considered in this exercise multiplies value of 1.50, 5, 10, 0.20, and 0.10 with the initial tangent stiffness of the PS.

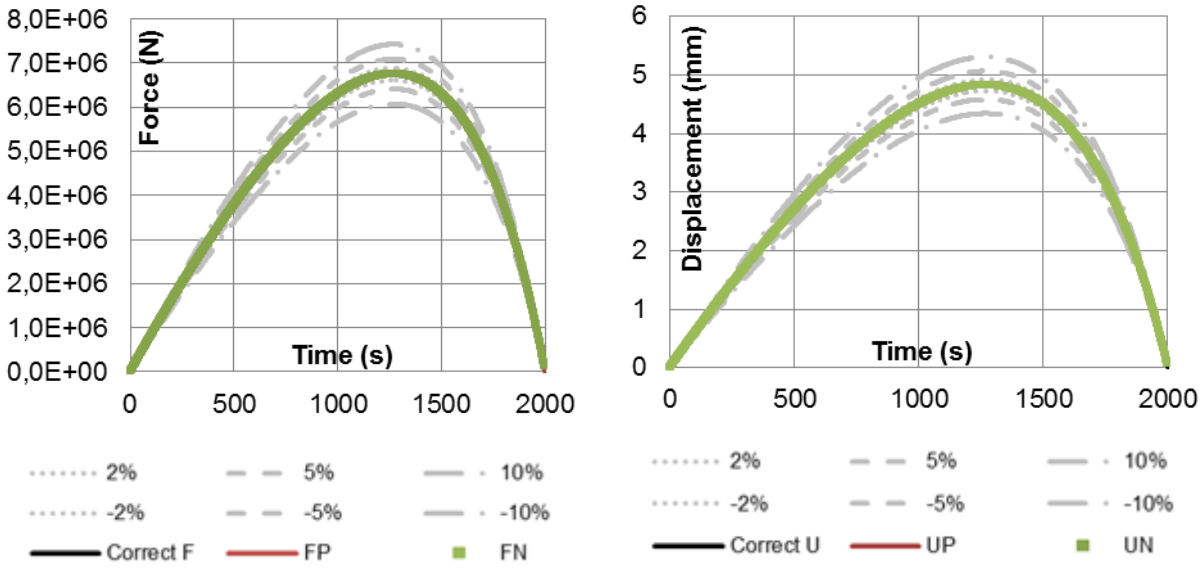


*a)* $K_P^* = 1.5\,K_P$

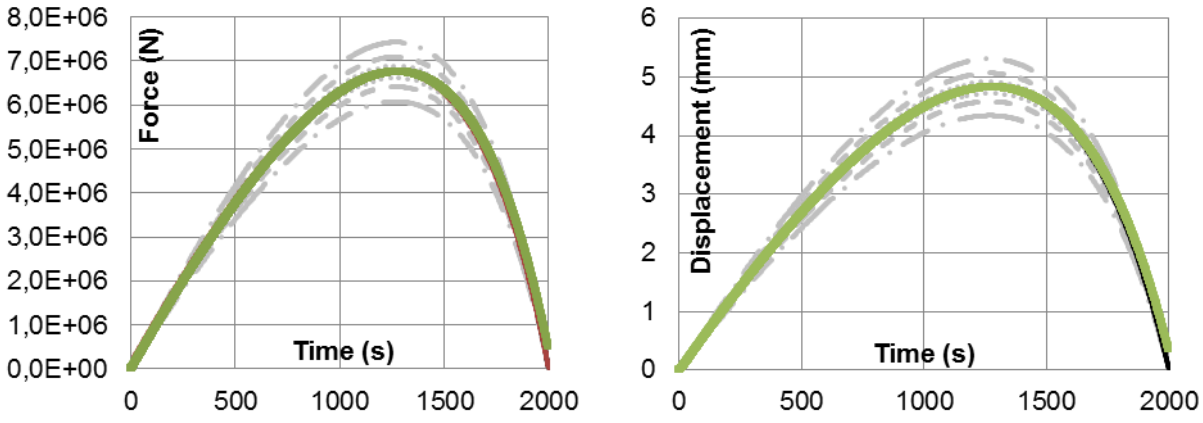


*b)* $K_P^* = 10\,K_P$

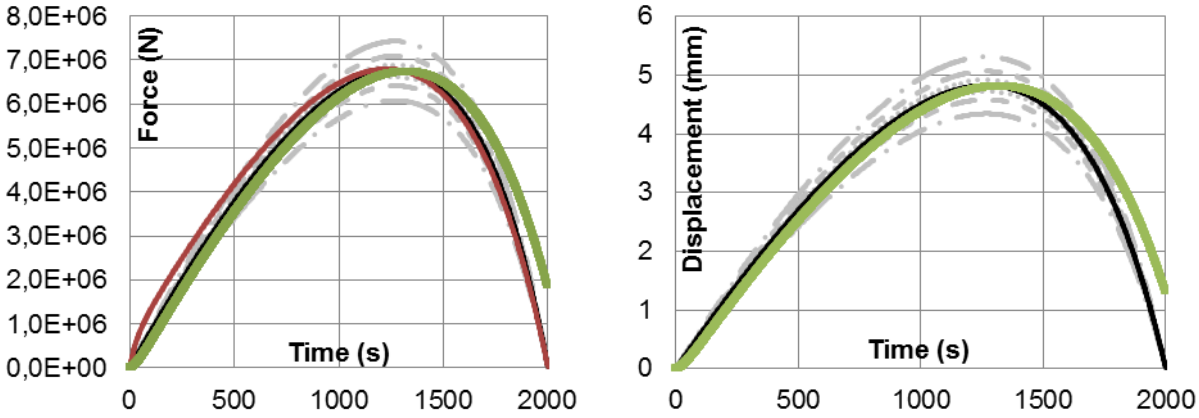


*c)* $K_P^* = 50\,K_P$

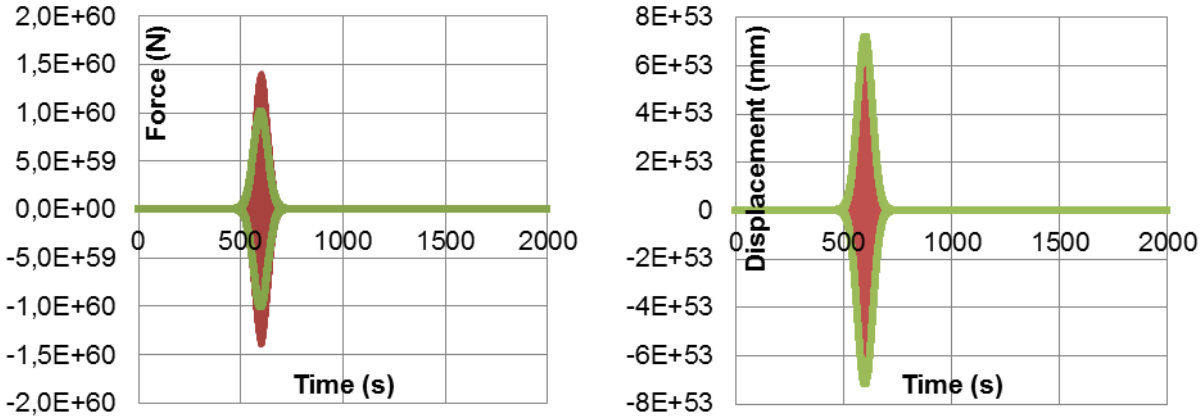


*d)* $K_P^* = 0.1\,K_P$

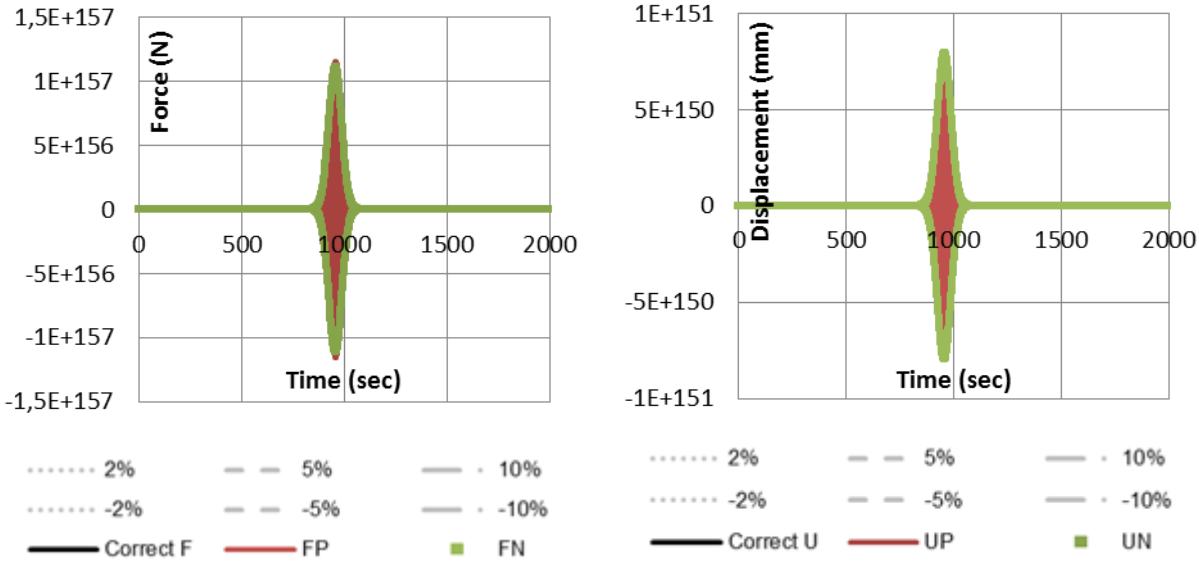


*e)* $K_P^* = 0.01\,K_P$

*The interface force* *The interface displacement*

**Figure 5-10. The boundary conditions when $R < 1$ and the stiffness of the PS varies**

The stiffness of the PS is requested to be known if using the new methodology. The degradation of the PS due to the fire exposure is difficult to be predicted during the test, this being the main reason why a constant value of the stiffness will be considered in the hybrid process. But it is still important to estimate the stiffness of the PS at ambient temperature and to use it in the calculations. If the value of the PS's stiffness used in the calculations overestimates the correct value, then this can lead to the loss of equilibrium and deviation from the correct value. In the examples presented this phenomenon is obvious when the stiffness of the PS is 50 times overestimated. But even like that the errors are not significant. What is important to be noticed is that instability during the tests can still occur if the stiffness of the PS is underestimated. The phenomenon can be observed in the same figure when the stiffness is underestimated 5 or 10 times. Please note that the value of forces and displacements printed in the same graph are not physically possible, the representation is used just to make the reader visualize the risk of instability in certain cases.

Figure 5-11 presents the evolution in time of the boundary conditions in the same conditions as mentioned, when the stiffness ratio between the substructures is bigger than one. The stiffness value considered in this exercise multiplies value of 1.50, 5, 10, 0.20, and 0.10 with the initial tangent stiffness of the PS.

In this situation, no matter the value of the PS's stiffness, good results are obtained (compatibility and equilibrium satisfied as well as the reproduction of the correct solution).

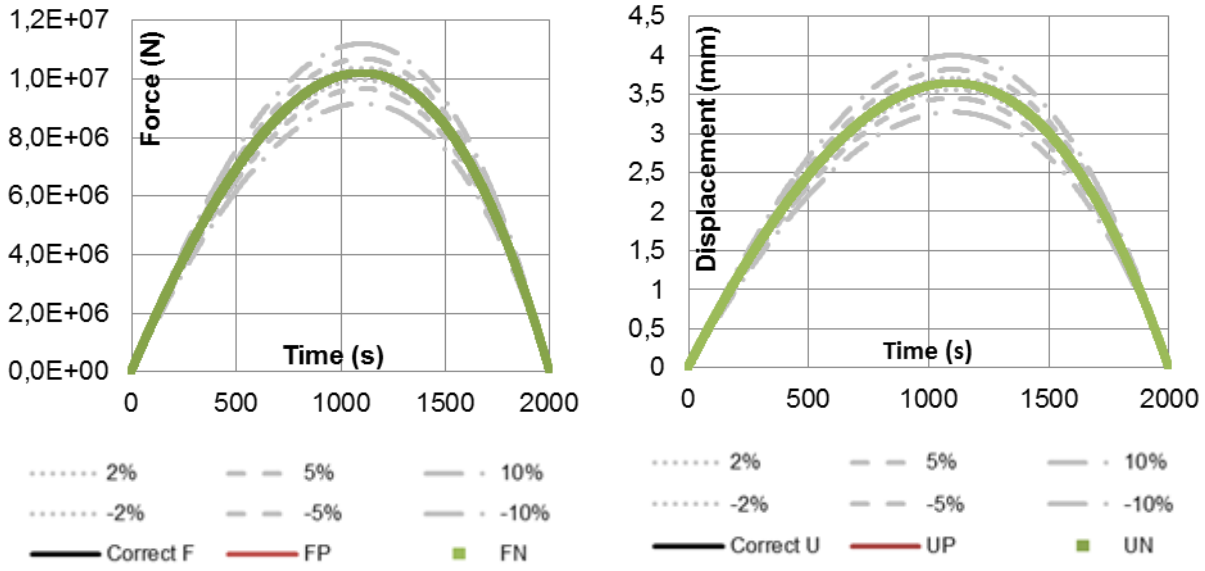


***a)*** $K_P^* = 1.5\,K_P$

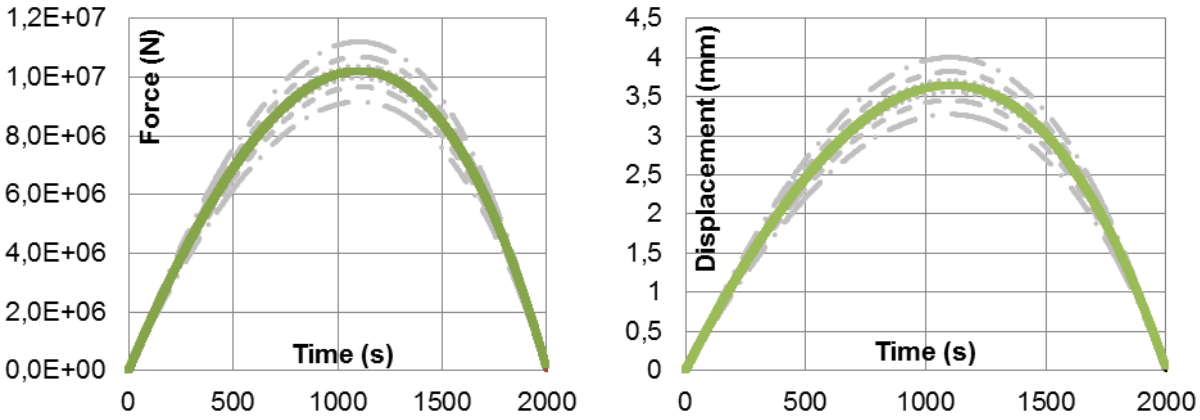


***b)*** $K_P^* = 10\,K_P$

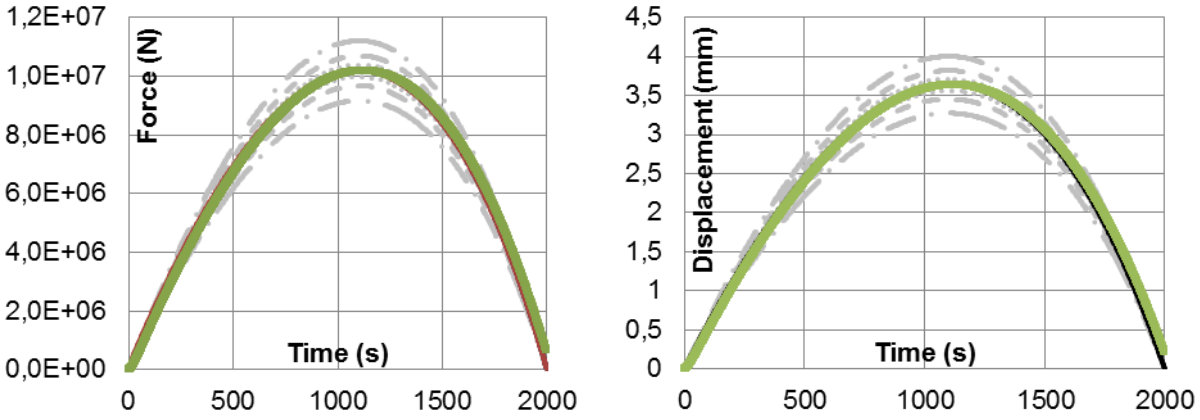


***c)*** $K_P^* = 50\,K_P$

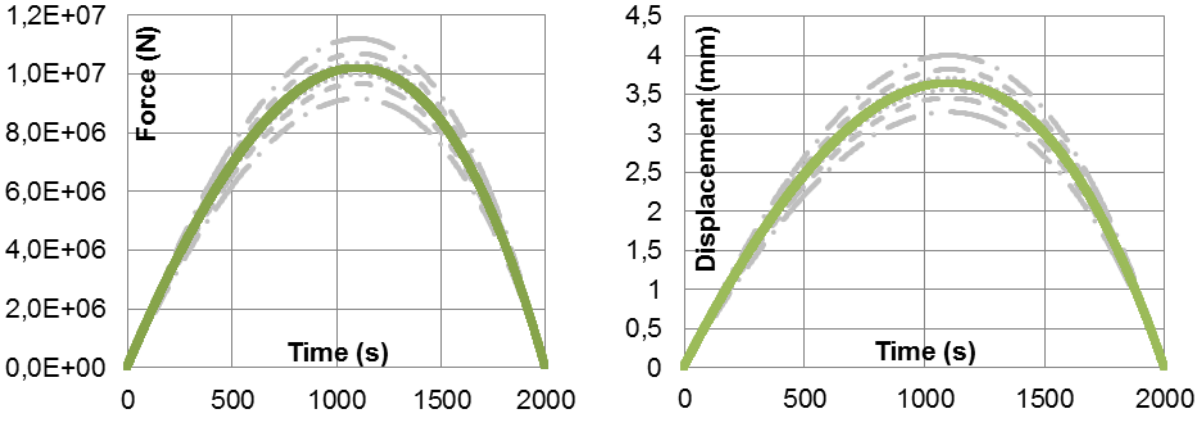


***d)*** $K_P^* = 0.1\,K_P$

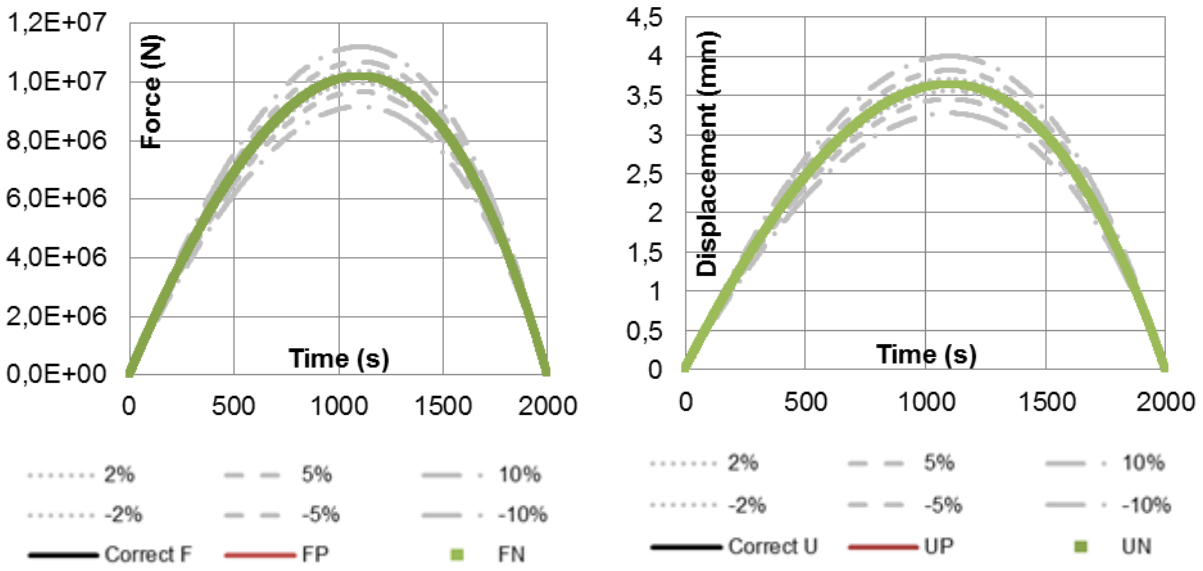


***e)*** $\boldsymbol{K_P^* = 0.01\, K_P}$

*The interface force* *The interface displacement*

**Figure 5-11. The boundary conditions when $R > 1$ and the initial tangent stiffness of the PS varies**

As it was observed, there is a risk of instability if the PS's stiffness chosen to be used in the calculation is not appropriate. This problem occurs especially in the situations when the PS is stiffer than the NS, i.e. $R < 1$**.** Thus, if the value of stiffness is underestimated then is almost equivalent with using the first generation method, where in the update of the interface solutions account just for the stiffness of the NS. And since a displacement control procedure is considered when applying the new methodology this leads to instability.

If the stiffness of the PS is smaller compared to the stiffness of the NS, then the results are not so much affected if the PS's stiffness is overestimated or underestimated since the NS's stiffness is the most significant. Thus the problem it almost reduces to the first generation method where the stiffness of the NS is the most important. In the first generation method a displacement control procedure is requested in the case of a stiffness ratio bigger than one. In this case then, the correct procedure is applied and this is why the value of the PS's stiffness in the calculations does not have a big effect on the results since the stiffness of the NS is driving the direction of the values to be imposed.

In real hybrid fire tests the difficulty comes from the fact that mainly multiple DoFs are requested to be controlled. For some DoFs the stiffness ratio is smaller than one while for the other the stiffness ratio is bigger than one for ambient temperatures. Thus is important the selected value of the PS's stiffness to be considered in the calculations. The chosen value should not underestimate the initial tangent stiffness since this can induce instability in the process. On the contrary, if the PS's stiffness value is too much overestimated then the loss of equilibrium and deviation from the correct solution can occur. It is recommended for the user to perform a preliminary study in order to choose the appropriate value. It is recommended to overestimate the PS's stiffness by a reasonable amount, thus the instability is avoided and the

equilibrium is still satisfied. In practice a factor of 1.50 is recommended to overestimate the measured value of the stiffness matrix at the ambient conditions.

### 5.4.3. Influence of the stiffness ratio on the results

The new methodology is applied for the same example when the stiffness ratio of the substructures at ambient conditions varies. The other coefficients are set constant during the test, such as the time step is set to 1 s while the initial tangent stiffness matrix is considered in the calculations. The results are presented in the Figure 5-12. It can be observed that the method is stable during the test no matter the stiffness ratio between the substructures if the time step and the stiffness of the PS are set correctly at the beginning of the test. Not only the stability is ensured but also the accuracy of the results is satisfactory.

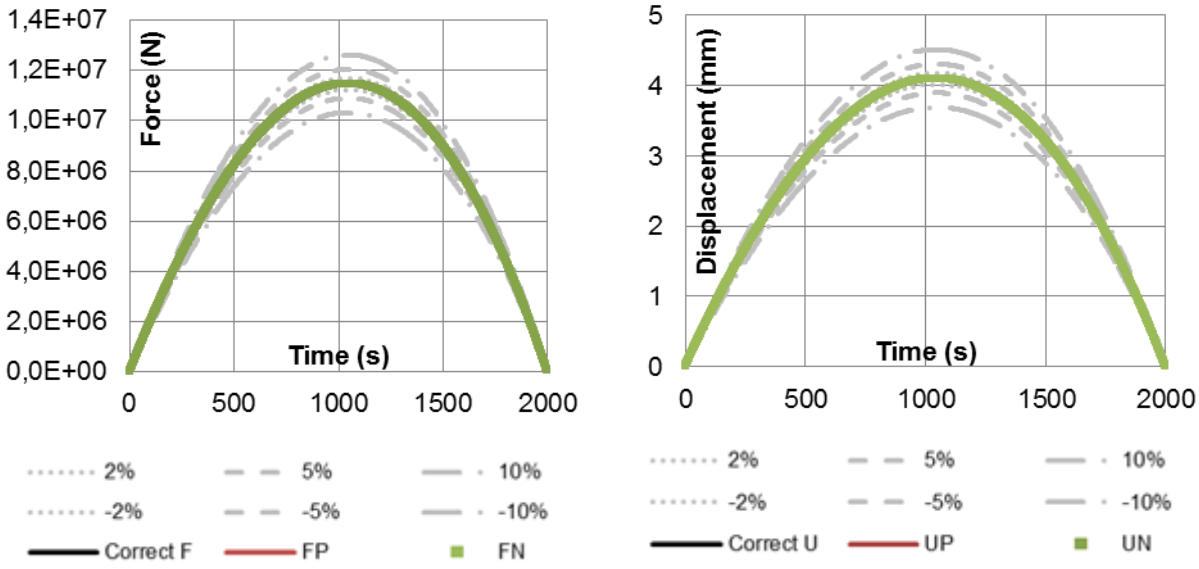


*a)* $R = 5$

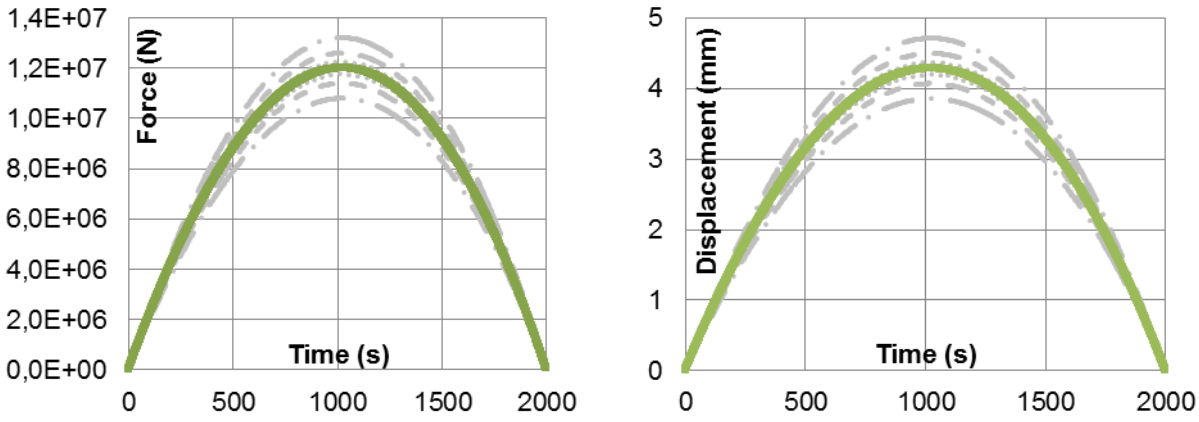


*b)* $R = 10$

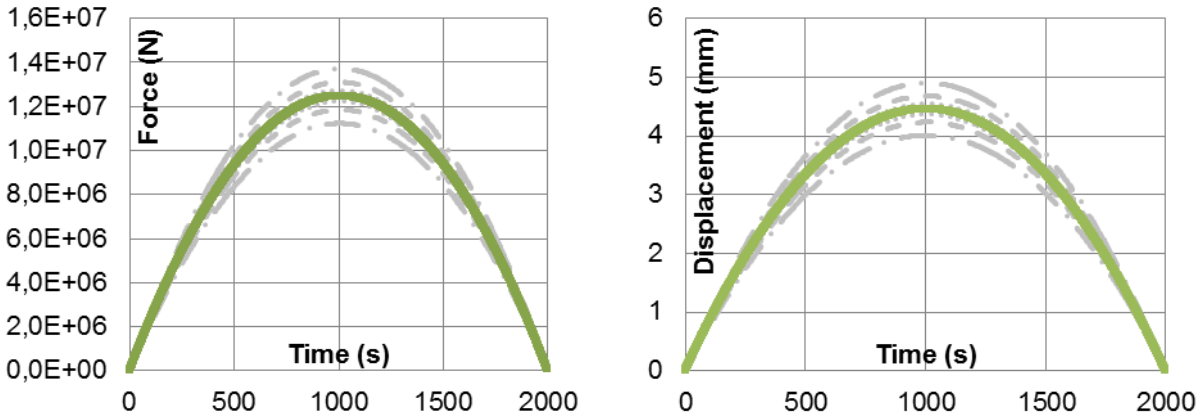


*c)* $\boldsymbol{R = 50}$

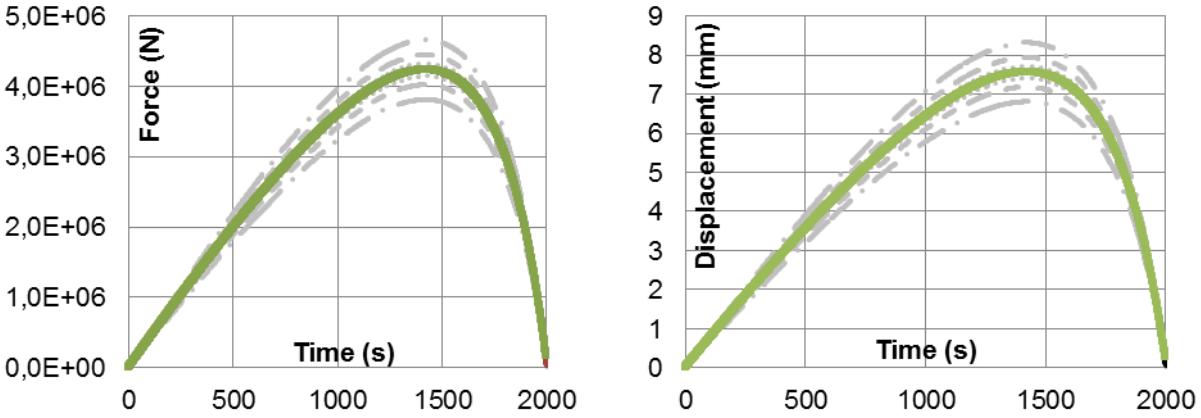


*d)* $\boldsymbol{R = 0.20}$

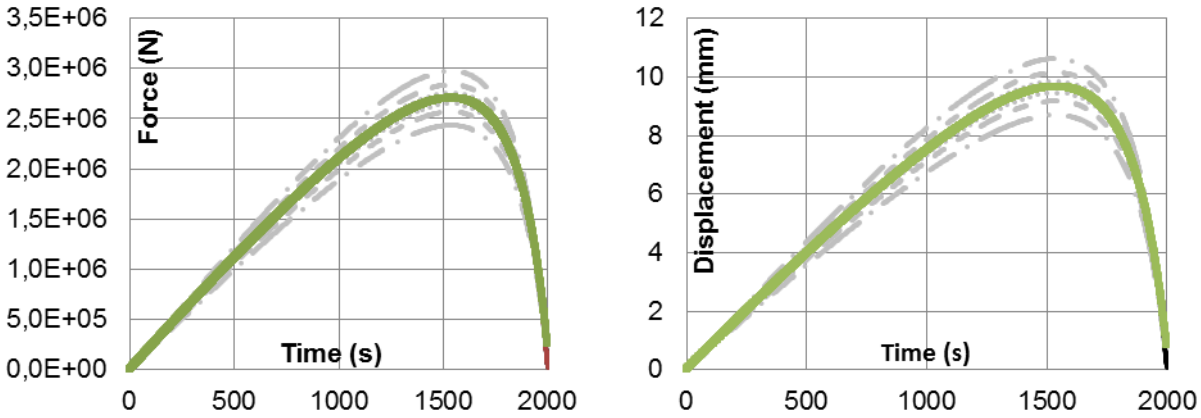


*e)* $\boldsymbol{R = 0.10}$

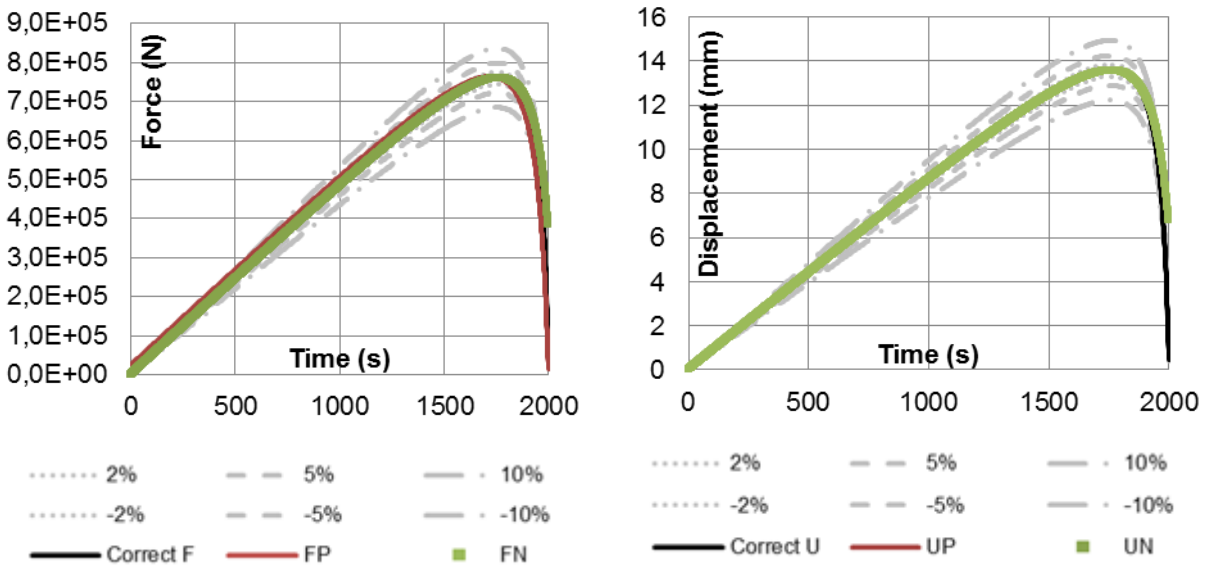


***f)*** $\boldsymbol{R = 0.02}$

*The interface force* *The interface displacement*

**Figure 5-12. The boundary conditions when the stiffness ratio varies**

Important to be observed in this exercise is the fact that the equilibrium might be affected for the case when the stiffness of the PS is significantly bigger than the one of NS. This is the case when the stiffness ratio between the substructures is set to be equal to 0.02, i.e. the stiffness of the PS is 50 times bigger than the stiffness of the NS. Thus the stiffness of the NS is insignificant in the computations process. Thus, right from the first step of the hybrid process, the reaction force of the PS is significantly different of the reaction force of the NS. To restore the equilibrium would request in this situation an important number of iteration. Since in fire tests the heat continues to affect the PS, thus the reaction force of the PS, the equilibrium will request even a bigger number of iterations. To produce better results is enough to reduce the time step. In this example the time step is set to be equal to 1s, so a smaller time step is possible but again the fire facility dictates if this is possible or not. On the other hand, in practice is unlikely to find structural system where the PS is 50 stiffer than the NS. If this specific situation is yet encountered, then it would be more economical to study the PS exposed to fire without updating the boundary conditions during the tests (traditional tests).

### 5.4.4. Conclusions

The presented exercise offers the possibility to understand better the new methodology and the parameters which affect the accuracy of the results and in some case even the stability of the process.

The selected time step depends on the furnace facility as well as on the stiffness ratio between the substructures. The reduction of the time step will lead to more accurate results.

The stiffness of the PS to be used in the calculation is important to be properly defined especially in the cases where the stiffness of the PS is more important (bigger) compared with the stiffness of the NS. In this situation an underestimation of the PS's stiffness can lead to instability, while the overestimation can lead to loss of equilibrium and deviation from the correct solution. If the stiffness of the NS is more important than the stiffness of the PS, then it is not so important the values of the PS's stiffness to be used.

The stiffness ratio between the substructures is important especially when the time step and the PS's stiffness to be used in the calculation are selected. If the NS's stiffness tends to infinity compared with the stiffness of the PS, then it might be possible to perform traditional tests on the PS with fixed boundary conditions. If the stiffness of the PS is much more significant compared with the stiffness of the NS (the stiffness of the PS tends to infinity), then the PS is tested in a traditional way with free boundary conditions.

The hybrid simulation represents interest when the stiffnesses of the substructures are in the same range of values, i.e. $\boldsymbol{R \cong 1}$**.** By writing that the stiffness ratio is approximately equal to one ($R \cong 1$) refer to the similar values of stiffnesses. By similar values we refer to all the cases when the traditional test with fixed or free conditions is not a proper solution.

All these details are analyzed prior the hybrid fire tests to be performed in order to select properly the parameters to be used.

## 5.5. Particularities of the new method in force versus displacement control

When performing standard fire tests, the most common tradition is to apply forces or displacements on the physical substructures which remain constant through the tests. The forces or the displacements transmitted to the tested specimen can likewise vary during the fire test, but most of the cases the function of variation is defined before the test.

When performing hybrid fire testing, the forces or displacements to be applied on the PS vary depending on the actual behavior of the PS during the fire test and depending on the characteristics of the NS.

Every fire facility is unique and developed for different purposes characterized by the possibility to work in displacement control or in force control. Nevertheless, some facilities dispose of force control and of displacement control method.

A displacement control strategy is the most common applied worldwide. In this case, the static equation is solved every time step for a target displacement that the PS must move to.

A force control procedure implies solving the static equation for a target force to be applied on the PS. The force control strategy is recommended for stiff physical specimen where the specimen can be moved using reasonable size force increments.

The actuator's Proportional, Integral, Derivative (PID) control parameters can be tuned for displacement control without requiring a specimen. For a force control procedure, a specimen

is necessary for tuning in order to receive force feedback. The force control tuning is also stiffness dependent, therefore using force control for a specimen with changing stiffnesses may not produce smooth results, because the actuator can only be tuned for one stiffness value.

Independent on the type of the procedure to be applied in the fire facility, the new methodology can be applied when solving for displacements (displacement control procedure) as well when solving for forces (force control procedure).

The particularities of the procedures lay in how the stiffness of the PS and NS is accounted for. The novelty of the new method compared with the first generation method is that the stiffness of the PS is not neglected anymore in the calculations. In other words, the stiffness of the PS and the stiffness of the NS are considered when solving for new solutions every time step.

It is next explained how the stiffnessess of the substructure are considered in displacement control procedure versus force control procedure.

*Displacement control procedure.*

The discussion will be done considering the system presented in the Figure 5-13 which is described in details in the Chapter 4.

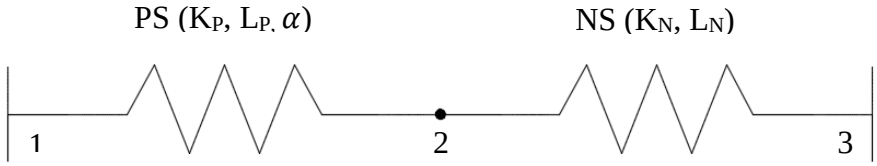


**Figure 5-13. The simple elastic system**

In displacement control procedure, the same displacement is imposed to be developed by the PS as well as for the NS.

Therefore, the displacement of the PS, i.e. $u_P$, and the displacement developed in the NS, i.e. $u_N$, is equal to the target displacement $u$ applied in the node 2 (see Eq. (67)).

$$u = u_P = u_N \tag{67}$$

The total force $F$ induces by the imposed displacement $u$ equals the sum of the forces developed in each substructure (see Eq.(70)).

$$F = F_P + F_N \tag{68}$$

The forces induced in the PS and NS by the target displacement $u$ are expressed in the Eq. (69).

$$\begin{aligned} F_P &= K_P * u \\ F_N &= K_N * u \end{aligned} \tag{69}$$

Therefore, the target displacement $u$ imposed in the node 2 of the system presented in Figure 5-13induces a force expressed by the Eq.(70).

$$F = (K_P + K_N) * u \tag{70}$$

*Force control procedure.*

In force control procedure, the forces developed at the interface of the substructures are equal as presented in the Eq. (71).

$$F = F_P = F_N \tag{71}$$

The force $F$ generates the displacement $u_P$ at the interface of the PS and the displacement $u_N$ at the interface of the NS (see Eq. (72)).

$$u_P = \frac{1}{K_P} * F$$

$$u_N = \frac{1}{K_N} * F \tag{72}$$

The total displacement $u$ induces by the imposed force $F$ equals the sum of the displacements developed in each substructure (see Eq.(73)).

$$u = u_P + u_N \tag{73}$$

In this specific case, the target force $F$ imposed in the node 2 of the system presented in Figure 5-13 is expressed by the Eq.(74).

$$F = \left(\frac{1}{K_P} + \frac{1}{K_N}\right)^{-1} * u \tag{74}$$

In conclusion, the solution of hybrid fire testing to be solved every time step $t_n$ is presented next for the displacement control procedure as for the force control procedure.

In the case of displacement control procedure, the incremental displacement computed every time step $t_n$ is solved based on the Eq. (75) .

$$\Delta\mathbf{u}(t_n) = (K_P + K_N)^{-1}\Delta\boldsymbol{F}(t_n) \tag{75}$$

In the case of force control procedure, the incremental force computed every time step $t_n$ is solved based on the Eq. (76).

$$\Delta \boldsymbol{F}(t_n) = \left(\frac{1}{K_P} + \frac{1}{K_N}\right)^{-1} \Delta \mathbf{u}(t_n) \tag{76}$$

*Example simple elastic truss*

This section presents the evolution of the interface displacement and force for the elastic system presented in the chapter 5.4 when the new methodology is considered in the calculations. Figure 5-14 presents the mentioned results in the case of the displacement control procedure while the Figure 5-15 presents the results for the case of the force control procedure.

The stiffness ratio between the substructures is $R = 0.50$ while the time step considered in the calculations is equal to $\Delta t = 50\ s$. The Young modulus decreases once with the fire exposure, nevertheless, the initial tangent stiffness is considered in the calculation of the new solution. All the characteristics of the system i.e. Young modulus, area, temperature evolution etc., are presented in detail in the Chapter 4 and 5.4.

The objective of this example is just to show that the new method is applicable in displacement control procedure as well as in the force control procedure.

No instability occurs when the new method is applied in force control or displacement control procedure.

The interface solution presented in the Figure 5-14 shows that the interface equilibrium is not satisfied and the solution deviates from the correct solution towards the end of the hybrid simulation. This is due to the improper time step selected to perform the iterations. The influence of the time step on the results is analyzed in the section 5.4.

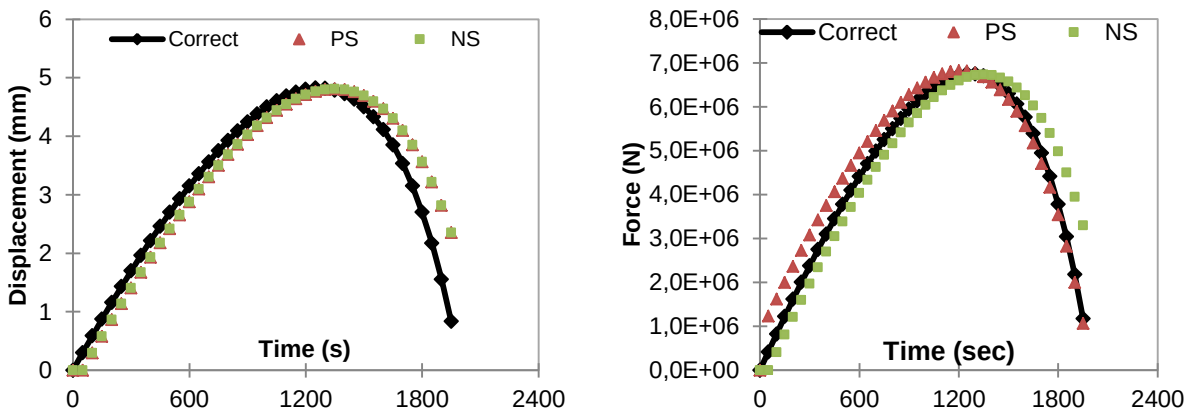


**Figure 5-14. Interface conditions for elastic system. Displacement control procedure.**

The solution presented in the Figure 5-15 shows that the compatibility is not ensured. As mentioned in the case of displacement control procedure, the time step is not properly

selected. The influence on the results of the time step as well as the influence of the PS's stiffness used in the calculations is not analyzed in this section. More analysis needs to be done in order to observe the characteristics of the force control procedure.

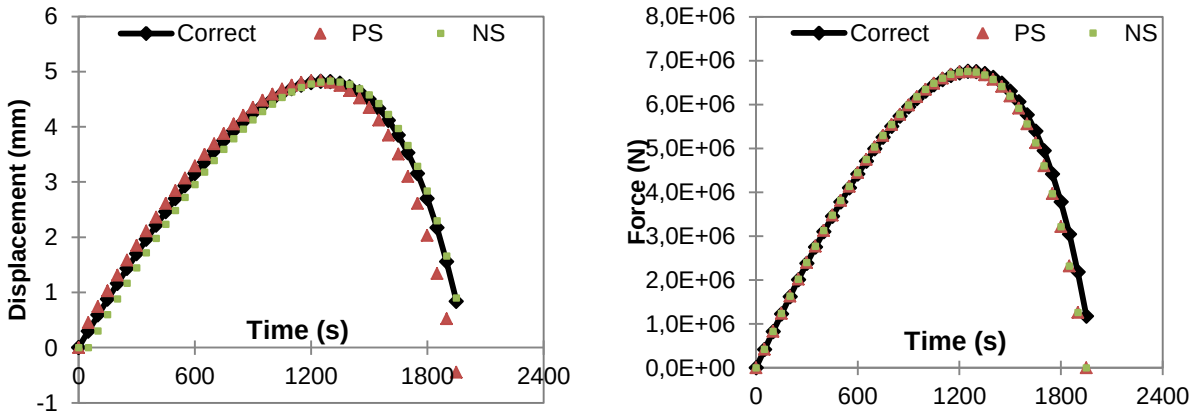


**Figure 5-15.Interface conditions for elastic system. Force control procedure.**

The objective of the graphs presented above is to underline that the new method is stable in force control procedure and displacement control procedure, with the mention that the force control procedure was not analyzed in detail in this thesis. A proper selection of the time step, as well as the proper stiffness of the PS need to be selected in order to ensure equilibrium, compatibility and moreover, to reproduce the correct solution.

In conclusion, the new method can be applied in force and displacement control procedure. The new solution to be imposed on the interface of the substructures is computed based on the Eq. (75) in the case of displacement control procedure, and based on the Eq. (76) in the case of the force control procedure.

# 6. HYBRID SIMULATION CASE STUDY

## 6.1. Introduction and motivation

The objective of this chapter is to analyze the behavior of a certain structure exposed to a certain fire scenario by means of hybrid fire simulation.

The former tests presented in the literature are performed on columns and slabs making use of the first generation method. One DoF is controlled during the tests, when the PS is represented by columns (Korzen and Mostafaei), while three DoFs are controlled when the slab is tested by means of hybrid fire test (Robert).

The objective of this thesis was to perform hybrid fire test on a structural element which has not been tested previously and to control multiple DoFs during the test. Thus, the selected structure for the case study is a moment resisting frame in the conditions when the roof floor beam is exposed to fire while the rest of the structure is not. The analyzed structure, i.e. the moment resisting concrete frame, is selected due to the common use in practice. The selected configuration allows testing a structural element which has not been tested before, i.e. a concrete beam, and the number of DoFs to be controlled at the interface is bigger than one.

The applicability of the first generation method as well as the new method is first analyzed in a numerical environment.

Next, the new methodology is implemented in the Promethee furnace facility in order to test the beam in a hybrid environment. The objective of the hybrid fire tests is, first, to test the methodology and, second, to observe the effect of the experimental site on the results (the equipment available in the furnace facility influences the results during the hybrid fire testing and one of the objectives was to identify the capability of the available equipment).

The support conditions during a fire test influence the behavior of the tested specimen, e.g. the failure time and mode. The traditional fire tests (common fire tests) are performed with simplified boundary conditions e.g. simply supported structural elements, fixed supports of the structural elements etc. The hybrid fire testing is a methodology which permits modelling the real boundary conditions during the entire tests by updating the supports conditions. Therefore, one of the case study interests is to show how behavior varies depending on the adopted boundary conditions during testing.
The standard fire curve ISO-834 is considered in the analysis.

## 6.2. Case study

### 6.2.1. Description

**Analyzed structure**

The analyzed building is an office building with 4 longitudinal bays of 5.6 m each and 2 transversal bays of 4 m, while the height of one storey is equal to 3 m. Figure 6-1 presents the plan view of the analyzed structure while the Figure 6-2 shows the elevation plan of the structure in the longitudinal direction.

The building frame is composed of reinforced concrete beams and columns, supporting concrete floor slabs which are 150 mm thick. The exterior and interior walls are made of masonry.

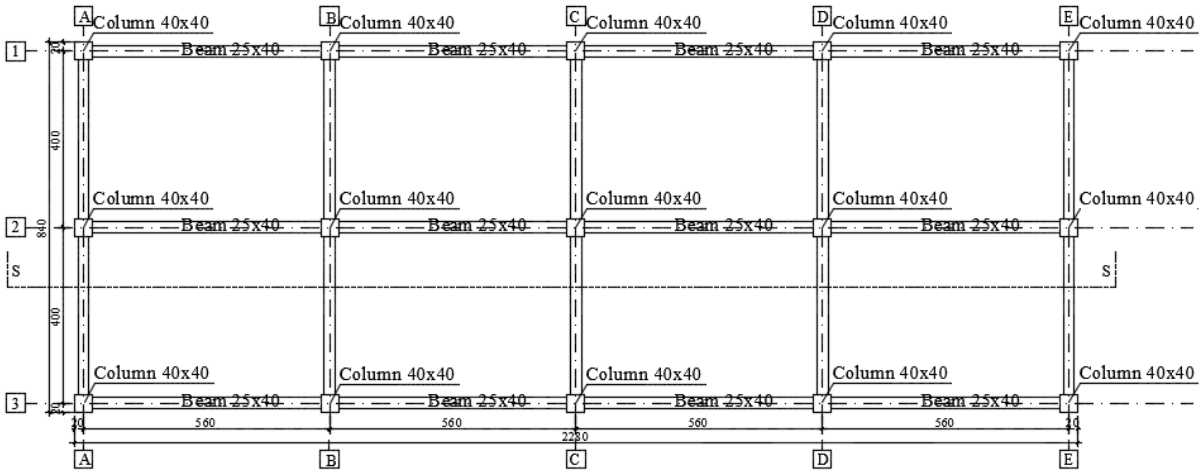


**Figure 6-1. Plan view of the building**

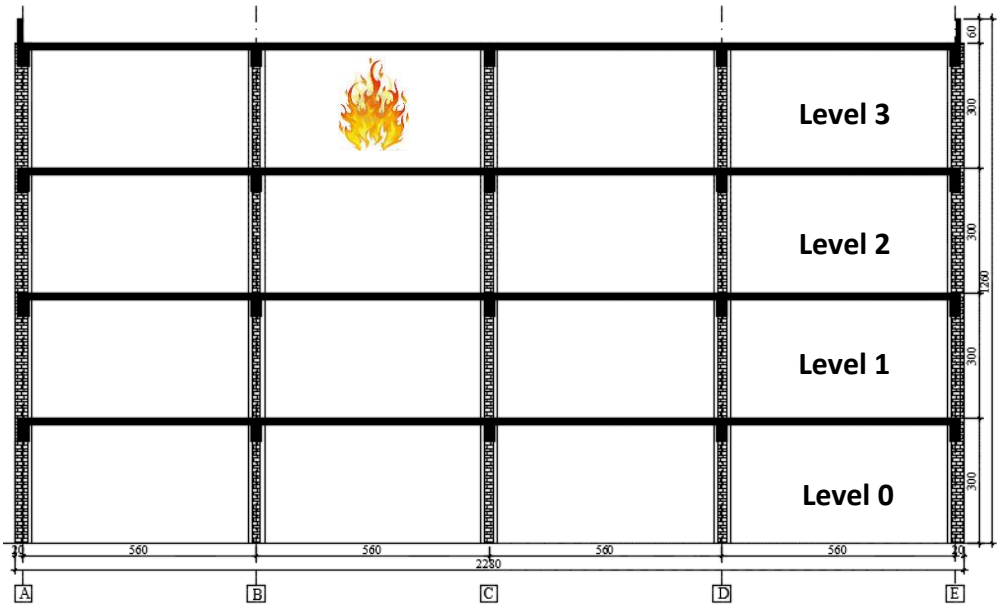


**Figure 6-2. Elevation of the structure. Section S-S**

The fire compartment is considered to be placed in the second bay, at level 3. For simplicity in the analysis we consider only the beam above the fire compartment exposed to fire while the rest of the structural elements inside the compartment are considered as unexposed.
Further on, only the central longitudinal frame, i.e. axis 2, is analyzed and considered in the calculations.

- **Structural members**

*Columns*

The cross section of the column is equal to 0.16 $m^2$ and is presented in Figure 6-3. The materials considered in the analysis are C30/37 concrete and cold worked steel, grade 500 class B. The nominal cover of the longitudinal reinforcement is equal to 35 mm (axis distance equal to 43 mm).

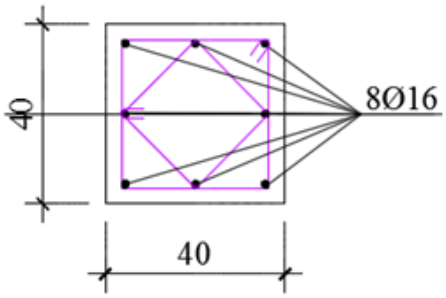


**Figure 6-3. The cross section of the column**

*Beams*

Different reinforcement areas will be used at the ends of the beams, at intermediate supports and in the span as presented in Figure 6-4. The cross section of the beam is equal to 0.25x0.40 $m^2$. The considered materials are concrete with the compressive strength of 48 MPa and cold worked steel, grade 500 class B. For the exposed beam (the specimen) additional shear stirrups have been included to avoid a possible shear failure during the hybrid test as can be seen in Figure 6-4 for the mid-span section and intermediate support. The effect of shear force on the exposed beam is assessed based on the simplified calculation presented in Annex D of EN 1992-1-2 [87] followed by the numerical analysis in the FE model VecTor2 [86].

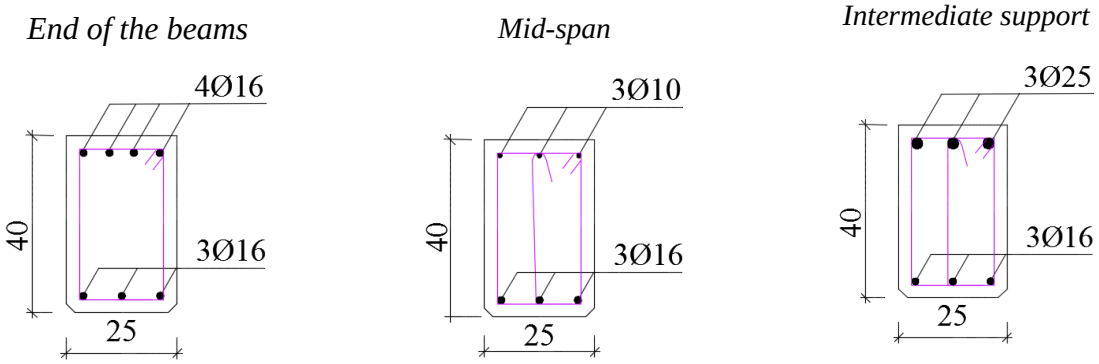


**Figure 6-4. The sectional configuration of the beam**

Table 6-1 presents the longitudinal reinforcement and the nominal cover of the reinforcement.

**Table 6-1. Longitudinal reinforcement and the nominal cover of the beam**

| *Type beam* | *Position reinforcement* | *Number and diameter* | *Nominal cover (Xdim × Ydim)* |
|---|---|---|---|
| **Perimeter** | bottom | 3 $\phi$ 16 | 40mm x 30mm |
| | top | 4 $\phi$ 16 | 40mm x 46mm |
| **Mid-span** | bottom | 3 $\phi$ 16 | 40mm x 30mm |
| | top | 3 $\phi$ 10 | 40mm x 71mm |
| **Intermediate** | bottom | 3 $\phi$ 16 | 40mm x 30mm |
| | top | 3 $\phi$ 25 | 40mm x 46mm |

- **Loads**

The characteristic values of the existing loads in the building are presented in Table 6-2**.**

**Table 6-2. Existing loads**

| | Load name | Value of load | Unit |
|---|---|---|---|
| Dead load | Self-weight of the structural elements | 25 | kN/m$^3$ |
| | Dead load of interior slabs | 1.50 | kN/m$^2$ |
| | Dead load of the roof | 4.50 | kN/m$^2$ |
| | Dead load of the exterior wall | 5.17 | kN/m$^2$ |
| | Dead load of the interior wall | 3.50 | kN/m$^2$ |
| | Dead load attic | 3.40 | kN/m$^2$ |
| Live load | Category A (areas for domestic and residential activities) | 2.00 | kN/m$^2$ |
| | Roof (no circulation) | 0.75 | kN/m$^2$ |
| | Snow | 0.56 | kN/m$^2$ |
| | Wind | ( Belgium Annex) | |

The load combination for the ultimate limit state (ULS) considered to design the structural members is presented in Eq. (77), where $G_{k,j}$ is the permanent action $j$, $Q_{k,1}$ is the dominant variable load, $Q_{k,i}$ is the variable load $i$ and $\gamma_{G,j}$, $\gamma_P$, $\gamma_{Q,1}$, $\gamma_{Q,i}$, $\psi_{0,i}$ are the safety coefficients defined in EN 1990 (no prestressed force is considered in this example).

$$\sum_{j\geq 1} \gamma_{G,j}\, \mathrm{G}_{k,j}\text{"} + \text{"}\gamma_{Q,1}\mathrm{Q}_{k,1}\text{"} + \text{"} \sum_{i>1} \gamma_{Q,i}\, \psi_{0,i}\mathrm{Q}_{k,i} \qquad \textbf{(77)}$$

The mechanical action in fire situation was determined in accordance with EN 1990 by using the load combination presented by Eq. (78).

$$\sum_{j\geq 1} \mathrm{G}_{k,j}\text{"} + \text{"}(\psi_{1,1}\ or\ \psi_{2,1})\mathrm{Q}_{k,1}\text{"} + \text{"} \sum_{i>1} \psi_{2,i}\, \mathrm{Q}_{k,i} \qquad \textbf{(78)}$$

According to the Belgian National Annex, the wind load is multiplied by the coefficient $\psi_{1,1} = 0{,}2$ while the live load for domestic areas and residential activities is affected by the coefficient $\psi_{2,2} = 0{,}3$.

So the load combination considered in the fire analysis can be written as "Dead load + 0.2 Wind + 0.3 Live Load".
The geometric imperfections are applied as horizontal forces in the nodes, based on the section 5.2. of EN 1992-1-1 [88].

### 6.2.2. The definition of the predetermined matrix

The NS can be represented in a FE model during the test or can be described by a predetermined matrix.

If the FE model is chosen then, for every time step of hybrid test, the FE model is running to get the interface data to be used in the update of the boundary conditions. The running time of the analysis can be an important factor that influences the quality of the results in terms of equilibrium and compatibility at the interface. Moreover, if the NS is represented in the FE model then the reduction from the global DoFs to local DoFs (and vice versa) needs to be implemented.

If the predetermined matrix is used instead then there is no need of running the FE analysis every time step. Therefore, the time to compute the reactions of the NS is reduced to virtually zero. In this situation the matrix is determined for the number of DoFs controlled at the interface without having the need to do this additional operation during the test. Moreover, the predetermined matrix includes the effects of the loads on the structure before the start of the fire.

This section presents the method to establish the predetermined matrix for the studied example.

*Structure, configuration, loads*

The first step in defining the predetermined matrix is to perform the analysis of the considered structure before the substructuring. Thus the moment resisting frame was loaded with the distributed loads, vertical concentrated forces (reactions from the transversal frame), and horizontal forces (imperfections and wind). The load combination considered is the one presented by Eq. (78). Figure 6-5 presents the FE model of the analyzed structure along with the considered loads in the nonlinear software SAFIR®.

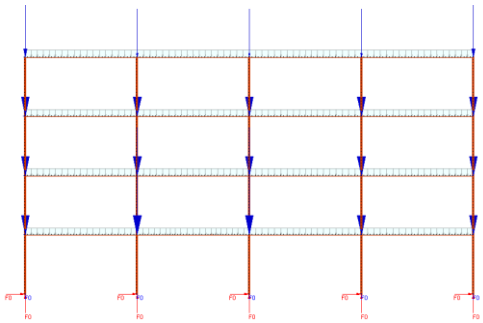

**Figure 6-5. FE model (SAFIR) of the analyzed structure.**

The next step is to define the equivalent structure which will serve to calculate the terms of the matrix. The equivalent structure is obtained by "cutting" the PS from the whole structure and introducing the equivalent forces at the interface. The equivalent forces (the horizontal force, the vertical force and a bending moment) in each node are obtained from the analysis of the entire building.

The beam is extracted from the analyzed structure as presented in Figure 6-6. The total number of DoFs at the interface is 6 for a 2D analysis, noted here from $D_1$ to $D_6$. To eliminate the rigid body modes, the beam will be simply supported in the furnace with only 3 DoFs controlled during the hybrid tests. The controlled DoFs are the axial displacement noted $D_{1L}$ and the support rotations $D_{2L}$ and $D_{3L}$. As specified before, the predetermined matrix will be defined directly for the number of DoFs controlled at the interface. Thus the predetermined matrix will have a dimension of [3x3].

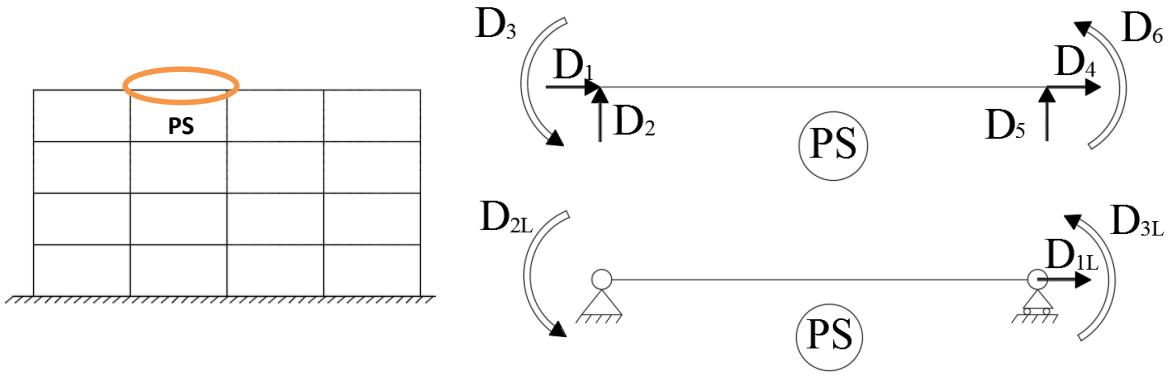


*The analyzed structure* *The PS with global and local DoFs*

**Figure 6-6. The PS extracted from the analyzed structure**

The predetermined matrix $K_N$ for the case study has the form presented by the Eq. (79). The displacement method is considered to determine the terms of the matrix.

$$K_N = \begin{bmatrix} k_{11} & k_{12} & k_{13} \\ k_{21} & k_{22} & k_{23} \\ k_{31} & k_{32} & k_{33} \end{bmatrix} \quad \textbf{(79)}$$

It will be explained next how the predetermined matrix of the NS is determined.

Please note that during the process of determining the predetermined matrix, the frame is loaded with the exterior loads. This is due to the fact that the predetermined matrix needs to represent the state of the building right before the start of the fire (tangent stiffness). Before the fire, the structure is loaded with possible cracks in the concrete.

*The first column of the matrix*

Figure 6-7 presents the SAFIR model used to compute the first column of the predetermined matrix related with the axial DoF.

The principle of the displacement method is to impose a displacement for one DoF while the rest of DoFs are blocked. Therefore, the terms of the stiffness matrix result by dividing the reaction forces which develop in the blocked DoFs by the imposed displacement.
The predetermined matrix has been computed to account for the DoFs which were blocked during the test in order to avoid the rigid body modes.
Thus in the numerical model the PS will be replaced by a rigid truss. The objective of the truss is to keep the two nodes connected. The truss will be heated in order to introduce a relative displacement between the two nodes. The displacements in the nodes will be different because the stiffness of the surrounding is different for one node compared to the other node. The material properties of the heated truss are kept constant. No degradation of the material is considered, only the thermal expansion to induce the relative displacement.
The support rotations are controlled during the test therefore in the FE analysis the rotations are blocked.
As a summary of the procedure the steps are presented simplified here below. Note that the left node in the structure will be the hinged support in the test while the right node will be the rolling support.

**Impose**:

- expansion of the truss;
- impose the rotation at the left node with the value coming from the analysis of the entire building;
- The same for the right node;

**Read**:

- the axial force in the truss $N_{truss}$;
- the reaction moment in the left node $R_l$;
- the reaction moment in the right node $R_r$;
- the elongation of the truss $u_t$;

**Results**:

- $k_{11} = -\frac{\Delta N_{truss}}{\Delta u_t}$
- $k_{21} = \frac{\Delta R_l}{\Delta u_t}$
- $k_{31} = \frac{\Delta R_r}{\Delta u_t}$

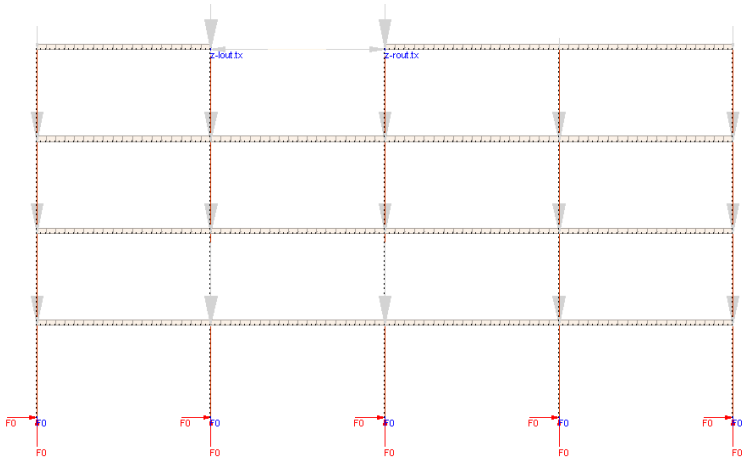

**Figure 6-7. SAFIR model to compute the first column of the predetermined matrix**

*The second column of the matrix*

The second column is related to the rotation of the left node. The FE model is built as in the previous case with the modifications specified here below.

The PS will be replaced by a cold rigid truss, to keep the same distance between the two nodes of the interface while the position of the nodes is changing.

The left rotation is imposed while the right rotation will be blocked.

As a summary:

**Impose**:

- the same distance between the node by using a rigid truss;
- impose an increase of the left support rotation $\theta_l$ compared with the value coming from the analysis of the entire building;
- block the rotation of the right support with the value coming from the analysis of the entire building;

**Read**:

- the axial force in the truss $N_{truss}$;
- the reaction in the left node $R_l$;
- the reaction in the right node $R_r$;
- the left support rotation $\theta_l$;

**Results**:

- $k_{12} = -\frac{\Delta N_{truss}}{\Delta \theta_l}$
- $k_{22} = \frac{\Delta R_l}{\Delta \theta_l}$
- $k_{32} = \frac{\Delta R_r}{\Delta \theta_l}$

*The third column of the matrix*

The last column of the matrix refers to the right support rotation. The process is the same as for the left node.

## 6.3. The configuration of the tests

The new methodology will be implemented and verified on two full scale fire tests in the Promethee furnace, CERIB, France. The analyzed structure is presented in the Figure 6-8.

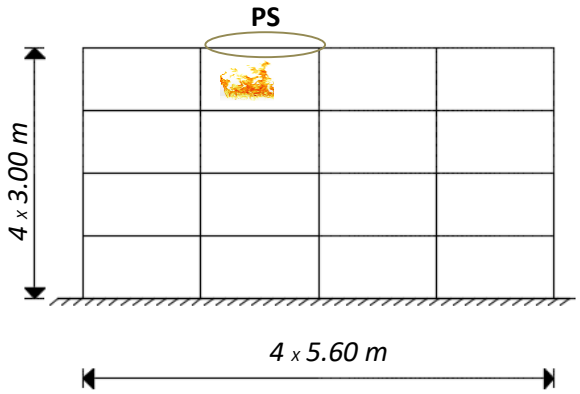


**Figure 6-8 – Moment resisting concrete frame.**

Figure 6-9 presents the configuration of the PS. A concrete beam of 0.25 m x 0.40 m x 8.00 m, will be tested in three different tests. The beam will be exposed to fire only between the supports (5.60 m), while the two cantilever parts of the beam are used to generate the support bending moment. The horizontal jacks $H$ is used to control the horizontal displacement $u$ of the specimen. The vertical jacks $P_{left}$ and $P_{right}$ are used to control the rotations $\theta_{left}$ and $\theta_{right}$. The jacks $P$ are used to apply the constant loads in the span.

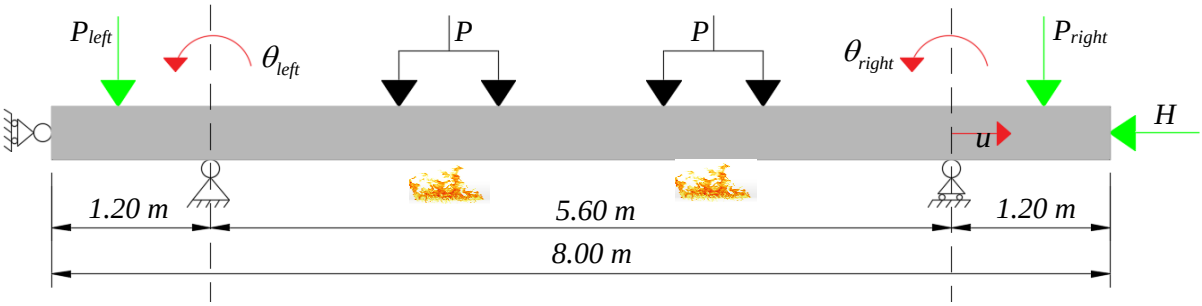


**Figure 6-9 – The configuration of the physical specimen PS.**

Table 6-3 presents a summary of the jacks and controlled DoFs during the different tests. The beam is simply supported and the condensation of the DoFs has been taken into account in the predetermined matrix. From the total number of 6 DoFs at the interface, only 3 DoFs will be controlled during the hybrid test.

**Table 6-3. Description of the jacks and controlled DoFs**

| Jacks | Controlled DoFs | TEST 1 | TEST 2 | TEST 3 |
|---|---|---|---|---|
| $H$ | $u$ | - | *Variable* | *Variable* |
| $P_{left}$ | $\theta_{left}$ | *Constant* | *Variable* | *Variable* |
| $P_{right}$ | $\theta_{right}$ | *Constant* | *Variable* | *Variable* |

The first test, Test 1, is a non-hybrid test (traditional test), where the effect of the surrounding is assumed constant during the test (constant negative moments applied at the supports and no axial restraint). Only the jacks $P_{left}$, $P_{right}$ and $P$ are active, applying constant forces during the test, due to the fact that no evolution of interaction with the NS is considered during the test. The horizontal jack $H$ is inactive meaning that no axial restraint is assumed during the test.

The next two tests, Test 2 and Test 3, are hybrid tests. In this case only the jacks $P$ will be applying a constant load during the test. However, the jacks $P_{left}$ and $P_{right}$ (generating the support bending moment) and $H$ (controlling the axial DoF) will apply varying forces, depending on the characteristics of the NS and PS. In the hybrid tests, the behavior of the NS will be pre-calculated, using a predefined matrix defined in the software which controls the furnace (Sauca et al. in [83]).

In order to ensure stability of the process, the first generation method would require using a force control procedure to control the axial DoF and a displacement control procedure to control the rotational DoFs. This illustrates the impracticability of the latter when several DoFs need to be controlled. Yet, the new method presented in this thesis can be applied and is stable independent on the stiffness ratio between the substructures as it will be next presented.

## 6.4. Numerical Analysis of the Hybrid Test (Virtual Hybrid Fire Testing)

Before performing the hybrid fire tests, predictions need to be done in a numerical environment.

The numerical analysis of a hybrid fire tests assumes the following actions:

- The NS is modeled aside in the FE software or by using the predetermined matrix;
- The PS is modeled in the FE software capable to deal with the heat transfer;
- The hybrid fire methodology serves to connect the PS and NS by ensuring the compatibility and equilibrium every time step. Moreover, the correct solution needs to be reproduced (the solution is deemed to be correct when the forces and displacement at the interface are the same in the HFT as in the analysis of the entire structure);

In the performed case study, the NS behavior is described by the predetermined matrix while the PS is modeled in SAFIR®. The interface displacements/forces of the PS and NS are

controlled every time steps using the hybrid fire methodology so the objectives of hybrid fire testing are satisfied.

We refer to the numerical analysis of the hybrid fire testing as virtual hybrid fire testing. This is due to the fact that the PS is modeled in the FE software i.e. “virtual furnace”.

The virtual hybrid testing is performed here using the first generation method and the new method.

For the real hybrid fire tests, the compression concrete strength of the concrete is measured on samples, in different days since the casting of the specimen. Using the Expressions (3.1) and (3.2) from EN 1992-1-1, the compression concrete strength in the day of the test is assumed to be equal to 48 MPa. In the virtual hybrid fire tests, the value of 48 MPa concrete compressive strength is considered.

All the results in the virtual environment (SAFIR) presented in this thesis are done based on the concrete model SILCONC_EN. It has been verified that the effects of the explicit consideration of transient creep strain (Gernay in [89], [90]) are not significant for this case study mainly due to the fact that ISO fire is used.

The predetermined matrix for the NS in this specific case is presented in the Eq. (80) and is determined as presented in section 6.2.2. All the values presented next are expressed in [N], [m] and [rad].

$$K_N = 10^6 \begin{bmatrix} 10.50 & -11.70 & 8.26 \\ -11.70 & 64.80 & -8.72 \\ 8.26 & -\ 8.72 & 63.60 \end{bmatrix} \tag{80}$$

The stiffness matrix of the PS is obtained considering the loaded beam as a start point (Eq.(81)).

$$K_P = 10^6 \begin{bmatrix} 479 & 0 & 0 \\ 0 & 25.60 & 12.80 \\ 0 & 12.80 & 25.60 \end{bmatrix} \tag{81}$$

Considering the three DoFs to be controlled during the hybrid tests, the stiffness matrix of the PS is computed as presented in the Eq.(82). The young modulus of the concrete material is calculated as presented in the Eq.(83), where $f_c$ is the compressive strength of the concrete.

$$K_P = \begin{bmatrix} \frac{EA}{L} & 0 & 0 \\ 0 & \frac{4EI}{L} & \frac{2EI}{L} \\ 0 & \frac{2EI}{L} & \frac{4EI}{L} \end{bmatrix} \tag{82}$$

$$E = \frac{2f_c}{2.5 \times 10^{-3}} \quad (83)$$

Where:

$E$ is the Young modulus, unit $[\frac{N}{m^2}]$;
$A$ is the cross sectional area, unit $[m^2]$;
$I$ is the moment of inertia, unit $[m^4]$;
$L$ is the length of the beam, unit $[m]$;

By comparing the predetermined matrix of the NS and the stiffness matrix of the PS some observations are done for the ambient temperature:

- The axial stiffness of the PS is higher than the axial stiffness of the NS;
- The rotational stiffness of the PS is smaller than the one of the NS;

### 6.4.1. The First Generation Method

The first generation method is sensitive to the stiffness ratio between the NS and PS. For this specific case study, the stiffness ratio is smaller than 1 for the axial DoF and bigger than 1 for the rotational DoFs. The force control procedure is requested for the axial DoF and the displacement control procedure is suitable for the rotational DoFs in order to avoid the instability of the process.

The virtual hybrid fire test is first performed using the first generation method. The force control procedure is considered during the example.

The following steps are performed during the virtual hybrid fire test:

- The PS is modelled in SAFIR with the concrete properties characteristic to the compression strength of 48 MPa;
- The span loads are applied in the FE model along with the initial interface forces. The initial interface forces are applied in the case of the force control procedure. If a displacement control procedure is used, then the initial interface displacements are applied in this step;
- The NS is modeled using the predetermined matrix, defined in an Excel file;
- Before starting heating the PS, the equilibrium at ambient temperature is restored;
- For the exercise the chosen time step is equal to 2 s and the delay time is equal to 1 s;
- The virtual fire test starts, i.e. the FE model runs during one time step. During this time step, the span loads and the initial forces at the interface are kept constant. The fire exposure induces changes in the interface displacements;
- The interface displacements are thus registered, and noted in the Excel file;
- The reaction forces of the NS can be computed since the interface displacements are known (the vector of reaction forces results by multiplying the predetermined matrix with the vector of the initial displacements);
- The reaction forces of the NS are imposed at the interface of the PS. The simulation is ready to run for one more step;

In this specific case, the communication between the PS (SAFIR) and the NS (Excel file) was done manually.

Figure 6-10 presents the evolution of interface displacements when the first generation method is applied in a virtual environment. Every graph illustrates the correct solution along with the interface solutions of the PS and NS. The correct solution represents the solution resulted when the building structure is numerically modeled as a whole.

Soon after the virtual hybrid fire test starts, the solution of the virtual hybrid fire testing oscillates around the correct solution leading to the failure of the beam.

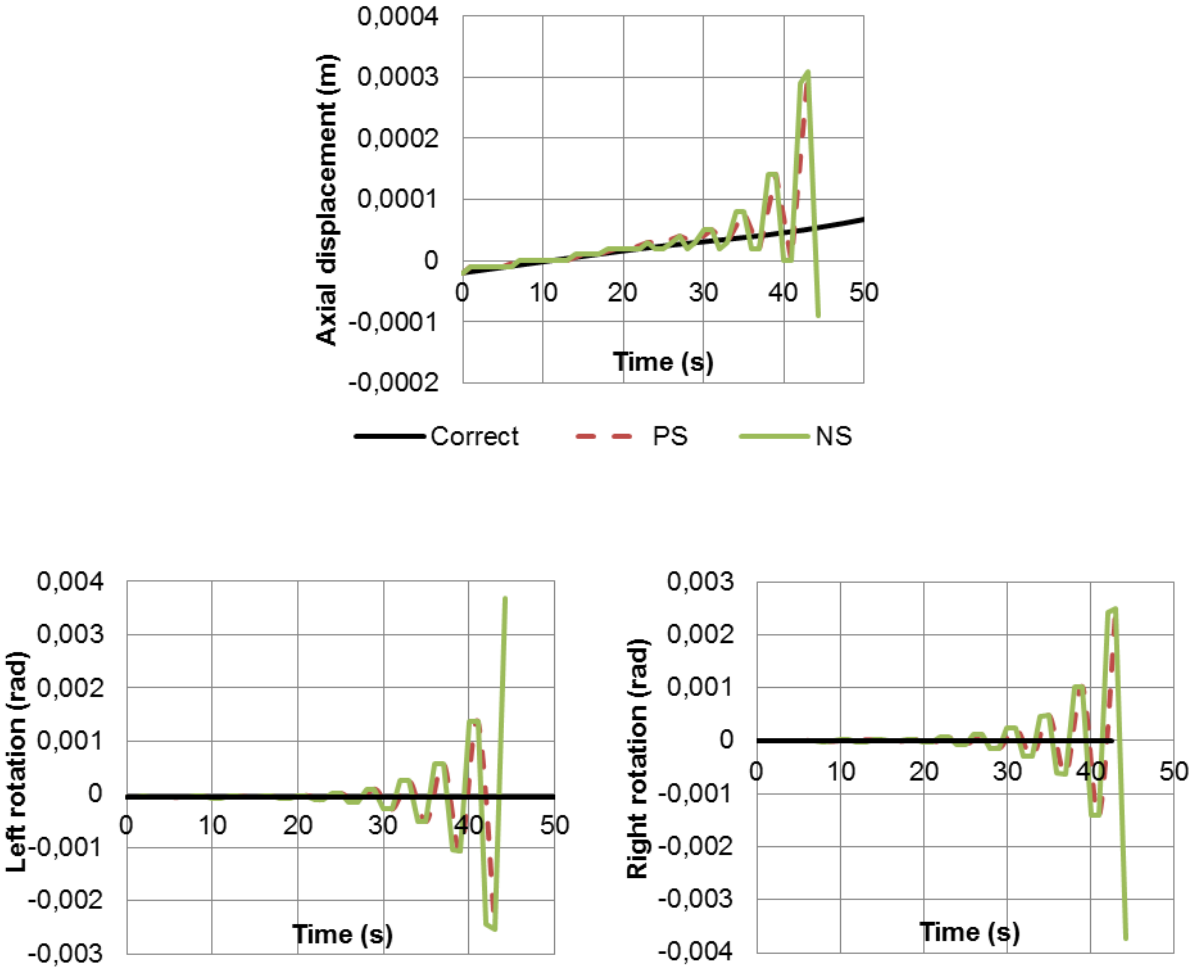


**Figure 6-10. The case study results in a virtual environment when the first generation method is considered**

The exercise is repeated with different time steps leading to instability every time. Figure 6-10 presents the evolution of the interface displacements when the time step is elected to be equal to 2 s.

This example supports the conclusions presented in chapter 4, the first generation method is sensitive to the stiffness ratio between the substructures (Sauca et al. [84]).

Since the force control procedure is appropriate for the axial DoF, for the rotational DoFs the displacement control procedure needs to be applied. A mixed force/displacement control procedure could be applied, meaning that for the axial DoF the force control is adopted and a displacement control procedure for the rotational DoFs. From the experimental point of view, it is complex and might not be suitable for all the furnace facilities. Moreover, even if the mixed force/displacement control procedure is applied successfully, the force control procedure does not offer the possibility to simulate experimentally the failure mode in the unstable regime. More than that, for successful results in force control procedure, the stiffness ratio needs to be smaller than 1 during the entire test. Since the stiffness of the PS is degrading due to the fire exposure, at one moment during the tests the ratio can become bigger than 1and thus the instability is induced in the inappropriate time.

Another solution is to switch from force control procedure to displacement control procedure when the stiffness ratio changes. From theoretical point of view, the solution is applicable. From the experimental point of view, it is complex and risky to identify the moment to switch the procedures.

Even though from the theoretical point of view solutions exist to use the first generation method in all possible cases, from the experimental point of view some of the mentioned solutions are difficult or even impossible to be realized.

The new methodology is suitable to be applied independently on the stiffness ratio between the structures. The next section has the objective to analyze the new methodology in the virtual environment and to see the proper characteristics to be chosen in order to generate accurate results.

### 6.4.2. The New Method in displacement control procedure

The virtual hybrid fire testing is performed by using the new methodology proposed in this thesis.

The new methodology ensures equilibrium, compatibility at the interface along with the reproduction of the correct solution, independently on the stiffness ratio between the substructures (Sauca et al. [85]). Before the start of the hybrid fire tests, some inputs are required such as the time step and the initial tangent stiffness matrix of the PS. Based on the discussions from chapter 5 the input values dictate the accuracy of the results. The main objective of this section is to observe the results of the virtual hybrid fire testing in different conditions, when different values are selected as an input of the hybrid fire tests. This exercise helps to choose the proper characteristics to be defined before the start of the real hybrid fire tests.

In the previous section, the exchange of the information between the PS and NS was done manually. This tedious exercise could be performed only because instability occurred early in the process.

Two solutions are presented and described to perform virtual hybrid fire testing automatically:

- Matlab routine;
- SAFIR - new subroutine implemented;

*Matlab routine*

A Matlab code is written to compute the solution to be imposed at the boundaries of the substructures every time step and to ensure the connection between the PS and NS.

The advantages of the Matlab routine are:

- Avoids the human error;
- Computation time reduces;

The steps implemented in the Matlab routine are:

- The PS is modelled in SAFIR and loaded with the span loads;
- The predetermined matrix of the NS is defined in the Matlab routine;
- The time step is defined in the Matlab routine along with the initial tangent stiffness of the PS;
- The initial displacements are applied at the interface of the PS (in SAFIR) and the numerical analysis of the PS is ready to run;
- The Matlab routine orders to the SAFIR executable to run the analysis when the span loads and the initial displacements are applied on the interface of the PS at ambient conditions;
- The next step in the Matlab routine corresponds to opening of the output file generated by the SAFIR executable and to read the reaction forces;
- The reaction forces at ambient temperature are compared with the reactions of the NS at ambient temperature. If the equilibrium is not ensured, then new displacements are computed based on the out of balance forces and imposed on the substructures, until the equilibrium at ambient conditions is satisfied;
- Once the equilibrium is satisfied, the Matlab routine induces the numerical analysis to run. During the entire time step, the interface displacements are kept constant. The fire exposure induces a change in the reaction forces of the PS;
- The reaction force of the PS is different than the reaction force of the NS. Based on the out of balance forces, new displacements are computed and imposed on the substructures. At the same time the PS is exposed to fire;
- Every time after the numerical analysis stops running, the output file is opened and the reaction forces are saved and used further in the calculations;
- The procedure is repeated until the end of the virtual hybrid fire tests;

The FE software SAFIR does not give the possibility to the user to pause the analysis every time step, while the modification of boundary conditions is done, and then to restart the calculations from the previous time step. Every time step when the boundary conditions of the PS are modified, the analysis restarts from the beginning. The adopted solution worked well

but it was not the most efficient in terms of the total time needed to perform the virtual hybrid fire testing.

*SAFIR - HFT, new subroutine implemented*

The new methodology presented in this thesis is implemented in SAFIR and makes possible to perform virtual hybrid fire testing entirely in SAFIR. The subroutine is developed for the case when the NS is defined by the predetermined matrix.

The main advantage of the subroutine is the economy of time. The running time of analysis reduces considerably compared with the previous solution i.e. the Matlab routine.

The HFT subroutine computes the interface displacement to be imposed on the interface of the substructures every time step.

Before the start of the virtual hybrid fire test, the user defines the following:

- the initial tangent stiffness of the PS;
- the predetermined matrix of NS;
- the initial interface forces;
- the initial interface displacements;

To perform virtual hybrid fire tests some small changes are implemented as well in the input file used by the SAFIR executable.

The changes in the considered input file to run virtual hybrid fire test in SAFIR are next described.

A procedure is presented to define the time step in order to permit the iterations at ambient conditions at the very beginning of the fire analysis.

- The time step of the virtual hybrid testing is defined as the time step of the usual structural analysis. An example is presented and explained here below:

*TIME*
*0.01* *0.05* -> the time defined for the iteration at ambient temperature
0.95 1.00 -> the time step defined for the hybrid fire testing
*1.00* *20000.00*
*ENDTIME*

The first defined line refers to the time step needed for the iterations at ambient temperature. The user will observe the needed number of iterations at ambient temperature to restore the equilibrium between the substructures. The restoring of equilibrium is done in the first second of the analysis, thus the fire effect is negligible. In our example the equilibrium at the ambient temperature is restored in 0.05s. Such a short time step is not suitable if a dynamic analysis is performed.

Next, the time step afferent to the hybrid fire testing is defined, which is equal to 1 s in this example.

- The DoFs to be controlled during the virtual hybrid fire test are specified in the input file which describes the PS. Some modifications are applied to the "FIXATION" command.

The changes in the descriptions of "FIXATION" command presented in the USER SAFIR MANUAL are presented here below:

'FIXATIONS'

Supports and imposed displacements fixed blocks.

One line for each node where the solution follows a defined function of time and the reaction must be calculated.

'BLOCK', NNO, CBLOCK(1,NNO), …, CBLOCK(NDOFMAX,NNO)

NNO = Number of the specific node where the solution must not be calculated.

CBLOCK(1,NNO) = Function describing displacement for first D.o.F. at this node with respect to time. Type NO if the displacement is not prescribed for this DoF. **Type HFT1.txt if the displacement is controlled during the hybrid test.**

CBLOCK(2,NNO) = Function describing displacement for second D.o.F. at this node with respect to time Type NO if the displacement is not prescribed for this DoF. **Type HFT2.txt if the displacement is controlled during the hybrid test.**

…

CBLOCK(NDOFMAX,NNO) = Function describing displacement for last D.o.F. at this node with respect to time. Type NO if the displacement is not prescribed for this DoF. **Type HFTNDOFMAX.txt if the displacement is controlled during the hybrid test.**

For each degrees of freedom NDL, from 1 to NDOFMAX, CBLOCK(NDL,NNO) is "NO" if the displacement is not imposed at this DoF or the name of the function describing the evolution of the displacement at this node with respect to time. "F0" is a common function, used to model a fixed support. **If the degree of freedom is controlled during the virtual hybrid fire test, the function describing the evolution of displacements is defined as HFTNDL.txt. The txt file will include no information, it will just serve to know that the respective DoF is controlled in the virtual hybrid process**.

The example presented bellow has three DoFs to be controlled during the virtual hybrid test. For the node "1" the first and the third DoFs are controlled, while for the node "2" only the third DoF is controlled.

```
FIXATIONS
   BLOCK   1   HFT1.txt   F0   HFT3.txt
   BLOCK   2   F0          F0   HFT3.txt
END_FIX
```

*Results of the virtual hybrid fire testing*

The new method is described in details in chapter 5. The stability and accuracy of the tests depend on the time step and on the value chosen for the stiffness of the PS.

Before the real hybrid fire test, the virtual HFT is performed in order to choose the proper value of the time step as well as the proper values of the PS's stiffness.

- The influence of the time step on the results

In the first stage of the exercise, the influence of the time step on the results is observed.

At the same time, the stiffness of the PS is considered constant during the virtual hybrid fire testing. The chosen value for the calculations is based on the recommendations mentioned here below.

Before the real hybrid fire testing the stiffness of the PS is recommended to be measured. To avoid the experimental possible errors when the stiffness of the PS is measured, the recommendation is to overestimate the measured values of the stiffness with a factor of 1.50 as presented in the Eq. (84).

$$K_P^* = 1.50 K_P \tag{84}$$

Where:

$K_P^*$ is the stiffness of the PS considered in the calculation process during the HFT;

$K_P$ is the measured tangent stiffness of the PS;

Before the virtual hybrid fire testing, the initial tangent stiffness of the PS is determined in the numerical environment and the resulted value for this exercise is presented in the Eq. (81). The resulted values are then multiplied with 1.50 and defined in the HFT SAFIR subroutine.

The cases presented in the Table 6-4 are next analyzed.

**Table 6-4. The variation of the time step in the virtual hybrid fire testing**

| | Time step | The PS's stiffness |
|---|---|---|
| **Case 1** | $t = 1\ s$ | $K_P^* = 1.50K_P$ |
| **Case 2** | $t = 10\ s$ | |
| **Case 3** | $t = 30\ s$ | |
| **Case 4** | $t = 60\ s$ | |
| **Case 5** | $t = 5\ min$ | |
| **Case 6** | $t = 10\ min$ | |

Six graphs are presented for every case, 3 of them illustrate the evolution of interface forces for every DoF, while the other 3 present the evolution of the interface displacements for every DoF.

Every graph illustrates the "correct solution" along with the solution registered at the interface of the PS and the solution computed at the interface of the NS. The "correct solution" results from the numerical analysis of the structure when no substructuring is done. The interface solutions of the PS result from the virtual hybrid fire testing analysis. The NS is defined using a constant matrix, called "predetermined stiffness matrix" and the interface solution are computed during the virtual hybrid fire testing. The correct solution is represented using the continuous black line, the solution of the PS is represented using the dashed red line while the solution of the NS is represented by the continuous green line.

The first objective of the HFT is to ensure the equilibrium and compatibility between the substructures during the entire process. In the graphic representation the equilibrium and the compatibility are ensured when the solution of the PS matches the solution of the NS. If the interface forces of the PS and NS match, then the equilibrium is achieved, while the compatibility is achieved when the displacement of the PS match the displacement of the NS.

During the hybrid fire testing, the correct solution needs to be reproduced. This condition is available in a virtual environment based on the hypothesis of the hybrid fire testing. The hybrid fire testing is normally performed when the behavior of the PS is unknown prior the testing; the "correct solution" is thus unknown in a real hybrid fire test. On the contrary, in a virtual environment, the "correct solution" is known and therefore the new methodology should be able to reproduce the exact solution.

In this particular example the NS is defined by the predetermined matrix which is considered constant during the entire virtual hybrid fire test. When the PS is exposed to fire, the interface displacements and forces vary in time. In the exact solution, these variations induce plasticity in the NS even if it is not exposed to fire. Since the predetermined matrix is constant, the changes induced in the NS are not captured in this specific case study. This is the main reason why in the presented graphs the solution of the virtual hybrid fire test does not match the "correct solution", especially at the end of the tests. Despite the mentioned fact, the "correct solution is chosen to be plotted. The solution of the virtual hybrid fire test is observed to diverge from the correct solution when the plasticity starts to be developed in the cold NS. The time when this occurs has been extracted from the numerical analysis of the entire

moment resisting frame and it corresponds with the time when the solution of the hybrid fire testing starts diverging from the correct solution.

A deviation of 2%, 5% and 10 % from the solution of the NS is plotted in every graph. It is assumed that the accuracy of the results is ensured if the solution is within the mentioned range. The user defines the possible deviation during the hybrid fire testing depending on the objectives of the project. The deviations are represented with light grey color, more specific, the 10% deviation with continuous line, the 5% deviation with dashed line while the 2% deviation with the dotted line.

**Case 1**

The time step to be used in a real hybrid fire test is selected based on some criteria such as the calculation time of the solution during the time step and the time requested to reach the target values in the furnace. The virtual hybrid fire testing is performed in order to predict the behavior of the PS during the test and to establish the proper value of the time step and of the PS's stiffness. To predict the behavior of the PS during the tests serves to prepare the configuration of the tests, while a proper value of the time step and PS's stiffness ensured stability during the test and the accuracy of the results.

Based on the characteristics of the Promethee facility, the time step of *1 s* is reachable. Thus, Figure 6-11 presents the evolution of the interface forces and displacement when the time step is equal to *1 s*.

In the graph:

$H$ is the axial force in the beam;
$P_{left}$ is the force on the cantilever inducing the hinged support bending moment;
$P_{right}$ is the force on the cantilever inducing the rolling support bending moment;
$u$ is the axial displacement of the beam;
$\theta_{left}$ is the rotation on the hinged support;
$\theta_{right}$ is the rotation on the rolling support;

The solution of the PS matches the solution of the NS, therefore the compatibility and equilibrium are satisfied. The results encourage the election of the time step equal to 1 s.

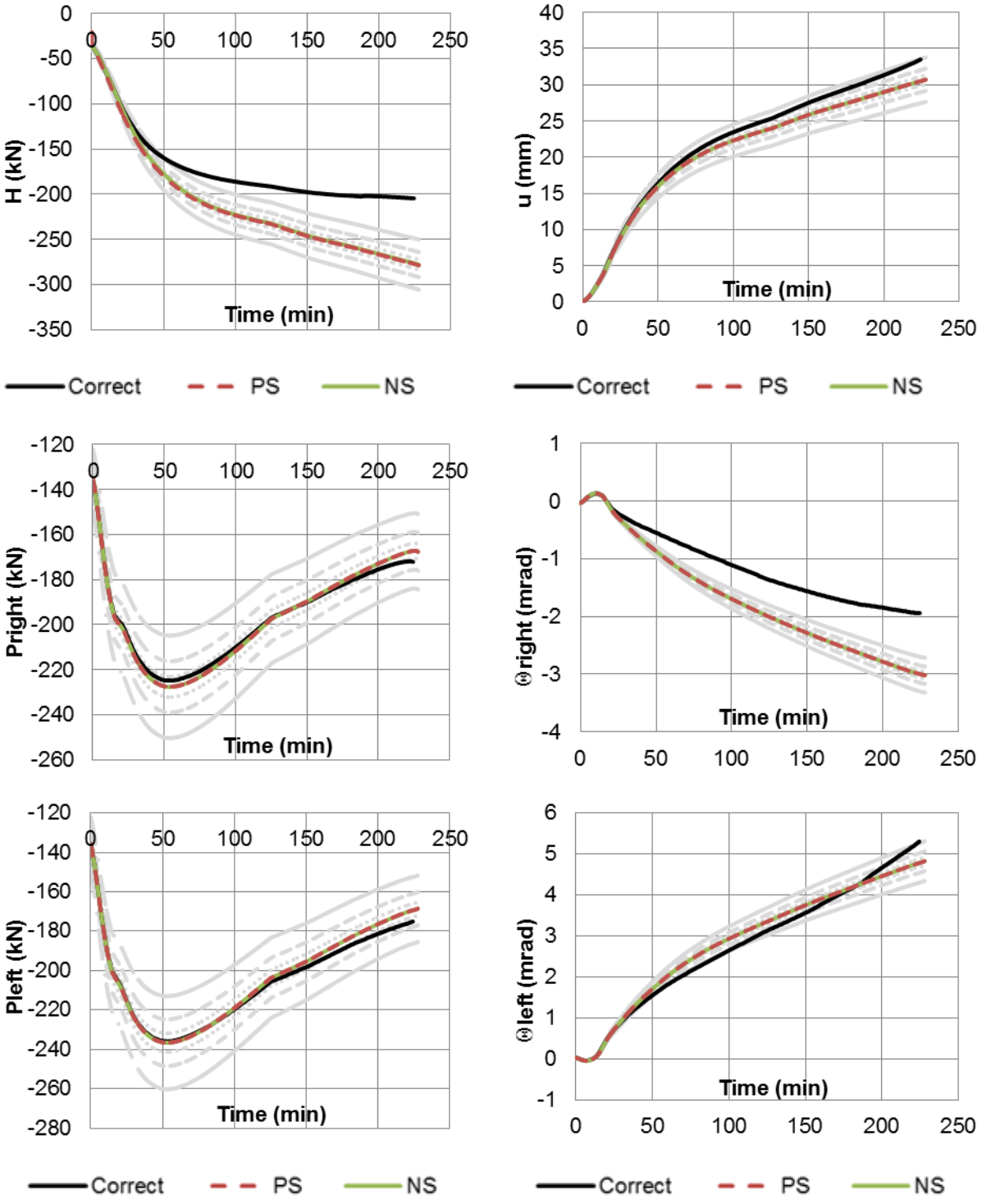


*Interface forces* *Interface displacements*

**Figure 6-11. Virtual HFT when $t = 1\ s$ and $K_P^* = 1.50K_P$**

**Case 2**

Figure 6-12 presents the evolution of the interface forces and displacements when the time step is equal to *10 s*.

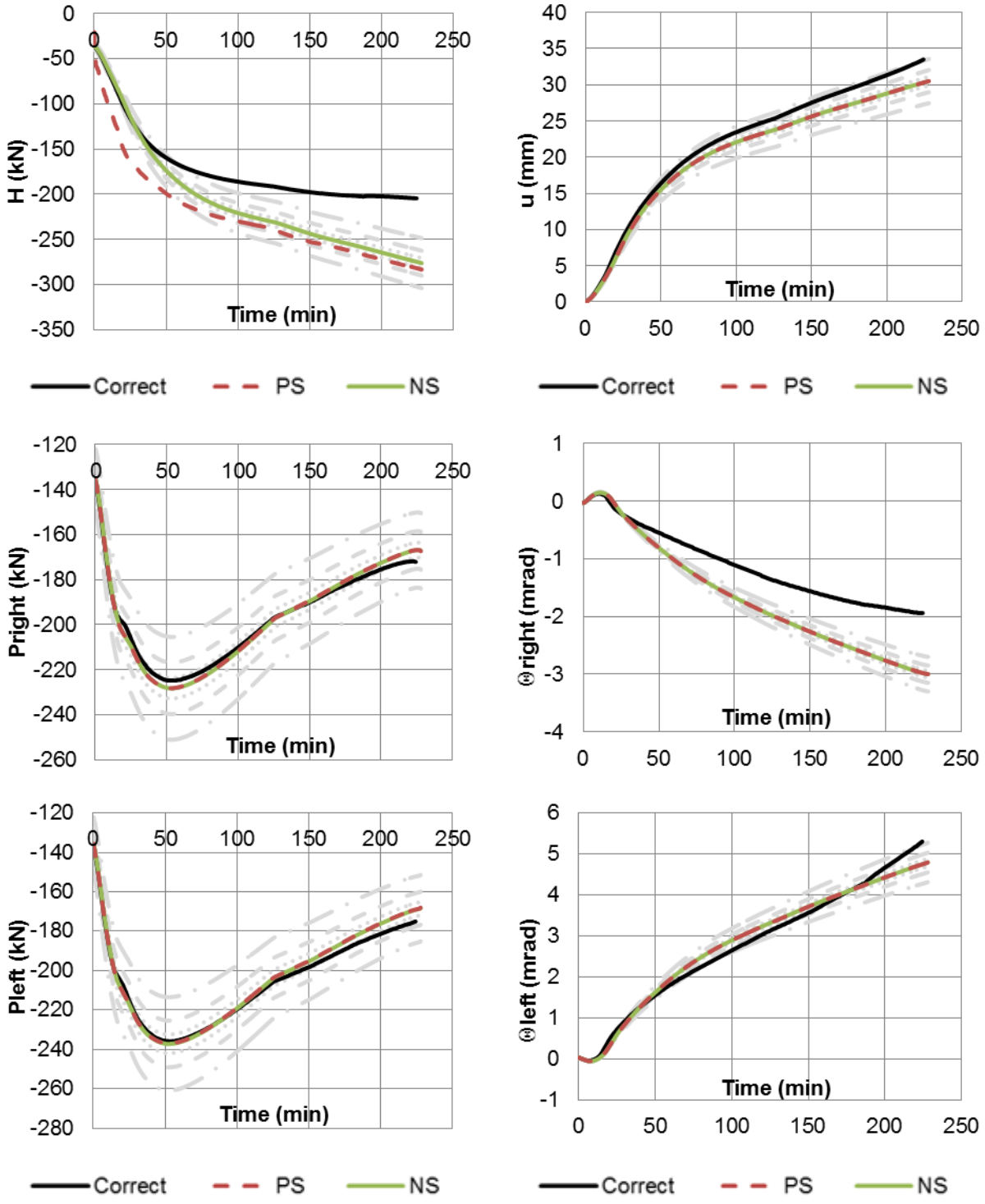


*Interface forces* *Interface displacements*

**Figure 6-12. Virtual HFT when $t = 10\ s$ and $K_P^* = 1.50K_P$**

The solution of the PS matches the solution of the NS for the rotational DoFs. For the axial DoF, the reaction force of the PS differs from the reaction force of the NS. The same displacements are imposed on the PS as for the NS.

The stiffness ratio for the rotational DoFs is bigger than one, meaning that the NS is stiffer than the PS. Moreover, during the hybrid fire test, the stiffness of the PS degrades. Thus, in

the calculation process, the results are influenced by the stiffness of the NS even if the stiffness of the PS is accounted in the calculations. For the rotational DoFs, the first generation method can be applied successfully in displacement control procedure. In the cases of a stiffness ratio bigger than one and when a displacement control procedure is considered, the influence of the PS on the results is in a small percentage.

For the axial DoF, the stiffness ratio is smaller than one, i.e. the PS is stiffer than the NS. In this case, the stiffness of the PS has an important role in the results. In the case of the first generation method, the displacement control procedure induces instability in the process. The new methodology makes use of the PS's stiffness in order to ensure the stability.

The stiffness of the PS is unknown during the hybrid fire test, thus the initial tangent stiffness matrix is considered during the entire test. The solution computed to be imposed at the interface of the PS differs from the measured solution in the furnace when the target displacements are imposed. This is just because the real stiffness of the PS differs from the stiffness considered in the calculation process. Thus the idea is to continue, within each time step, computing new solutions based on the out of balance forces, until the equilibrium and compatibility are reached (equivalent with the iteration process).

The specific characteristic of hybrid fire testing is the exposure to fire of the PS during the entire test. In between two time steps, the reaction of the PS varies due continuous heating. Thus, the displacements computed every time step to be imposed on the interface of the substructures induces reaction on the PS which differ from the one expected due to the (i) the stiffness used in the calculations and (ii) the reaction force of the PS used in the calculations. The stiffness degrades in time and does not match the initial tangent stiffness considered in the calculations. The reaction force from the time of the calculation until the time when the new displacements are imposed at the interface changes due to the fire exposure.

The consequence of a longer time step used in the calculations is that the equilibrium is not satisfied. The difference between the NS's axial force and PS's axial force in the first 50 min is not in the defined range of acceptable deviations. Starting from 100 min until the end of the test, the difference between the reaction forces is less than 5% of the defined deviation. In the first stage of fire exposure, the changes of the interface displacements and forces are more significant than the changes after the first stage. This is why the measured solution of the PS tends to the solution of the NS after 100 min of fire exposure.

The theoretical explanation of the phenomenon is explained in the chapter 3.6 while the numerical example of the elastic truss system presented in the chapter 5.4 underlines the importance of selecting the time step and the initial tangent stiffness on the results.

**Case 3**

Figure 6-13 presents the evolution in time of interface displacements and forces when $t = 30\ s$ and $K_P^* = 1.50K_P$.

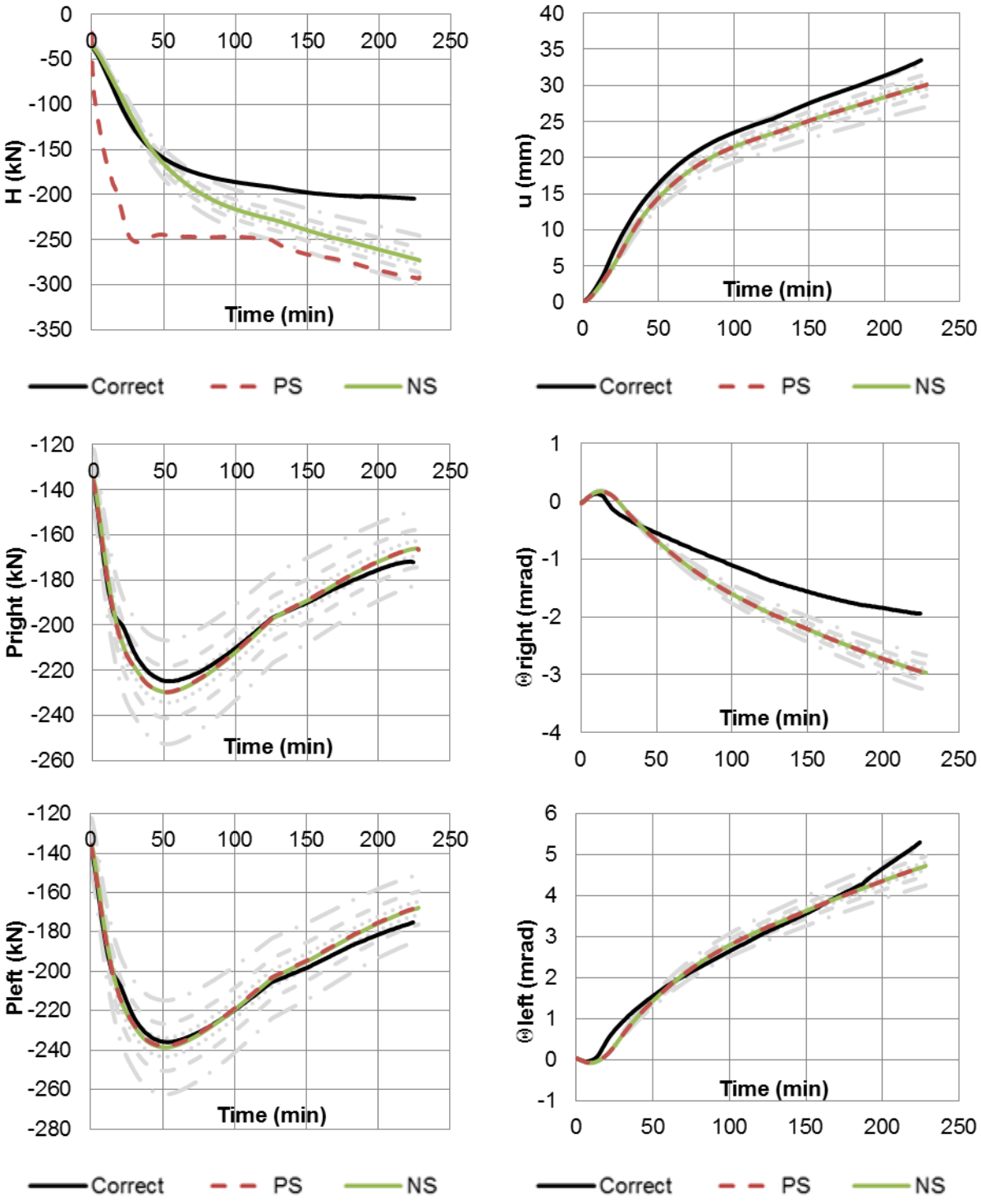


*Interface forces* *Interface displacements*

**Figure 6-13. Virtual HFT when $t = 30\ s$ and $K_P^* = 1.50K_P$**

The axial DoF is the most affected since the solution of the PS does not match the solution of the NS i.e. no equilibrium satisfied. The difference between the PS's axial force and the NS's axial force is more important in the early stage of the test and it reduces from the minutes 100 until the end of the test. Thus, after 100min of fire exposure, the solution of the PS exceeds the solution of the NS with 10%.

Good agreement is observed between the PS and NS forces and displacements characteristic to the rotational DoFs.

**Case 4**

Figure 6-14 presents the evolution in time of interface displacements and forces when $t = 60\ s$ and $K_P^* = 1.50K_P$.

It is observed that with the increase of the time step, the PS's solution diverges from the solution of the NS for the axial DoF.

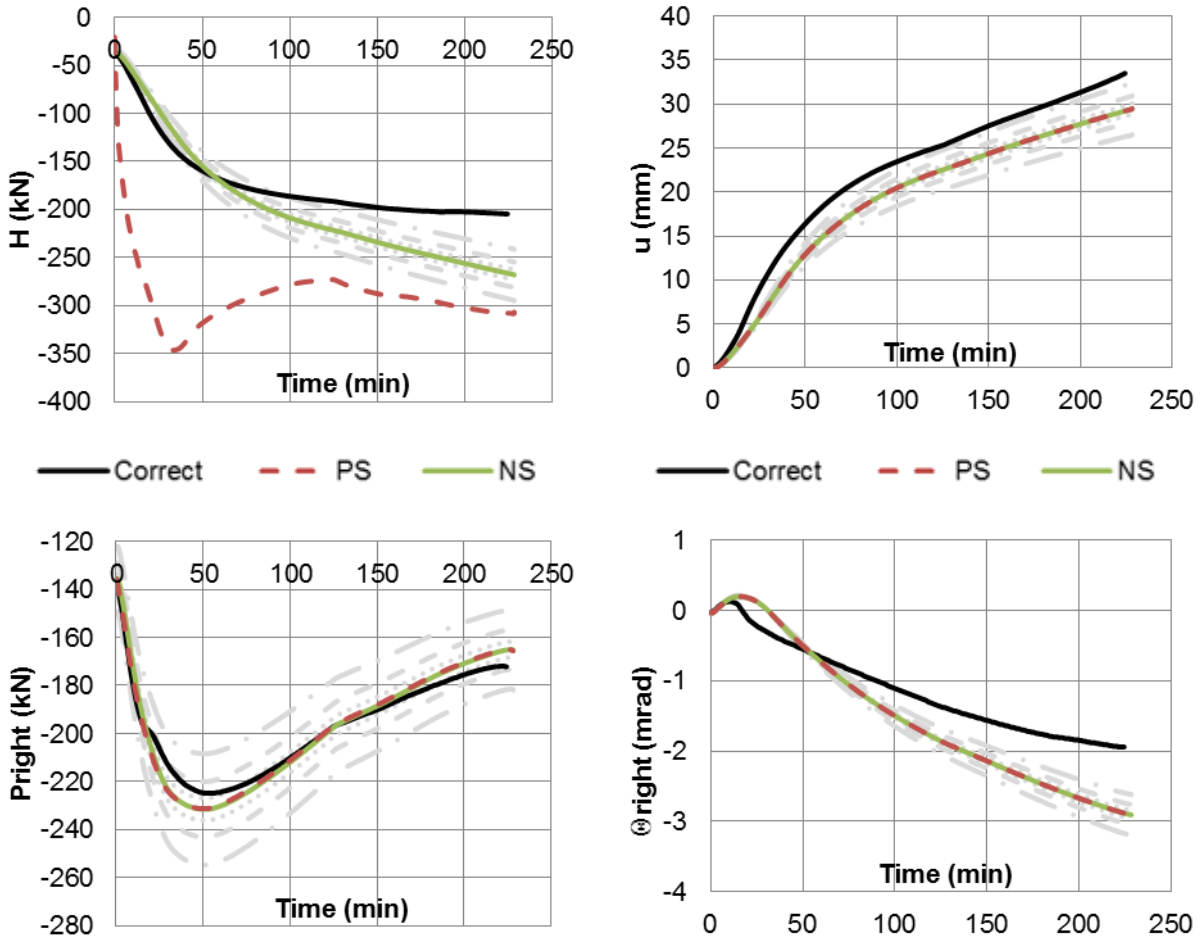

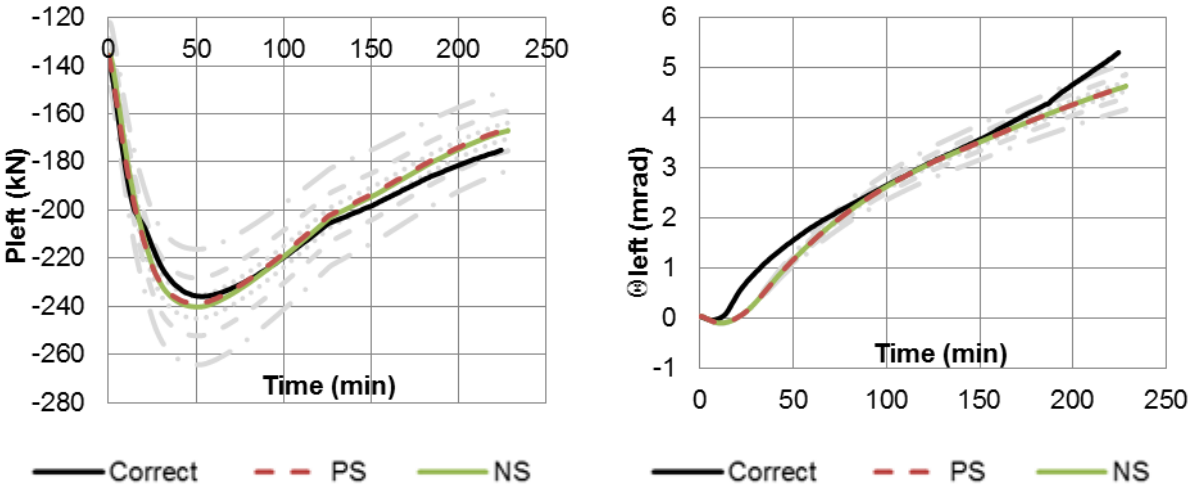


*Interface forces* *Interface displacements*

**Figure 6-14. Virtual HFT when $t = 60\ s$ and $K_P^* = 1.50K_P$**

**Case 5**

Figure 6-15 presents the evolution in time of interface displacements and forces when $t = 300\ s$ and $K_P^* = 1.50K_P$.

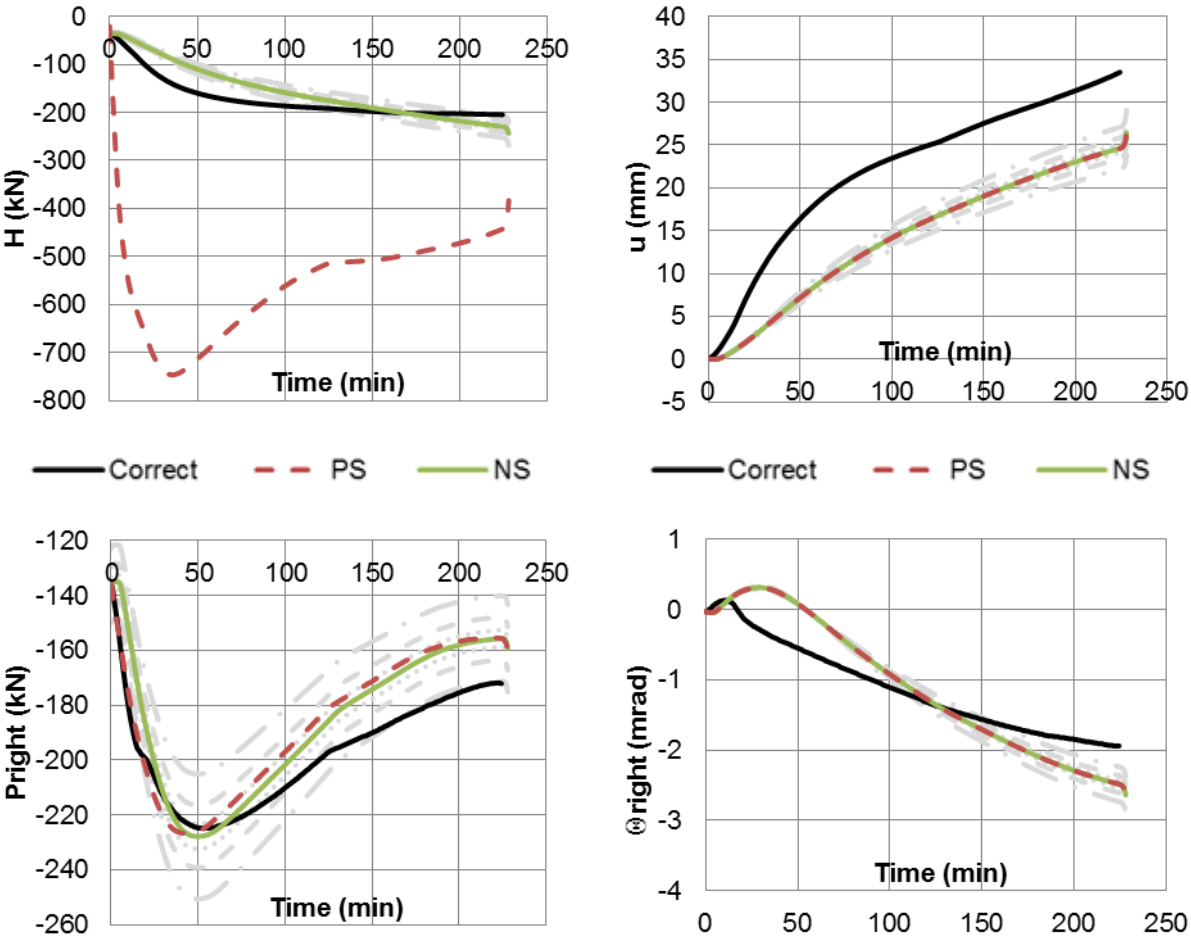

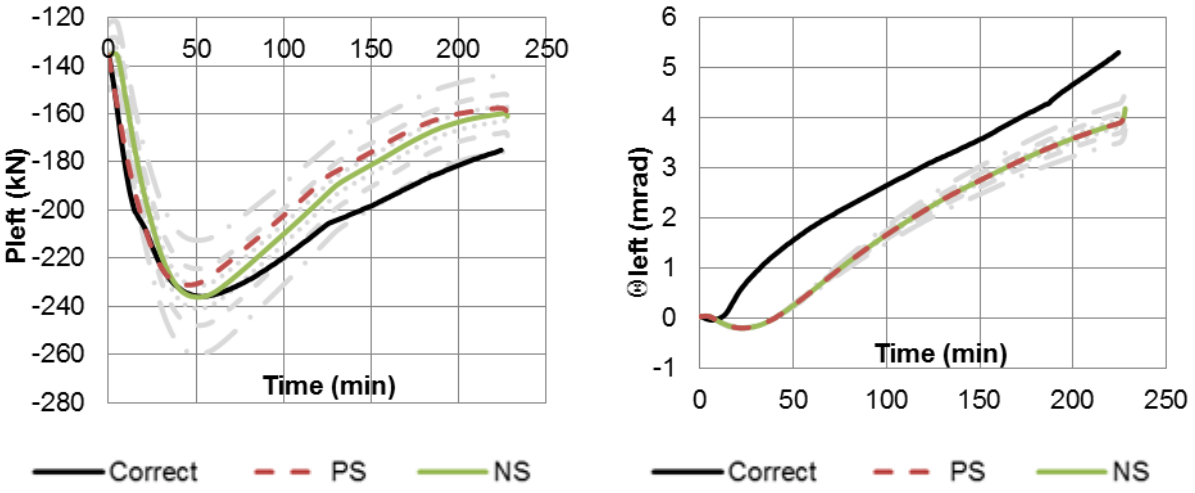


*Interface forces* *Interface displacements*

**Figure 6-15. Virtual HFT when $t = 300\ s$ and $K_P^* = 1.50K_P$**

In this case, the increase of the time step induces modifications not only for the axial DoF but for the rotational DoFs too. The difference between the solution of the PS and NS is in the limit defined by the user for the rotational DoFs, but this is not the case for the axial DoF. The axial force induced in the PS differs from the axial force of the NS and no equilibrium is ensured.

**Case 6**

Figure 6-16 presents the evolution in time of interface displacements and forces when $t = 600\ s$ and $K_P^* = 1.50K_P$. The interface solution is updated every 10min and no equilibrium is satisfied at the interface. The difference between the PS's solution and NS's solution increases with the increase of the time step along with the deviation from the correct solution.

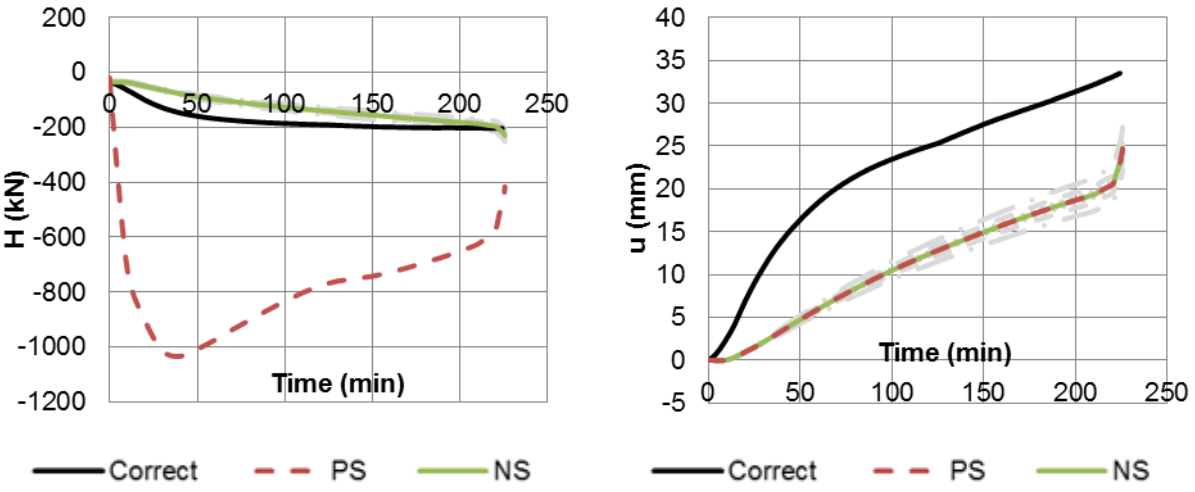

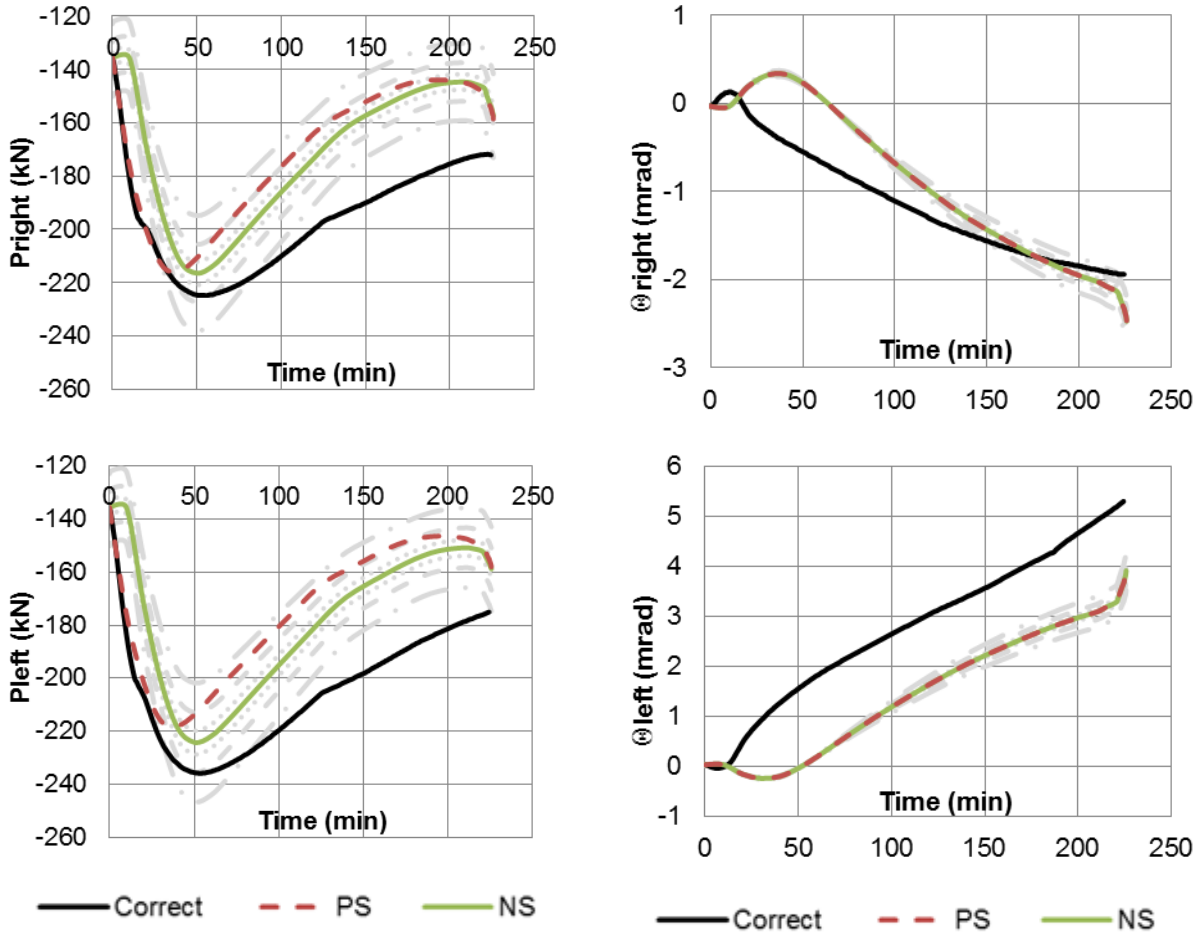


*Interface forces* *Interface displacements*

**Figure 6-16. Virtual HFT when $t = 600\ s$ and $K_P^* = 1.50K_P$**

## Conclusions

The objective of the exercise was to underline the importance of the time step value in the accuracy of the results. In all the cases presented, no instability occurred with the increase of the time step.

Figure 6-17 presents the evolution of the increment of the displacement vector in time when the time step varies. Reduced time steps lead to more updates of the boundary displacements than in the case when bigger time steps are considered. Thus, the difference between the displacements in two consecutive steps (increment of displacements) is reduced compared with the case with a bigger time step.

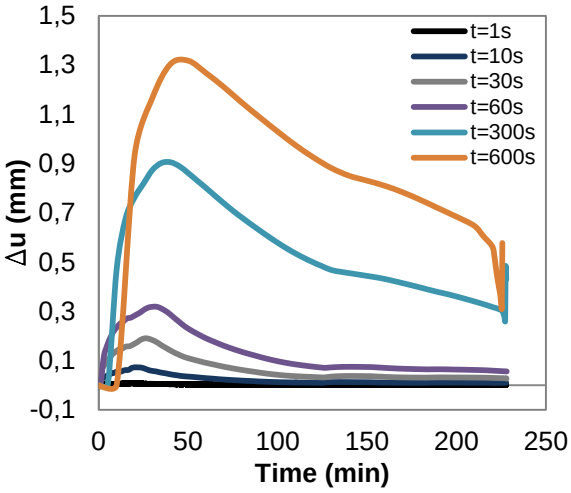


*Horizontal displacement*

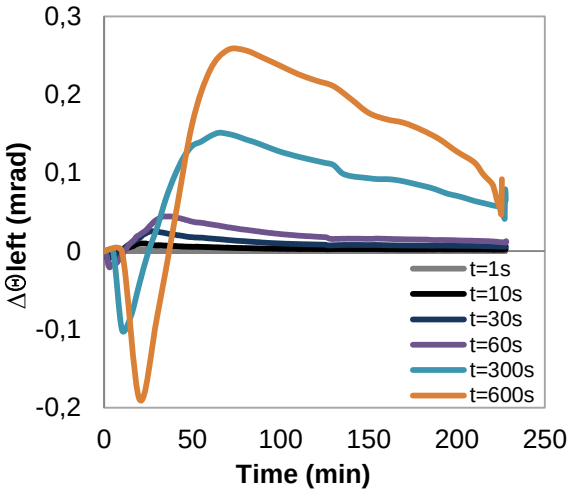


*Rotation left support*

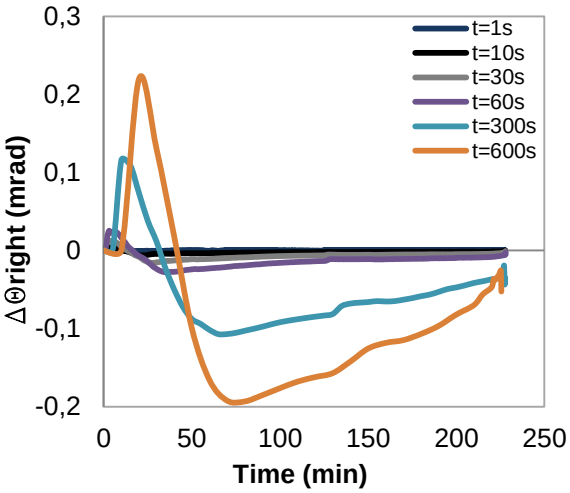


*Rotation right support*

**Figure 6-17. The increment of the interface displacements and rotations**

When a time step equal to *1 s* is considered for this specific example, the equilibrium and compatibility are ensured and good results are obtained. For a time step of *30 s* and *60 s*, the equilibrium is not anymore satisfied. The increment in displacement is next plotted for these three cases in Figure 6-18.

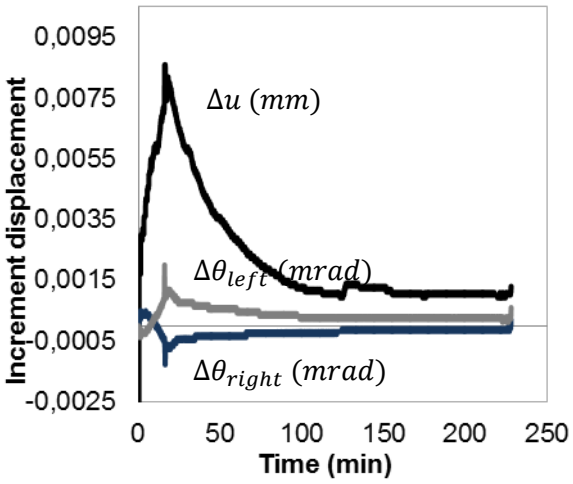


$\boldsymbol{t = 1\ s}$

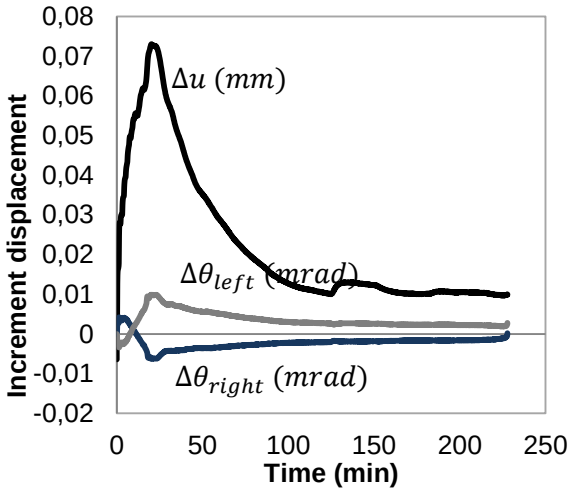


$\boldsymbol{t = 10\ s}$

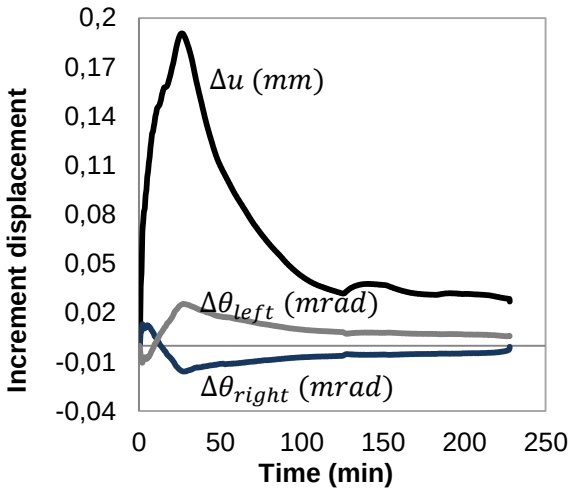


$\boldsymbol{t = 30\ s}$

**Figure 6-18. Incremental displacement and rotations when time step is 1 s, 10 s and 30 s**

The increment of displacement and rotations increases in the first 30 min of the test. Right after that moment the increment of displacements starts decreasing. Moreover, after the minute 100, the increment of displacement and rotations is almost constant with a tendency of decreasing.

The incremental displacements needs to be imposed on the boundary of the PS and NS every time step. Observations are done regarding the small value of the incremental displacements to be imposed for the three cases.

Applying small incremental displacements implies the use of very precise and high resolution measurement equipment. The noise during the measurement process will have an important role in the results.

During the hybrid fire testing process, every time step new interface displacements are computed and imposed at the interface of the substructures. If, during one time step, the

incremental displacement cannot be imposed and measured in the furnace because it is too small, then no variation of displacement is imposed and the process continues to the next step.

For the studied case, a smaller time step of iteration produces better results, meaning that the equilibrium and the compatibility are ensured during the hybrid test. The disadvantage of a small time step is the small values of incremental displacements and rotations to be imposed every time step. From the experimental point of view this can be tricky and can lead to the loss of equilibrium.

- The influence of the PS's stiffness

Here, the influence of the value considered for the PS's stiffness on the results is observed.

From the observations made when the influence of the time step on the results is observed, a time step equal to 1 s ensures the equilibrium and compatibility in the virtual environment. Thus the value of the time step considered in this section is set to 1 s.

The cases presented in Table 6-5 are analyzed.

**Table 6-5. The variation of the PS's stiffness in the virtual hybrid fire testing**

| | Time step | The PS's stiffness |
|---|---|---|
| **Case 1** | $t = 1\ s$ | $K_P^* = 5K_P$ |
| **Case 2** | | $K_P^* = 10K_P$ |
| **Case 3** | | $K_P^* = 50K_P$ |
| **Case 4** | | $K_P^* = 0.50K_P$ |

The results are presented in the same format as before.

**Case 1**

In the case 1, the stiffness used in the calculation process is equal to 5 times the initial tangent stiffness of the PS. Figure 6-19 presents the interface solution for the mentioned case. The equilibrium is satisfied for the rotational DoFs. For the axial DoF, a slight difference between the PS's solution and NS's solution can be observed in the first 50 min of the tests. After the minute 50, the axial forces of the PS tend to the values of the NS. The errors do not exceed the defined values and the results are considered as acceptable.

By overestimating the stiffness of the PS affects only the axial DoF since the axial stiffness of the PS is bigger than the stiffness of the NS.

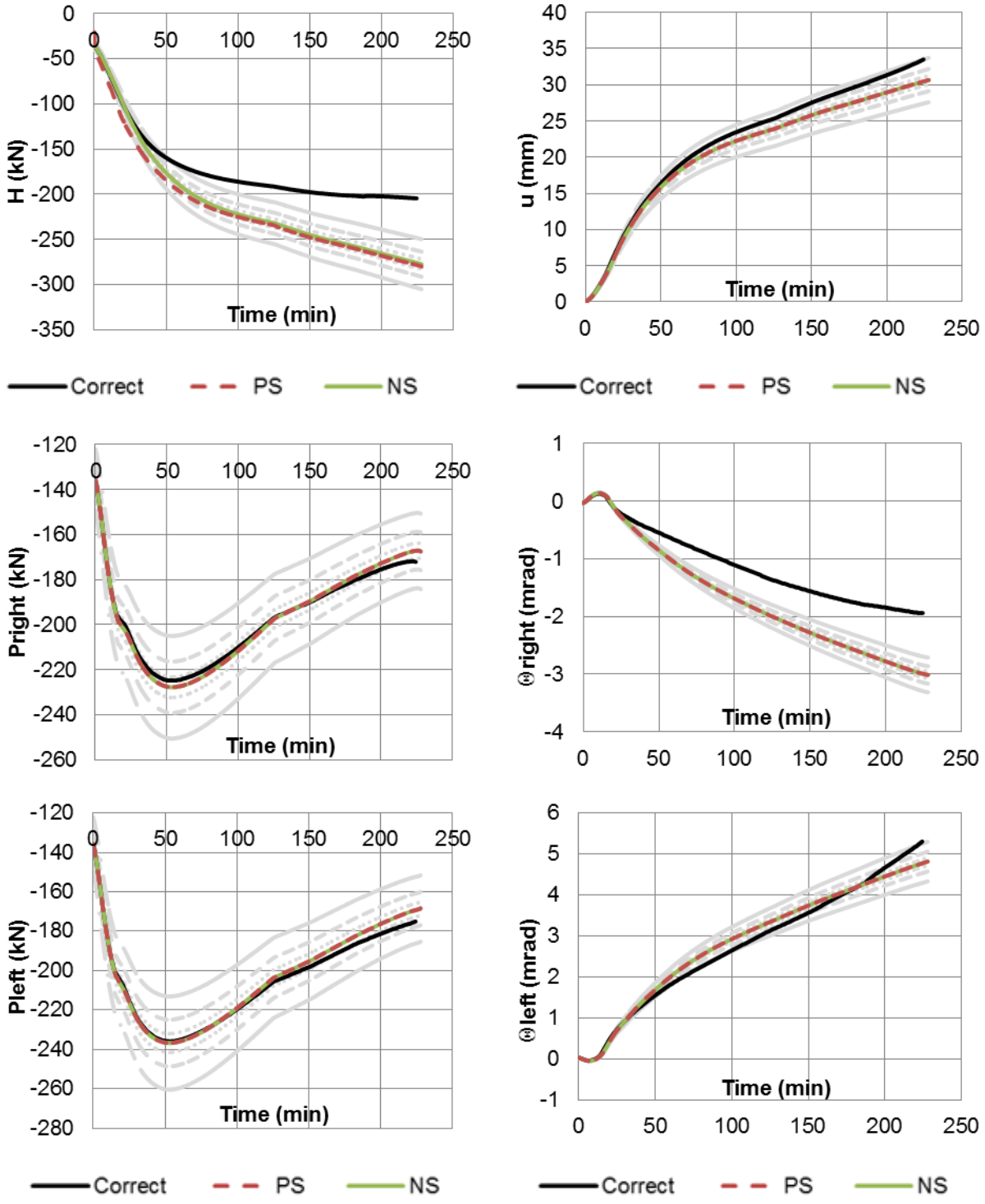


*Interface forces* *Interface displacements*

**Figure 6-19. Virtual HFT when $t = 1\ s$ and $K_P^* = 5K_P$**

**Case 2**

Figure 6-20 presents the interface solutions for the case when the stiffness considered in the calculation process overestimates the initial tangent stiffness by 10.

The axial DoF is the most affected. The axial force registered in the PS slightly differs from the axial force of the NS at the beginning of the tests. The difference exceeds the defined limits, but the results can be found appropriate depending on the objectives of the project. From minute 100, the difference considerably reduces.

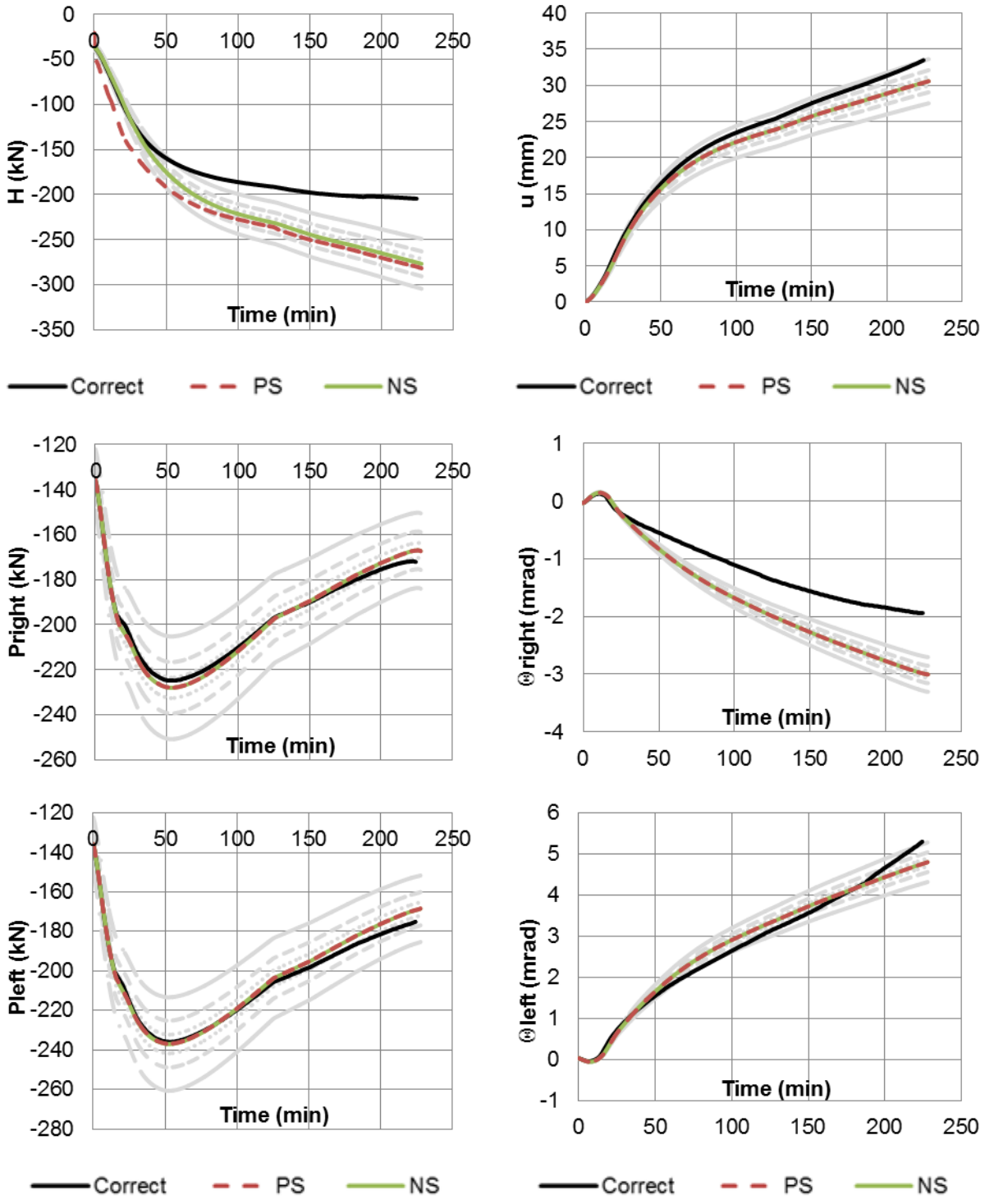


*Interface forces* *Interface displacements*

**Figure 6-20. Virtual HFT when $t = 1\ s$ and $K_P^* = 10K_P$**

**Case 3**

Figure 6-21 presents the interface forces and displacement in the virtual hybrid fire testing when the initial tangent stiffness of the PS is 50 times overestimated.

The equilibrium is not ensured, since the axial force of the PS does not match the axial force of the NS, the difference between the two solutions is significant especially in the first 120 minutes of the test. From this moment, until the end of the hybrid fire test, the axial force of the PS exceeds the axial force of the NS by 10%.

The rotational DoFs are not affected in this case; the forces of the PS are equal to the forces of the NS. Since the same displacements are imposed on the substructures, the compatibility is ensured.

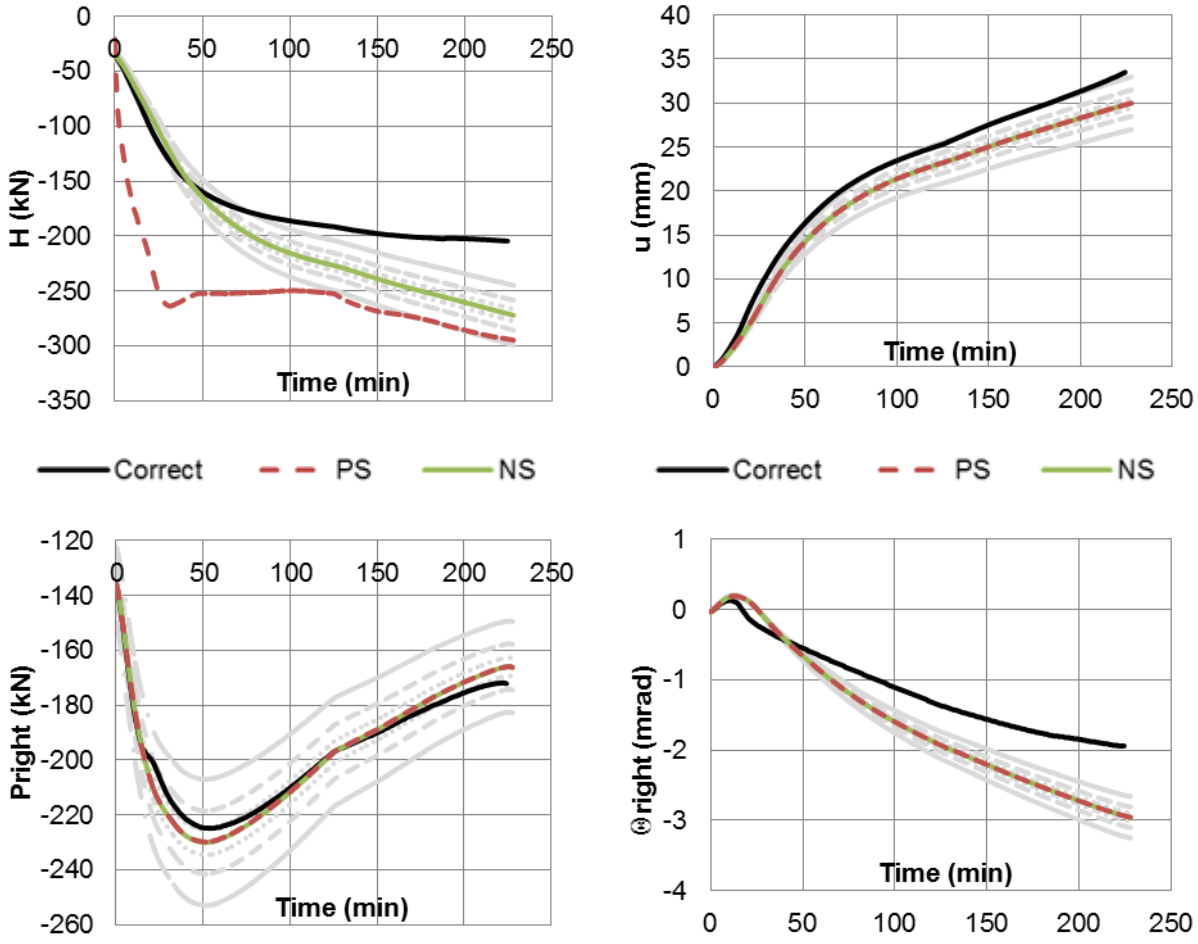

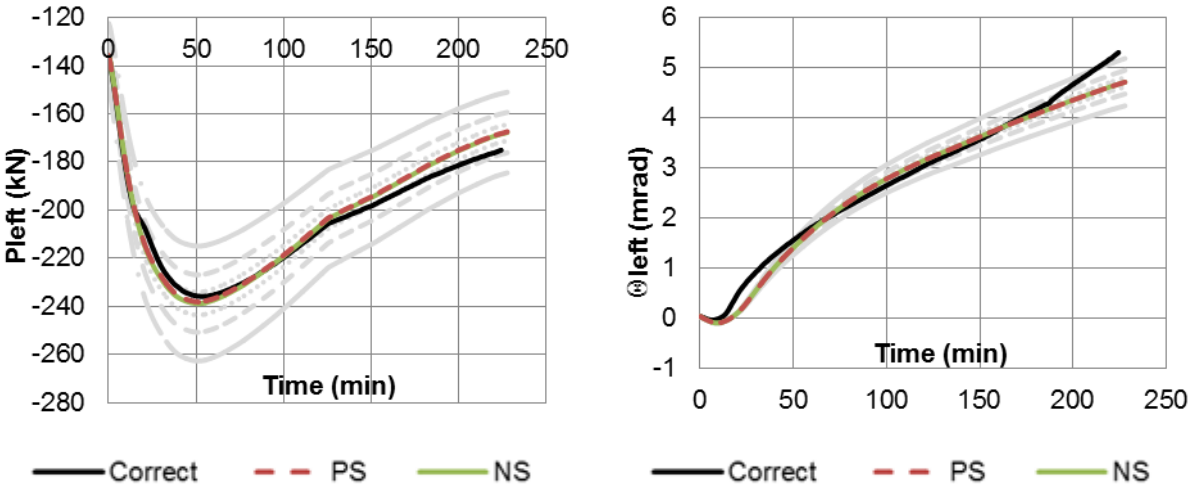


*Interface forces* *Interface displacements*

**Figure 6-21. Virtual HFT when $t = 1\ s$ and $K_P^* = 50K_P$**

**Case 4**

Figure 6-22 presents the results of the virtual hybrid fire testing when the stiffness of the PS is underestimated with a 0.50 factor.

Right at the beginning of the virtual hybrid test the solution tends to be unstable.

To underestimate the stiffness of the PS is not recommended since this can lead to the instability early in the hybrid fire testing.

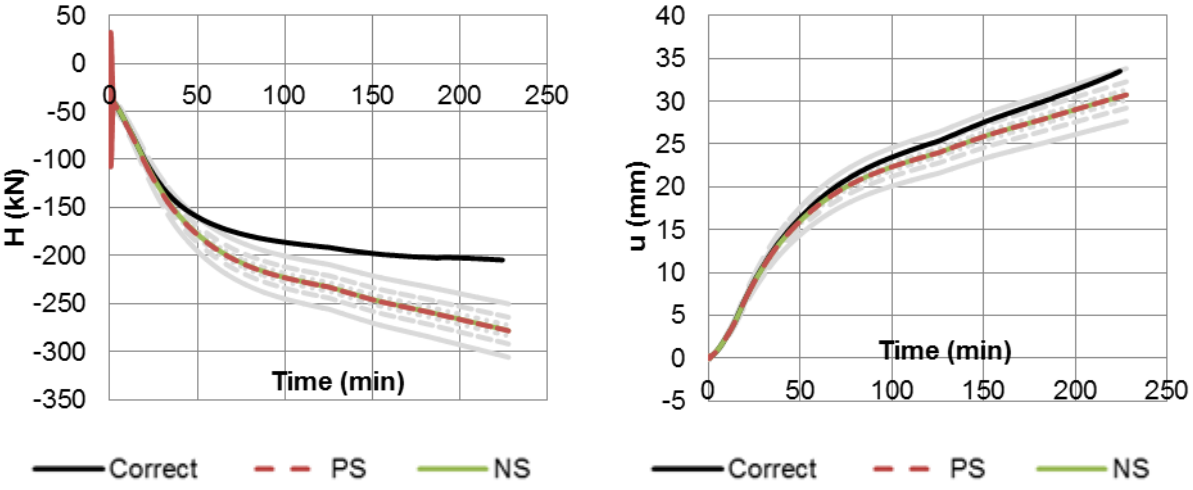

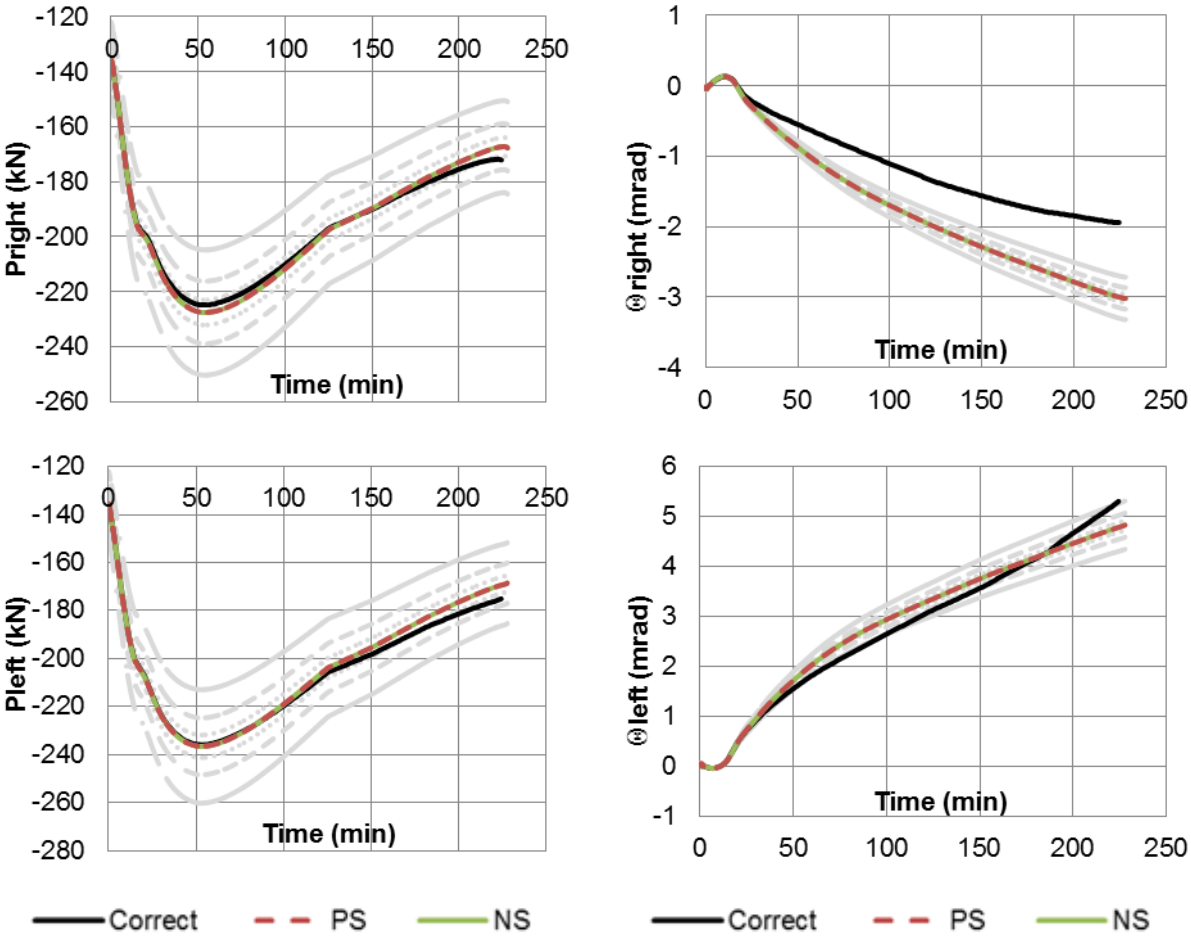


*Interface forces* *Interface displacements*

**Figure 6-22. Virtual HFT when $t = 1\ s$ and $K_P^* = 0.50K_P$**

**Conclusions**

The stiffness value to be used in the hybrid process must be defined properly in order to ensure the stability of the process and to provide accurate results.

If the stiffness value is overestimated, then the equilibrium is not satisfied. The difference between the PS's solution and NS's solution depends on how much the stiffness of the PS is overestimated in the calculations process. It is more dangerous to underestimate the stiffness of the PS in the calculation process, since the instability of the process can be triggered early in the hybrid fire testing.

It is important to estimate properly the initial tangent stiffness of the PS before the hybrid fire testing, this is why before the tests it is recommended to measure the stiffness of the specimen.

### 6.4.3. The New Method in force control procedure

The focus during the thesis was to analyzing the new method when displacement control procedure is considered.

Nevertheless, the new method can be applied even in the case when a force control procedure is selected to be applied in the practice.

The virtual hybrid fire test of the case study has been performed when the force control procedure is considered.

To do so, a new subroutine has been developed in SAFIR, which gives the possibility to solve for the incremental force to be applied on the substructures interface every time step.

Figure 6-23 presents the evolution of the interface forces versus the interface displacements for the horizontal DoF and for the rotational DoFs when the force control procedure is considered. For the virtual hybrid fire tests, the time step is set to 1s and the initial tangent stiffness matrix is overestimated with a factor of 1.50.

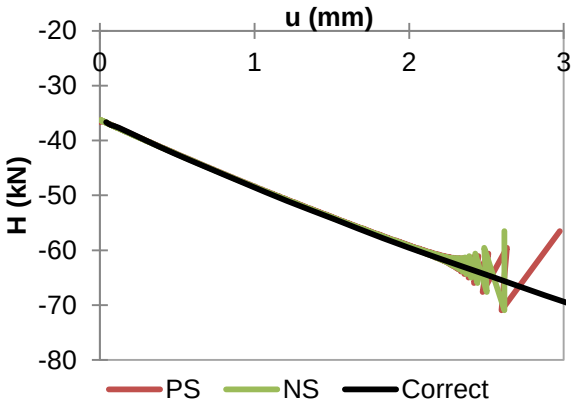


*a) Axial force **H** versus horizontal displacement **u***

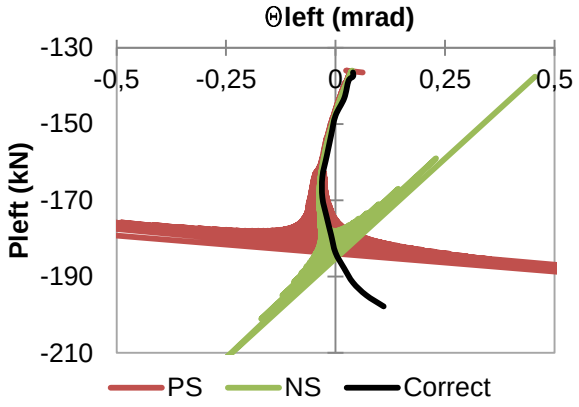


*b) Vertical force $P_{left}$ versus rotation on the left support $\theta_{left}$*

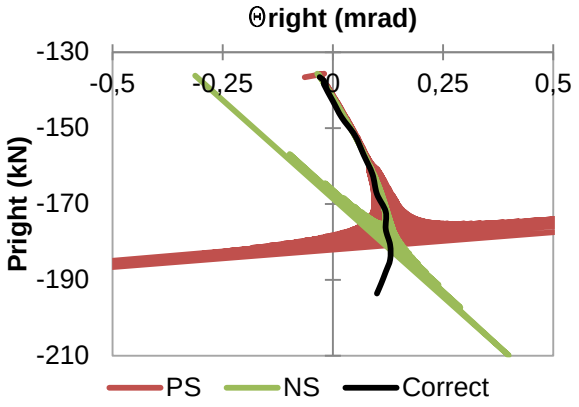


*c) Vertical force $P_{right}$ versus rotation on the left support $\theta_{right}$*

**Figure 6-23. Interface conditions when force control procedure is considered**

The model runs successfully only for 9 minutes. The compatibility and the equilibrium are ensured and moreover the correct solution is correctly represented for the first 6 minutes of the analysis. The solution starts diverging from the correct solution in the last part of the analysis.

The force control procedure becomes instable when the stiffness of the PS is ill conditioned or when the size of the load increment is greater than the limit load.

In the evolution of the vertical forces acting on the cantilever beam versus the support rotations, i.e. $P_{left}$ -$\theta_{left}$ and $P_{right}$ -$\theta_{right}$, the change of the slope can be observed. When the slope changes, the force control procedure is not capable to reproduce the solution. The imposibility to reproduce the solution in this area can be explained if the the size of the incremental load is to large such as the the limit load is exceded.

In the present case study the force control procedure cannot be applied succesfully until the end of the virtual hybrid fire test due to the specified reasons. Nevertheless, the solution produces for the first minutes of the virtual hyrid fire tests show that the equilibrium and the compatibility are ensured and the correct solution is reproduced for a portion of the test.

This example indicates that the new method offers the possibility to solve for incremental force, i.e. force control procedure, with the mention that problems might occur when there is a change in the behavior of the tested elements such as for example the softenning of the material.

## 6.5. Hybrid simulation at CERIB equipment site

Figure 6-24 presents the architecture of the equipment site available at CERIB.

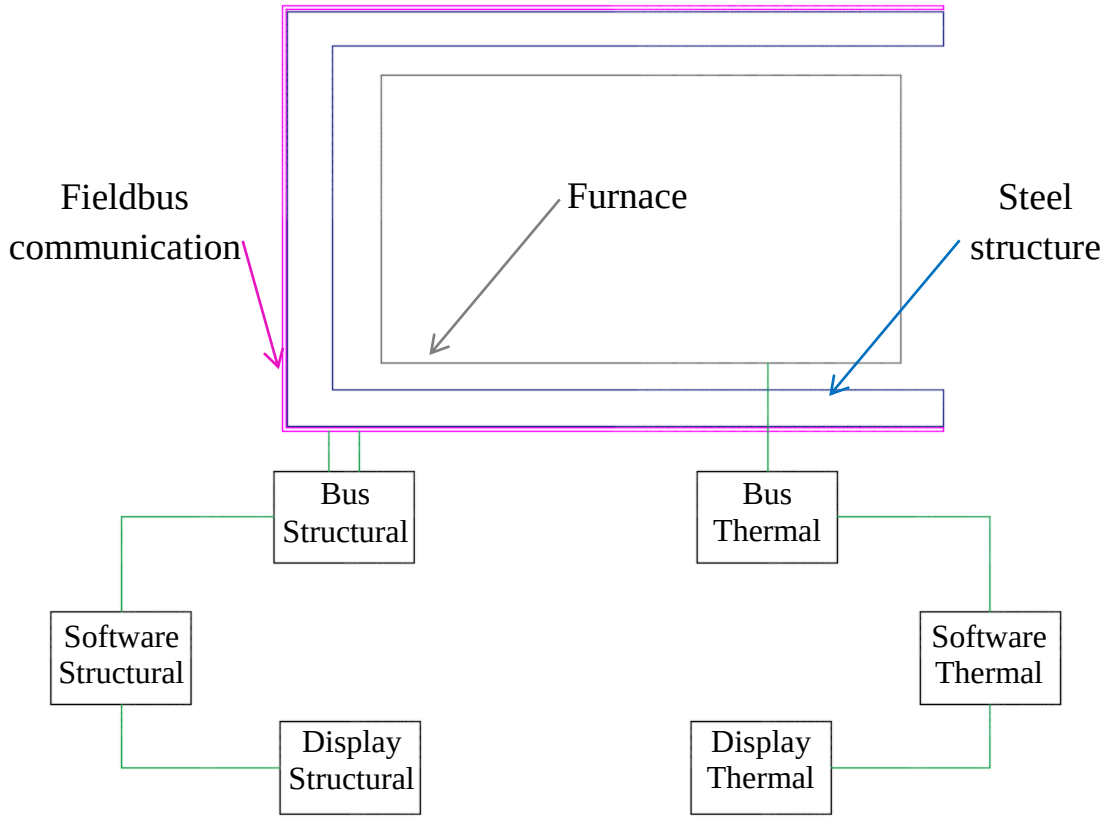


**Figure 6-24. Architecture of the equipment site at CERIB-Promethee**

The main components of the equipment are:

- The furnace;
- The steel structure surrounding the furnace;
- The Fieldbus communication;
- Bus structural / Bus thermal;
- Software Structural / Software Thermal;
- Display Structural / Display Thermal

Please note that the structural control is independent on the thermal control.

*The furnace* is a closed space where the structural elements will be placed and exposed to fire. The burners produce the increase of the temperature while the pyrometers are measuring the temperature reached in the furnace.

*The steel structure surrounding the furnace* has the role of supporting the jacks in different configurations for different types of tests.

*Fieldbus communication* refers to a family of industrial computer network protocols used for real-time distributed control. The distributed control system represents an organized hierarchy of controller systems. In this hierarchy, there is usually a Human Machine Interface (HMI) at the top, where an operator can monitor or operate the system. This is typically linked to a middle layer of Programmable logic controllers (PLC). At the bottom of the control chain is the fieldbus that links the PLCs to the components that actually do the work, such as sensors, actuators and valves.

The main advantage of choosing the fieldbus communication is that it requests less wiring and less hardware. The disadvantage of using the fieldbus communication is that only specific sensors can be connected to the system. If other sensors have to be implemented, then an intervention is needed.

In the case of Promethee, the servo valves and the displacements transducers are connected to the fieldbus communication. The inclinometers used in the measurement process needed special implementation since it was not possible to connect them to the fieldbus communication. Thus all the information is collected in the *Bus structural*. The Bus structural collector is connected with the *Structural Software* developed to perform fire tests. The user operates the system making use of the *Display Structural*.

For the thermal control the structure is identic as in the case of the structural control. Thus the temperature in the thermocouples is registered along with the temperature in the pyrometers. The regulation of the pressure and the oxygen level are controlled by this section.

Figure 6-25 presents the Promethee fire laboratory. The operator can send target values to be reached in the furnace and at the same time to read the response.

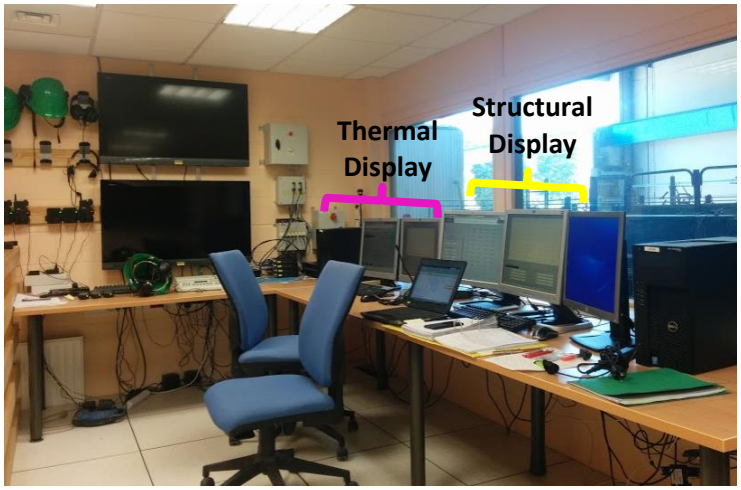


**Figure 6-25. Promethee fire laboratory**

## 6.6. Test 1

The first performed test, Test 1, is a non-hybrid test. The test is performed in a traditional manner where the effect of the surrounding is assumed constant during the test (constant negative moments applied at the supports and no axial restraint). The configuration of the test is presented in the Figure 6-9.

### 6.6.1. Motivation

The main reason of the TEST 1 is to compare the results of a standard test with the hybrid fire test results, i.e. TEST 2 and TEST 3.
The traditional test is performed on structural elements without considering the real boundary conditions.
The hybrid fire tests are performed on structural elements under real boundary conditions.
The standard tests and the hybrid fire test induce different behavior of the PS as presented in the section 1.2. The difference lays in the failure time as well as in the failure mode.

### 6.6.2. Test Setup and Procedure

The beam and the furnace are prepared properly before the fire tests. After the beam is positioned in the furnace, the data acquisition system is placed in the position in order to measure the evolution of displacements during the fire test. The transfer system (actuators) is used to apply the loading during the fire test. The thermocouples serve to measure the temperature evolution of the PS. Thus the fire test is ready to start. For more information about the test setup see Appendix D.

### 6.6.3. Test Results and Interpretation

*Temperature evolution*

After the test is finished, the measured temperatures are compared with the predicted temperature in SAFIR. Good agreement is observed between the two.

Figure 6-26 presents the evolution of temperature for the longitudinal rebars. The numerical solution (black dashed line) matches the measured solution by a multitude of thermocouples for the bottom corner and middle rebars. The position of the thermocouples is presented in the section D.3 (see Figure D-6).

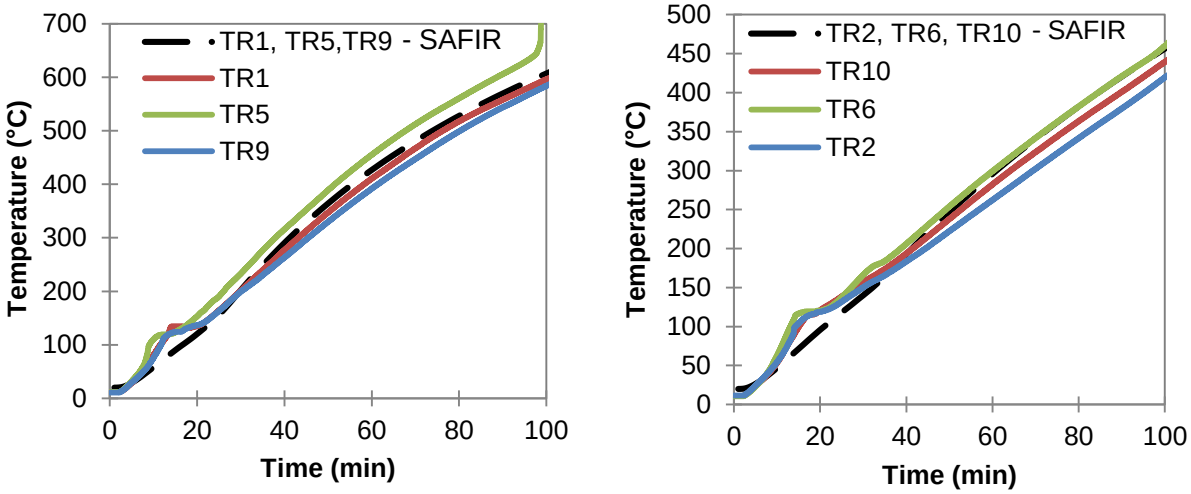


*Bottom corner rebars* *Bottom middle rebars*

**Figure 6-26. Temperature evolution in the longitudinal rebars**

*Structural response*

**The failure of the beam occurred at 99 min since the fire exposure**. The failure is due to the plastic hinge formed in the mid-span of the beam. During the test, the falling of the concrete occurs close to the failure time. The first falling occurred at 85 minutes, followed by the second failure at 93 minute, and the last failure before the test stopped, at 97 min.

Figure 6-27 shows the beam after the fire exposure. The areas with the fallen concrete during the test are underlined in the mentioned figure. In the same figure, the mid-span plastic hinge is presented.

Only one plastic hinge is formed since the standard tests are performed with simply supported boundary conditions. In the case of the hybrid fire testing, the failure would occur later since more than one plastic hinge is needed in order to lead to failure.


**Figure 6-27. The beam after the fire exposure.**

Numerical analysis performed in SAFIR predicted the failure to be reached after 115 min of fire exposure (the last step of convergence). Good agreement between the numerical solution and the measured solution is observed.

Figure 6-28 present the evolution of the mid-span vertical displacement measured during the test and the solution computed in SAFIR. The evolution of the measured mid-span displacement shows a similar trend with the mid-span displacement from the numerical analysis.

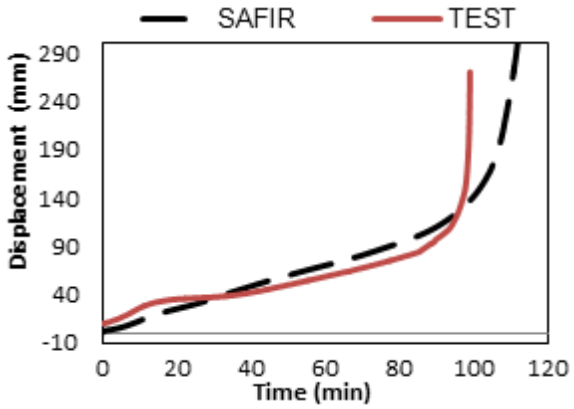


**Figure 6-28. The evolution of the mid-span vertical displacements in Test 1**

Other measurements, such as the horizontal displacements of the rolling support, the rotation of the supports and other vertical displacements, are recorded during the test but are not presented in this thesis.

## 6.7. Test 2

In the numerical analysis of the moment resisting frame with the studied beam exposed to fire, the effects (efforts) on the beam in time vary, depending on multiple reasons. The fire scenario, the stiffness of the exposed beam along with the stiffness of the surrounding structure influences the behavior of the exposed beam. Thus the evolution of the bending

moment along with the evolution of the axial force is dependent on the mentioned causes. The bending moment varies during the test along with the axial force. For the cold design it is assumed that the axial force in the beams is insignificant while once with the increase of temperature the values of the axial force are so significant that they cannot be neglected.
The variation of the bending moment and axial force is unknown before the tests and depends on different factors. The surrounding effect can be accounted by applying the hybrid fire testing methodology, thus the global effect is represented during the test.

Thus the objective of the Test 2 is to take into consideration the effect of the surrounding on the tested element. To achieve that objective, the hybrid fire methodology is applied during the test. The configuration of Test 2 is presented in Figure 6-9.

### 6.7.1. Motivation

Different reasons motivated the Test 2.

Since a new hybrid fire method is proposed and validated numerically in this thesis, the Test 2 has the purpose to validate the method experimentally.

More than that, the fire facility Promethee disposes of possibility to perform such tests. Thus one of the motivations is to test the capability of the facility and to try to learn from the present experience to be able to implement future development.

### 6.7.2. The analysis of the testing equipment

Before starting the hybrid fire tests, it is important to know the exact characteristics of the data acquisition system and transfer system.

The thermal action is equivalent to a mechanical static load with long duration. The fire effect induces changes of the boundary conditions i.e. changes in the interface forces and displacements. Generally, the changes occur slowly in the process, thus a static equation is solved to determine the solution of the boundary conditions every time step. The tested substructure can experience large deformation before failure. The final deformation can increase significantly in a short time. In concrete structures the deformation of the physical substructure may be influenced by the spalling of the concrete.

In these particular situations dynamic effects can be significant and a dynamic approach of the method needs to be developed. Rather than that, the deformation of the PS develops slowly in time, meaning that the difference between the displacements in the previous time step and the displacement from the current time step is small. This difference depends also on the characteristic (mainly the stiffness) of the PS and NS as well as on the time step chosen to perform the hybrid fire test.

The data acquisition system needs to be accurate enough in order to register the changes of the boundary condition. If the PS is a stiff structural element, then large reaction forces are produces by small displacements. Thus, for small reading errors of displacements, the reaction

force registered by the transfer system varies. These errors can produce inaccurate results and in some cases instability of the process.

This is why knowing the capability of the testing facility is crucial, in order to be able to produce correct results.

- **Transducers and inclinometers**

*Configuration adopted during the Test 2*

The horizontal displacement of the beam is measured using WS19KT cable extension position sensor. The rotation is measured using high performance digital and analogue servo-inclinometer SX41100. The horizontal displacement is measured on the rolling support. Since the supports of the PS are positioned in the furnace, the respective area of the beam is protected. Thus the transducer is positioned out of the furnace and the measurement is done as presented in Figure 6-29. Additional metallic system helps to attach the transducers and to attach a wheel to redirect the direction of the transducer's cable.

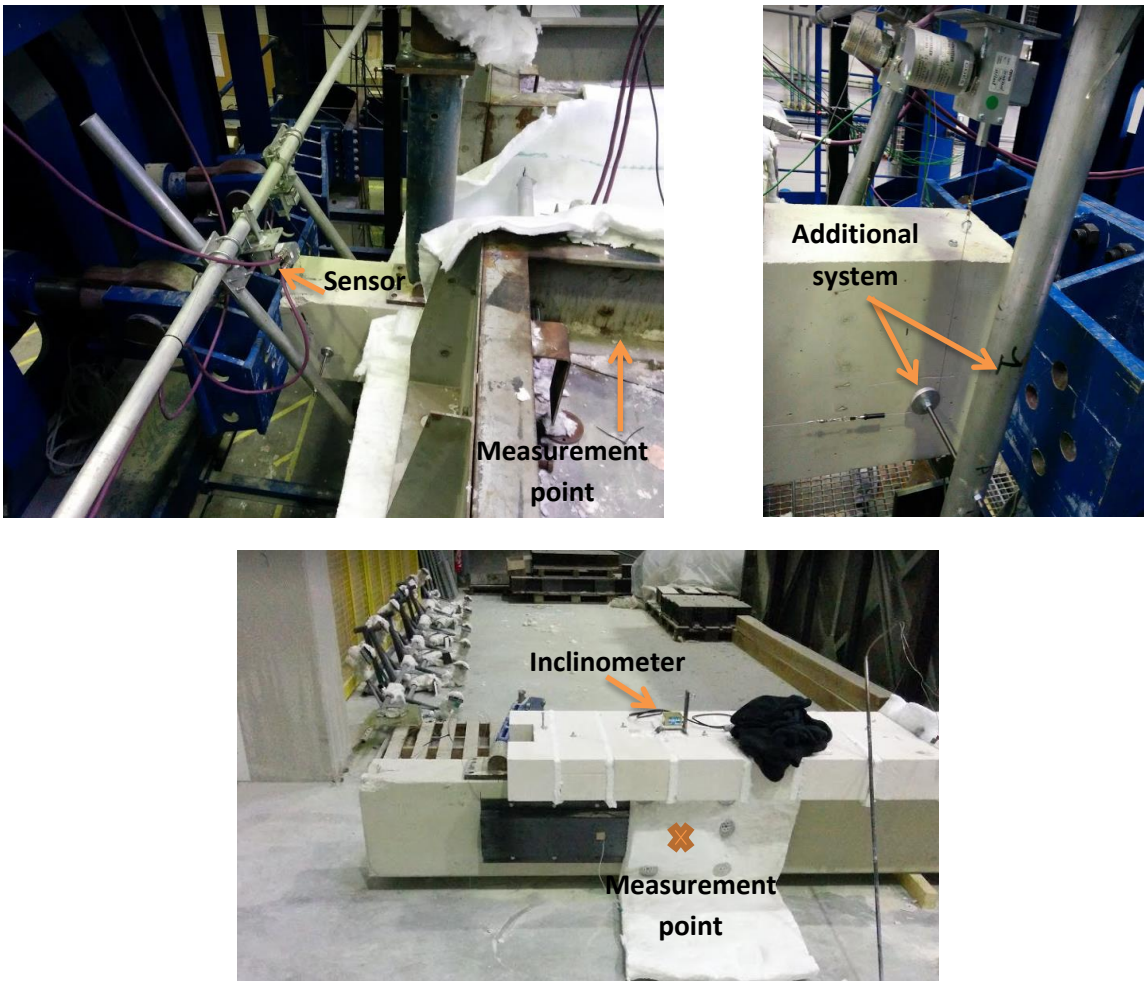


**Figure 6-29. The measurement of the horizontal displacement and rotation during the Test 2**

The measurement point of the horizontal displacements is marked in the same figure.

In Promethee configuration, the supports of the tested structural element are placed inside the furnace. The mineral wool is used to protect the specific area. The metallic cover ensures that the cable of the transducers is always in the correct position and it will not be affected during the test by exterior factors such as the contact with the roof of the furnace or the mineral wool placed in that area.

One of the questions, when designing the configuration of the tests, was related to the temperature evolution in the area when the cable of the transducer is placed. The temperature is not expected to increase based on the protection provided in the needed zone. Nevertheless, thermocouples have been placed in different positions to measure the temperature evolution in the mentioned areas. An increase in the temperature leads to the dilatation of the transducer's cable and thus the results can be compromised. Another solution to avoid the problem is to make use of quartz cables in the areas which can be affected by the temperature. The protection assured in the configuration of the TEST 2 is considered proper to avoid the increase of the temperature in the transducer's cable.

The same figure presents the position of the inclinometer, which is placed outside the furnace. Promethee facility had previously implemented a formula to compute the horizontal displacement on the supports by measuring the supports rotation and other additional displacements measured on the unexposed side of the beam. By measuring multiple displacements and rotations and then the transformation into the needed measurements can induce errors in the process. This is the reason why the direct horizontal displacement of the rolling support is measured during the TEST 2.

*Characteristics of the considered data acquisition system*

The tested beam is simply supported and the aim is to impose every time step rotations on the supports along with the horizontal displacements. The support rotation is imposed by the vertical jacks acting on the cantilever cold part of the beam. The horizontal displacement is imposed by the horizontal jack acting on the cold cantilever part of the beam close to the rolling support. Close to the hinged support, no horizontal displacement is admitted. To stop the horizontal displacement close to the hinged support the jack presented in the Figure 6-29 is provided. Thus the horizontal displacement is blocked during the tests but at the same time the vertical displacement and rotation are allowed.

A simple calculation to estimate the stiffness of the metallic structure supporting the jacks has been done to check if the horizontal displacement on the hinged support is not possible. After the calculations, it was decided to measure the both horizontal displacement, on the hinged support as well as on the rolling support. Thus, the horizontal displacement controlled during the hybrid test is the sum between the horizontal displacement measured on the hinged support and horizontal displacement measure on the rolling support. The displacements are summed due to the fact that the transducers to measure the mentioned displacements are positioned in the opposite directions (see the sign convention for the transducers in Appendix B).

The resolution of the transducers is checked making used of the system presented in Figure 6-30.

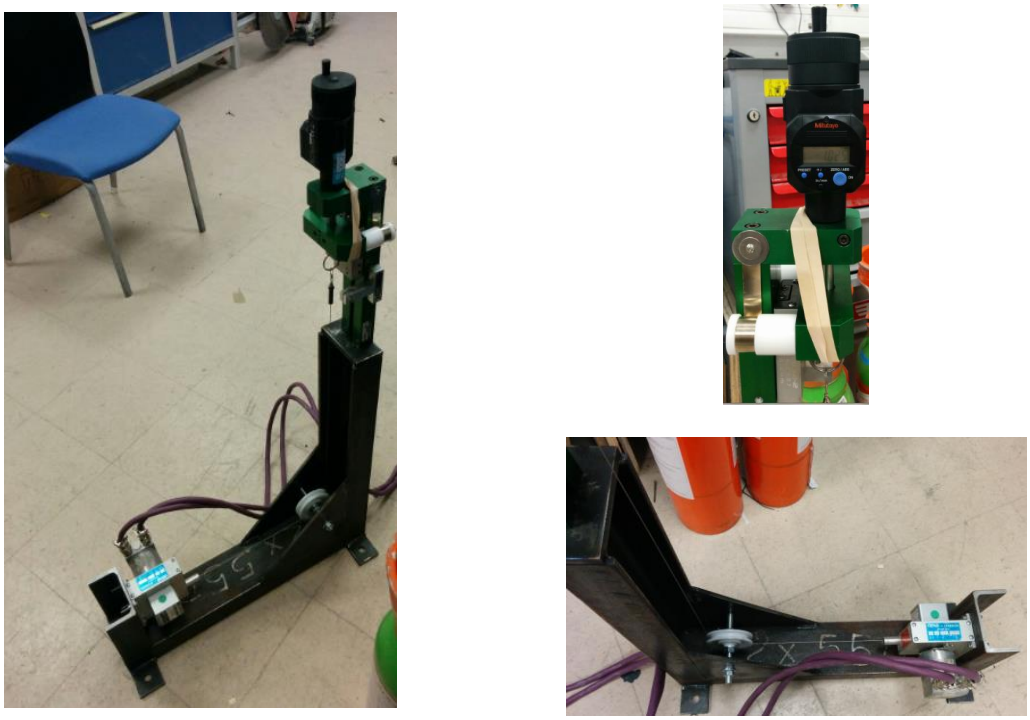

**Figure 6-30. The system used to check the resolution of the transducers**

A steel piece is designed where the transducer used in the measurement is attached and connected to the micrometric transducers. The micrometric transducer has the objective to impose displacements while the measurement done by the sensor is registered and then compared with the imposed value. The wheel redirects the direction of the cable in order to simulate the conditions during the test. The wheel is important to be stiff and in the same time to allow the needed displacement.

Figure 6-31 presents the evolution of target displacements versus the measured displacements for the two transducers used in the hybrid test. The demonstration is done in the interval 0 mm to 1 mm. The resolution of the transducers is deduced from the mentioned plots, thus the transducer 1 has a resolution of 0.0625 mm, while the transducer 2 has a resolution of 0.039 mm. The resolution of the inclinometers is equal to 0.018 mrad.

*Transducer 1* *Transducer 2*

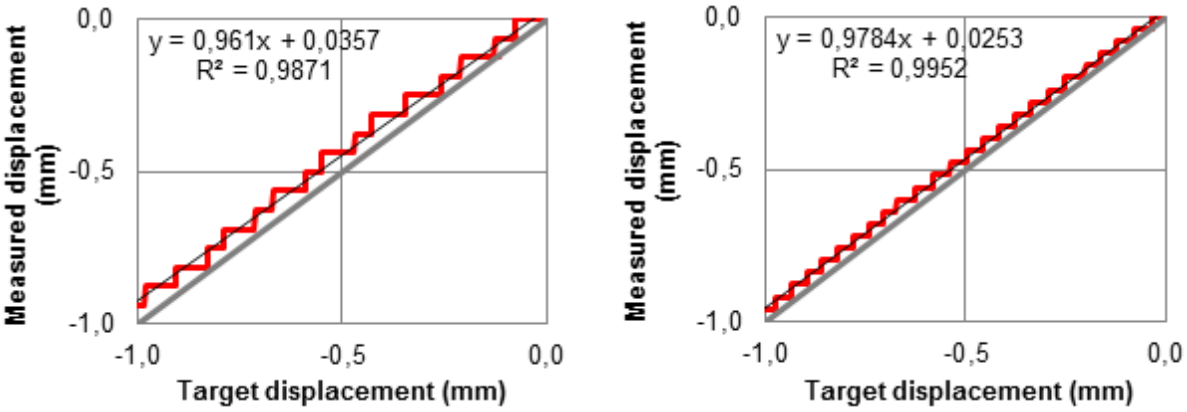


**Figure 6-31. Resolution of the transducers**

- **The actuators**

*Characteristics and some observations*

Figure 6-32 presents the hydraulic actuator to control the supports rotations. The position of the actuator is vertical with a capacity of 50 tons.

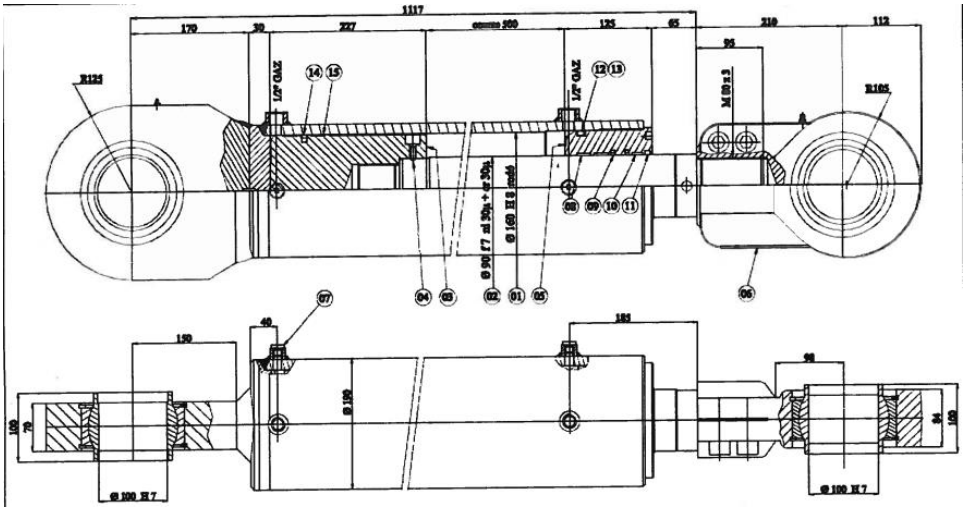

**Figure 6-32. The actuators controlling the support rotations**

Figure 6-33 presents the hydraulic actuator to control the horizontal displacement. The position of the actuator is horizontal with a capacity of 120 tons.

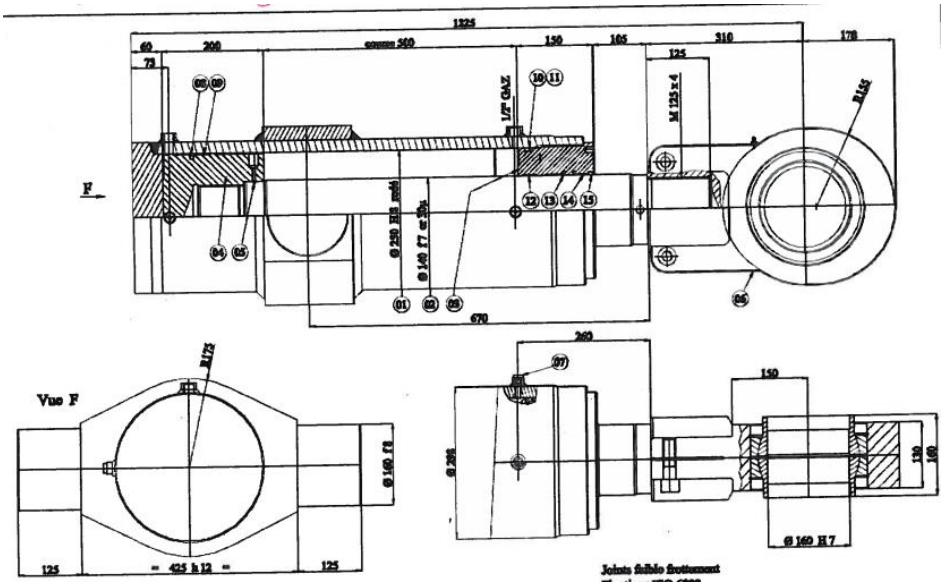


**Figure 6-33. The actuator controlling the horizontal displacement**

The following observations are done towards the actuators for a proper regulation:

- The oil chambers are recommended to have the same dimensions, which is not the case for the facility of the Promethee furnace.
- The mechanical friction joints (the case of Promethee facility) are characteristic of industrial jacks. The mechanical friction joints induce errors in the reading force when the direction of the jack changes. One solution to avoid the errors produced by the joints is to use load cells for measuring the forces. Another solution is the possibility of using jacks which dispose of hydraulic friction joints.
- The capacity of the horizontal actuators is 120 tons while the maximum expected force during the test is less than 50 tons. When working in the low range of action of the actuators the precision is affected.
- The use of auto-adaptive systems for the control would adjust depending on the occurred event during the tests.

*Transducer test with the actuator*

The next step was to test the transducer with the actuator in the laboratory. One of the transducer (resolution of 0.039 mm) is attached to the horizontal jack as presented in Figure 6-34.

The objective of this step is to check if the jack can induce the target displacement and to see the variation of the force in the jack depending on the variation of the displacements. The imposed target displacement is not a multiple of the transducers resolution. Thus the jack is changing directions in order to find the proper value, inducing variation of forces.

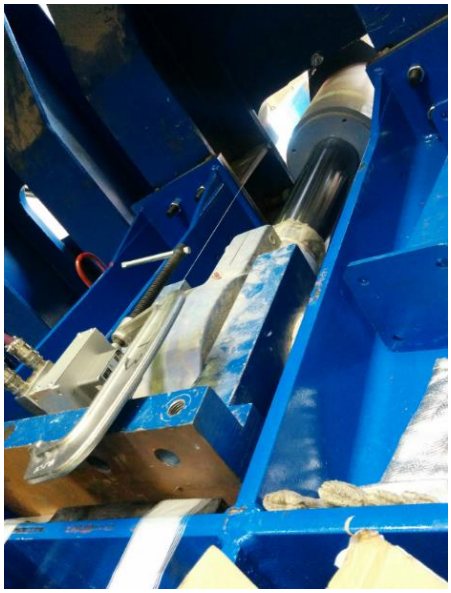

**Figure 6-34. Test transducer using the actuator**

Figure 6-35 presents how the measured displacement oscillates around the target displacement. In this example the target displacement is 3mm. The measured data are registered and plotted every 3 seconds thus. It has been observed that the oscillation of displacement induced a force variation of 2 tons in this specific configuration.

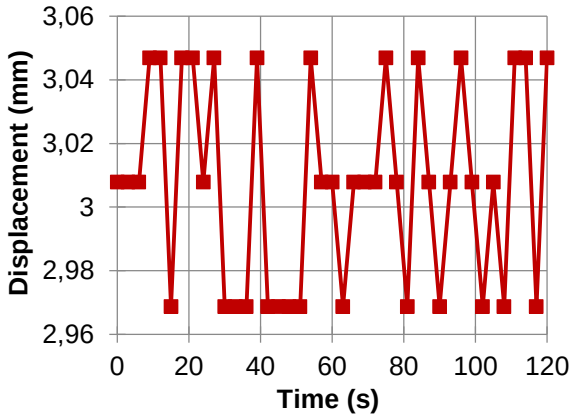


**Figure 6-35. The variation of displacement in time while controlling actuator**

The objective of the exercise was to check the force variation induced by the resolution of the transducers. Small variation of displacement induced significant variation of force. A higher resolution of the transducers would reduce the force variation. It is expected that the noise induced during the test to have a bigger impact on the results than the resolution of the transducers.

### 6.7.3. Test Setup and Procedure

*Beam preparation*

The same steps described for the preparation of the beam during the TEST 1 are applied when the TEST 2 is performed (for more details see Appendix D). The only difference is about the measurement of the horizontal displacement on the supports, as presented in the section 6.7.2.

*Furnace preparation*

The same as described in the preparation process of the TEST 1 (for more details see Appendix D).

*Instrumentation layout*

- Transducers/inclinometers

Vertical and horizontal displacements are measured in different positions along with the support rotations.

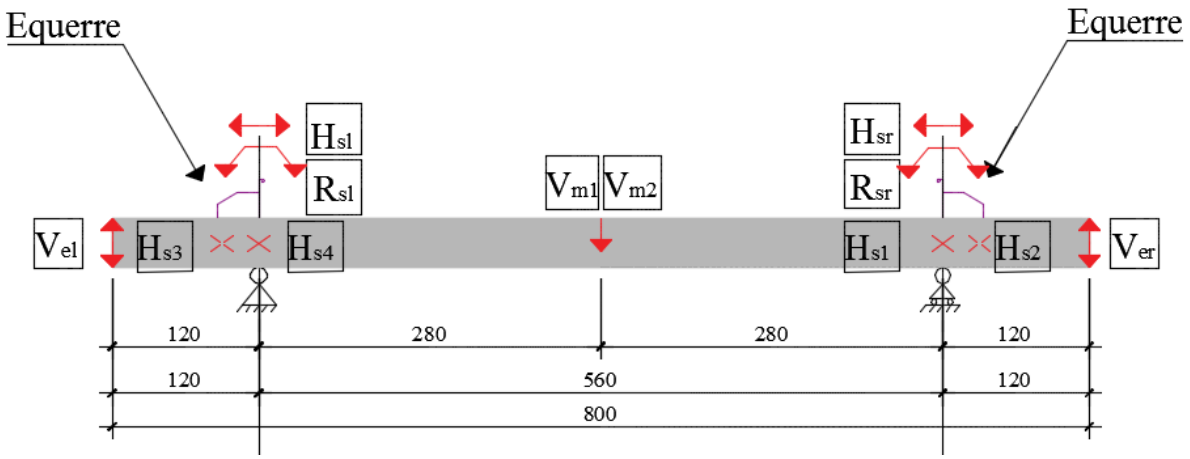


**Figure 6-36. The measured displacements and rotations during the Test 2**

The vertical displacements are measured in the mid-span $V_{m1}$ and $V_{m2}$, along with the vertical displacements of the cold extremities $V_{el}$ and $V_{er}$.

For the hinged support several displacements and rotations are measured. The horizontal displacement $H_{sl}$ and the rotation $R_{sl}$ are measured on the unexposed side of the beam.

For the rolling support, the horizontal displacement $H_{sr}$ and the rotation $R_{sr}$ are measured.

The measured horizontal displacements on the rolling support are $H_{s1}$ and $H_{s2}$ while on the hinged support are $H_{s3}$ and $H_{s4}$. The displacements $H_{s1}$ and $H_{s4}$ are measured in the axis of the support, while the displacements $H_{s2}$ and $H_{s3}$ are measured 30 cm distance from the supports. In the ***hybrid process the sum of the measured displacements $H_{s2}$ and $H_{s3}$ is considered***. The displacement $H_{s2}$ and $H_{s3}$ are chosen for control in order (i) to avoid the

effect of possible plastic effects in the area of the supports; (ii) to avoid the effect of temperature in the area of the supports which can lead to the dilatation of the transducers cable. The vertical displacements of the cantilever unexposed beam are expected to be small based on the virtual hybrid fire test, thus the horizontal displacement measured 30 cm distance from the support is not affected by the vertical displacement of the cold extremity.

The ***rotations controlled during the hybrid process are $R_{sl}$ for the hinged support and $R_{sr}$ for the rolling support***.

- The configuration of the jacks

The same configuration of the vertical jacks is considered during the TEST 2 as in the TEST 1 (for more details see Appendix D). In addition, the horizontal jacks are added in the TEST 2 to model the restrain given by the surrounding structure. Figure 6-37 shows some pictures of the horizontal jacks in the furnace.

**Figure 6-37. The configuration of the horizontal jacks**

- Configuration of the thermocouples

The configuration of the thermocouples is presented in Appendix D3.

## 6.7.4. Test Results and Interpretation

### 6.7.4.1. The input data of the algorithm

A new methodology is proposed in this thesis and the algorithm of the new methodology is described in section 5.3.

The input data to perform the TEST 2 are described in this section. The units of the expressed values are in [N], [m] and [rad].

The concrete property, i.e. the compressive strength, is known in different stages since the beams are casted. The strength result after performing the specific tests on samples, in different days from the casting of the specimen. Thus, a prediction is done based on EN 1992-1-2, to assume the value of the concrete strength in the day of the TEST 2.

*The number of controlled degrees of freedom*

First, the number of controlled degrees of freedom at the interface between the PS and NS is defined (see Eq. **(85)**). In this example, three degrees of freedom are controlled, namely the horizontal displacement on the roller support and the two rotations. Please note that the number of controlled degrees of freedom during the tests differ from the total number of degrees of freedom existing at the interface between the PS and NS, see section 6.2.2. The first component of the displacement vector is the horizontal displacement, the second component is the left rotation (hinged support) while the last component of the vector is the right rotation (rolling support).

$$\text{nDOF} = 3 \tag{85}$$

*The stiffness of the NS*

The NS is represented by the predetermined matrix computed after the steps presented in the section 6.2.2. The matrix is kept constant during the hybrid fire tests. It is assessed that in the day of the TEST 2, the compressive strength of the concrete will reach the value of 48 MPa. The predetermined matrix is presented by the Eq. **(86)** .

$$K_N = 10^6 \begin{bmatrix} 10.50 & -11.70 & 8.26 \\ -11.70 & 64.80 & -8.72 \\ 8.26 & -\ 8.72 & 63.60 \end{bmatrix} \tag{86}$$

*The stiffness of the PS*

The initial tangent stiffness of the PS is computed in SAFIR assuming the compressive concrete strength is equal to 48 MPa. The resulted value is presented by the Eq. (87). If the stiffness matrix of the PS is compared with the predetermined matrix of the NS it can be observed that the axial stiffness of the PS is much higher compared with the axial stiffness of the NS, while the rotational stiffness of the PS is smaller than the rotational stiffness of the PS.

$$K_P = 10^6 \begin{bmatrix} 479 & 0 & 0 \\ 0 & 25.60 & 12.80 \\ 0 & 12.80 & 25.60 \end{bmatrix} \tag{87}$$

The stiffness of the PS is constant during the calculations of hybrid fire testing. It is recommended to measure the stiffness of the PS before the test and to multiply the measured stiffness value with a factor of 1.5 just to avoid the possible errors during the measurements. Before performing the real hybrid tests, the stiffness of the PS was not measured. But at the same time, the valuable information is extracted from the preloading stage of the beam, before starting the fire. More details will be explained later in the thesis. Therefore, the stiffness value of the PS defined in the algorithm is the value resulted from the numerical analysis multiplied with 1.5 (see the Eq. (88)).

$$K_P = 10^6 \begin{bmatrix} 718.5 & 0 & 0 \\ 0 & 38.40 & 19.20 \\ 0 & 19.20 & 38.40 \end{bmatrix} \tag{88}$$

*The vector of interface forces of the NS at ambient temperature*

The vector of interface forces at ambient temperature is described for the NS by the Eq. **(89)**.

$$F_{N,initial} = \begin{bmatrix} H_{N,initial} \\ M_{N,left,initial} \\ M_{N,right,initial} \end{bmatrix} \tag{89}$$

Where:
$H_{N,initial}$ is the axial force of the NS at ambient temperature;
$M_{N,left,initial}$ is the bending moment on the left (hinged) support at ambient temperature;
$M_{N,right,initial}$ is the bending moment on the right (rolling) support at ambient temperature;
$H_{N,initial}$, $M_{N,left,initial}$, and $M_{N,right,initial}$ result from the analysis of entire structure at ambient temperature.
The interface forces defined for the NS will have the opposite signs compared with the interface forces defined for the PS.
Equation (90) presents the values defined as an input before the start of the TEST 2.

$$F_{N,initial} = \begin{bmatrix} 36650 \\ -95535 \\ 95589 \end{bmatrix} \tag{90}$$

*The vector of interface displacements at ambient temperature*

The vector of interface displacements at ambient temperature is presented by the Eq. (91). The first component of the vector refers to the horizontal displacement, the second component of the vector refers to the left rotation (hinged support) while the last component of the vector refers to the right rotation (rolling support). The vector of interface displacements results from the analysis of the entire structure (before substructuring) at ambient temperature.

$$u_{initial} = \begin{bmatrix} 0.00004 \\ 0.00004 \\ -0.00003 \end{bmatrix} \quad (91)$$

*The transformation matrix for forces*

The transformation matrix presented by the Eq. **(92)** is established based on the position of the jacks related to the global system of coordinates GSC (see Appendix B).

$$T_P = \begin{bmatrix} -1 & 0 & 0 \\ 0 & arm_{left} & 0 \\ 0 & 0 & -arm_{right} \end{bmatrix} = \begin{bmatrix} -1 & 0 & 0 \\ 0 & 0.7 & 0 \\ 0 & 0 & -0.7 \end{bmatrix} \quad (92)$$

*Transformation matrix for displacements*

The transformation matrix for displacements (Eq. (93)) is built based on the position of the transducers and inclinometers in the furnace compared with the GSC (see Appendix B).

$$T_u = \begin{bmatrix} -1 & 0 & 0 \\ 0 & 1 & 0 \\ 0 & 0 & 1 \end{bmatrix} \quad (93)$$

*The hydraulic jacks to apply the constant loads*

Two hydraulic jacks are considered to apply the constant load in the mid-span of the beam (Eq. (94)).

$$nP = 2 \quad (94)$$

The value to be imposed during the hybrid fire testing is expressed by the Eq. **(95)**.

$$P = \begin{bmatrix} P_1 \\ P_2 \end{bmatrix} = \begin{bmatrix} 73928 \\ 73928 \end{bmatrix} \quad (95)$$

*The time step*

The time step chosen for the TEST 2 is presented in the Eq. (96) and is chosen based on the numerical analyses presented in the section 6.4.

$$\boldsymbol{\Delta t = 1} \quad (96)$$

*The tolerance for the convergence*

The tolerance for the convergence is defined by user in the Eq. **(97)**.

$$\boldsymbol{eps} = 2\text{x}10^{-3} \quad (97)$$

### 6.7.4.2. Preloading stage

Before starting the hybrid fire tests, the beam must be loaded in the mid span with the load $\boldsymbol{P}$ and the interface displacements $\boldsymbol{u_{initial}}$ must be imposed.

The user chooses the proper solution to apply the initial loads depending on the existing possibility of the furnace facility.

The mid span loads and the interface displacements can be both applied gradually in time.

In this specific case it is chosen to apply the loads in 3 different stages described below and summarized in Table 6-6. The solution is chosen based on the possibilities of the furnace facility.

*Stage 1*: Only half of the span force is applied on the beam **P/2**. All the support displacements are free. In the first stage of preloading the beam is simply supported and cannot support the total load **P.**

*Stage 2*: The mid-span load is equal with the load applied in the Stage 1, i.e. **P/2**. The initial interface displacements $\mathbf{u_{initial}}$ are imposed on the supports.

*Stage 3*: The mid-span load is totally applied, i.e. **P**. At the same time the interface displacements are forced to have the same values as in the Stage2, thus initial interface displacements $\mathbf{u_{initial}}$.

**Table 6-6. Stages of loading TEST 2**

| STAGE | $\boldsymbol{P}$ (N) | $\boldsymbol{u}$ (m) | $\boldsymbol{\theta_{left}}$ (rad) | $\boldsymbol{\theta_{right}}$ (rad) |
|---|---|---|---|---|
| **1** | 18 482 x 4 = 73 928 | not controlled | not controlled | not controlled |
| **2** | 18 482 x 4 = 73 928 | 0.00004 | 0.00004 | -0.00003 |
| **3** | 36 964 x 4 = 147 856 | 0.00004 | 0.00004 | -0.00003 |

The values presented in the Table 6-6 are expressed in the global system of coordinates

*Observations in preloading stage*

The evolution of forces in the jacks along with the evolution of displacements/rotations at the interface is next discussed.

Figure 6-38 presents the evolution of mid-span force in the preloading stage 1 and 2.

Figure 6-39 presents the evolution of axial force in the preloading stage 1 and 2.

Figure 6-40 presents the evolution of horizontal displacement in the preloading stage 1 and 2.

Figure 6-41 presents the evolution of vertical forces in the jacks acting on the cantilever side of the beams, in the preloading stage 1 and 2.

Figure 6-42 presents the evolution of rotations in the preloading stage 1 and 2.

Note that the values illustrated in the graph are expressed based on the local system of coordinates. The positive displacement shows elongation of the transducers cable, while the positive rotation illustrates a counter clockwise rotation in the local system of coordinates. A positive force is measured when the jacks are pushing on the PS.

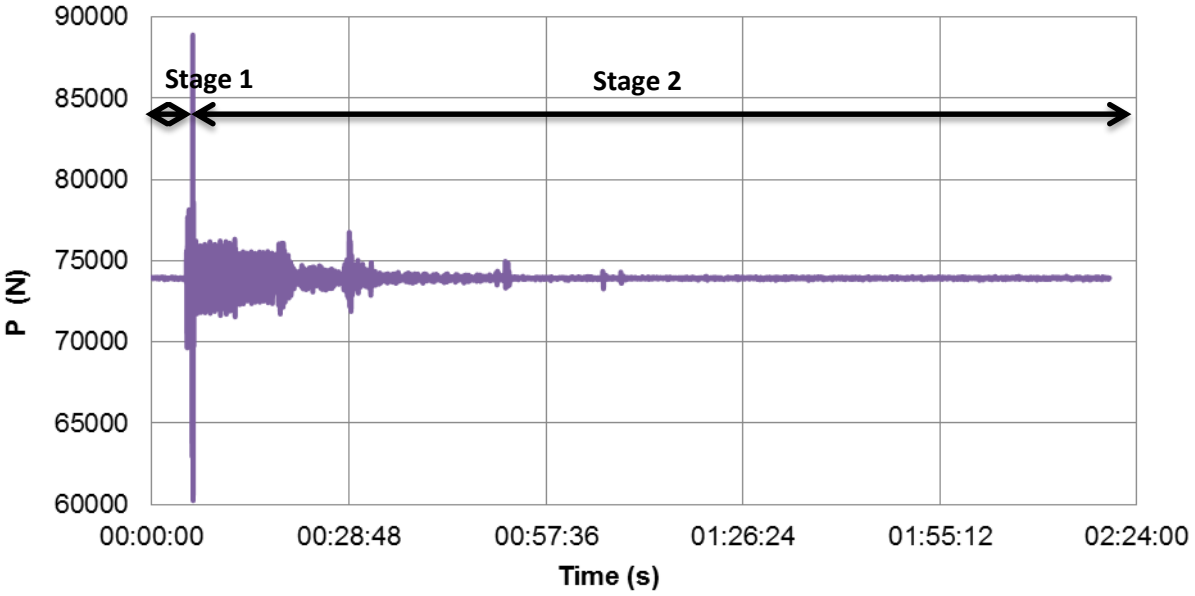


**Figure 6-38. The mid-span load in the preloading stage 1 and 2**

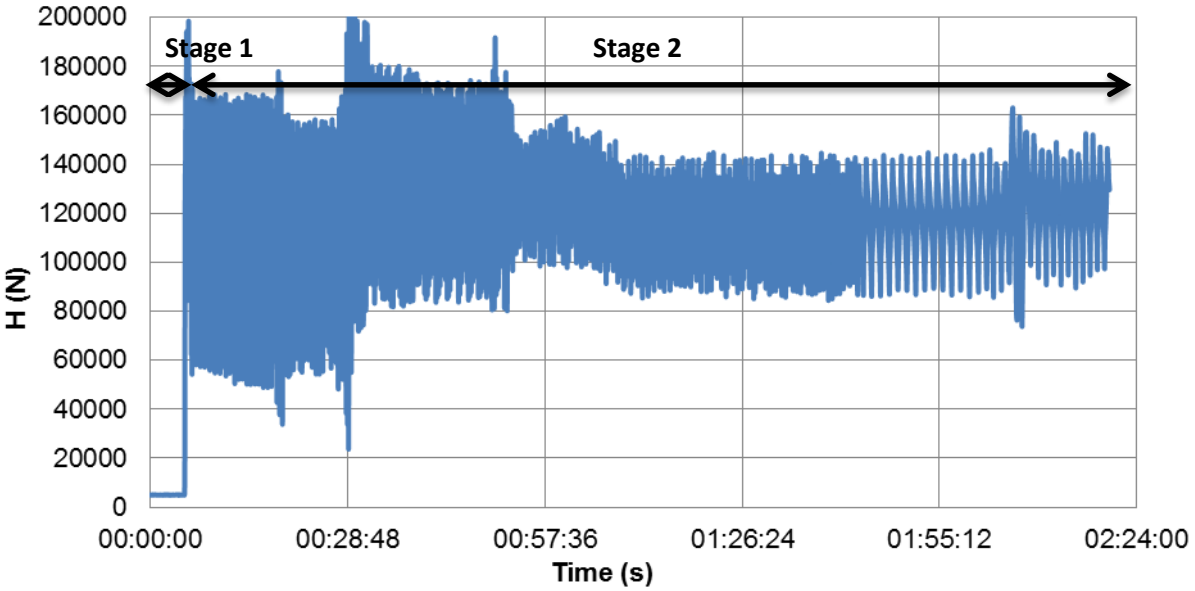


**Figure 6-39. The axial force in the preloading stage 1 and 2**

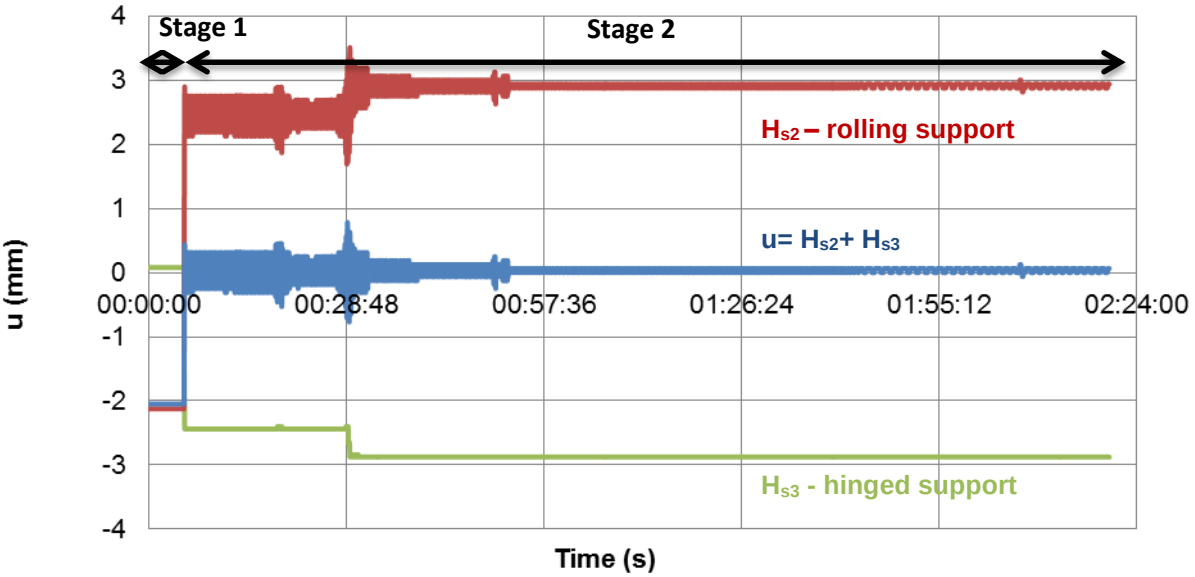


**Figure 6-40. The axial displacement in the preloading stage 1 and 2**

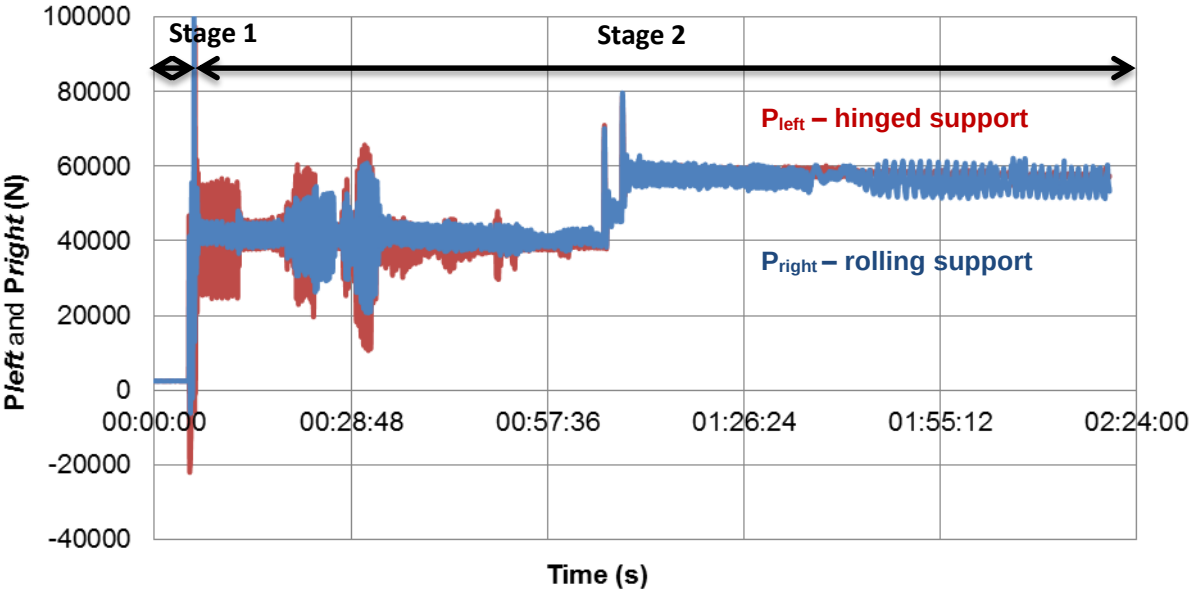


**Figure 6-41. The vertical forces in the preloading stage 1 and 2**

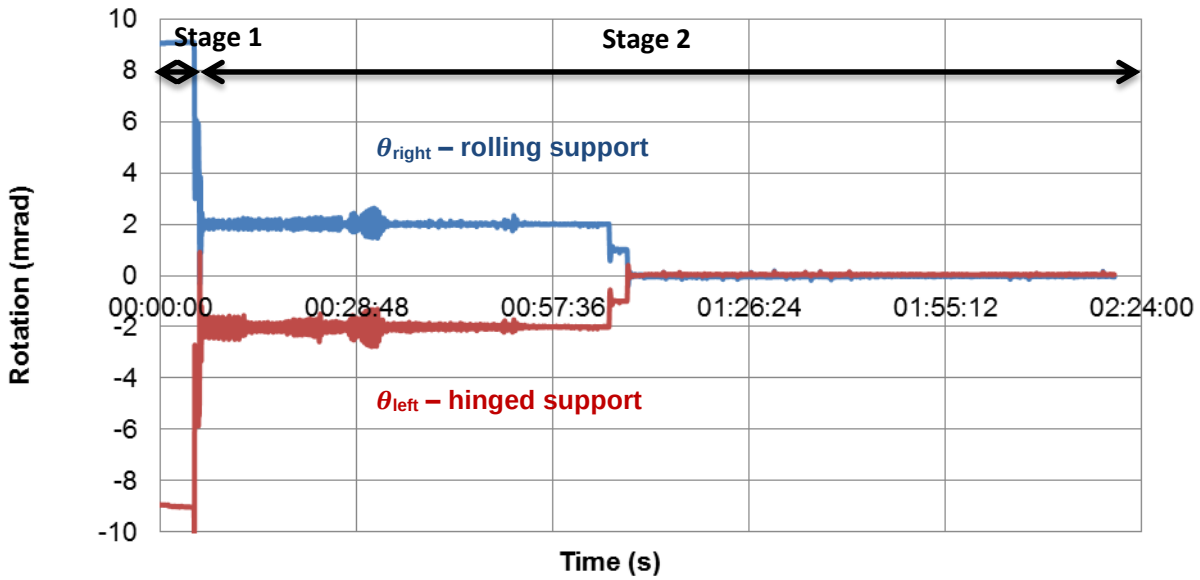


**Figure 6-42. The rotations in the preloading stage 1 and 2**

Stage 1

In the first stage of preloading only half of the span load is applied (P=73 928 N). Table 6-7 summarizes the interface displacement in the Stage 1 in the local system of coordinates LSC as well as in the global system of coordinates GSC.

The horizontal displacement $u$ is the sum of the horizontal displacement of the hinged support and the horizontal displacement of the rolling support. In the first stage no horizontal displacement is measured on the hinged support (the hinge does not allow the horizontal displacement). On the rolling support a negative displacement is measured (the cable of the transducer shortens) in the local system of coordinates LSC. The displacement in the global system of coordinates results by multiplying the measured value with the first term of the transformation matrix for displacements, thus a positive displacement in the global system of coordinates GSC is measured (elongation of the beam).

A negative rotation is measured on the hinged support $\theta_{left}$ while a positive rotation is measured for the rolling support $\boldsymbol{\theta_{right}}$. The values of the transformation matrix of displacements afferent to the rotations are equal to one, thus the measured rotations in the furnace represent the values in the LSC as well as in the GSC.

**Table 6-7. Interface displacement/rotation in Stage 1**

| **Stage 1** | $\boldsymbol{u}$ (mm) | $\boldsymbol{\theta_{left}}$ (mrad) | $\boldsymbol{\theta_{right}}$ (mrad) |
|---|---|---|---|
| **LSC** | -2.047 | -8.931 | 9.019 |
| **GSC** | 2.047 | -8.931 | 9.019 |

Stage 2

After the first stage is done the next step is to force the interface displacement and rotations to be equal to the initial displacements $\mathbf{u_{initial}}$.

From a value of 2.047 mm (GSC), the horizontal displacement needs to reach a value of 0.04 mm (GSC). The horizontal jack pushes on the beam in order to impose a displacement approximately equal to zero.

From a value of -8.931 mrad (GSC), the rotation on the hinged support needs to reach a value of 0.04 mrad (GSC). Thus the vertical jack acting on the cantilever beam close to the hinged support pushes on the beam until the measured rotation is equal to the defined value of 0.04 mrad.

From a value of 9.019 mrad (GSC), the rotation on the rolling support needs to reach a value of -0.04 mrad (GSC). Thus the vertical jack acting on the cantilever beam close to the rolling support pushes on the beam until the measured rotation is equal to the initial defined value of -0,03mrad.

All the jacks will register a positive value of forces.

The first observation is done based on the registered forces in the horizontal jack (see Figure 6-39). The force varies from 5 tons to 17 tons. The horizontal jack influences the registered values in the jacks P, $P_{left}$ and $P_{right}$ and continuous oscillations in the readings are observed. The horizontal measured displacement on the hinged support is between 2 and 3 mm. At the same time the imposed rotations on the support are 2 mrad on the rolling support and -2 mrad on the hinged support.

Next, the focus was to fix the values of PID in order to reduce the oscillations. It can be observed in the graphs above that the values are adjusted in such way that the oscillation in readings is reduced as much as possible in all the jacks acting on the beam.

The improvement in the readings is observed around the 57 min since the preloading stage started. Soon right after, the induced support rotations are equal to the initial defines values.

The measured axial force varies from 9 tons to 14 tons. The measured forces on the cantilever vary from 5.50 tons to 6 tons. The oscillation is slightly bigger in the vertical jack positioned close to the horizontal jack.

To be mentioned that the transducer positioned close to the rolling support has a resolution of 0.0625 mm, while the transducer positioned close to the hinged support has a resolution of 0.039 mm. The section 6.7.2 presents the oscillation of horizontal displacement around the target value due to the resolution of 0.039 mm of the transducers. The same section mentions a variation equal to 2 tons within the mentioned resolution. A variation of axial force of 5 tons during the TEST 2 is justified by the fact that one of the transducers used in the measurements has a resolution of 0.0625mm.

The stage 2 of preloading was possible only after some corrections in the control process (software). The first identified error refers to the incorrect implemented unit system. Other error refers to the impossibility of the jacks to apply the target displacement. Corrections were implemented, and finally the preloading stage was possible to be performed. The unit system was corrected and the jacks were able to apply the target displacements.

Stage 3

The last stage assumes the total span load and the initial interface displacements.

Figure 6-43 to Figure 6-47 present the forces acting on the beam in the stage 3 as well as the interface displacements and rotations.

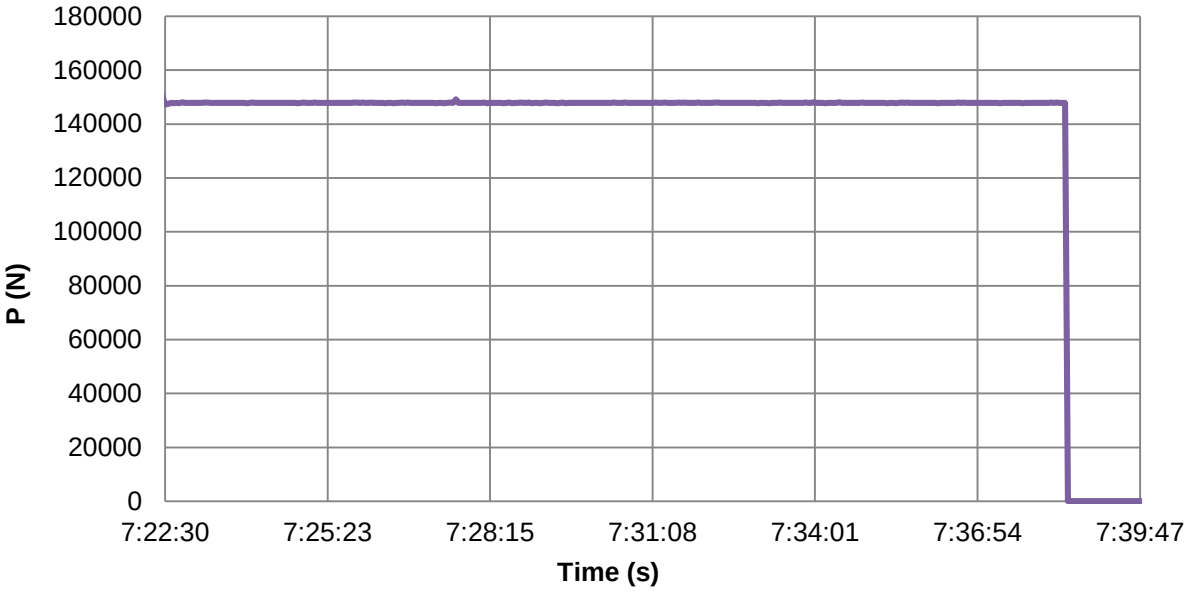


**Figure 6-43. The mid-span load in the preloading stage 3**

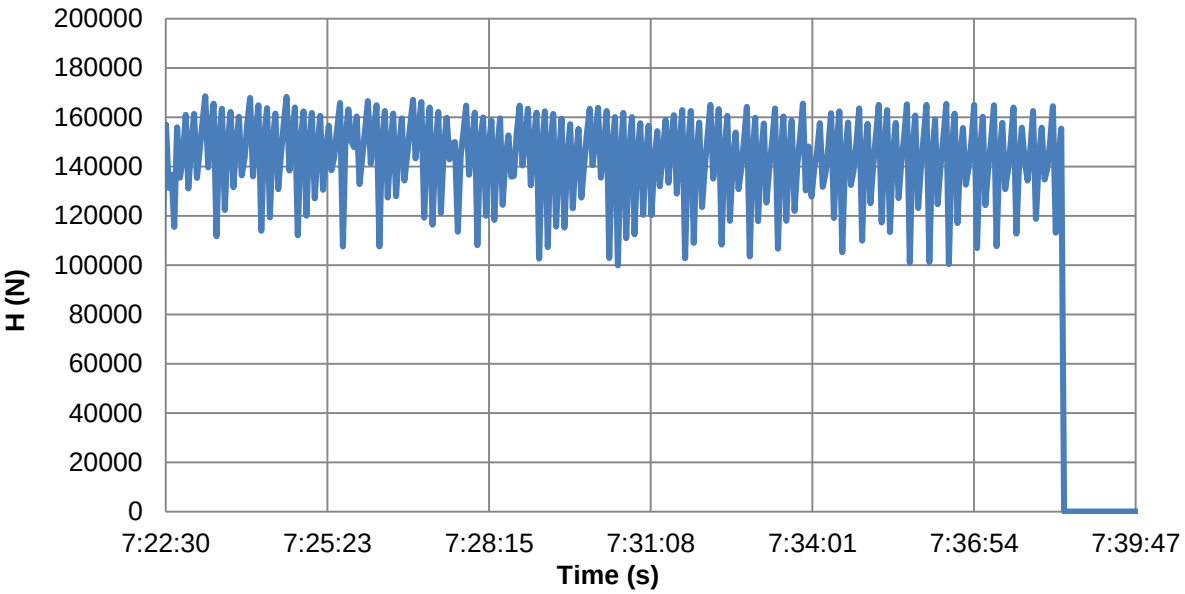


**Figure 6-44. The axial force in the preloading stage 3**

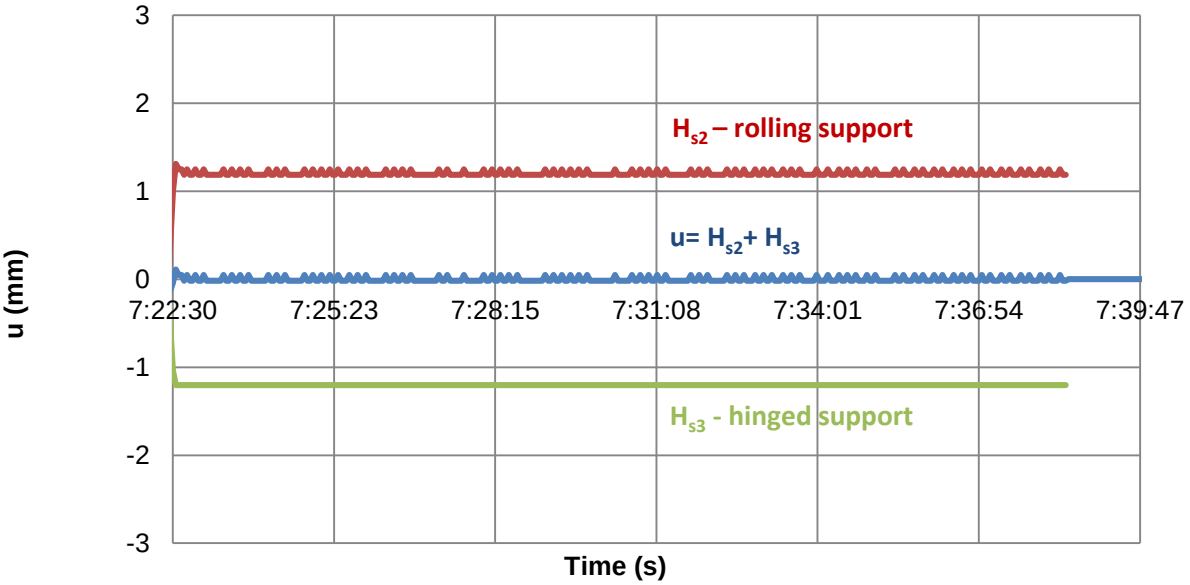


**Figure 6-45. The horizontal displacements in the preloading stage 3**

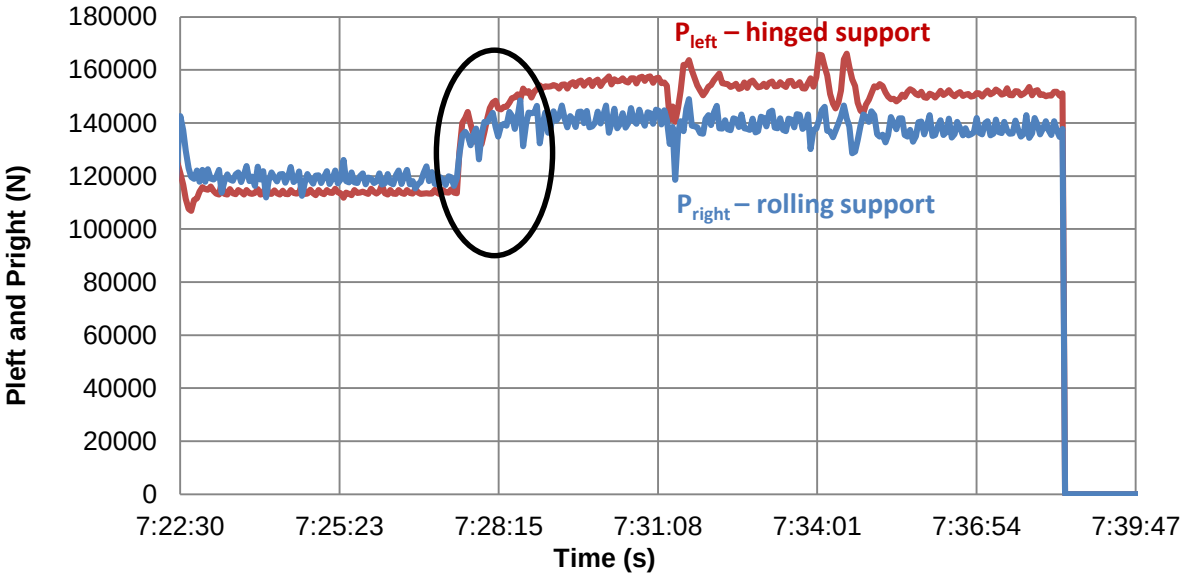


**Figure 6-46. The forces in the vertical jacks in the preloading stage 3**

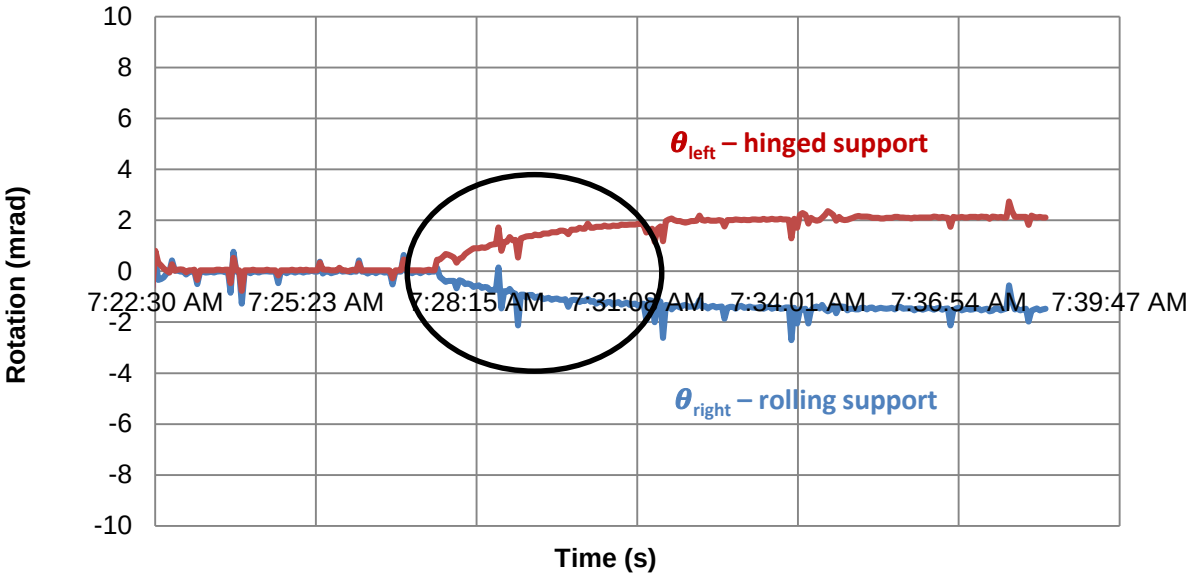


**Figure 6-47. The support rotations in the preloading stage 3**

In the stage 3 of preloading, the total force $\boldsymbol{P}$ is applied in the span along with the initial interface displacements $\mathbf{u}_{\mathbf{initial}}$.

After the preloading in stage 2 and before the preloading in stage 3, the PID is continued to be tuned in order to get the best possible response of the actuators.

It can be observed that the oscillation in the force $P_{right}$ is more pronounced compared with the oscillation in the force $P_{left}$ (the 2 actuators and 2 inclinometers have identic characteristics). The horizontal actuator influences the response of the vertical actuator $P_{right}$.

*Observations in the preloading stage*

Table 6-8 presents the measured values of the interface forces and displacements/rotations in the TEST 2. The measurements are expressed in the global system of coordinates and are presented for the 3 defined preloading stages.

**Table 6-8. Measured values in the TEST 2**

| STAGE | $H$ (N) | $P_{left}$ (N) | $P_{right}$ (N) | $u$ (m) | $\theta_{left}$ (rad) | $\theta_{right}$ (rad) | $V_{m1}$ (m) | $V_{el}$ (m) | $V_{er}$ (m) |
|---|---|---|---|---|---|---|---|---|---|
| **1** | 0 | 0 | 0 | 0.00205 | -0.00891 | 0.00902 | -0.01631 | 0.00981 | 0.00975 |
| **2** | -104404 | -58510 | -59115 | -0.00006 | 0.00004 | -0.00004 | -0.00306 | -0.00144 | -0.00138 |
| **3** | -162341 | -112790 | -120213 | 0.00002 | 0.00006 | 0 | -0.00750 | -0.00275 | -0.00344 |

In the first stage of preloading, i.e. Stage 1, only half of the span loads are applied on the specimen. Since the beam is simply supported and no interface conditions imposed, the beam can uphold only half of the span loads in this stage. The interface displacements and rotations, i.e. $u$, $\theta_{left}$ and $\theta_{right}$, are measured along with the mid-span vertical displacement $v_{m1}$ and vertical displacements on the cantilever extremities, i.e. $V_{el}$ and $V_{er}$. Since the interface displacements/rotations are free, the forces $H$, $P_{left}$, and $P_{right}$ are equal to zero.

In the next stage, i.e. Stage 2, half of the span loads act on the beam along with the interface displacements and rotations $u_{initial}$, $\theta_{initial,left}$ and $\theta_{initial,right}$. The horizontal jack $H$ imposes the horizontal displacement $u_{initial}$ while the vertical jacks $P_{left}$, and $P_{right}$ impose the support rotations $\theta_{initial,left}$ and $\theta_{initial,right}$. The effective measured values at the interface $u$, $\theta_{left}$ and $\theta_{right}$ are presented in the same table. Please observe that the measured values in the furnace, i.e. $u$, $\theta_{left}$ and $\theta_{right}$, slightly differ from the imposed target values, i.e. $u_{initial}$, $\theta_{initial,left}$ and $\theta_{initial,right}$. The developed interface forces $H$, $P_{left}$, and $P_{right}$ are expressed in the same table. The mid-span vertical displacements and the vertical displacements of the cantilever are measured and expressed in the same table.

In the Stage 3 the initial interface displacements are imposed in the furnace and the total span load. The initial interface displacements need to be kept in the Stage 3 as in the Stage 2. In other words, the measured interface displacements $u$, $\theta_{left}$ and $\theta_{right}$ are the same in the Stage 2 as in the Stage 3. The measured interface displacements in the furnace during the Stage 2 and 3 are presented in the Table 6-8 and it can be observed a slightly difference. As in the previous stage, the difference occurs due to the resolution of the transducers. The target value is not a multiple value of the transducers and inclinometers resolution. Thus, the measured value varies around the target value without the possibility to achieve the target value. Nevertheless, the interface forces $H$, $P_{left}$, and $P_{right}$ increases since the span load increased compared from the previous stage. The mid-span vertical displacement and the vertical displacement of the cantilevers increases in the Stage 3 compared with the Stage 2.

### 6.7.4.3. Equilibrium at ambient conditions

Once the loading of the beam is completed (Stage 1, Stage 2 and Stage 3), the interface reaction forces of the PS should be in equilibrium with the interface forces of the NS at ambient temperature. The interface forces of the NS at ambient temperature are defined by Eq. **(90)**.

Table 6-9 presents the interface forces of the PS versus the interface forces of the NS at ambient conditions and it can be observed that no equilibrium is ensured. The differences will be analyzed in the section "Post-analysis of the Test 2". Nevertheless, the equilibrium needs to be ensured before starting the hybrid fire tests.

**Table 6-9. Interface forces at ambient temperature in the Test 2**

| | ***PS*** | ***NS*** |
|---|---|---|
| $\boldsymbol{H}$ *[N]* | −162341 | 36650 |
| $\boldsymbol{M_{left}}$ *[Nm]* | 78953 | −95535 |
| $\boldsymbol{M_{right}}$ *[Nm]* | −84149 | 95589 |

The interface compatibility needs to be ensured along with the interface equilibrium. In the preloading stages, the initial displacement is imposed on the interface of the PS, meaning that the compatibility should be ensured. Table 6-10 presents the interface displacements measured in the furnace versus the initial displacement of the NS. The small differences are caused by the resolution of the data acquisition system.

**Table 6-10. Interface displacements at ambient temperature in the Test 2**

| | ***PS*** | ***NS*** |
|---|---|---|
| $\boldsymbol{u}$ *[m]* | 0.00002 | 0.00004 |
| $\boldsymbol{\theta_{left}}$ *[rad]* | 0.00006 | 0.00004 |
| $\boldsymbol{\theta_{right}}$ *[rad]* | 0 | −0.00003 |

To restore the equilibrium at ambient temperature, the same algorithm is applied as in the case of fire. Based on out of balance forces, the interface displacement is corrected until the equilibrium and compatibility are ensured.

The equilibrium at ambient temperature is initiated at the time 7:27:30 and the evolution of the span force, interface forces and interface displacements is presented in the Figure 6-43 to Figure 6-47 (the circled area corresponds to the initiation of the calculations).

Every second out of 10 min, new interface displacements have been computed and imposed on the interface until the iteration process stopped. When the iteration process stopped it suggested that the equilibrium and compatibility are satisfied.

It was curios that no changes were registered in the horizontal jack but only in the vertical jacks acting on the cantilever.

The evolution of the interface forces and displacement raised questions, therefore the beam was unloaded in order to analyze the results.

During this time, some modifications were done in the control process by the person in charge.

The preloading of the beams was redone and the equilibrium at ambient temperature was launched one more time. The results showed once again a behavior which was not expected and some spikes in the forces which indicate some instability. All this actions happened in a short time and during this time different modifications were done in the control software. All these modifications were not identified in the post-analysis of the hybrid fire test.

In order to analyze the results, the test was canceled.

By the time when the test was cancelled, the restoring of the equilibrium at ambient temperature did not work properly. In conclusion, the hybrid fire test was not launched.

The beam did not undergo plastic deformation during the Test 2 despite the different stages of loading which have been applied. Therefore, the same beam will be reused in the following test.

Please note that the hybrid fire testing algorithm was implemented in the control process of Promehee. The software which makes possible the hybrid fire test is specially designed for Promethee furnace by an external company. The hybrid fire test is operated by a

representative of the external company which is responsible to implement all the requested actions during the test.

#### 6.7.4.4. Post-analysis of the Test 2

*Identified problems in the preloading stage during the Test 2*

The preloading process was possible after a number of trials. Different modifications were done in the control software in order to be able to perform the preloading stages of the Test 2.

The following problems were identified in the preloading stage of the Test 2:

- The unit system of measurements is defined with some errors;
- The horizontal and the vertical jacks were not able to impose the target displacements, i.e. $u_{initial}$.

Modifications were done in the control software such as the preloading stages of the Test 2 were possible.

*Preloading stages*

Differences between the interface forces of the PS and NS are registered in the preloading stage. In order to understand the differences, the preloading stages have been analyzed in SAFIR after the test.

The model is build such as for every stage the corresponding span loads and the interface loads are applied. In the Stage 1 only half of the span load is applied. In the Stage 2 only the half of the span loads are applied and the interface forces as follows: $H = -104404\ N$, $P_{left} = -58510\ N$, and $P_{right} = -59115\ N$. During the Stage 3, the total span load is applied along with the interface forces $H = -162341\ N$, $P_{left} = -112790\ N$, and $P_{right} = -120213\ N$.

Once the model is built, the analysis runs and the displacements $u$, $\theta_{left}$, $\theta_{right}$, $V_{m1}$, $V_{el}$ and $V_{er}$ are computed and extracted.

The SAFIR analysis is done in two configurations, i.e. Configuration 1 and Configuration 2. The Configuration 1 refers to the SAFIR model in which the tensile strength of the concrete is neglected (equal to zero). The Configuration 2 refers to the SAFIR model in which the tensile strength of the concrete is considered.

Only the compression strength of the concrete is measured in the day of the test. The tensile strength is computed based on the Table 3.1 of the EN 1992-1-1. The compression test revealed a compressive strength of the concrete equal to 41 MPa in the day of the Test 2. Before the Test 2, all the preliminary calculations to prepare the tests are done with the assumption that the compressive strength of the concrete is equal to 48 MPa. The values to be defined as the input of the hybrid fire testing are computed when the compressive strength of the concrete is assumed to be equal to 48 MPa.

The post-test analysis in SAFIR is done considering the real compression strength of the concrete in the day of the Test 2, i.e. 41 MPa.

Table 6-11 presents the displacements which result when the SAFIR model is built in the configuration 1, with no tensile strength.

**Table 6-11. Displacements computed in SAFIR in configuration 1 (no tensile strength)**

| STAGE | $H$ (N) | $P_{left}$ (N) | $P_{right}$ (N) | $u$ (m) | $\theta_{left}$ (rad) | $\theta_{right}$ (rad) | $V_{m1}$ (m) | $V_{el}$ (m) | $V_{er}$ (m) |
|---|---|---|---|---|---|---|---|---|---|
| **1** | 0 | 0 | 0 | 0.00228 | -0.01115 | 0.01115 | -0.01992 | 0.01338 | 0.01338 |
| **2** | -104404 | -58510 | -59115 | -0.00003 | -0.00047 | 0.00045 | -0.00282 | -0.00005 | -0.00008 |
| **3** | -162341 | -112790 | -120213 | 0.00029 | -0.00184 | 0.00160 | -0.00722 | 0.00102 | 0.00066 |

Table 6-12 present the displacements which result when the SAFIR model is built in the Configuration 2 when the tensile strength is considered.

**Table 6-12. Displacements computed in SAFIR in configuration 2 (with tensile strength)**

| STAGE | $H$ (N) | $P_{left}$ (N) | $P_{right}$ (N) | $u$ (m) | $\theta_{left}$ (rad) | $\theta_{right}$ (rad) | $V_{m1}$ (m) | $V_{el}$ (m) | $V_{er}$ (m) |
|---|---|---|---|---|---|---|---|---|---|
| **1** | 0 | 0 | 0 | 0.00064 | -0.00568 | 0.00568 | -0.01132 | 0.00682 | 0.00682 |
| **2** | -104404 | -58510 | -59115 | -0.00002 | -0.00096 | 0.00095 | -0.00306 | 0.00085 | 0.00084 |
| **3** | -162341 | -112790 | -120213 | 0.00004 | -0.00187 | 0.00172 | -0.00600 | 0.00156 | 0.00132 |

The measured results are better suited when no tensile strength is considered in the numerical model.

The account of the tensile strength in the numerical model has an impact on the reaction forces measured at the interface of the PS. This is due to the different distribution of the strain depending on the tensile strength of the concrete. Different distribution of the strain induces different displacement in the two configurations.

The axial degree of freedom is the most affected by the value of the tensile strength defined in the numerical model. In the Configuration 1, the horizontal displacement induced by the half of the span loads is bigger than in the Configuration 2 (0.00228 m versus 0.00064 m). The difference between the target axial displacement (to be imposed in the furnace) and computed displacement in SAFIR is bigger for the Configuration 1 than in Configuration 2. Therefore, the reaction axial force in the Configuration 1 is bigger than the reaction axial force in the Configuration 2.

To observe this effect, the beam has been modelled in SAFIR when loaded with the corresponding span loads and the interface displacement for the Stage 2 and Stage 3. The interface displacements $u_{right}$, $\theta_{left}$ and $\theta_{right}$ measured during the Test 2 are applied only in the Stage 2 and Stage 3.

The computed reactions in the Configuration 1 (no tensile strength considered) are presented in the Table 6-13 whereas the computed reactions in the Configuration 2 (tensile strength considered) are presented in the Table 6-14.

**Table 6-13. Reaction computed in SAFIR in Configuration 1 (no tensile strength)**

| STAGE | $H$ (N) | $P_{left}$ (N) | $P_{right}$ (N) |
|---|---|---|---|
| **2** | -96960 | -62786 | -62786 |
| **3** | -183600 | -129614 | -127671 |

**Table 6-14. Reaction computed in SAFIR in Configuration 2 (with tensile strength)**

| STAGE | $H$ (N) | $P_{left}$ (N) | $P_{right}$ (N) |
|---|---|---|---|
| **2** | -44220 | -64857 | -64857 |
| **3** | -53510 | -129729 | -127043 |

The differences between the measured reaction forces during the Test 2 and the computed reaction forces in SAFIR (in the Configuration 1 and Configuration 2) are next discussed.

During the stage 2 of the preloading, the measured axial force during the Test 2 is equal to -104404 N. In the SAFIR analysis, in the same stage, the axial force is equal to -96960 N in the configuration 1 (model with no tensile strength) and equal to -44220 N in the configuration 2 (model with tensile strength). The $P_{left}$ force has the following values: -58510 N in the furnace, -62786 N in the configuration 1 and -64857 N in the configuration 2. The force $P_{right}$ has the following values: -59115 N in the furnace, -62786 N in the configuration 1 and -64857 N in the configuration 2.

During the stage 3 of preloading, the measured axial force in the Test 2 is equal to -162341 N. SAFIR analysis, in the same stage, reveals values of the axial force equal to -183600 N in the configuration 1 (model with no tensile strength) and -53510 N in the configuration 2 (model with tensile strength). The $P_{left}$ force has the following values: -112790 N in the furnace, -129614 N in the configuration 1 and -129729 N in the configuration 2. The force $P_{right}$ has the following values: -120213 N in the furnace, -127671 N in the configuration 1 and -127043 N in the configuration 2.

The Configuration 1 (SAFIR model with no tensile strength considered) reveals more appropriate results to the real values measured in the TEST 2. The effect of the tensile strength of the concrete is more visible for the horizontal DoF.

*Discussion about preloading stages*

The concrete tensile strength has a major impact on the behavior of the PS at ambient temperature, as it was discussed here above.

In the global analysis of the structure (the numerical analysis of the entire structure) the tensile concrete strengths does not have such an important impact on the results as when modeling the PS sole at ambient temperature.

The reason why the tensile strength of the concrete at ambient temperature has a bigger impact when modelling the PS sole than when performing the global analysis of the entire structure will be next explained.

- Concrete tensile strength effect in the analysis of the PS at ambient temperature

The following steps are accomplished in the furnace activity before the start of the hybrid fire tests. The PS is prepared and placed in the correct position in the furnace. No loads are acting on the beam excepting the self-weight of the beam. The next step is to start the preloading stage, i.e. the span loads and the initial interface displacements are applied in different stages. In the first stage, half of the span load is applied and the beam is simply supported. In this stage of loading the tensile strength of the concrete might be exceeded. In the Stage 2 the interface initial displacements are applied thus the mid-span bending moment developed in the Stage 1 is redistributed on the supports. In the Stage 3 the total span load is applied and the interface conditions are kept as in the previous stage. Therefore, the preloading of the PS influences the reaction forces developed at the interface and which are next used in the hybrid process. Moreover, before the test, the PS is kept in special conditions for approximately one year. The shrinkage phenomenon is another factor to affect the tensile strength of the concrete.

- Concrete tensile strength effect on the global behavior at ambient temperature

The global numerical analysis at ambient temperature is needed in order to determine the initial interface forces and displacements. In other words, the input data of hybrid fire testing are defined after the global analysis is performed.

For the Test 2, the input data (the initial interface forces and displacements, the tangent stiffness of the PS and NS) have been defined by accounting for the tensile strength of the concrete.

In the global analysis of the structure performed at ambient temperature, the reaction forces at ambient temperature are not so much influenced by the value of tensile strength used in the SAFIR model. The loading of the structure in the global analysis is done in such way that the tensile strength does not have an important impact on the reaction forces at ambient temperature.

In other word, in the global analysis, the PS is loaded with the total span load in one step. The action of the load is redistributed in the mid-span and on the supports. The modeling of the real boundary conditions of the beam reduces the influence of the concrete tensile strength on the results at ambient temperature.

It was explained how the tensile strength of the concrete influences the results at ambient conditions when the PS is loaded in the conditions described in the Test 2 (3 preloading stages) versus the loading in the global analysis.

This explains the differences between the reaction forces measured during the Test 2 and the initial reaction forces defined as the input of the hybrid fire testing. The equilibrium at ambient temperature needs to be restored before the start of the hybrid fire tests.

*Recommendation about preloading stage*

The preloading of the PS during the Test 2 was done in 3 stages, as it was presented.

In order to reproduce the conditions of loading as in the case of global analysis, the following strategy is considered appropriate:

- Place the PS in the furnace;
- Impose the initial displacements at the interface $u_{initial}$;
- Impose the span load $P$;

The mentioned strategy would imply the real boundary conditions before the span loads are applied.

*The equilibrium at ambient temperature*

During the Test 2, the interface reaction forces of the PS were not in equilibrium with the interface reaction forces of the NS at ambient temperature.

Before the start of the hybrid fire test, the equilibrium at ambient conditions must be restored. The restoring of the equilibrium at ambient temperature during the Test 2 revealed unexpected behavior.

This section is committed to understand the behavior observed during the Test 2 when the equilibrium at ambient temperature was about to be restored.

Figure 6-43 to Figure 6-47 show the evolution of forces and interface displacement after the preloading stage and during the restoring process of equilibrium at ambient temperature.

*Observations and actions during the Test 2 when restoring the equilibrium at ambient temperature*

The following observations are done during the TEST 2:

- The support rotations ($\theta_{left}$ and $\theta_{right}$) and the afferent vertical forces ($P_{left}$ and $P_{right}$) experience a behavior which is not expected and understood;
- The changes registered by the horizontal force $H$ and the horizontal displacement $u$ are insignificant;
- The attention during the Test 2 was directed on the behavior of the vertical actuators and inclinometers since important changes were registered during the calculations;
- Another reason to focus the attention on the vertical actuators and inclinometers was due to the problems identified in the preloading stages related these specific DoFs. In the preloading stage, the vertical actuators were not able to impose the target rotations

moreover, the rotations imposed by the vertical jacks were always exceeding the target rotations.

The following actions are done during the Test 2:

- checking of the control software and some modifications which have been done by the person in charge with the control process;
- The modifications which have been done cannot be named now since there was no written list of the modifications during the test. In this way, not all the actions and the time of implementations were recorded;

Recommendations for the future:

- registration of all the modifications done in the control system in order to keep track of the actions and to help in the post-analysis of the test;

*Post-test analysis of Test 2 when restoring equilibrium at ambient temperature*

In the post-test analysis of the Test 2, the following observations can be done about the action of restoring equilibrium at ambient temperature:

- The calculation performed to restore the equilibrium starts at the time 7:27:30;
- Modifications are observed in the evolution of forces/displacements for some DoFs;
- The support rotations ($\theta_{left}$ and $\theta_{right}$) and the vertical force ($P_{left}$ and $P_{right}$) records some changes;
- No changes are observed in the evolution of the horizontal force $H$ and horizontal displacement $u$;
- The changes are registered for 10 min since the starts of the calculations;
- When no changes are registered signifies that the equilibrium has been reached;

The activities performed to restore the equilibrium at ambient conditions are next discussed more in details.

Right before the start of the calculation performed to restore the equilibrium at ambient temperature, the measured displacements in the furnace as the measured reaction forces are presented in the Table 6-15. The measured values are presented in the global system of coordinated GSC.

**Table 6-15. The measured displacements and reaction forces at the starts of the calculations in the GSC**

| **Measured displacement [m, rad]** | | | **Measured reaction force [N, m]** | | |
|---|---|---|---|---|---|
| $u_{right}$ | $\theta_{left}$ | $\theta_{right}$ | $H$ | $M_{left}$ | $M_{right}$ |
| 0,000157 | 0,000210 | -0,000176 | -146763 | 79848 | -83151 |

The first observation concerns the measured values of displacements which are not equal with the initial interface displacements. Figure 6-45 and Figure 6-47 show the measured displacements and rotations in the preloading Stage 3 and during the calculations needed to restore the equilibrium. Before the start of the calculations, the displacements oscillate around the target displacements i.e. the initial interface displacements. The oscillation is due to the resolution of the data acquisition system.

The values presented in the Table 6-15 are used to compute the new interface displacement to be imposed at the interface of the PS and NS substructures. The new computed interface displacements are presented in the Table 6-16.

**Table 6-16. The computed displacements in the first iteration**

| **Computed displacements [m, rad]** | | | | | |
|---|---|---|---|---|---|
| *Expected values* | | | *Values of the Test 2* | | |
| $\boldsymbol{u_{right}}$ | $\boldsymbol{\theta_{left}}$ | $\boldsymbol{\theta_{right}}$ | $\boldsymbol{u_{right}}$ | $\boldsymbol{\theta_{left}}$ | $\boldsymbol{\theta_{right}}$ |
| 0.000313 | 0.000395 | -0.000335 | 0.000156 | 0.000211 | -0.000175 |

The expected values refer to the displacements which results from the calculation process when the measure reaction force and measured displacement are considered. The values computed during the Test 2 are different compared with the expected values and this can be observed from the first iteration.

To restore the equilibrium at ambient temperature, first the out of balance force is computed. To do so, the measured reaction force in the furnace is used along with the computed reaction force of the NS. The computation of the NS's reaction force makes use of the measured displacements in the furnace.

The out of balance force is used in the computation of new incremental displacement vector. Therefore, the new interface displacement to be updated in the furnace is computed based on the incremental displacement vector and the previous interface displacement measured in the furnace.

To compute expected values every iteration time step, the reaction forces along with the measured displacements in the furnace are considered.

The values computed during the Test 2 (see Table 6-16) do not match the expected value due to the fact that the measured displacement in the furnace is neglected in the calculation process. In other words, instead of using the measured displacement in the furnace, the computed displacement in the previous time step is considered.

Since the discussion is done for the first iteration calculations, no previous displacements are computed. Therefore, zero displacement vector is saved in the memory. The effective value of displacements is computed based on the zero displacement vector and not on the measured displacement vector presented in the Table 6-15.

To be more precise, the intuitive procedure to compute and impose displacements during the hybrid fire testing is illustrated by the Figure 6-48. Right at the start of the hybrid procedure at ambient temperature, the measured displacement in the furnace $\boldsymbol{u_0^m}$ is equal to the computed displacement $\boldsymbol{u_0^c}$, i.e. $\boldsymbol{u_0^m = u_0^c = u_{initial}}$. The arrow from the computed value towards the measured displacement suggests that the next step calculation can start once the measured value in the furnace equals the computed value. Once the equality is fulfilled, the measured displacement in the furnace $\boldsymbol{u_0^m}$ is next considered in the calculations to establish the computed value $\boldsymbol{u_2^c}$ of the next step. The reason why the measured value is considered in the calculations is due to the fact than in reality, the measured value $\boldsymbol{u_i^m}$ will not be exactly equal to the computed value $\boldsymbol{u_i^c}$, i.e. $\boldsymbol{u_i^m \neq u_i^c}$. The difference occurs due to the limitations and challenges of the data acquisition system during the test. Nevertheless, the difference between the two values should be as small as possible in order to reproduce valuable results during the hybrid process.

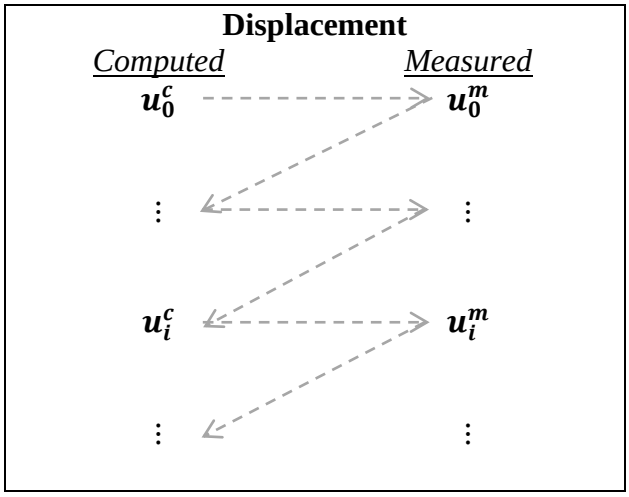


**Figure 6-48. The intuitive procedure to compute and impose displacement**

The considered procedure to compute displacements during Test 2 is presented in Figure **6-49**. Right at the beginning of the hybrid fire tests, the computed displacement i.e. the initial interface displacement, is imposed on the PS, therefore the measured displacement $u_0^m$ is equal to computed displacement $u_0^c$. For the calculation of the new displacements $u_1^c$, the measured displacements $u_0^m$ is neglected and the previous computed displacement $u_0^c$ is considered. The arrow from the computed displacement $u_i^c$ towards the measured displacements $u_i^m$ suggests that the computed displacement is imposed in the furnace. At the same time for the calculation of the new solution $u_{i+1}^c$ only the previous computed solution $u_i^c$ is accounted for.

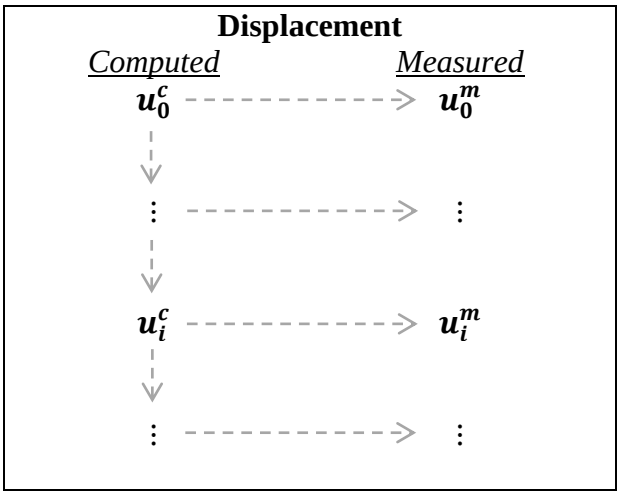


**Figure 6-49. The considered procedure to computed displacements during Test 2**

The computed value by the algorithm during the Test 2 should be equal with the measured values in the furnace.

The measured versus computed interface displacements are presented in the Figure 6-50. The same figure presents the measured reaction forces of the PS versus the reaction forces of the PS used in the calculations process.

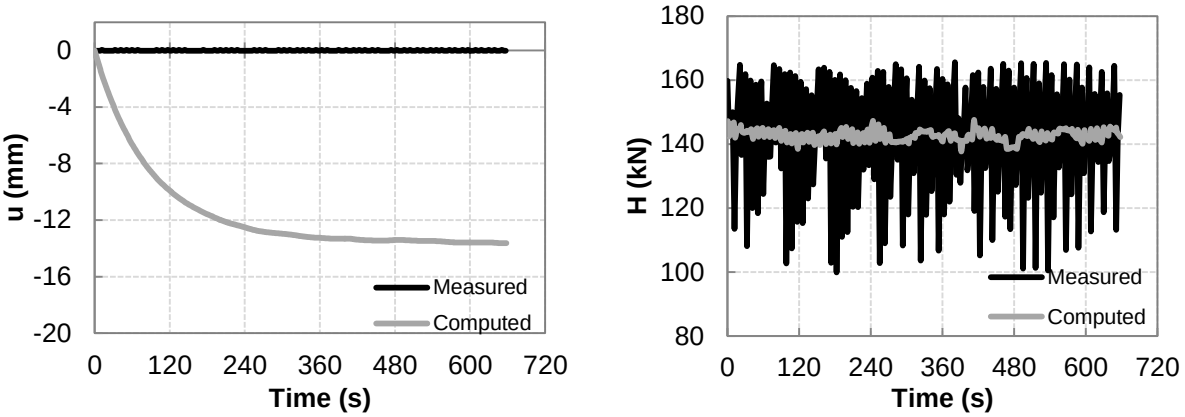


*a) Axial DoF*

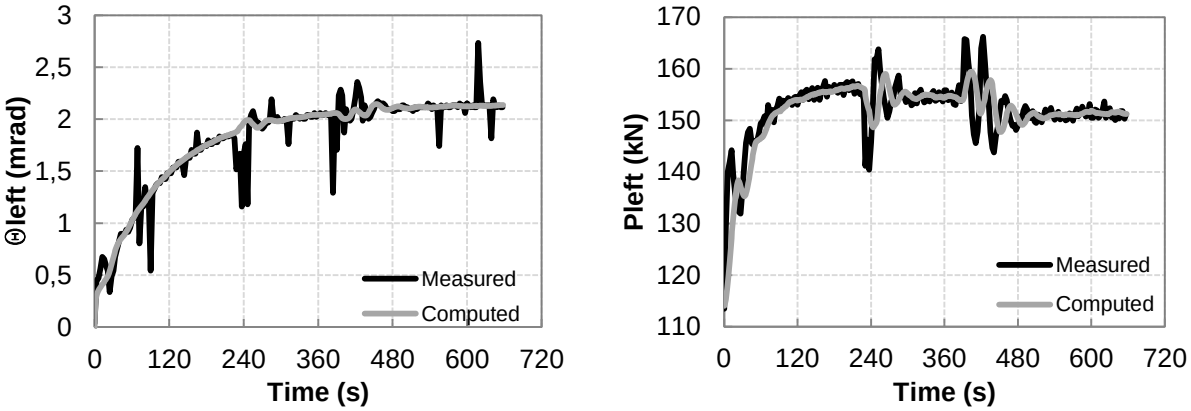


*b) Rotational DoF – hinged support*

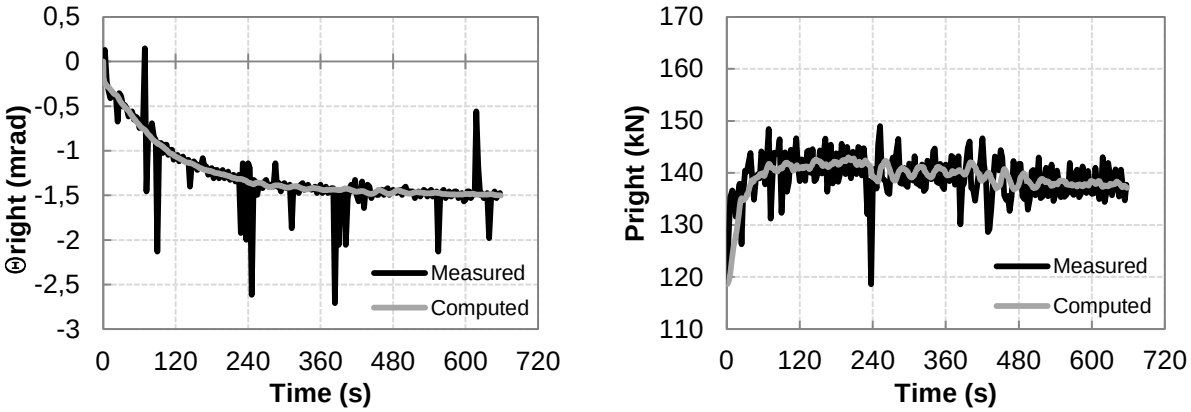


*c) Rotational DoF – rolling support*

**Figure 6-50. Restoring of the equilibrium at ambient temperature. Measured versus computed values of the PS**

The first observation is done related the reaction forces which are measured in the furnace. It is evident that the measured reaction forces plots contain spikes. These occur when the actuator changes directions. The direction changes when the value to be imposed cannot be registered by the transducers and inclinometers.

To smooth the plot of the measured reaction forces, a new plot is presented where the current value of the reaction force is computed based on the mean of the previous 10 values. The computed reaction forces do not only smooth the measured values but also delays the measured effects. In the calculation process of restoring the equilibrium at ambient temperature the computed reaction forces are used to calculate the new interface displacements.

Based on the computed reaction forces, the computed displacements are plotted versus the measured displacements in the furnace. If the measured support rotations follow the computed displacement (the imposed displacement) not the same conclusion can be done regarding the axial DoF. It is obvious from the Figure 6-50 a) that the measured horizontal displacement in the furnace remains constant and does not follow the computed displacement (imposed displacement).

The horizontal actuator did not impose the target displacements (computed displacements) in the furnace. The impossibility to impose the target displacements appears only when the equilibrium at ambient temperature starts to be searched. In the preloading stage, the horizontal actuator along with the vertical actuators is capable to impose the target values.

Nevertheless, we observe that the calculation stopped after 10 min which is a sign that the equilibrium is reached. This is possible to achieve due to the fact that in every step calculation, the measured value in the furnace is neglected. All the calculations are done based on the computed values of displacements in the previous step. The reaction forces were still registered from the furnace. Therefore, it is assumed that the computed values are reached in the furnace even if in reality the computed axial displacement is not reached.

In conclusion, two main observations are done about the activity of restoring equilibrium at ambient temperature:

- The measured displacement in the furnace is neglected in the computation process;
- The actuator to control the axial displacement does not impose the target values;

Despite the identified defaults, the procedure looks promising when the future adjustments will be done to correct the mentioned drawbacks.

*The resolution of the data acquisition system*

The resolution of the data acquisition system influences the results of the hybrid fire test

The computed displacement $\boldsymbol{u_i^c}$ characteristic to the time step $\boldsymbol{i}$ represents the displacements to be imposed in the furnace. If the computed displacement is not multiple of the data acquisition system resolution, then the measured displacement in the furnace $\boldsymbol{u_i^m}$ does not coincide with the computed displacement $\boldsymbol{u_i^c}$.

The effect of the resolution of the data acquisition system will be next studied in the two configurations mentioned above. One of the configurations refers to the case when the measured displacement is accounted in the calculations whereas the other configuration refers to the case when the measured displacement in the furnace is neglected.

*The effect of measured/computed displacement on the results, in the virtual HFT*

Figure 6-48 presents the every time step results for the case when the intuitive procedure is considered. The update of interface displacements needs to account for the value of displacements measured on the PS in the real hybrid fire test.

Figure 6-49 presents the results for the case when the procedure during the Test 2 is considered. In this specific case, the real displacement measured on the PS is neglected. The calculations are done based on the previous computed displacements.

The virtual hybrid fire tests are performed considering the time step equal to 1 s and the initial tangent stiffness of the PS is overestimated with a factor of 1.50.

- The account of the measured displacements in the calculations

Figure 6-51 presents the evolution of the interface forces and displacements in the case when the measured displacements in the furnace are accounted in the calculations of the next step solution.

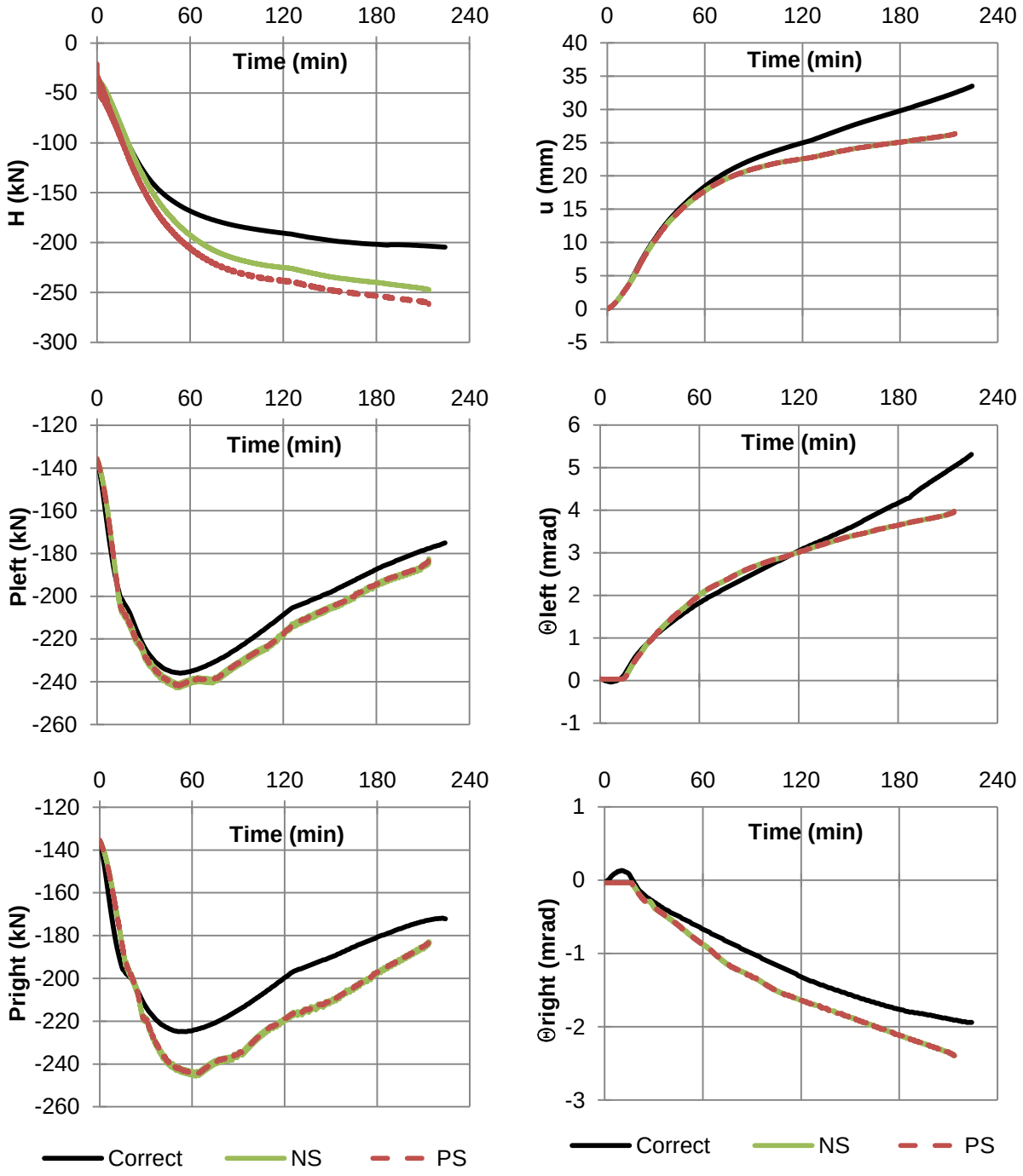


**Figure 6-51. The boundary conditions when the measured displacements are considered in the calculation process**

For the axial DoF, the equilibrium is not ensured, whereas for the rotational DoFs the equilibrium is satisfied. The slightly divergence from the correct solution is due to the simplifications used in the modeling of the NS (constant matrix).

The resolution of the transducers in this example is set equal to 0.039 mm while for the inclinometers is equal to 0.018 mrad, based on the characteristics of the data acquisition system available in CERIB.

To observe the influence of the resolution, the evolution of the axial force and axial displacements is next presented for the first minutes of the analysis.

Figure 6-52 presents the evolution of the axial force and axial displacement in different stages of the hybrid fire test, i.e. the first 2 min of the analysis, between the 6$^{th}$ and 8$^{th}$ min and between 150$^{th}$ and 152$^{nd}$ min.

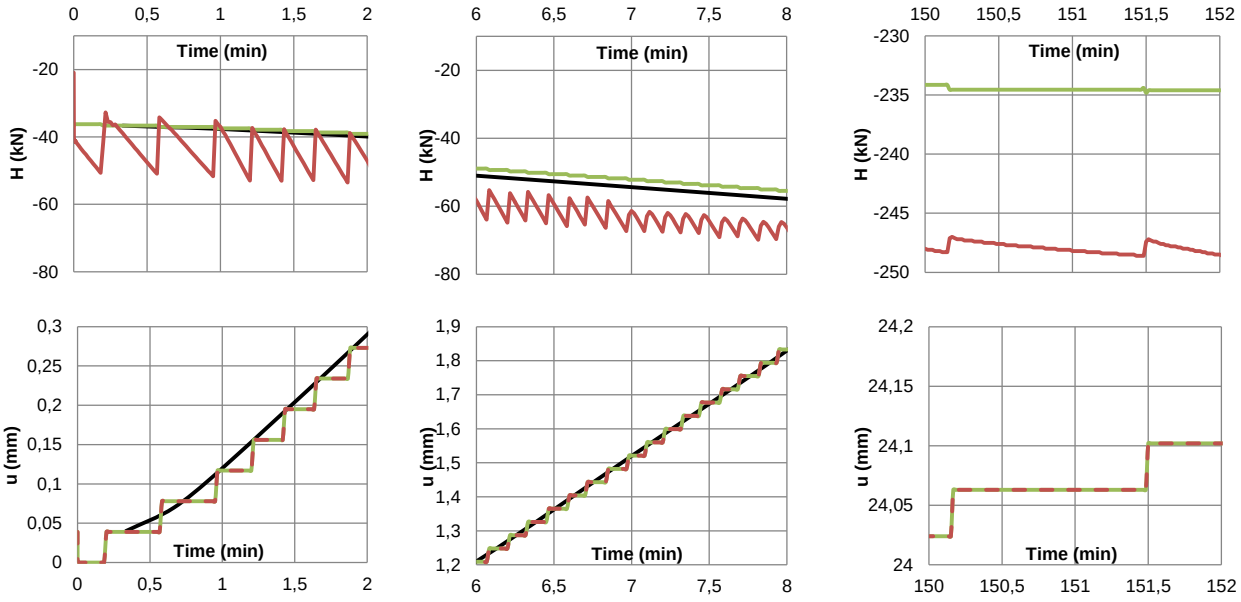


**Figure 6-52. The influence of the resolution on the axial DoF in different stages of the test (the measured displacement considered in the calculations)**

The resolution of the transducer induces spikes in the reaction force. The spikes are more pronounced in the early stage of the hybrid fire testing. The reaction force of the PS does not equal the reaction force of the NS, therefore no equilibrium is satisfied. The cause is the impossibility to reach the equilibrium at ambient temperature. The displacement which can ensure the equilibrium at the ambient temperature cannot be measured by the transducers. Therefore, the value measured by the transducer induces a reaction force of the PS which is not in equilibrium with the reaction force of the NS.

The fire starts even if the equilibrium at ambient temperature is not reached and is the main cause why during the test the equilibrium is not ensured for the axial DoF. For the ambient temperature, 20 kN variation in reaction force is induced by the resolution of 0.039 mm which confirms the observations during the test. Once the fire is turned on (the start of the hybrid fire test) in between two steps, the measured value of axial displacement is constant, while the

reaction force increases due to the fire exposure. The increase of the reaction force is more important at the beginning of the test compared with the final stage of the test. This is due to the decrease of the PS's stiffness once the exposure advances. This phenomenon can be observed in the mentioned figure, for different stages of the hybrid fire test. Therefore, the spikes in the reaction forces are more pronounce in the early stage of the hybrid fire test. In time, the spikes are not anymore obvious.

Since the inclinometers used to measure the support rotations are more precise, i.e. 0.018 mrad, the spikes for the vertical forces acting on the cantilever are not so obvious.

- The computed displacements used in the calculations

Figure 6-53 presents the evolution of the interface displacements and forces when in the calculation process the measured displacement is neglected. The displacements applied in the furnace account for the resolution of the data acquisition system. In this case the equilibrium is ensured for every DoF. The plot of the axial reaction force shows spikes in the first stage of the hybrid fire test. For the rotational DoFs the spikes are negligible due to a better resolution of the inclinometers.

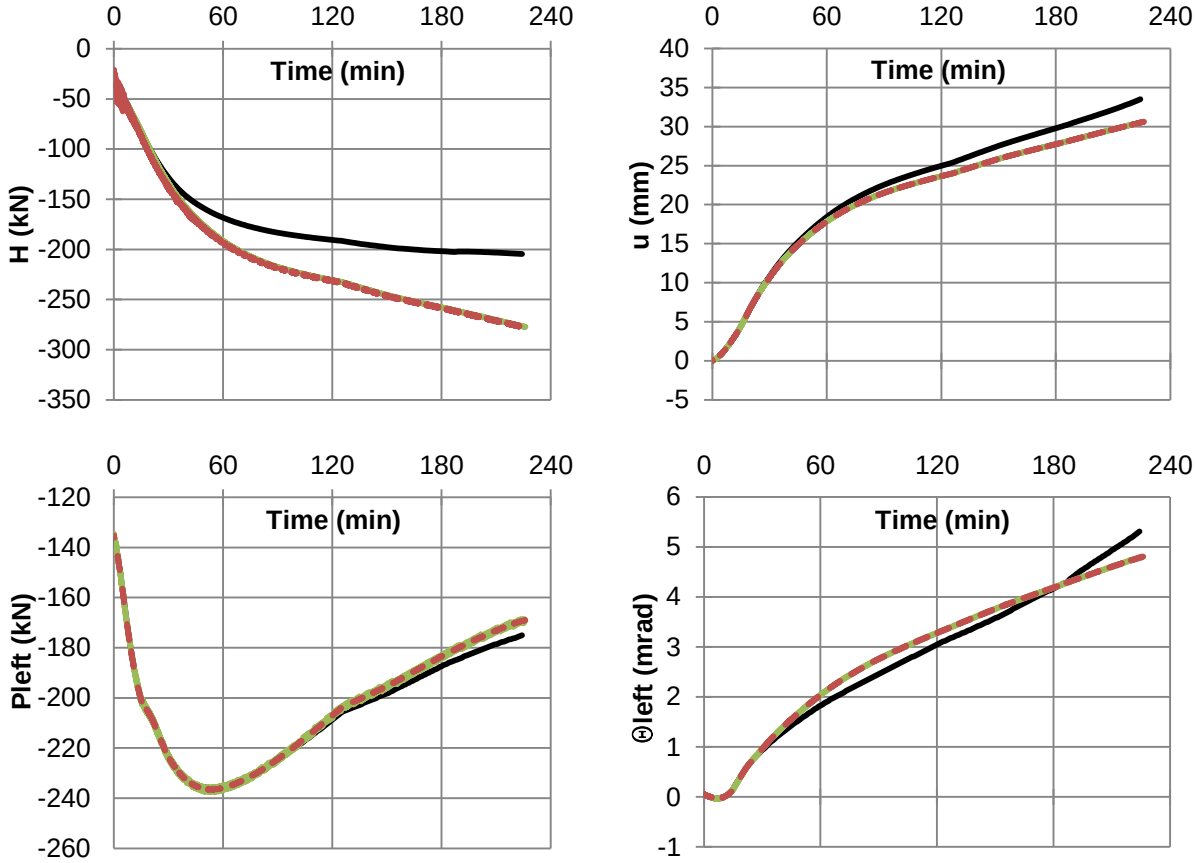

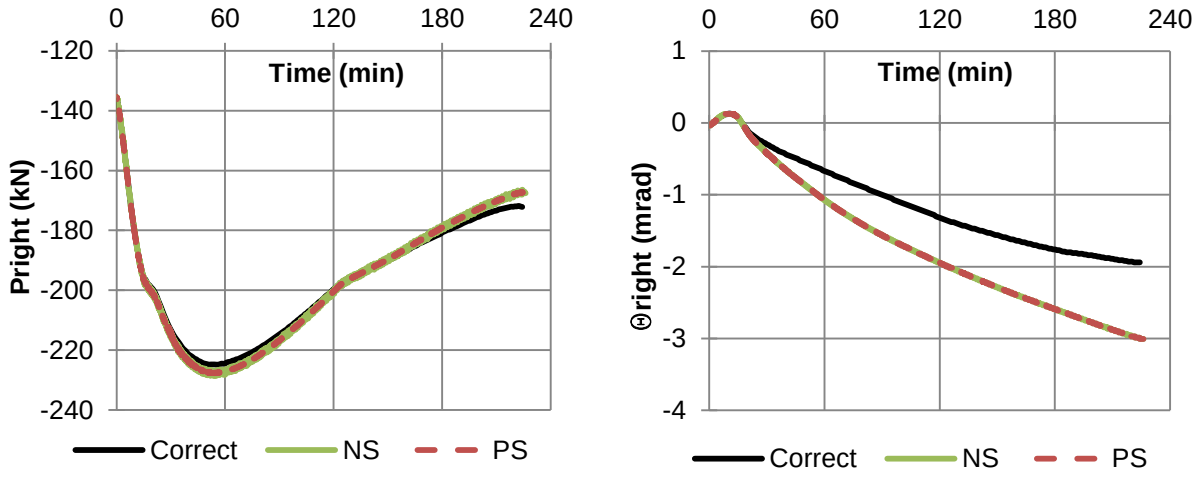


**Figure 6-53. The boundary conditions when the measured displacements are neglected in the calculation process**

Figure 6-54 presents the evolution of axial force and axial displacement for different stages of the test. The zoom aims the first 2 min of the test, followed by the period between 6$^{th}$ and 8$^{th}$ min and one close to the final stage of the test, between 150$^{th}$ and 152$^{nd}$ min.

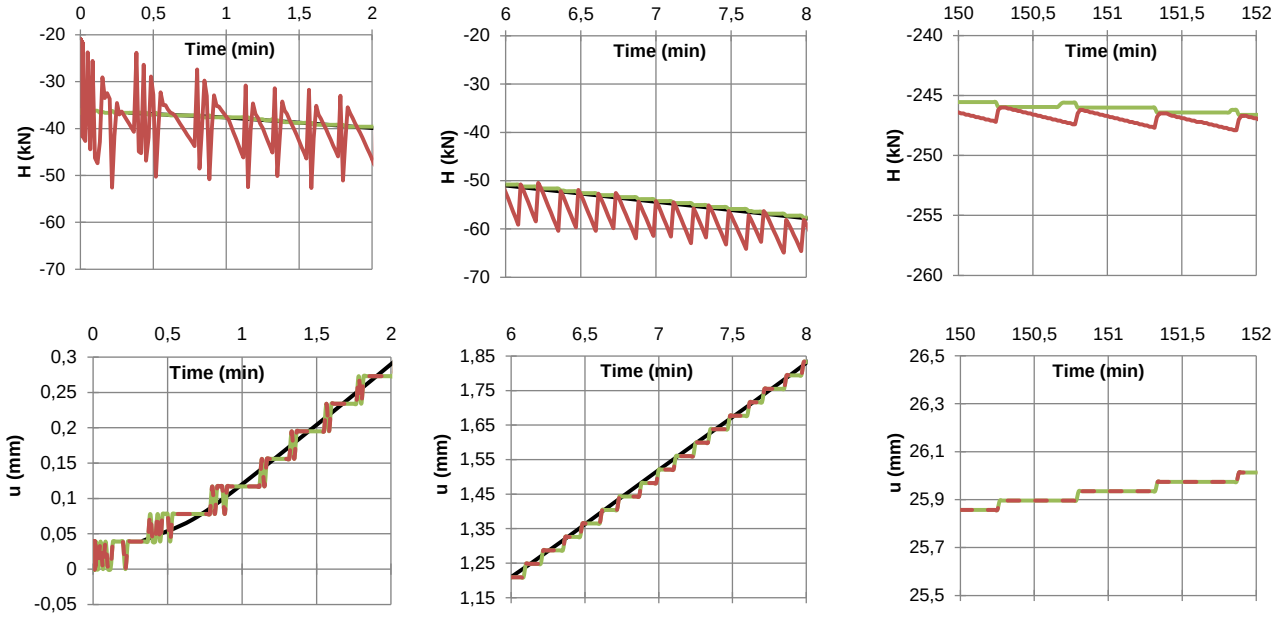


**Figure 6-54. The influence of the resolution on the axial DoF in different stages of the test (the measured displacement in the furnace is neglected)**

For the update of the boundary conditions, the real values of displacements measured in the furnace are neglected. It means that the computed value in the previous step is considered in the computation for the current time step. This is the reason why more spikes are registered in this configuration compared with the configuration when the measured displacements are accounted in the calculations.

When the measured displacements are accounted for the calculations, the displacement is constant for a certain time until the fire action increases and induces a displacement which can

be registered in the furnace by the data acquisition system. Since the displacement is constant, the reaction of the NS is constant while the reaction of the PS modifies due to the fire exposure.

When the computed displacement is used in the calculations, it means that every time step the reaction of the NS modifies along with the computed displacements. The fire induces modifications in the PS's reaction force. When the reaction of the NS and PS modifies every time step, despite the measured displacement in the furnace is constant, the evolution of displacements and reaction forces differs compared with the previous case, i.e. the reaction of the PS modifies due to the fire exposure while the reaction of the NS is constant once the displacement in the furnace is constant.

Next the comparison between different solutions is discussed.

Figure 6-11 presents the evolution of the interface displacements and forces in the virtual environment, i.e. the resolution of the data acquisition is infinite. In this case, the every time step computed displacement is assumed to be applied in the furnace, with other words, the computed displacements is equal with the measured displacement.

Figure 6-51 presents the evolution of the interface displacements and forces when the resolution of the data acquisition system is accounted for. Besides that, for the computation of every new solution, the measured displacement in the furnace is accounted in the process.

Figure 6-53 presents the evolution of the interface displacements and forces when the resolution of the data acquisition system is considered. The computation of the new solutions to be imposed on the substructures is done neglecting the measured displacement in the furnace, with other words, the computed displacement in the previous time step is considered.

The solution presented in the Figure 6-53 presents some variation of force (spikes) during the proces, due to the resolution of the data acquisition system. Beside the mentioned aspect, the solution generated in this case is reproducing very well the solution presented in the Figure 6-11. The two solutions are almost identic due to the fact that in the calculation process of the solution presented in the Figure 6-53 the measured values in the furnace are neglected.

The solution presented in the Figure 6-51 is different compared with the solution presented in the Figure 6-11. More than that, the spikes in the reading of the reaction force are present since the effect of the resolution is accounted. The differences between the two solutions are due to the effect of the resolution and due to the fact that the measured displacement in the furnace is considered in the calculations process.

Therefore, it has been observed that the characteristics of the furnace facility, e.g. the resolution of the data acquisition system, lead to solutions which are different compared with the solution in the virtual environment when the effect of the resolution is neglected.

*Conclusions related the effect of the resolution and the effect of the measured/computed displacement on the results*

The following conclusions can be done:

- The resolution of the data acquisition system influences the results of the hybrid fire tests as proved in the previous exercise performed in the virtual environment;
- No sensitive analysis has been done to observe the influence of the time step, the stiffness of the PS and different resolutions on the results;
- The previous exercise shows that the results of the hybrid fire testing are more accurate when the measured displacement in the furnace is neglected in the calculations;
- Neglecting the measured displacement in the hybrid fire calculations show better results for the selected resolution of the transducers and inclinometers, for the time step selected and for the stiffness of the PS;
- For different examples, the observations underlined in the previous example might not be applicable.

The following recommendations are underlined:

- More detailed analysis is needed in order to observe the effect of the resolution on the results and the effect of the measured displacement versus the computed displacement.

### 6.7.4.5. Summary of the Test 2

The Test 2 helped identifying problems in the control process and at the same time helped improving the configuration of the tests.

The lessons learned during the Test 2 are the following:

- The system used to measure the horizontal displacement is too flexible;
- The resolution of the data acquisition system has an important impact on the results;
- The control system needs to be developed properly for successful hybrid fire tests. Many errors have been identified in the control system when trying to perform the Test 2;
- The expected axial forces during the hybrid fire tests represent less than 50% of the total capacity of the horizontal jack;

Because of the problems identified on the day of the test after the preloading stage, it was decided that it would not be safe, for the specimen, for the testing equipment and, possibly, for the personal, to start the real fire test, i.e. starting increasing the temperature in the furnace. It was decided to allow some month for analyzing and fixing the errors in the control system, to improve the displacement measuring system and to verify the theoretical procedure that had been developed.

## 6.8. Test 3

### 6.8.1. Motivation and Description

The objective of the TEST 3 is to repeat the TEST 2 but at the same time to improve some aspects in order to be able to produce better results. Thus, the TEST 3 represents somehow the continuation of the TEST 2.

The position of the jacks is kept the same as in the configuration of the Test 2. Moreover, the same beam which has been used for the TEST 2 is reused for the TEST 3. The solicitations during the TEST 2 did not induce plastic behavior and no cracks have been observed. The area of the beam in the contact with the horizontal jacks is slightly damage (falling of the concrete in some parts). Even like that the beam is considered proper to perform a new test, i.e. TEST 3.

### 6.8.2. The testing equipment

- **Transducers and inclinometers**

The same type of transducers and inclinometers are used in the TEST 3 as in the TEST 2.

It has been discussed that the oscillation of the force is directly affected by the step resolution of the transducers and inclinometers. The resolution of inclinometers is concluded to be appropriate since the force oscillation in the jacks controlling the rotations is not significant.
The oscillation of force in the horizontal jack is significant and is induced by the resolution of the transducers. The section 6.7.2 presents the effect of the resolution, i.e. 0.039 mm, on the measured horizontal forces. The same effect is observed during the TEST 2.

Even though a better resolution of transducers would reduce the oscillation of forces, in the end the decision is to continue the TEST 3 with the same type of the data acquisition system. The pro argument weights more than the argument against. Table 6-17 presents the mentioned arguments.

**Table 6-17. The arguments to decide the type of the transducers in the TEST 3**

| *Arguments against* | *Pro arguments* |
|---|---|
| • The resolution of the transducers, i.e. *0.039 mm* and *0.625 mm*, induces important oscillation of the axial force. | • The induced noise once the burners are turned on cancel the positive contribution of the transducers with a better resolution. |

- **The configuration of the measurements**

The same displacements and rotations are measured during the TEST 3 as in the TEST 2. The difference in the TEST 3 consists in a new system to help measuring the horizontal displacements of the supports.

The new system is presented in the Figure 6-55 and serves to attach the transducers and to attach a wheel which helps redirecting the direction of the transducer's cable. The system is stiff and does not affect the displacements. The wheel is stiff but at the same time permits the rotation needed when the cable of the transducer shortens or elongates.

The place where the horizontal displacement is measured did not change. Only the system needed to make possible the measurement changed.

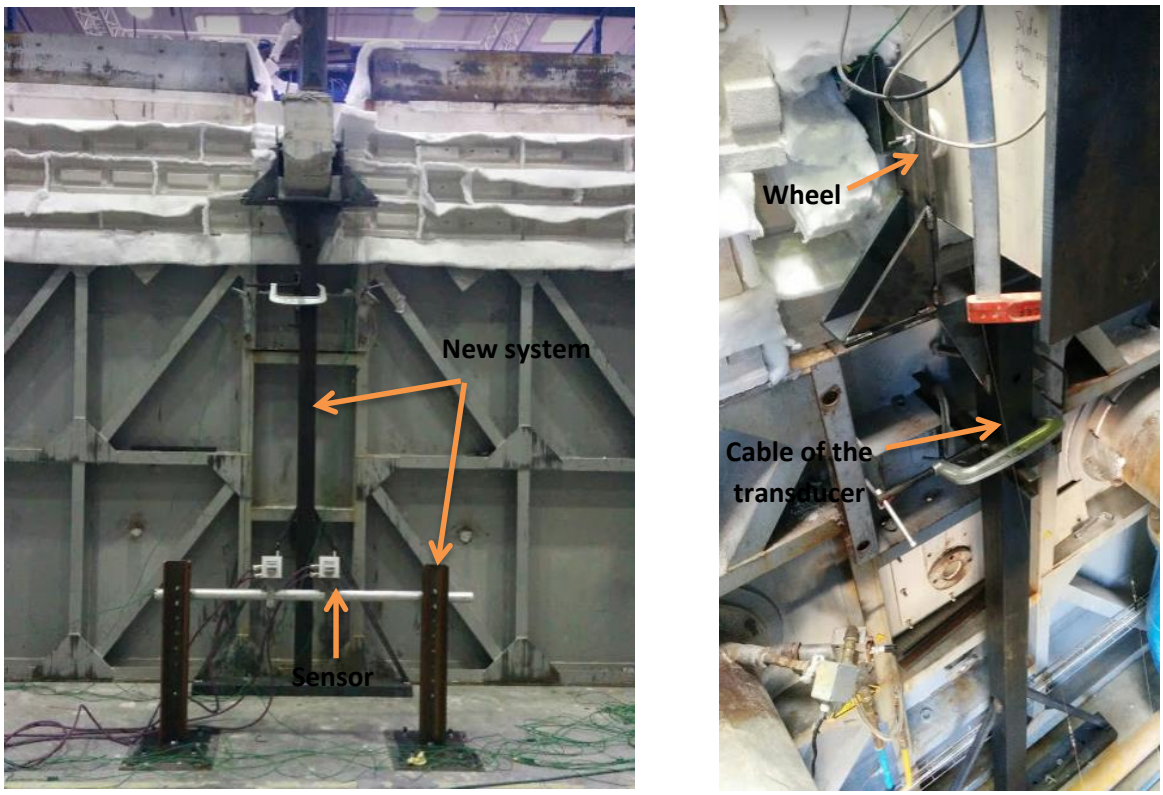


**Figure 6-55. The new system to measure the horizontal displacement in the TEST 3**

- **The actuators**

The section 6.7.2 describes the available equipment in the CERIB fire facility.

The actuators have been analyzed in the same sections and some observations are done.

One of the observations refers to the effect of the hydraulic friction joints. The hydraulic friction joints induce errors in the reaction force when the direction of the actuator is changed. Thus, jacks with mechanical friction joints are recommended in hybrid fire tests.

Changes or replacements of some parts of the fire testing facility are not economical and intermediate solutions can be adopted in order to improve the final results.

To cancel the negative effect of the hydraulic joints, the loads cell is placed on the horizontal jack (see Figure 6-56).

In order to be able to use the readings of the load cell in the hybrid algorithm, modifications of the control process are required. The modifications were not done for the Test 3 but the

load cell is still placed on the horizontal jack. A comparison of the values used in the calculations with the one measured by the load cell is planned to be done at the end of the test. The loads cell did not register the measured forces at ambient temperature (it was not turned on) and it was due to be turned on once with the start of fire.

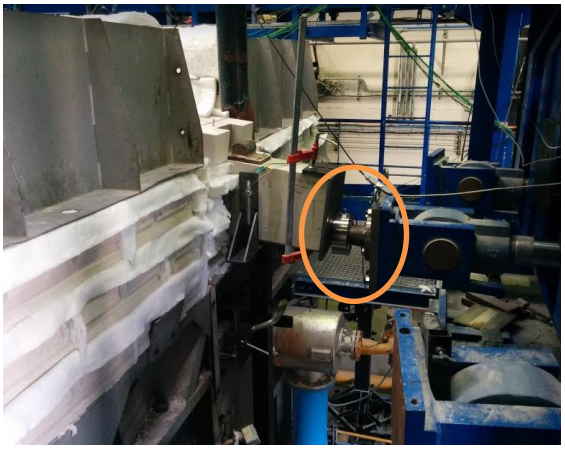

**Figure 6-56. The load cell placed on the horizontal jack**

### 6.8.3. Test Setup and Procedure

*Beam preparation/ Furnace preparation/ Instrumentation layout*

Since TEST 3 is a continuation of the TEST 2, the beam preparation, the furnace preparation along with the instrumentation layout are repeated for the TEST 3.

### 6.8.4. Solution proposed to increase the axial force

The expected axial force to be induced in the beam represents less than 50% of the capacity of the horizontal jack.

Thus, the jack operates with the inferior capacity. The errors induced in the reading process are significantly higher if the actuators are not used at the full capacity.

A new structural system is proposed for the TEST 3 (see Figure 6-57).

The modifications in the TEST 3 are the following:

- The arc is introduced in the span number three to increase the axial force in the tested beam;
- The loads acting on the arch are doubled compared with the loads acting on the roof beams. The curved part of the roof serves to develop a plantation, therefore the loads are doubled;
- The analyzed structure is considered to be built besides a stiff building. The stiff building represents a bracing system for the analyzed structure, so no horizontal displacements in the left sight of the building are allowed.

The other characteristics are kept as in the configuration proposed for the TEST 1 and TEST 2.

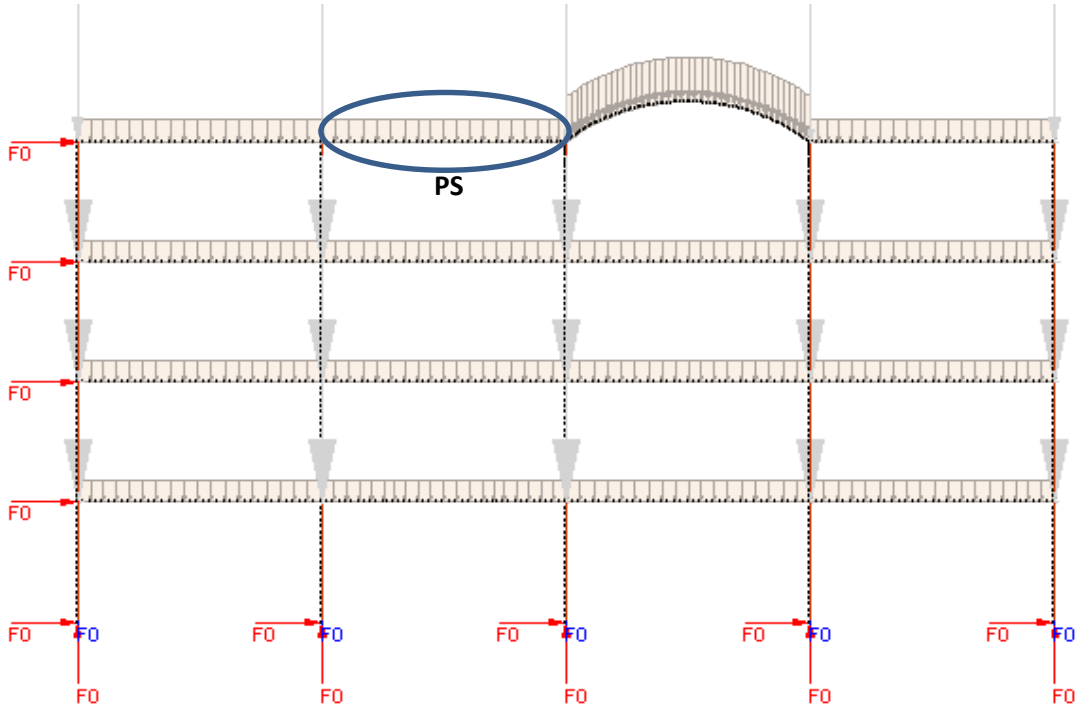


**Figure 6-57. The structural system proposed for the TEST 3.**

## 6.8.5. Test Results and Interpretation

### 6.8.5.1. The input data of the algorithm

Since the configuration of the analyzed structure changed, some of the input data of the algorithm modify i.e. the stiffness of the NS and the initial forces and displacements at ambient temperature.

Before the TEST 2, the compressive strength of the concrete is determined based on the measured values at 7 days, 28 days and during the TEST 1. Therefore, a value of 48 MPa concrete compression strength is assumed for the TEST 2. The compressive tests of samples, performed in the day of the TEST 2, showed a compressive strength of 40 MPa.

All the preliminary analysis made for the TEST 3 are done with a concrete compressive strength of 40 MPa.

The stiffness of the PS is defined for the characteristic compression strength of 48 MPa.

Next are presented all the input values which have been changed during the TEST 3.

*The stiffness of the NS*

The predetermined matrix used for the TEST 3 is presented by the Eq. (98). The compressive strength of the concrete is considered equal to 40 MPa.

$$K_N = 10^6 \begin{bmatrix} 20.10 & -2.76 & 17.60 \\ -2.76 & 86.30 & -1.63 \\ 17.60 & -1.63 & 89.40 \end{bmatrix} \quad (98)$$

*The vector of interface forces of the NS at ambient temperature*

Equation (99) presents the interface forces of the NS at ambient temperature for the TEST 3.

$$F_{N,initial} = \begin{bmatrix} 71\,750 \\ -97\,633 \\ 96\,309 \end{bmatrix} \quad (99)$$

The increase of the axial force at the ambient temperature can be observed in the configuration of the TEST 3 compared with the configuration of the Test 2 (71 750 N versus 36 650 N). For comparison, see Eq. (99) and Eq.(90).

*The vector of interface displacements at ambient temperature*

The vector of interface displacements at ambient temperature is presented by the Eq.(100).

$$u_{initial} = \begin{bmatrix} -0.00004 \\ 0.00016 \\ -0.00023 \end{bmatrix} \quad (100)$$

All the other input values are equal with the one defined for the Test 2.

### 6.8.5.2. Preloading stage

*Plan*

Some recommendations are presented in section 6.7 on how to apply the loads on the PS. During the Test 3 these recommendations are not used since they have been derived at a later stage.

The summary of the span loads and interface displacements applied on the PS is presented in Table 6-18 in the global system of coordinates.

**Table 6-18. Loading of the PS in the TEST 3**

| STAGE | $P$ (N) | $u$ (m) | $\theta_{left}$ (rad) | $\theta_{right}$ (rad) |
|---|---|---|---|---|
| **1** | 18 482 x 4 = 73 928 | Not applied | Not applied | Not applied |
| **2** | 18 482 x 4 = 73 928 | -0.00004 | 0.00016 | -0.00023 |
| **3** | 36 964 x 4 = 147 856 | -0.00004 | 0.00016 | -0.00023 |

*Observations made during the preloading stages in the Test 3*

In the first stage of preloading only half of the span load is applied on the beam. The developed displacements are measured and compared with the one computed in the SAFIR model. It was observed that the measured values are comparable with the computed values.
The stage 2 of preloading is ready to start. During this activity, the interface initial displacements should be applied. It was yet quickly observed that the jacks were not able to impose the target displacements prescribed by the developed theory, revealing that the corrections made by the person in charge of the control process have not been successful. Some aspects of the control process that had been solved at the end of Test 2 (the jacks were able to impose the target displacements in the preloading stage) revealed to be unstable again, whereas, according to the person in charge, no modification should have been made on these aspects.
The beam was thus unloaded in order to save it from destruction and allow some time for analyzing the problem.
When the beam was unloaded to search the reasons why the preloading process is not possible, the person in charge with the control process was distracted by a question from a technician who entered in the control room. Because of the distraction, the automatic loading of the beam was unwillingly and inadvertently activated. This implied the increase of the horizontal force along with the increase of the vertical forces acting on the cantilever part of the beam. The negative bending in the span combined with a big compression force created a solicitation for which the specimen had not been designed and this caused the sudden failure at mid span, with the jacks loading the span loosing support and being expelled violently. Figure 6-58 presents some pictures of the beam after failure

**Figure 6-58. The failure mode of the beam in the TEST 3**

*Conclusions of the Test 3*

During the Test 3 the specimen was destroyed before being able to reproduce at least the activities from the Test 2.

In these conditions the proposed algorithm for hybrid fire testing could not be tested experimentally.

## 6.9. Summary

The chapter 6 presents the implementation of the proposed hybrid fire testing methodology on a case study. The case study refers to a moment resisting frame where the PS is represented by the roof beam. The detailed description of the case study is presented along with the procedure to define the predetermined matrix of the NS.

The configuration of the tests is next presented for the traditional test and for the hybrid tests.

Before performing the hybrid fire test, a detailed analysis is done in the virtual environment. The analysis in the virtual environment was possible due to the developments implemented in SAFIR.

First, the first generation method is analyzed in the virtual environment showing that the instability occurs at the beginning of the fire test.

The new method showed good results in displacement control procedure and no instability occurred. Sensitive analysis was performed in order to select the proper value of the time step and the stiffness of the PS. The displacement control procedure is selected to be implemented in the real hybrid fire test.

The new method was implemented in SAFIR also for the force control procedure. The virtual hybrid fire tests performed in force control procedure showed some limitations in the moment when the behavior of the PS registered some changes. No sensitive analysis was performed for the case when the force control procedure is applied. Not much attention was payed to force control procedure and more research is needed to make some final conclusions.

The real hybrid fire test is ready to be performed in CERIB furnace facility.

The first performed test, i.e. Test 1, was a traditional test made in the purpose to compare the results of the standard test with the one of hybrid fire test. The results of the Test 1 showed good agreement with the SAFIR predictions.

The Test 2 was designed to be a hybrid fire test. Before starting the test, the available equipment is analyzed in details and the resolution of the data acquisition system is observed to have an impact on the reaction forces. The following steps need to be fulfilled when performing the test (i) the preloading of the beam, (ii) the restoring of the equilibrium at ambient conditions and (iii) the hybrid fire test itself. Only the first two steps have been successful when performing the Test 2. Different errors of the control process have been identified while performing the first two steps. Some of them have been corrected during the

preloading stage. When performing the equilibrium at ambient temperature, the horizontal jack was not capable to induce the target displacements and the measured displacements in the furnace have been neglected in the calculation process. These facts have been concluded in the post-analysis of the Test 2. Since the equilibrium at ambient temperature induced unexpected behavior, the Test 2 was called out in order to understand the causes.

The following test, Test 3, was a continuation of the Test 2 in the conditions that some improvements are implemented, first, in the control process. Also, the configuration of the tests is modified in order to generate bigger axial force than in the previous case. The system considered to measure the horizontal displacements is modified, in order to ensure a better environment for the measurement of the horizontal displacements. During the Test 3 the same steps as in the Test 2 should be followed: (i) the preloading of the beam, (ii) the restoring of the equilibrium at ambient conditions and (iii) the hybrid fire test itself. In the preloading stage of the PS, unexpected behavior of the control system occurred. While reflecting on the possible reasons of the errors, the person in charge with the control process get distracted and inadvertently activated the automatic loading of the PS which led to destruction of the PS.

In the mentioned conditions, no hybrid fire test was performed. The proposed algorithm for hybrid fire testing was not checked experimentally since from the first actions of the test (preloading stages and restoring of the equilibrium at ambient temperature) many errors of the control process have been identified.

# 7. GENERAL CONCLUSIONS

## 7.1. Summary

The hybrid fire methodology considered in the full scale hybrid fire tests is analyzed in the first part of the thesis. The "first generation method" of hybrid fire testing refers to the methodology considered in the former hybrid test performed on full scale structural elements. It is shown that the applicability of the first generation method depends on the stiffness ratio between the NS (the part of the structure modeled aside) and PS (the part of the structure tested in the furnace). For a stiffness ratio bigger than one, i.e. the NS is stiffer than the PS, the displacement control procedure is requested to be applied during the test in order to avoid the instability of the process early in the tests. A force control is applied when the stiffness ratio is smaller than one, i.e. the PS is stiffer than the NS. The stiffness ratio between the substructures varies during the tests due to the fire exposure. The force control procedure or a displacement control procedure is selected to be applied based on the stiffness ratio values. The modification of the stiffness ratio is not easy to be predicted before the hybrid test, moreover in the condition that some specific phenomenon such as spalling can occur. Therefore, is not easy and safe to select the procedure to be used during the hybrid fire test in order to avoid the early instability during the tests. The possibility to switch from one procedure to another during the tests or to use mixed force/displacement control procedure has its own limitations. To be able to switch from one procedure to another first the perfect time needs to be selected in order to be successful. Moreover, the facility where the hybrid fire test is performed needs to give the possibility to work in force and displacement control, depending on the structural case proposed for analysis. To be able to apply the displacement control procedure and the force control procedure in the same facility introduces complex tuning activities. Even if from theoretical point of view the first generation method is applicable in different cases when the force and displacement control procedures are mixed, from experimental point of view is challenging.

Every time step when the boundary conditions of the substructures are updated, the stiffness of the PS is neglected in the calculations process. The only use of the NS's stiffness causes the dependency of the first generation method on the stiffness ratio between the substructures. The first generation method is exemplified on a simple elastic truss system. The exercise helps underlining the characteristics of the first generation method, such as the advantages and the drawbacks.

The new methodology considers the stiffness of the PS along with the stiffness of the NS in the update process of the new boundary conditions during the test. Therefore the new methodology is stable independently on the stiffness ratio between the substructures. The new method is implemented in displacement control procedure in order to be able to capture the failure of the specimen. Since the update of the PS's stiffness during the hybrid test is not

done, the initial tangent stiffness of the PS is used in the calculations. Therefore the selection of the time step to update the boundary conditions of the substructure is important in order to achieve equilibrium and compatibility at the interface. Moreover, it is important to establish the correct value of the initial tangent stiffness of the PS in order to ensure stability and accurate results. The values of the time step as well as the value of the initial tangent stiffness matrix are chosen based on the type of analyzed structure. The influence of the time step and the initial tangent stiffness on the results is observed when the new method is applied for the case of the simple truss system.

The new method is implemented in Promethee furnace facility and a concrete beam is planned to be tested by means of hybrid fire testing. The rest of the structure is represented by means of a constant predetermined matrix. The tested beam is part of the moment resisting concrete frame. The "virtual" hybrid fire test is performed prior the real hybrid fire test in SAFIR. A new subroutine is developed in SAFIR which gives the possibility to run virtual hybrid fire tests. The scope of the "virtual" hybrid fire tests is to predict the behavior of the PS during the test and to help choosing the correct value of the time step and initial tangent stiffness matrix.

The beam is first tested as a singular component, with no interaction with the rest of the structure. Such test is a traditional test performed in most of the cases. The results are planned to be compared with the results of the hybrid fire tests.

The first hybrid fire test is prepared and planned to be performed. Before starting the hybrid fire test, the beam is loaded with the exterior loads and interface conditions at ambient temperature. This stage of the test already reveals some experimental difficulties. The data acquisition system and transfer system might not be accurate enough to ensure good results. The resolution of the measurement system is considered insufficient compared with the values to be updated every time step. The noise produced during the tests does not support the use of a more accurate data acquisition system. Before turning the burners on in the furnace, the equilibrium at ambient condition between the substructures is restored. In this stage of the test unexpected results are observed and the test is called out in order to understand the errors. The unexpected results are produced due to some error in the code of the control system. The post-analysis of the Test 2 helped identifying the issues of the control system and are analyzed in details in the thesis.

The beam tested during the first trial of hybrid fire testing is reused for the next hybrid fire test referred to as the Test 3. Some improvements have been done based on the observations from the previous tests, i.e. Test 2. The system to measure the horizontal displacement is replaced, being stiffer than in the previous case. As mentioned previously, the resolution of the transducers is limited; nevertheless, the same transducers are used based on the hypothesis that the noise during the hybrid test has a bigger influence than the resolution of the transducers. In the previous test the axial force to be reproduced during the tests is considered too small in comparison with the capacity of the horizontal jack. Therefore, the configuration of the analyzed structure is modified to increase the value of the axial force. In the early stage of the test, the person in charge with the control process activated by mistake the loading of the beam which lead to failure.

No hybrid fire test has been performed.

## 7.2. Conclusion

This thesis presents the development and the implementation of a hybrid fire testing method which was applied numerically on a concrete structure with elastic boundary conditions.

The main contributions and observations of this thesis are summarized here below.

*Methodology of hybrid fire testing*

- The "first generation method", i.e. the method considered in the former tests where the numerical structure is considered separately from the physical structure, is conditionally stable on the stiffness ratio between the NS and PS. In the cases when the PS is stiffer than the NS, a force control procedure is stable, while a displacement control procedure is stable in the case when the NS is stiffer than the PS.
- The instability of the first generation method is due to the fact that in the calculation process of the boundary conditions only the stiffness of the NS is considered.
- In order to ensure stability, independently on the stiffness ratio of the substructures, the stiffness of the PS must also be considered in the calculation process of the boundary conditions.
- The second generation method is stable independent on the stiffness ratio due to the fact that when the boundary conditions are updated, the stiffness of the NS and PS are both considered.
- The second generation method is recommended to be implemented in displacement control procedure since the force control procedure may be unstable even if the stiffness of both substructures is considered at the interface and, also, because a displacement control may allow following the large displacements of the system at the later stage of the test, when the PS becomes unstable, giving a better insight into the failure mode.
- The second generation method was developed considering a predetermined matrix in order to represent the behavior of the NS. The limitations of the predetermined matrix are that the nonlinearities in the NS are neglected and the NS cannot be exposed to fire.
- The case when the nonlinearities of the NS are considered would need some additional strategies in order to implement the method in a fire facility. The strategies refer to the appropriate development of the FE model in order to be suitable for hybrid fire testing, the proper selection of the parameters to produce accurate results, or the strategies referred to the proper control system in the fire facility.

*Hybrid fire testing*

- To be able to perform successful hybrid fire tests, an adequate control system is required.
- The proposed hybrid fire test in this thesis was not successful but important observations are done after the trials.
- The loading of the system (with the exterior loads and the interface displacements) at ambient temperature turned out to be sensitive to the data acquisition system and transfer system.
- A proper solution must be adopted in order to avoid the experimental errors. The system considered to help measuring the horizontal displacements was improved after the first trial of the hybrid fire test.
- The resolution of the data acquisition system has an important impact on the results since the interface equilibrium can be affected along with the accuracy of the results.
- The capacity of the transfer system, i.e. actuators, should be selected appropriate for the range of expected reaction forces.
- Different results of virtual hybrid fire testing are obtained depending whether, in the calculation process, the measured displacements or the calculated displacements are considered. Better results are observed when the measured displacement in the furnace is neglected in the calculation process for this specific case study. More analysis needs to be done to explain the influence of this factor on the hybrid fire results.

*Numerical implementation*

- The virtual hybrid fire testing was possible after some modifications were implemented in the FE software SAFIR.
- The implementation was developed only for the case when the NS is represented by a predetermined matrix.

## 7.3. Future work

In the analyzed case study, the NS is chosen to be represented by the constant predetermined matrix. The predetermined matrix is only appropriate when the NS is not exposed to fire. The heated PS can induce plasticity in the cold surrounding hence the constant matrix does not reflect the real behavior of the NS. The next step of the future work aims the study of hybrid fire testing when the NS is modelled in FE software and eventually is exposed to fire. The use of the FE model influences the possible minimum time step to be used during the hybrid fire test. Thus, the effect of the calculation time needs to be further study.

In the case when the NS is represented in the FE software, a strategy needs to be developed in order to make possible the connection between the FE model and the furnace facility.

Until now, the static equation is solved during hybrid fire testing. In the final stage of the hybrid tests, when large deformation occurs and the PS is unstable, a dynamic approach might be needed to succeed the test until the failure.

One of the further developments is the possibility to update the temperature in the FE model, based on the measured temperature in the furnace. The influence of the temperature updates should be analyzed.

From the experimental point of view, the first objective is to perform the tests described in this thesis. Every time when a new development is done, the experimental approach is aimed to be performed in order to validate the imposed improvements.

An important aspect that should be analyzed in details is the propagation of errors in the process, e.g. rounding or truncating the calculated values, lack of accuracy of the different sensors, limited resolution of the sensors, delay between the time when the request is sent to the actuators and the time when it is actually processed.

# REFERENCES

[1]. Tondini, N., Rossi, B., & Franssen, J.-M. (2013). Experimental investigation on ferritic stainless steel columns in fire. *Fire Safety Journal, 62*, 238-248.

[2]. Tondini, N., Hoang, V. L., Demonceau, J.-F., & Franssen, J.-M. (2013). Experimental and numerical investigation of high-strength steel circular columns subjected to fire. *Journal of Constructional Steel Research, 80*, 57-81.

[3]. Lennon, T. (2003). Whole building behavior – Results from a series of large scale tests. *CIB-CTBUH International Conference on Tall Buildings*, 8-10 May 2003, Malaysia.

[4]. Newman, G. M., Robinson, J. T., & Bailey, C. G. (2000), Fire Safe Design, A New Approach to Multi-storey Steel Framed Buildings, SCI P-288, *The Steel Construction Institute*, Ascot (United Kingdom).

[5]. Armer, G. S. T., & Moore, D. B. (1994), Full-Scale Testing on Complete Multistorey Structures, *The Structural Engineer*, Volume 72, No 2/18 January 1994, pp 30-31.

[6]. René De Borst, Mike A. Crisfield, Joris J. C. Remmers and Clemens V. Verhoosel (2012), Non-linear finite element Analysis of Solids and Structures, Second edition, *John Wiley & Sons Ltd.*

[7]. Schellenberg, A.H., Mahin, S.A., Fenves G.L., (2009). *Advanced implementation of Hybrid Simulation.* PEER Report 2009/104, University of California, Berkeley

[8]. Takanashi, K., et al. (1975), Non-linear earthquake response analysis of structures by a computer-actuator online system – Part 1: detail of the system. *Transactions of the Architectural Institute of Japan* (229): 77-83.

[9]. Takanashi, K., and Nakashima, M., (1987), Japanese activities on on-line testing. *Journal of Engineering Mechanics* 113(7): 1014-1032.

[10]. Mahin, S. A., and Williams, M. E., (1980), Computer controlled seismic performance testing. Dynamic Response of Structures: Experimentation, Observation, Prediction and Control, *American Society of Civil Engineers*, New York, NY.

[11]. Shing, P. B., and Mahin, S. A., (1983), Experimental error propagation in pseudodynamic testing. *Berkeley, CA, Earthquake Engineering Research Center*: 175 pages.

[12]. Thewalt, C. R., and Mahin, S. A., (1987). Hybrid solution techniques for generalized pseudodynamic testing. *Berkeley, CA, Earthquake Engineering Research Center*: 142 pages.

[13]. Mosqueda, G., et al. (2005). Implementation and accuracy of continuous hybrid simulation with geographically distributed substructures. *Berkeley, CA, Earthquake Engineering Research Center.*

[14]. Shing, P. S. B., and Mahin, S. A., (1984). Pseudodynamic test method for seismic performance evaluation: theory and implementation. *Berkeley, CA, Earthquake Engineering Research Center*: 162 pages.

[15]. Newmark, N. M., (1959). A method of computation for structural dynamics. *Journal of Engineering Mechanics*, ASCE 67.

[16]. Dermitzakis, S. N., and Mahin, S. A., (1985). Development of substructuring techniques for on-line computer controlled seismic performance testing. *Berkeley, CA, Earthquake Engineering Research Center*: 153 pages.

[17]. Hughes, T. J. R. and Liu, W. K., (1978). Implicit-explicit finite elements in transient analysis: implementation and numerical examples. *Journal of Applied Mechanics*, ASME 45(2): 375-378.

[18]. Hughes, T. J. R. and Liu, W. K., (1978). Implicit-explicit finite elements in transient analysis: stability theory. *Journal of Applied Mechanics*, ASME 45(2): 371-374.

[19]. Mahin, S. A. and Shing, P. S. B., (1985). Pseudodynamic method for seismic testing. *Journal of Structural Engineering* 111(7): 1482-1503.

[20]. Nakashima, M., (1985). Part 1: Relationship between integration time interval and response stability in pseudo dynamic testing (stability and accuracy behavior of pseudo dynamic response). *Journal of Structural and Construction Engineering (Transactions of AIJ)* (353): 29-36.

[21]. Nakashima, M., (1985). Part 2: Relationship between integration time interval and accuracy of displacement, velocity, and acceleration responses in pseudo dynamic testing. *Journal of Structural and Construction Engineering (Transactions of AIJ)* (358): 35-42.

[22]. Nakashima, M., and Kato, H., (1988). Part 3: experimental error growth in pseudo dynamic testing (stability and accuracy behavior of pseudo dynamic response). *Journal of Structural and Construction Engineering (Transactions of AIJ)* (386): 36-48.

[23]. Nakashima, M., and Kato, H., (1989). Part 4: Control of experimental error growth in pseudo dynamic testing-- Stability and accuracy behavior of pseudo dynamic response. *Journal of Structural and Construction Engineering (Transactions of AIJ)* (401): 129-138.

[24]. Takanashi, K., and Nakashima, M., (1987). Japanese activities on on-line testing. *Journal of Engineering Mechanics* 113(7): 1014-1032.

[25]. Thewalt, C. R., and Mahin, S. A., (1987). Hybrid solution techniques for generalized pseudodynamic testing. *Berkeley, CA, Earthquake Engineering Research Center*: 142 pages.

[26]. Hilber, H. M., et al. (1977). Improved numerical dissipation for time integration algorithms in structural dynamics. *Earthquake Engineering and Structural Dynamics* 5(3): 283-292.

[27]. Nakashima, M., et al. (1988). Feasibility of pseudo dynamic test using substructuring techniques. *Proceedings, Ninth World Conference on Earthquake Engineering*. Tokyo, Japan.

[28]. Nakashima, M., et al. (1990). Integration techniques for substructure pseudo dynamic test. *Proceedings, Fourth U.S. National Conference on Earthquake Engineering*. Palm Springs, CA.

[29]. Hughes, T. J. R., et al. (1979). Implicit-explicit finite elements in nonlinear transient analysis. *Computer Methods in Applied Mechanics and Engineering* 17(18): 159-182.

[30]. Mahin, S. A., et al. (1989). Pseudodynamic test method - current status and future directions. *Journal of Structural Engineering* 115(8): 2113-2128.

[31]. Dorka, U. E. and Heiland, D. (1991). Fast online earthquake utilizing a novel PC supported measurement and control concept. *4th Conference on Structural Dynamics*. Southampton, UK.

[32]. Dorka, U. E. (2002). Hybrid experimental - numerical simulation of vibrating structures. *International Conference WAVE2002*. Okayama, Japan.

[33]. Bayer, V., et al. (2005). On real-time pseudo-dynamic sub-structure testing: algorithm, numerical and experimental results. *Aerospace Science and Technology* 9(3): 223-232.

[34]. Shing, P. S. B., et al. (1991). Implicit time integration for pseudodynamic tests. *Earthquake Engineering & Structural Dynamics* 20(6): 551-576.

[35]. Shing, P. S. B. and Vannan, M. T. [1991]. Implicit time integration for pseudodynamic tests: convergence and energy dissipation. *Earthquake Engineering & Structural Dynamics* 20(9): 809-819.

[36]. Shing, P. B., et al. (1994). Pseudodynamic tests of a concentrically braced frame using substructuring techniques. *Journal of Constructional Steel Research* 29(1-3): 121-148.

[37]. Bursi, O. S., et al. (1994). Pseudodynamic testing of strain-softening systems with adaptive time steps. *Earthquake Engineering & Structural Dynamics* 23(7): 745-760.

[38]. Nakashima, M., et al. (1992). Development of real-time pseudo dynamic testing. *Earthquake Engineering & Structural Dynamics* 21(1): 79-92.

[39]. Schneider, S. P. and Roeder, C. W., (1994). An inelastic substructure technique for the pseudodynamic test method. *Earthquake Engineering & Structural Dynamics* 23(7): 761-775.

[40]. Thewalt, C. R. and Roman, M., (1994). Performance parameters for pseudodynamic tests. *Journal of Structural Engineering* 120(9): 2768-2781.

[41]. Campbell, S. and Stojadinovic, B. (1998). A system for simultaneous pseudodynamic testing of multiple substructures. *Proceedings, Sixth U.S. National Conference on Earthquake Engineering*. Seattle, WA.

[42]. Magonette, G. E. and Negro, P. (1998). Verification of the pseudodynamic test method. *European Earthquake Engineering* XII(1): 40-50.

[43]. Horiuchi, T., et al. (1996). Development of a real-time hybrid experimental system with actuator delay compensation. *Proceedings, 11th World Conference on Earthquake Engineering*. Acapulco, México.

[44]. Horiuchi, T., et al. (1999). Real-time hybrid experimental system with actuator delay compensation and its application to a piping system with energy absorber. *Earthquake Engineering & Structural Dynamics* 28(10): 1121-1141.

[45]. Magonette, G. (2001). Development and application of large-scale continuous pseudo-dynamic testing techniques. *Philosophical Transactions of the Royal Society: Mathematical, Physical and Engineering Sciences* 359(1786): 1771-1799.

[46]. Pan, P., et al. (2005). Online test using displacement-force mixed control. *Earthquake Engineering & Structural Dynamics* 34(8): 869-888.

[47]. Pan, P., et al. (2005). Online hybrid test by internet linkage of distributed test-analysis domains. *Earthquake Engineering & Structural Dynamics* 34(11): 1407-1425.

[48]. Elkhoraibi, T. and Mosalam, K. M. (2007). Towards error-free hybrid simulation using mixed variables. *Earthquake Engineering & Structural Dynamics* 36(11): 1497-1522.

[49]. Wu, B., et al. (2007). Equivalent force control method for generalized real-time substructure testing with implicit integration. *Earthquake Engineering & Structural Dynamics* 36(9): 1127-1149.

[50]. Bonnet, P. A., et al. (2008). Evaluation of numerical time-integration schemes for real-time hybrid testing. *Earthquake Engineering & Structural Dynamics* 37(13): 1467-1490.

[51]. Bursi, O. S., et al. (2008). Novel coupling Rosenbrock-based algorithms for real-time dynamic substructure testing. *Earthquake Engineering & Structural Dynamics* 37(3): 339-360.

[52]. Saouma, V.E. & Sivaselvan, M.V. (2008). *Hybrid simulation: Theory, implementation and application*, Taylor and Francis, London, UK. 2008.

[53]. Schwarz, H. A. (1870), Gesammelte Mathematische Abhandlungen, volume 2, pages 133–143. 1890. First published in *Vierteljahrsschrift der Naturforschenden Gesellschaft* in Zürich, volume 15, 1870, 272-286.

[54]. Takanashi K. et al. (1975), *Nonlinear Earthquake Response Analysis of Structures by a Computer Actuator On-Line System*. Bull. Of Earthquake Resistant Structure research Center, Institute of industrial Science, University of Tokio, No. 8

[55]. Dermitzakis, S.N., Mahin, S.A. (1985), *Development of Substructuring Techniques for On-Line Computer Controlled Seismic Performance Testing*. UCB/EERC Report No. 85/04, Earthquake Engineering Research Center, University of California.

[56]. Magonette, G., (1991), *Digital Control of Pseudo-Dynamic Tests* in: J. Donea, P.M. Jones (eds.): Experimental and Numerical Methods on Earthquake Engineering, Dordrecht 1991, 63-69

[57]. Korzen, M., Magonette, G. & Buchet, Ph. (1999), Mechanical Loading of Columns in Fire Tests by Means of the Substructuring Method, *Zeitschrift für Angewandte Mathematik und Mechanik*, 1999, Vol. 79, pp. S617-S618.

[58]. Korzen, M., Ziener, K.-U. & Riemen, S., (2002), Some Remarks on the Substructuring Method Applied to Fire Resistance Tests of Columns, *World Congress on Housing*, Housing Construction-An Interdisciplinary Task, 9-13 September 2002, Coimbra, Portugal

[59]. Korzen, M., Rodrigues, J.P.C. & Correia, A.M., (2009), Thermal Restraint effects on the fire resistance of steel and composite steel and concrete columns, *Application of Structural Fire Engineering*, 19-20 February 2009, Prague, Czech Republic.

[60]. Korzen, M., Rodrigues, J.P.C. & Correia, A.M., Composite Columns Made of Partially Encased Steel Sections Subjected to Fire, Proceedings of the Sixth International Conference Structures in Fire, pp. 341–348, June 2010, Michigan, USA.

[61]. Correia, A.M., Rodrigues, J.P.C., Korzen, M., (2012), Experimental Research on the Load-Bearing Capacity of Partially Encased Steel Columns Under Fire Conditions, Journal of Structural Fire Engineering, Volume 3, Number 1, 2012, pp 81-94.

[62]. Robert, F., (2008), *Comportement des bétons sous haute température et en cas d'incendie: caractérisation multi-échelle*, (Unpublished doctoral thesis). L'Ecole Normale Supérieure de Cachan, Cachan, France, 2008.

[63]. Robert, F., Rimlinger, S., Collignon, C., (2009), Promethee, Fire Resistance Facility Taking Into Account the Surrounding Structure, *1st international Workshop on Concrete Spalling due to Fire Exposure*, 2009, 3-5 sept.

[64]. Robert, F., Rimlinger, S., Collignon. C., (2010), Structure fire resistance: a joint approach between modelling and full scale testing (substructuring system), *3rd fib International Congress*

[65]. Mostafaei, H. (2013), Hybrid fire testing for assessing performance of structures in fire –Application, *Fire Safety Journal*, 2013, 56, 30–38.

[66]. Mostafaei, H. (2013), Hybrid fire testing for assessing performance of structures in fire –Methodology, *Fire Safety Journal*, 2013, 58, 170–179.

[67]. Franssen, J.-M., (2005), SAFIR, A Thermal/Structural Program Modelling Structures under Fire, *A.I.S.C. Engineering Journal*, 2005, 42 (3), 143–158.

[68]. Whyte, C.A., Mackie, K.R. and Stojadinovici, B. (2016). "Hybrid Simulation of Thermomechanical Structural Response", Journal of Structural Engineering, 142(2): 04015107-1 – 04015107-11.

[69]. OpenFresco 2016. "Open Framework for Experimental Setup and Control."

[70]. OpenSees 2016. "Open System for Earthquake Engineering Simulation."

[71]. Whyte, C.A., Mackie, K.R., Abbiati G. and Stojadinovici, B. (2016). "Optimal Tuning of Thermomechanical Hybrid Simulation Parameters", 9th International conference on Structures in Fire, 8-10 June, pg. 1055-1062.

[72]. Tondini, N., Abbiati, G., Posidente, L. and Stojadinovici, B. (2016). "A Static Partitioned Solver for Hybrid Fire Testing", 9th International conference on Structures in Fire, 8-10 June, pg. 827-835.

[73]. Schulthess, P., Neuenschwander, M., Knoblock, M. and Fontana, M. (2016). "Consolidated Fire Analysis – Coupled Thermo-mechanical Modelling for Global Structural Fire Analysis", 9th International conference on Structures in Fire, 8-10 June, pg. 819-826.

[74]. ABAQUS `ABAQUS Documentation', Dassault Systèmes, Providence, RI, USA.

[75]. Bonelli, A., Bursi, O. S. (2004) *Generalized-alpha methods for seismic structural testing*. Earthquake Engineering and Structural Dynamics, 33:1067–1102

[76]. Bisby, L., Mostafaei, H., Pimienta, P. (2014). *State-of-the-Art on Fire Resistance of Concrete Structure Structure-Fire Model Validation*, DRAFT Submitted to: Applied Research Associates

[77]. Garlock, M., Kruppa, J., LI, G-Q., Zhao, B. (2014). *Fire behavior of steel structures*.

[78]. Whyte, C., A., Stojadinovic, B., (2014). *High-precision displacement control for hybrid simulation of the seismic response of stiff reinforced concrete shear walls.* Tenth U.S. National Conference on Earthquake Engineering Frontiers of Earthquake Engineering, July 21-25, Anchorage, Alaska

[79]. Hung, C.-C. and El-Tawil, S. (2008). *A method for estimating specimen tangent stiffness for hybrid simulation.* Earthquake Engineering and Structural Dynamics, 38:115-134.

[80]. Elkhoraibi T., Mosalam K.M. (2007). *Generalized hybrid simulation framework for structural systems subjected to seismic loading*, PEER Report 2007/101, Pacific Earthquake Engineering Research Center, University of California, Berkeley, CA.

[81]. Farhat, C. and Roux, F.-X. (1991). *A method of finite element tearing and interconnecting and its parallel solution algorithm.* International Journal for Numerical Methods in Engineering, 32:12051227.

[82]. P.L.C. van der Valk. (2010). *Model reduction and interface modeling in dynamic substructuring. Application to a multi-megawatt wind turbine.* MSc. Thesis, January 14.

[83]. Sauca, A., Gernay, T., Robert, F. & Franssen, J.M. (2015). Characteristics and implementation of Hybrid Fire Testing (HFT), presented at the *Engineering Mechanics Institute Conference*, 2015, June 16-19.

[84]. Sauca, A., Gernay, T., Robert, F., Tondini, N. & Franssen, J.M. (2016). Stability in Hybrid Fire Testing, *9th International Conference on Structures in Fire*, 2016, June 8-10.

[85]. Sauca, A., Gernay, T., Robert, F., Tondini, N. & Franssen, J.M. (2016). A novel method for Hybrid Fire Testing, *6th European Conference on Structural Control*, 2016, July 11-13.

[86]. VecTor2, University of Toronto, http://www.civ.utoronto.ca/vector/software.html accessed on 16th December 2016.

[87]. EN 1992-1-2:2004 – Eurocode 2: Design of concrete structures – Part 1-2: General rules – Structural fire design.

[88]. EN 1992-1-1:2004 – Eurocode 2: Design of concrete structures – Part 1-1: General rules and rules for buildings.

[89]. Gernay, T., & Franssen, J.-M. (2012). *A formulation of the Eurocode 2 concrete model at elevated temperature that includes an explicit term for transient creep*. Fire Safety Journal, 51, 1-9

[90]. Gernay, T. (2012). *Effect of Transient Creep Strain Model on the Behavior of Concrete Columns Subjected to Heating and Cooling*. Fire Technology, 48(2), 313-329

# A. APPENDIX A: CERIB FIRE FACILITY

## A1. The dimensions of the furnace

Promethee furnace allows performing tests on structures with representative dimensions (furnace 6m long and 3.60m wide) having the possibility to test 10 m long structural elements which are heated only for a distance of 6m. Vertical elements (columns or walls) with the dimensions of 3m height and 3m wide are possible to be tested. The specimens can be horizontally and vertically loaded and as fire loads, conventional thermal loading (ISO 834, hydrocarbon fire curve or modified hydrocarbon fire curve) along with the natural fires can be reproduced. The innovative part of the facility is the possibility to perform hybrid fire testing.

Thus the actual dimensions of the structure to be tested are (i) 6m long, (ii) 4m wide and (iii) from 2.6m to 6m height.

Figure A-1 present the fire facility of CERIB known as Promethee furnace.

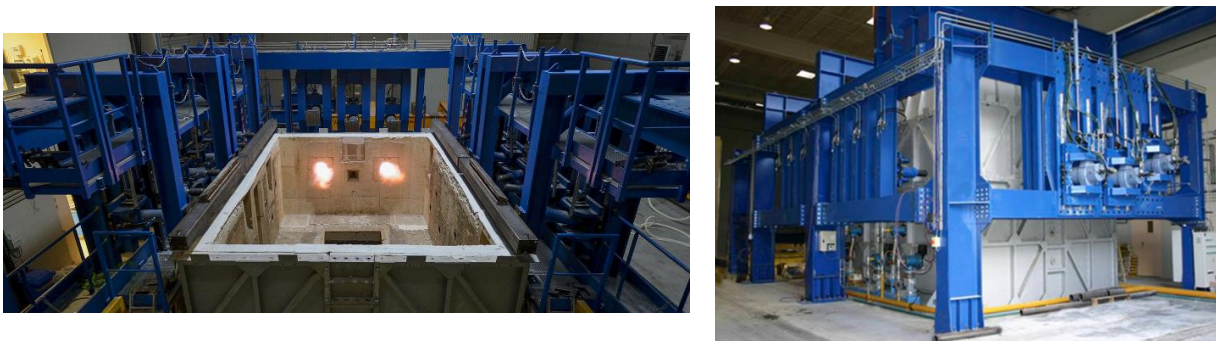

**Figure A-1. Promethee furnace.**

## A2. Mechanical characteristics

Promethee furnace disposes of the following jacks:

- 18 vertical jacks working in compression
  - 1 with 300 tons capacity and stroke of 50cm;
  - 4 with a 50 tons capacity and stroke of 50cm;
  - 4 with a 30 tons capacity and stroke of 40cm;
  - 9 with a 5 tons capacity and stroke of 50cm;
- 9 horizontal jacks
  - 3 with 125 tons capacity in compression and 60 tons in tension, with a stroke of 50 cm;
  - 6 with a 50 tons capacity in compression and stroke of 40cm;

- 2 vertical jacks with a 30 tons capacity in compression and stroke of 100cm which are applied at the extremities of the cantilever of a test element. These jacks are used when testing connections are characterized by rotations up to 10°.

## A3. Other specific characteristics

A series of displacements sensors and inclinometers can be used. The temperatures on the different faces of the structure and inside the tested element are monitored by thermocouples. The forces to be applied by the jacks are computed by hydraulic pressure sensors. All these measurements are completed by endoscopic view of the test elements during the test.

The total power of the furnace is 10.8 MW and is generated by 16 gas burners. The furnace is controlled by 30 regulating thermocouples.

A large number of fire scenarios can be generated where temperatures up to 1320°C are possible. This includes the ISO 834 curve, the standard hydrocarbon curve, and the modified hydrocarbon curve.

The structural elements to be tested are air-conditioned stored. The storage room is characterized by a surface of 350 $m^2$, 8m height with 23°C and 50% relative humidity.

Before this thesis, the first generation method was implemented in force control procedure where the interaction is produced by simulating the rigidity of the cold surrounding using the external forces at the extremities of the specimen. These forces are computer controlled to apply loads in accordance with the measured displacements.

As a result of this thesis, the novel method to perform hybrid fire testing is implemented in a displacement control procedure. The displacements are computer controlled to apply displacements in accordance with the measured forces. In the same time the cold surrounding (NS) is model via the predetermined matrix and since the stiffness of the PS is required during the procedure, the initial tangent stiffness is also defined.

# B. APPENDIX B: LOCAL VERSUS GLOBAL SYSTEM OF COORDINATES IN THE NEW IMPLEMENTED METHODOLOGY SPECIFIC TO CERIB FIRE FACILITY

The transformation from the global system of coordinates GSC to the local system of coordinates LSC (and other way around) in CERIB fire facility is presented in this appendix.

*Data acquisition system*

During a fire test the common data to be measured are:

- Temperature evolution for specific locations of the PS;
- Displacements and rotations;
- Forces;

The update of the boundary conditions can make use of all this information. In the former hybrid tests only the displacements and forces are used in the update of the boundary conditions. The temperatures can be used in the hybrid process if there is interest in updating the temperatures of the NS in real time. Nevertheless, the utility of updating the temperatures during the hybrid process still needs to be studied along with a definition of cases when there is needed to do so. To consider the temperature as a component of hybrid fire testing was not the aim of this project. One of the main reasons was due to the fact that the NS of the proposed case study was cold during the hybrid test.

Nevertheless, the data acquisition system is presented in Figure B-1. The temperature is measured by thermocouples, the displacements are measured by transducers, the rotations are measured by the inclinometers while the loads are measured using the load cells. Other possibility to measure the loads is the pressure of the actuators.

*Thermocouple* *Transducer and Inclinometer* *Load cell*

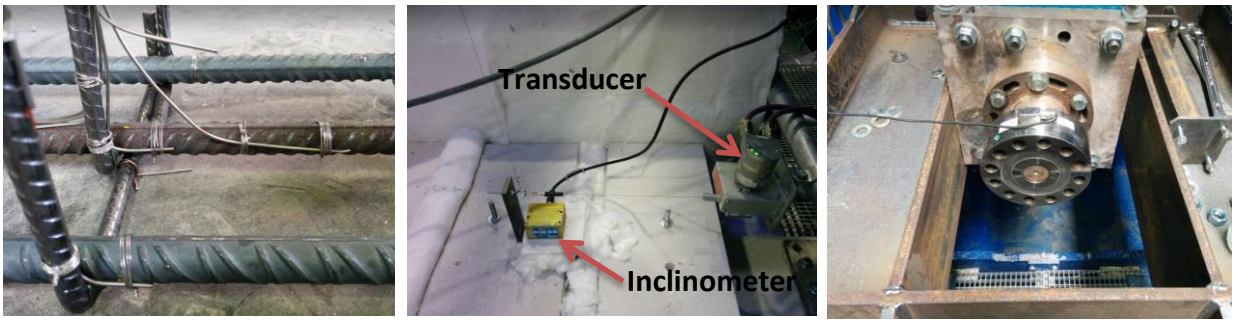


**Figure B-1. The data acquisition system used by Promethee**

*Transfer system*

The transfer system refers to the part of the furnace which induces the new boundary conditions.

The new boundary conditions can be enforced by applying at the interface of the substructures:

- Displacements (displacement control procedure);
- Forces (force control procedure);

The displacements/rotations and the forces/moments are applied by jacks as presented in Figure B-2. The jacks can have different orientations depending on the action that is required.

For vertical forces and vertical displacements, the jacks will be vertically oriented while for the horizontal displacements and forced the jacks will be horizontally oriented. To induce rotations some additional parts of the PS are needed. One example is presented in the Figure B-2 where to induce the rotation and the bending moment for a beam, a vertical jack is acting with a lever arm on the cold cantilever part of the tested beam. Some other solutions can be adopted depending on the furnace facility.

*Vertical jacks* *Horizontal jacks* *Moment effect*

**Figure B-2. The transfer system used by Promethee**

*The sign convention for data acquisition system*

- The inclinometers

Figure B-3 presents the sign convention for the registered rotation. Depending on how the inclinometer is fixed on the specimen, positive or negative rotation will be registered. A positive rotation is registered for counter clock direction while clock wise direction defines the negative rotation. The specified convention is available only if the position of the inclinometer is the one presented in the figure (the "+" sign in the left while the "-" sign in the right). Please note that if the inclinometer is turned with 180° (the "-" sign in the left and the "+" sign in the right) then a positive rotation is defined by the clock wise direction, while the negative rotation is defined by the counter clock wise direction.


**Figure B-3. The sign convention of the inclinometer**

In conclusion the sign of rotation can be imposed by the user by taking care of the inclinometers position.

- The transducers

Figure B-4 refers to the sign convention of the transducer. The sign depends on the entry or exit of the transducers cable. If the wire entries the transducer, then a negative displacement is registered while if the wire exits the transducer a positive displacement is registered.

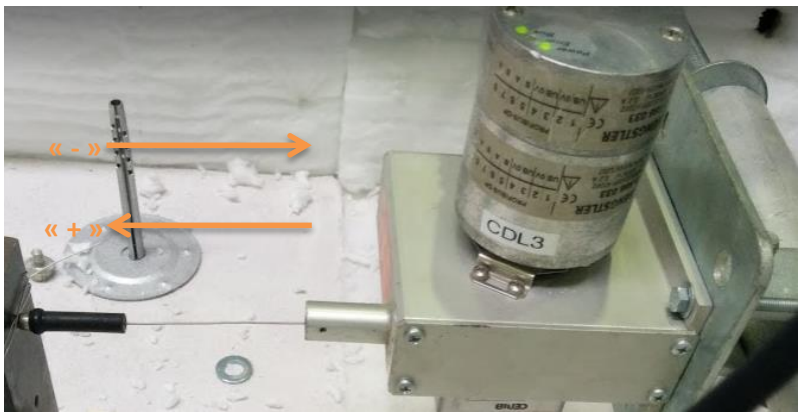


**Figure B-4. The sign convection for the transducers**

- The jacks

Figure B-5 presents the sign convention for the jacks. The sign of the registered force depends on the entry or exit of the jack. For entries of the jacks negative forces are registered while for the exit of the jack positive forces are registered.

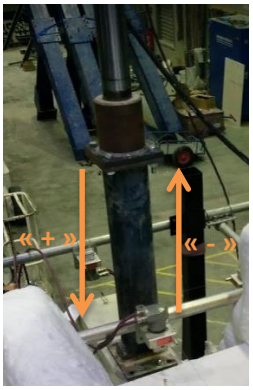


**Figure B-5. The sign convention for jacks**

*The sign convention for the transfer system*

While the transfer is composed of jacks, the sign convention is the same as the one presented in the Figure B-5.

*Transformation matrices*

The transformation matrices have been conceived for the transformation of the coordinates from the local/global system of coordinates to the global/local system of coordinates. The principle of the transformation matrices is relatively simple and it will be explained next in details.
The first step is to define the global system of coordinated GSC in the furnace as presented in Figure B-6. Along with the global system of coordinates we define the displacements: $u$ as the horizontal displacement, $v$ as the vertical displacement and $\theta$ the rotation.

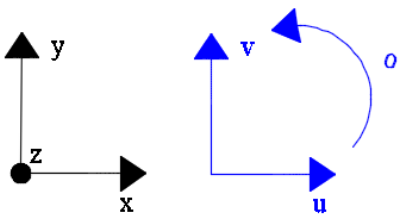


Where

$u \parallel x; \qquad u = x_n - x_{n-1}$
$v \parallel y; \qquad v = y_n - y_{n-1}$

**Figure B-6. The definition of the global system of coordinates**

- **Force sign convention**

Let us not with $F_G$ the force in GSC and $F_J$ the measured force in the jack. The measured forced by the jack depends on the position of the jack in the furnace. Different cases will be next presented in the Figure B-7 depending on the position of the jack compared with the global system of coordinates. The position of the jacks will define the transformation matrix.

The arrow shows the direction of the forces in the GSC while the thinner part of the jack indicates the direction of the jack. The jacks can have the same direction with the axes of the GSC thus the transformation factor is equal positive one (Case 2 and Case 4). When the direction of the jack does not coincide with the direction of the GSC axes then the transformation factor is equal negative one (Case 1 and Case 3).

*Case 1*: $\boldsymbol{F_J = -1 * F_G}$


*Case 2*: $\boldsymbol{F_J = 1 * F_G}$


*Case 3*: $\boldsymbol{F_J = -1 * F_G}$

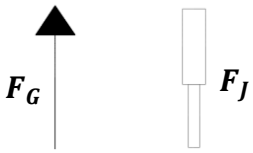


*Case 4*: $\boldsymbol{F_J = 1 * F_G}$

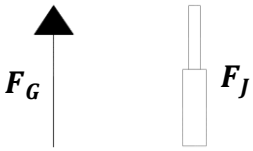


**Figure B-7. Position of the jacks compared with the axis of the GSC.**

Let us consider the body presented in Figure B-8 loaded with different loads in the global system of coordinates GSC.

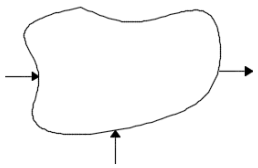

**Figure B-8. Body loaded with forces**

From the GSC the values need to be transformed in the LSC, depending on the solution chosen in the furnace to apply the loads (the jack's position).

In conclusion the transformation matrix for forces $T_P$ presented by Eq. (101) is defined as a diagonal matrix with positive or negative values of one, depending on the position of the jacks compared with the GSC. Usually the position of the jacks in the furnace is vertical or horizontal.

$$\boldsymbol{T}_P = \begin{bmatrix} \pm 1 & 0 & 0 \\ 0 & \pm 1 & 0 \\ 0 & 0 & \pm 1 \end{bmatrix} \tag{101}$$

Note that if the position of the jacks is different than vertical and horizontal, then the diagonal terms of the transformation matrix will have different values than positive or negative one. In this situation the trigonometric formulas will be used to compute the horizontal or the vertical component of the applied force.

If the transformation matrix is defined only by positive and negative values of one then the inverse of the transformation matrix is the transformation matrix itself as presented in Eq. (102).

$$\boldsymbol{T}_P = \boldsymbol{T}_P{}^{-1} \tag{102}$$

In conclusion if $\boldsymbol{F}_J$ is measured in the furnace and $\boldsymbol{F}_G$ is computed then $\boldsymbol{F}_G = \boldsymbol{T}_P * \boldsymbol{F}_J$. If $\boldsymbol{F}_G$ is computed and $\boldsymbol{F}_J$ needs to be applied in the furnace then $\boldsymbol{F}_J = \boldsymbol{T}_P * \boldsymbol{F}_G$.

- **Displacement sign convention**

The vertical and horizontal displacements are measured using the transducers presented in Figure B-9. The transformation matrix is defined by the orientation of the transducer compared with the axis of the GSC.


**Figure B-9. Representation of the transducer**

Figure B-14 presents different cases of different transformation values of the matrix. The transformation matrix of displacements is defined following the same principle as the transformation matrix of forces where the position of the transducers will induce positive or negative term in the main diagonal of the matrix. The transducer has the direction of the axis of the GSC in the Case 2 and Case 4, while for the Case 1 and Case 3 the transducer is oriented in the opposite direction of the GSC. The displacement in the GSC is noted with $u_G$ in this example while the displacement measured in the furnace with $u_J$.

<u>*Case 1*</u>: $\boldsymbol{u_J = -1 * u_G}$ <u>*Case 2*</u>: $\boldsymbol{u_J = 1 * u_G}$


<u>*Case 3*</u>: $\boldsymbol{u_J = -1 * u_G}$ <u>*Case 4*</u>: $\boldsymbol{u_J = 1 * u_G}$


**Figure B-10. The position of transducer compared with the axis of the GSC**

If we consider the body loaded with random displacements as presented in Figure B-11 then the transformation matrix $\boldsymbol{T}_U$ is defined by the Eq. **(103)**.

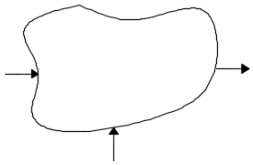

**Figure B-11. Body loaded with displacements**

The position of the transducers in the furnace compared with the GSC will define if the values in the main diagonal will be positive or negative. Note that in practice the transducers will be used in a parallel position with the axis of the GSC.

$$\boldsymbol{T}_U = \begin{bmatrix} \pm 1 & 0 & 0 \\ 0 & \pm 1 & 0 \\ 0 & 0 & \pm 1 \end{bmatrix} \tag{103}$$

In this case the transformation matrix of displacements has the property to be identic with the invers of the transformation matrix of displacements as presented in the Eq. (104).

$$\boldsymbol{T}_U = \boldsymbol{T}_U{}^{-1} \tag{104}$$

Hence if $u_J$ is measured in the furnace and $u_G$ is needed then $u_G = T_U * u_J$ while if $u_G$ is computed and $u_J$ needs to be applied in the furnace then $u_J = T_U * u_G$.

- **Sign convention for rotations**

The anticlockwise rotation is positive defined in the GSC as presented in Figure B-12. The measurement of the rotation in the furnace is done using the inclinometers. The inclinometers measure a positive or a negative rotation depending on how the inclinometer is placed on the PS compared with the GSC.

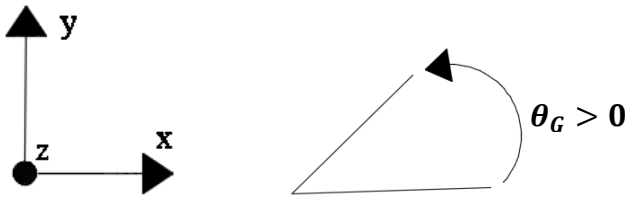


**Figure B-12. The GCS and the positive rotation**

The transformation from the calculated rotations (GSC) to the measured rotations in the furnace depends on the position of the inclinometer compared with the GSC, as presented in Figure B-13. In the Case 1 the positive rotation measured by the inclinometer is a counterclockwise rotation thus the transformation factor is equal to one. The Case 2 shows that the clockwise rotation is measured as positive, in this case the transformation factor is

negative one. The rotations measured in the furnace are noted $\theta_J$ while the rotation expressed in the GSC are noted with $\theta_G$.

<u>*Case 1*</u>: $\boldsymbol{\theta_J = 1 * \theta_G}$ <u>*Case 2*</u>: $\boldsymbol{\theta_J = -1 * \theta_G}$


**Figure B-13. The position of the inclinometers in rapport with the global system of coordinates**

The transformation matrix for rotations is a diagonal matrix with positive or negative values of one depending on how the inclinometer is positioned compared with the GSC. The same properties are valid as for the case of the transformation matrix of displacements.

- **Bending moment convention**

Figure B-14 presents the positive defined moment along with the global system of coordinates.

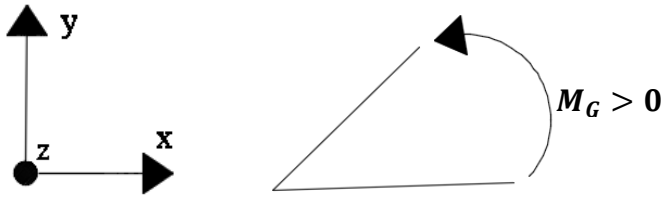


**Figure B-14. The GCS and the positive moment**

Different possibilities are available to induce a moment in the furnace. Usually the moments are induced by building in the furnace additional element loaded with force which along with the lever arm will produce the expected effect.

The transformation from the measured forces in the furnace into the moment in the GSC it is done using the transformation matrix.

The main diagonal of the matrix comprises the lever arm of the force with the corresponding sign.

Figure B-15 presents two different cases where the transformation factor is the negative level arm $-\boldsymbol{d}$ in the Case 1 and the positive level arm $\boldsymbol{d}$ in the Case 2. In this example $\boldsymbol{M_G}$ is the global moment while $\boldsymbol{F_J}$ is the force which creates the moment in the furnace.

*Case 1*: $\boldsymbol{M_G = -d * F_J}$ *Case 2*: $\boldsymbol{M_G = d * F_J}$

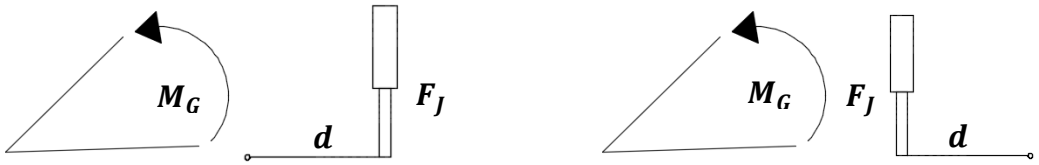


**Figure B-15. The induces moment in the furnace compared with the global moment**

- **General transformation matrix**

The transformation matrix for forces $T_P$ described by the Eq. (105) is a diagonal matrix which contains the value of the arm noted $arm$ of every reaction (restoring) force measured in the furnace and it will be used to calculate the moments. For a reaction force that must generate a moment the value of the lever arm will be introduced in the matrix in the right position. If a restoring force will not generate a moment, then the value of the lever arm will be equal to 1. The corresponding sign will be introduced based on the position of the jacks compared with the GSC as discussed previously.

$T_P$ is a diagonal matrix and the size is dependent on the number of DoFs to be controlled at the interface *nDOF*.

$$T_P = \begin{bmatrix} arm_1 & \dots & 0 \\ \vdots & \ddots & \vdots \\ 0 & \dots & arm_{nDOF} \end{bmatrix} \quad (105)$$

The transformation matrix for displacements $\boldsymbol{T_U}$ presented by Eq. (106) is a diagonal matrix which contains only positive or negative values of one. The sign depends on the position of transducers and inclinometers compared with the GSC.

$$T_U = \begin{bmatrix} \pm 1 & \dots & 0 \\ \vdots & \ddots & \vdots \\ 0 & \dots & \pm 1 \end{bmatrix} \quad (106)$$

# APPENDIX B: LOCAL VERSUS GLOBAL SYSTEM OF COORDINATES IN THE NEW IMPLEMENTED METHODOLOGY SPECIFIC TO CERIB FIRE FACILITY

# C. APPENDIX C: MATERIALS AND CONSTRUCTION OF THE PS

## C.1. Materials

All the three beams are casted in the same day (24.07.2015) using the same mix of concrete BPS XC1(F) C25/30 DMAX14 SF2 CEM I. The target class of the concrete is C25/30 and the maximum aggregate size is 14 mm. The chemical composition of the aggregates denotes siliceous aggregate. The composition of concrete is presented in the Table C-1. A quantity of 0,60 kg/m$^3$ polypropylene fibers are added to avoid the spalling during the fire tests.

**Table C-1. The composition of the concrete for m$^3$**

| | **Coarse aggregate (kg)** | **Fine aggregate (kg)** | **Cement (kg)** | **Filler (kg)** | **Water (kg)** | **Admixture Sika (%)** | **Polypropylene fibers (kg)** |
|---|---|---|---|---|---|---|---|
| **Beams** | 770 | 895 | 300 | 222 | 170 | 1.20 | 0.60 |

The casting of the beams is done by contractors. The instrumentation of the beam, meaning the instrumentation of the thermocouples is done by CERIB. After the casting, the beams are transported to CERIB in 29.07.2015 and stored in the air conditioning room of Promethee (CERIB). 30 cylindrical samples having the dimensions of 11 diameter x 22 tall along with the 5 cylindrical samples of dimensions 16 diameter x 25 tall are casted and store in the same conditions as the beams. The 30 samples are used to determine the compression and tensile strengths of the concrete for different periods especially in the days of the test along with the stress-strain test. The other 5 samples are used to determine the moisture content of the concrete in the day of the tests. The same samples are wrapped in aluminum in order to force the migration of the water in the transversal direction of the beam.

The cylinders have been tested incrementally for compressive strength as the specimens aged. Three specimens have been tested every time to determine a mean value of the compressive or tensile strength. Table C-2 presents the evolution of latest in time. The tensile strength is determined by splitting method in the day of the first day.

**Table C-2. The evolution of compressive and tensile strength in time**

| | **7 days** | **28 days** | *Test 1* *15.01.2016* **175 days** | *Test 2* *01.06.2016* **313 days** | Test 3 |
|---|---|---|---|---|---|
| **Compressive strength (MPa)** | 33.50 | 39.27 | 46.87 | 40.78 | - |
| **Tensile strength (MPa)** | - | - | 4,41 | - | - |

## C.2. Construction of the specimens

The specimens have been built by contractors where the first step was to assemble the cages as presented in Figure C-1. The chosen steel for the longitudinal rebars is B500B while for the transversal rebars B500A and is cold formed steel.

**Figure C-1. Assembled reinforced cage of the beam**

The next step is to instrument the cage with the thermocouples needed to measure the temperatures during the test. Three beams are casted but different thermocouples presented in the Figure C-3 are used for different specimens.

For the beam 1 the sheathed type K thermocouples are used. These consist of type K (nickel chromium/nickel aluminium) thermocouple wires, enclosed in a protective sheath made of metal alloy from which the wires are insulated by densely packed magnesium oxide. The metal alloy used to produce the sheath depends on the final use of the thermocouple. Inconel alloy is used for the case of high temperature or chemical environment. The diameter of the sheet varies from 0.25 mm to 11 mm where in this case 2 mm diameter was used. The measuring junction of the thermocouples can be produced in different configuration. In this case the configuration is presented in the Figure C-2 where “bead” refers to the measuring junction.

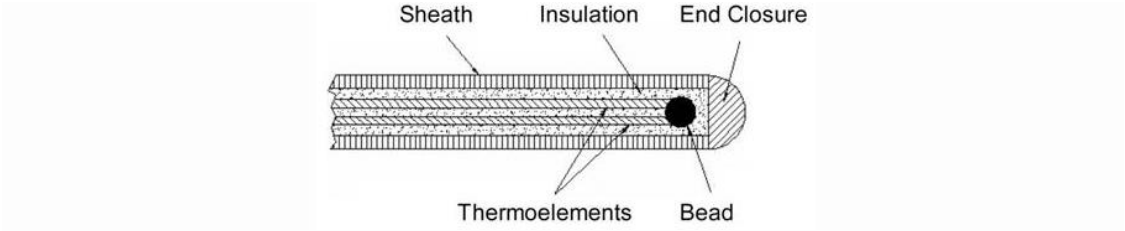


**Figure C-2. The measuring junction of the sheathed type K thermocouples thermocouples**

Twisted type K thermocouples are used for the beam 2 and beam 3. Twisted type K thermocouples consist of type K (nickel chromium/nickel aluminum) thermocouple fiber insulated wires (0.50 mm in diameter), whose extremity is uninsulated and twisted to produce the measuring junction.

The sheathed type K thermocouples are stiffer compared with the twisted type K thermocouples. Thus once the position of the thermocouple is fixed there is no risk that after the pouring of concrete the position changes. The thermocouples are attached to the rebars by wires as can be seen in the Figure C-3.

*Sheathed type K thermocouples*

*Twisted type K thermocouples*

**Figure C-3. The thermocouples used in the instrumentation of the beams**

Next the instrumented cages are placed in framework and are ready to be casted. Figure C-4 presents the beams framework, the position of the concrete thermocouples (TC) and the pouring process.

Before starting the pouring, it has been checked:

- The concrete cover;
- The position of the concrete TC;
- The protection of the TC;

The concrete cover is ensured by concrete additional elements (stiff elements) used in the process. The protection of the thermocouples wires (the part which will be plugged in the furnace) is ensured by some plastic bags. Once the checking has been done the pouring of the concrete starts. Self-compacted concrete is used for the casting. Polypropylene (PP) fibers are added to the concrete in the quantity of 0.50 kg/m$^3$. Once a temperature of 110 degrees Celsius is reached, the fibers in the concrete start to melt away and thus the water can evaporate avoiding the spalling.

*Beams Framework* *The position of the concrete TC* *Beam poured*

**Figure C-4. The casting process**

After the casting, the specimens are air-conditioned stored for specific conditions of humidity and temperature as presented in Figure C-5. The crane was used to store the beams in the air conditioning room and to place the specimens on the furnace after the needed instrumentation (see the Figure C-5).

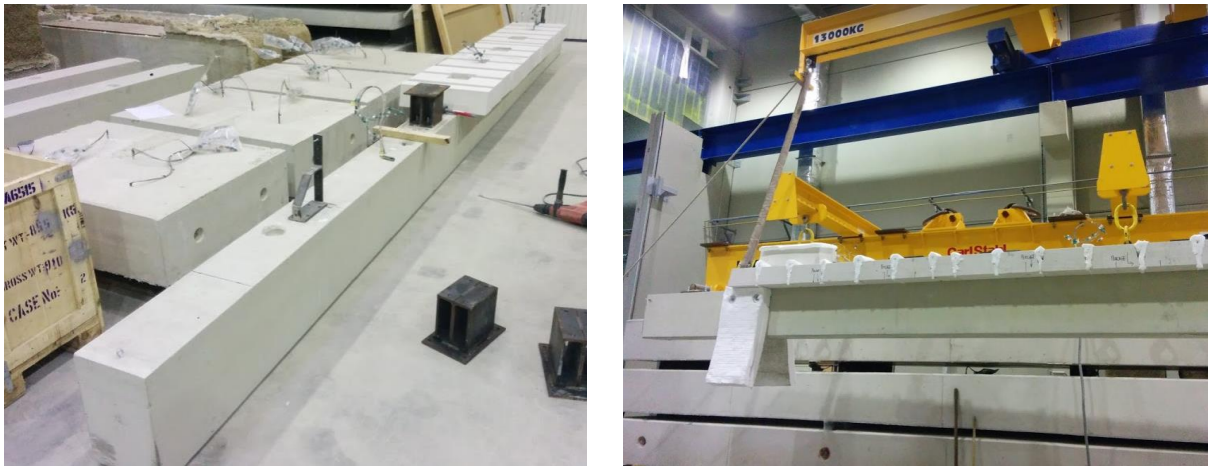


*The beam stored* *The transportation of the beams*

**Figure C-5. The beam stored and transported to the furnace**

# D. APPENDIX D: TEST SETUP

## D.1. Beam preparation

The setup of the specimens when tested in the furnace is a complex activity. The first step is to adjust all the additional elements needed during the fire tests as the one presented in Figure D-1. By additional elements we refer to:

- The cellular concrete and the mineral wool needed to form a closed space in the furnace;
- The pyrometers to measure the temperature inside the furnace;
- All the metallic pieces needed to apply the loads and measure the deformation of the specimen;

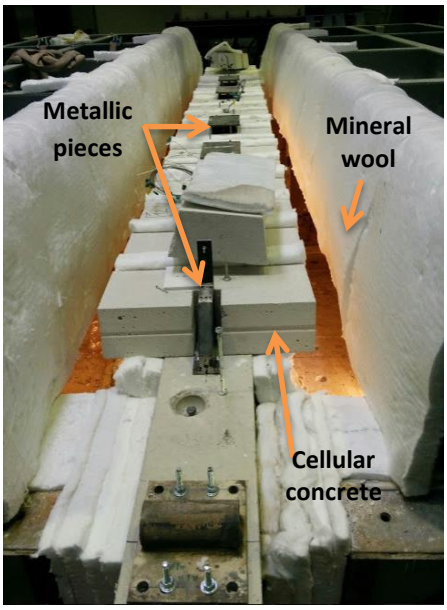


*The view of the beam above the furnace*

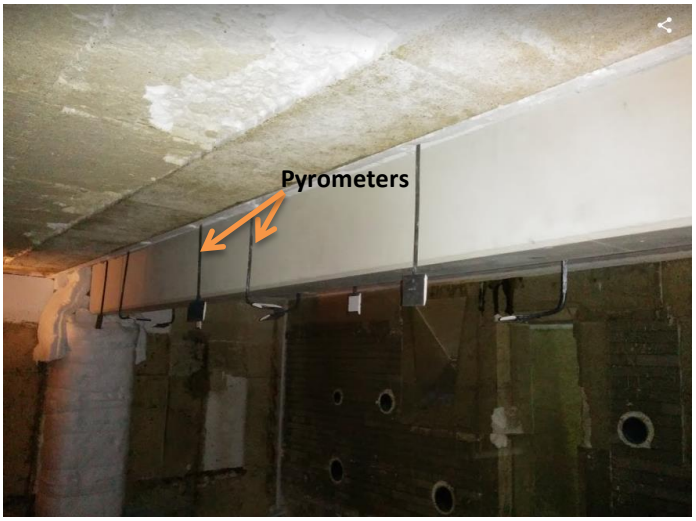


*The view of the beam from inside the furnace*

**Figure D-1. Preparation of the PS.**

## D.2. Furnace preparation

The next step is to prepare the furnace and one of the preparations is to provide the supports for the beam. The hinge and the roller are placed on the top of two columns located inside the furnace. The columns are used just when horizontal elements are needed to be supported and in order to protect them from the fire exposure they are wrapped with the mineral wools. Thus only 5,20m of the beam are exposed to fire whereas 20 cm close to the supports are protected (see Figure D-1). Figure D-2 presents the considered supports during the test with an inter-ax of 5,60m.

*Hinged support*

*The rolling support*

**Figure D-2. The supports of the beam**

When the furnace is prepared the next step is to place the beam on the supports.

## D.3. Instrumentation layout

- Transducers/inclinometers

Vertical and horizontal displacements are measured in different positions along with the support rotations.

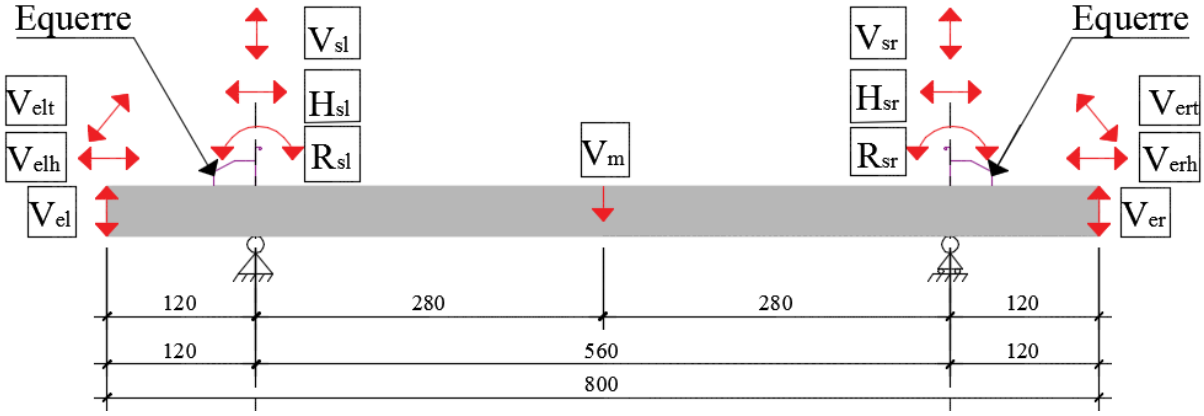


**Figure D-3. The measured displacements and rotations during the tests (configuration used during the Test 1)**

The vertical displacements are measured in the mid-span $V_m$, along with the vertical displacements of the cold extremities $V_{el}$ and $V_{er}$. The horizontal displacements are measured on the cold extremities $V_{elh}$ and $V_{erh}$. The transversal displacements $V_{elt}$ and $V_{ert}$ are measured just to check if there is no transversal movement during the test.

For the hinged support a couple of displacements and rotations are measured. The vertical displacement $V_{sl}$ (which is zero), the horizontal displacement $H_{sl}$ and the rotation $R_{sl}$ are used to back solve the horizontal displacement in the axis of the beam.

For the rolling support the vertical displacement $V_{sr}$, the horizontal displacement $H_{sr}$ and the rotation $R_{sr}$ are measured and used to back solve the displacement in the axis of the beam.

The position to place the transducers and inclinometers is limited in fire tests. To measure the displacement in the axis of the beam is challenging just because of the addition elements (mineral wool) used to protect the supports and to close the gap between the walls of the furnace and the beam. One solution is to make use of trigonometric relationships to back solve the needed displacements based on the couple of measured displacements.

Figure D-4 presents the instrumentation for the displacements and rotation measurement for the supports and for the cold extremities.

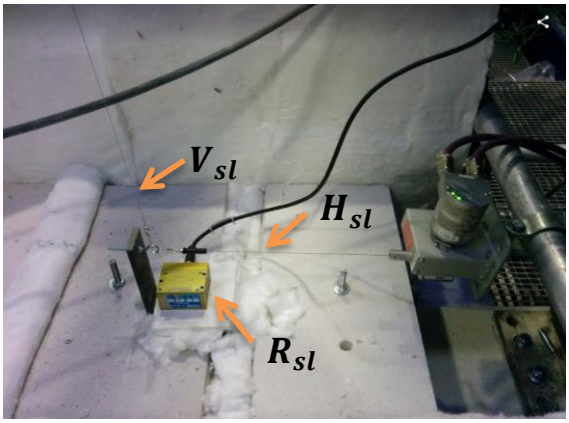


*Instrumentation to measure the hinged support displacements/rotations*

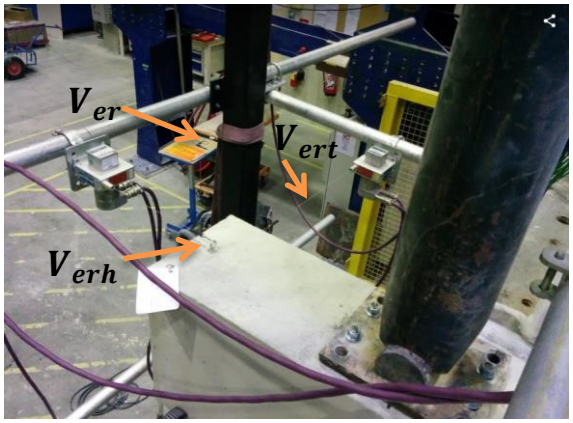


*Instrumentation to measure the cold extremity displacements/rotations (rolling support)*

**Figure D-4. The instrumentation for displacement/rotation measurements (configuration used during the Test 1)**

- The configuration of the jacks

Figure D-3 shows the configuration of the test and Figure D-5 presents pictures of the jacks from the furnace.

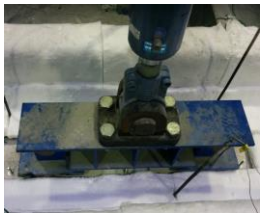

*The jack P*

*The jack $P_{left}$*

**Figure D-5. The configuration of the jacks**

- Configuration of the thermocouples

The thermocouples are used to measure the temperature evolution during the test in specific positions of the specimen.

Figure D-6 presents the position of the thermocouples for different sections of the beam.

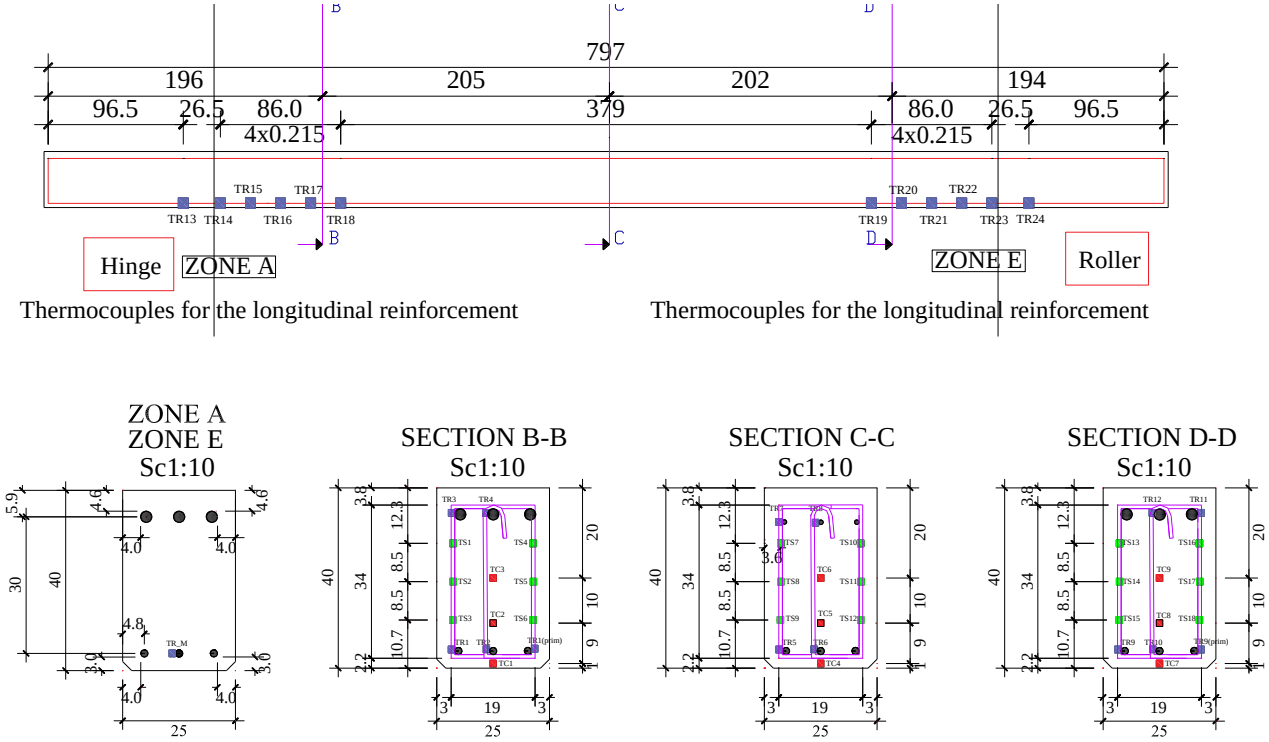


**Figure D-6. The configuration of the thermocouples**

Three types of thermocouples are defined:

- TC measuring the temperature in the concrete;
- TR measuring the temperature in the longitudinal rebars;
- TS measuring the temperature of the stirrups.

Three sections have been defined to measure the temperatures, Section B-B, Section C-C and Section D-D as presented in Figure D-6. The longitudinal temperature evolution is measured in Zone A (hinged support) and Zone E (rolling support).